Springer Series in Reliability Engineering

Enrico Zio

The Monte Carlo Simulation Method for System Reliability and Risk Analysis

Springer

Springer Series in Reliability Engineering

Series Editor

Hoang Pham

For further volumes:
http://www.springer.com/series/6917

Enrico Zio

The Monte Carlo Simulation Method for System Reliability and Risk Analysis

Springer

Enrico Zio
Chair on Systems Science and the Energetic Challenge
European Foundation for New Energy-Electricité de France
Ecole Centrale Paris and Supelec
France

and

Energy Department
Politecnico di Milano
Italy

ISSN 1614-7839
ISBN 978-1-4471-4587-5 ISBN 978-1-4471-4588-2 (eBook)
DOI 10.1007/978-1-4471-4588-2
Springer London Heidelberg New York Dordrecht

Library of Congress Control Number: 201290369

Printed on acid-free paper

Springer is part of Springer Science+Business Media (www.springer.com)

This book is passionately dedicated to
Giorgia, My teammate.
Thank you for making our team,
for giving it meaning, for filling it with love.

Preface

This book introduces the Monte Carlo simulation method for application to system reliability and risk analysis. Monte Carlo simulation is a modeling tool widely used in several scientific domains. The continuous improvements in computational power and software solutions allow its application to complex systems and problems.

The purpose of the book is to present basic and advanced techniques of Monte Carlo sampling and simulation for realistic system reliability and risk modeling. In the past, restrictive assumptions had to be introduced to the models in order to fit them to the analytical or numerical methods available for their solution, at the cost of drifting away from the actual system operation and at the risk of obtaining sometimes dangerously misleading results. Thanks to the inherent flexibility of Monte Carlo simulation, most of these assumptions can be relaxed so that realistic operating rules, including for example maintenance policies and component aging processes, can be accounted for in the model. This is of fundamental importance for systems and plants, such as those employed in the nuclear, aerospace, and chemical industry, which are safety-critical and must be designed and operated within a risk-informed approach. Yet, the efficient use of Monte Carlo simulation techniques is not trivial in large-scale applications, and the computational efforts involved may require appropriate "intelligent" techniques to obtain the results of interest in acceptable computing times.

This book collects, in a structured way, the material from a series of lectures held to senior undergraduate and graduate students at various Universities (e.g., Ecole Centrale Paris, Politecnico di Milano, Supelec, Universidad Politecnica de Valencia, Universidad Federico Santa Maria de Valparaiso, and others) and from research work carried out in the last 20 years by the author and his collaborators.

The material is organized as follows. In Chap. 1, a general introduction is offered on the types of problems that can be addressed by Monte Carlo simulation. Chapter 2 gives some basic concepts and definitions related to system reliability and risk analysis; some additional basic knowledge is given through Appendixes at the end of the book. In Chap. 3, basic procedures are given for sampling random numbers from some probability distributions commonly used in system reliability

and risk analysis, for solving definite integrals and linear integral equations, and for sensitivity analysis. Chapter 4 illustrates the use of Monte Carlo simulation for the problem of evaluating the reliability and availability of a system (formulated as a transport problem of the system states) and provides an operative procedure for its solution. The material in this chapter is completed by the presentation of a number of practical applications in the following Chap. 5. In Chap. 6, a number of advanced Monte Carlo simulation techniques are introduced to solve the problem of estimating the probability of system failure when this event is rare. These techniques include the classical Latin Hypercube Sampling and Importance Sampling, and also more recent techniques such as Cross-Entropy, Subset Sampling, Line Sampling. Examples of applications of some of these techniques are provided in Chap. 7, where sample space is given to comparisons with standard Monte Carlo simulation to appreciate the benefits offered by these techniques.

In preparing the book, efforts have been made to maintain a balance between the required theoretical and mathematical rigor in the exposition of the methods and the clarity in the illustration of the numerical examples and practical applications. For this reason, this book can serve well as a reference to both reliability and risk analysis researchers and engineers, and it would also prove useful for a university course on the subject at junior/senior undergraduate or graduate levels. Although the book is self-explanatory, a standard background in probability theory, mathematical statistics, and integral calculus is recommended.

Finally, it is with sincere appreciation that I thank all those who have contributed to prepare this book. In particular, I am grateful to Drs. Piero Baraldi, Edoardo Patelli, Nicola Pedroni, Luca Podofillini, and Professor Marzio Marseguerra for contributing the research that has provided the material for many parts of the book, and to Dr. Michele Compare, Samuele Baronchelli and Fabio Frassini for their careful editing work.

July 2012 Enrico Zio

Contents

Acronyms

AGREE	Advisory group on reliability of electronic equipment
BBN	Bayesian belief network
BDD	Binary digit diagram
c.o.v	Coefficient of variation
ccdf	Complementary cumulative distribution function
CE	Cross-entropy
CODR	Critical output-to-demand ratio
cdf	Cumulative distribution function
DOD	Department of defense
DIM	Differential importance measure
DR	Dimensionality reduction
EC	Electro-compressor
FTA	Fault tree analysis
FAR	Fatal accident rate
FORM	First order reliability method
IM	Importance measure
IS	Importance sampling
ISD	Importance sampling distribution
iid	Independent and identically distributed
LHS	Latin hypercube sampling
LSF	Limit state function
LS	Line sampling
LOCA	Loss of coolant accident
MTTF	Mean time to failure
mcs	Minimal cut sets
MC	Monte Carlo
MCMC	Markov Chain Monte Carlo
MCS	Monte Carlo simulation
NPP	Nuclear power plant
OA	Orthogonal axis
pdf	Probability density function

PF	Performance function
PLL	Potential loss of lives
PRA	Probabilistic risk assessment
RCA	Radio Corporation of America
rv	Random variable
RPS	Reactor protection system
SS	Subset simulation
TEG	Tri-ethylene glycol
TC	Turbo-compressor
TG	Turbo-generator

Chapter 1
Introduction

When designing a new system or attempting to improve an existing one, the engineer tries to anticipate future patterns of system operation under varying options. Inevitably, the prediction is done with a model of reality, which by definition can never fit reality in all details. The model is based on the available information on the interactions among the components of the system, the interaction of the system with the environment, and data related to the properties of the system components. All these aspects concur in determining how the components move among their possible states and, thus, how the system behaves. With the model, questions can be asked about the future of the system, for example in terms of its failures, spare parts, repair teams, inspections, maintenance, production and anything else that is of interest.

In this view, the Monte Carlo simulation (MCS) method is a powerful modelling tool for the analysis of complex systems, due to its capability of achieving a closer adherence to reality. It may be generally defined as a methodology for obtaining estimates of the solution of mathematical problems by means of random numbers. By random numbers, we mean numbers obtained through a roulette-like machine of the kind utilized in the gambling Casinos of the Monte Carlo Principate: then, the name of the method.

The random sampling of numbers was used in the past, well before the development of the present computers, by skillful scientists. The first example of what we would now call a MCS method seems to date back to the French naturalist Buffon (1707–88) who considered a set of parallel straight lines a distance D apart onto a plane and computed the probability P that a segment of length $L<D$ randomly positioned on the plane would intersect one of these lines [1]. The theoretical expression he obtained was

$$P = \frac{L/D}{\pi/2} \tag{1.1}$$

E. Zio, *The Monte Carlo Simulation Method for System Reliability and Risk Analysis*, Springer Series in Reliability Engineering,
DOI: 10.1007/978-1-4471-4588-2_1, © Springer-Verlag London 2013

Perhaps not completely convinced about the correctness of his result, Buffon had the idea of experimentally checking the above expression by actually drawing parallel lines and throwing a needle on the floor of its house, thus acquiring the honour of being the inventor of the MCS method. It is interesting to mention that, later on, Laplace observed that the Buffon's experiment represented a device for computing π by just throwing a needle on a floor [2].

In later years, MCS techniques were used by Lord Kelvin to solve integrals within the kinetic gas theory: he drew numbered cards from a drawer and wondered about possible correlations between the drawn numbers due to an imperfect mixing of the cards [3].

Many other scientists tackled probability problems with techniques based on random sampling. Among these, Gosset (Student), who in 1908 used a MCS method to estimate the correlation coefficient of his famous *t*-distribution [4].

Eventually, the revival of the method can be ascribed to Fermi, von Neumann and Ulam in the course of the Manhattan Project during the World War II. Back then, the MCS method provided, for example, the only option for solving the six-dimensional integral equations employed in the design of shielding for nuclear devices. It was probably the first case in human history in which solutions based on trial and error were clearly too risky.

Nowadays, MCS seems to be emerging unchallenged as the only method that can yield solutions to complex multi-dimensional problems. For about three decades it was used almost exclusively, yet extensively, in nuclear technology. Presumably, the main reason for this limited use was the lack of suitable computing power as the method is computer memory and time intensive for practical applications. Yet, with the increasing availability of fast computers the application of the method becomes more and more feasible in the practice of various fields. Indeed, the present power of computers allows uses of MCS otherways unimaginable.

The underlying tasks common to the various applications are:

- Simulation of random walks in a naturally stochastic environment or for the solution of equations, both differential and integral;
- Adoption of variance reduction methods for improving the efficiency of MCS calculations.

Two typical problems, one deterministic and one stochastic, which are addressed by MCS are described below, in general terms. As an example of a deterministic problem, let us consider the estimation of an *n*-dimensional Euclidean volume *V* of complex shape. The problem is formally equivalent to the evaluation of a definite integral. To this end, we place *V* inside a domain of volume *W* that can be readily evaluated (*W*, thus, is to be considered given). By randomly sampling a large number *N* of points inside *W* (we shall learn how to do this later in the book), *n* of these will fall inside *V*, while the remaining *N*–*n* will fall outside. Clearly, *n* is a random number that follows a binomial distribution characterized by the probability $p = V/W$ that a sampled point falls inside the volume *V*. Considering *n* as an estimate of the average number of successes we have:

$$n \simeq Np = N\frac{V}{W} \quad \text{and} \quad \hat{V} = \frac{n}{N}W$$

The statistical relative error of $\hat{V}$, estimate of V, can be immediately evaluated from the binomial distribution of n:

$$\frac{\sigma_V}{\hat{V}} = \frac{\sigma_n}{n} = \frac{\sqrt{Np(1-p)}}{Np} \simeq \frac{1}{\sqrt{N}}\sqrt{\frac{N-n}{n}} \tag{1.2}$$

where σ_V and σ_n are the standard deviations of the rvs $\hat{V}$ and n, respectively. For instance, for $V = W/2$, we have $n \simeq N/2$ and thus $\frac{\sigma_V}{\hat{V}} \simeq N^{-\frac{1}{2}}$, so that if we want to estimate V with a precision of 1%, we will have to sample $N = 10^4$ points. From this simple example, we see how it is possible to estimate a definite integral with an error tending to zero as the number N of sampled points increases.

As examples of intrinsically stochastic problems, let us consider the neutron (or photon) transport in a medium, and the reliability and risk analysis of an engineering system or plant, two problems that are apparently very different from each other.

The first case, of prominent interest in reactor physics and in medical or industrial dosimetry, aims at determining the position, energy, and flight direction of particles travelling in a medium of different materials and of complicated geometry, i.e., a fission reactor or a biological tissue [5–8]. If we suppose that the problem is linear, i.e., the particles do not interact with each other, and that the particles travel in an environment that is not modified in the course of the interactions, the idea is to successively simulate a great number of independent particle histories, each one describing the fate of a particle from its 'birth' from a radioactive source or a fission, to its 'death' by absorption or escape from the system. Each of these histories reproduces the life of a particle, which is simulated by a random walk in the so-called 'phase space' by extracting random numbers from appropriate probability distributions. In the course of the simulation, the occurrence of the events of interest in each history is recorded in appropriate counters, and at the end of the calculation the statistical estimates of the corresponding distributions are found. For example, in the case of neutron transport, each history begins with the sampling of the birth parameters of the neutron (position, flight direction and kinetic energy) from an appropriate source distribution. The neutron thus generated begins its 'flight' along a line segment whose length is dependent on the total macroscopic cross section of the material in which the neutron travels with the sampled kinetic energy, and is determined by random sampling. At the end of its flight along the line segment, the neutron interacts and the type of interaction is chosen among the various possibilities (i.e., scattering, radiative capture, fission) by sampling another random number: if as a result of the interaction the neutron is absorbed (radiative capture), the absorption event is tallied in an appropriate counter, the current history is ended and a new one begins. Alternatively, if one or more neutrons survive (from scattering or fission), for each of them a new flight direction is randomly chosen from the angular distribution of the collision, together with a new energy, and the simulation of the neutron life

continues. At the end of the calculation, the contents of the various counters in which the events of interest have been recorded allow obtaining the statistical estimates of the desired quantities. For example, by accumulating the number of fissions that occur in the different regions one can estimate the fission density; by classifying the energy of the neutrons that are exiting the system, one can estimate the escape spectrum, and so on.

By comparing the MCS approach to the neutron transport problem with the analytical–numerical solution to the neutron transport equation, the advantages and disadvantages of each method are evident. The principal advantages of the MCS method are:

- The direct use of nuclear data such as cross sections and angular distributions as a function of energy, with no need of resorting to approximations, such as, for example, the spherical harmonics representation for the transfer kernel and the methods based on energy groups;
- The possibility of considering extremely complicated geometries with no need of introducing simplifying, unrealistic assumptions such as the homogenization of heterogeneous regions.

On the other hand, the disadvantages of the MCS method are:

- A massive use of memory: the cross sections and angular distributions must be available for all nuclides and for all energies of interest;
- Long calculation times, which rapidly diverge with the desired accuracy.

Today, MCS neutronics calculations typically represent reference calculations that can be used to 'fix' empirically the approximate numerical calculations, which are generally faster.

The second example refers to the reliability and risk analysis of an engineering system or plant [9–12]. For simplicity, imagine that the system is made of a number of components placed in series or in parallel with k-over-N working logics. Each component is subject to random failures and repairs, and can be in one of several active states or in standby. The underlying idea of the MCS approach in this case is that of simulating successively a large number of independent histories of system life, each of which realizes the evolution of the state of the system from the starting time to the final (mission) time of interest. Each history, thus, reproduces one of the possible fates of the system, which is simulated with a random walk in the phase space by sampling random numbers from known failure, repair and state-transition distributions. From these distributions, it is possible to sample the time at which a first transition, say a failure, occurs and which component has failed. Then, the time at which the next transition occurs is sampled: this can be the time at which the failed component is repaired or the time at which the failure of another component occurs. The sequence of transitions is followed until the mission time is reached. During the simulation of each history, the events of interest, e.g., the system availability to function state, are recorded in appropriate counters. At the end of the simulation of all the histories, the contents of the counters allow obtaining the statistical estimates of the quantities of interest such as, for example, the failure probability of the system, its instantaneous unavailability, etc.

The MCS procedures described for the stochastic problems of particle transport and system reliability and risk analysis are based on phenomenological models and aim at estimating quantities that could, in principle, be calculated analytically, e.g., in the case of neutron transport, by solving the Boltzmann equation [13] and in the case of the system risk and reliability analysis, by solving the system of Markovian or Semi-Markovian differential equations [14–16]. The advantage of the MCS approach comes from the fact that it allows taking into account, in a realistic manner, the many phenomena that can occur, without additional complications in the modelling and in the solution procedure. For example, particle transport can be studied by MCS in complex geometries that are not solvable analytically: it is well known that the general solution of the Boltzmann transport equation is not known, and it is necessary to resort to various approximations which are more and more distant from the phenomenological reality. Analogously, if the reliability evaluation of a plant is performed using Markov equations, it would easily incur in the so-called *combinatorial explosion*, given by an exponential increase of the order of the system of differential equations: for example having 10 components, each of which can be in three states (working, failed, and standby) is described by $3^{10} = 59,049$ equations [17]; moreover, realistic aspects of system operation, such as component aging and maintenance, introduce significant complications in the analytical models whereas they can be treated straightforwardly by MCS [10, 18–20].

The principal disadvantage in the use of MCS in practice is the use of relevant calculation times, which diverge with the required accuracy. This disadvantage is decreasing thanks to the rapid development of computing power and to the availability of a number of techniques for efficient simulation, some of which will be illustrated in details in this book. Also, parallel computers are particularly useful for MCS because the various histories that contribute to the estimate of the solution are independent of each other and can thus be processed in parallel. On this account, in the future it can be foreseen that in many disciplines MCS will take the place of the more traditional numerical methods.

Finally, for comprehension of the book material, it is assumed that the reader has a background in probability theory, mathematical statistics and integral calculus, and is familiar with the basics of system availability and reliability theory, and risk analysis. Some Appendices are provided for background reference.

References

1. Comte de Buffon, G. Essai d'arithmetique morale. *Supplement a l'Histoire Naturelle*, *4*, 1777.
2. 7, Livre 2, Paris: Academie des Sciences, 365–366.
3. Lord Kelvin (1901). Nineteenth century clouds over the dynamical theory of heat and light. Phil. Matg. Serie 6, 2, 1.
4. Student (1908). Probable error of a correlation coefficient. *Biometrika*, *6*, 302.
5. Cashwell, E. D., & Everett, C. J. (1959). *A practical manual of the Monte Carlo method for random walk problems*. New York: Pergamon Press.

6. Gerbard, M., Spanier, J. (1969). *Monte Carlo principles and neutron transport problems*, Addison Wesley.
7. Dubi, A. (1986). *Monte Carlo calculation for nuclear reactors*, CRC Handbook of nuclear reactors calculations. In Y. Ronen (Ed.), CRC PRESS, *2*, 1.
8. Lux, I., Kobliner, L. (1991) *Monte Carlo particle transport methods: neutron and photon calculations.* CRC Press.
9. Lewis, E. E., & Bohm, F. (1984). Monte Carlo simulation of Markov unreliability models, Nuclear engineering and design. *77*, 49–62.
10. Wu, Y. F., & Lewins, J. H. (1992). Monte Carlo studies of engineering system reliability. *Annals of Nuclear Energy, 19*(10–12), 825–859.
11. Dubi, A. (2000). *Monte Carlo applications in system engineering*. Wiley: Chichester.
12. Marseguerra, M., Zio, E., *Principles of Monte Carlo Simulation for Application to Reliability and Availability Analysis*, Tutorials Notes of ESREL 2011, European Safety and Reliability Conference, 16–20 September 2001, Torino, Italy, 37–61.
13. Bell, G. I., Glasstone, S. (1979). Nuclear reactor theory. Krieger.
14. Dynkyn, E. B. (1965). *Markov processes I and II*, Springer.
15. Either, S. N., & Kurtz, T. G. (1986). *Markov processes characterization and convergence*. New York: John Wiley.
16. Davis, M. H. A. (1993). *Markov models and optimization*. Chapman and Hall.
17. Hoyland, A., Rausand, M. (1994). *System reliability theory*. (pp. 214–255) Wiley.
18. Borgonovo, E., Marseguerra, M., & Zio, E. (2000). A Monte Carlo methodological approach to plant availability modeling with maintenance. *Aging and Obsolescence, Reliability Engineering and System Safety, 67*, 59–71.
19. Barata, J., Soares, C. G., Marseguerra, M., & Zio, E. (2002). Simulation modelling of repairable multi-component deteriorating systems for 'on-condition' maintenance optimisation. *Reliability Engineering and System Safety, 76*, 255–264.
20. Marseguerra, M., Zio, E., & Cadini, F. (2002). Biased Monte Carlo unavailability analysis for systems with time-dependent failure rates. *Reliability Engineering and System Safety, 76*, 11–17.

Chapter 2
System Reliability and Risk Analysis

2.1 System Reliability Analysis

This introduction to system reliability analysis is based on [1]. Historically, it seems that the word reliability was first coined by the English poet Samuel T. Coleridge, who along with William Wordsworth started the English Romantic Movement [2]:

> "He inflicts none of those small pains and discomforts which irregular men scatter about them and which in the aggregate so often become formidable obstacles both to happiness and utility; while on the contrary he bestows all the pleasures, and inspires all that ease of mind on those around him or connected with him, with perfect consistency, and (if such a word might be framed) absolute reliability."

These lines were written by Coleridge in the year 1816, in praise of his friend the poet Robert Southey. From this initial 'familiar' use, the concept of reliability grew into a pervasive attribute worth of both qualitative and quantitative connotations. In fact, it only takes an internet search of the word 'reliability', e.g., by the popular engine Google, to be overwhelmed by tens of millions of citations [3].

From 1816 to today several revolutionizing social, cultural, and technological developments have occurred which have aroused the need of a rational framework for the quantitative treatment of the reliability of engineered systems and plants and the establishment of *system reliability analysis* as a scientific discipline, starting from the mid 1950s.

The essential *technical* pillar which has supported the rise of system reliability analysis as a scientific discipline is the theory of probability and statistics. This theory was initiated to satisfy the enthusiastic urge for answers to gaming and gambling questions by Blaise Pascal and Pierre de Fermat in the 1600s and later expanded into numerous other practical problems by Laplace in the 1800s [3, 4].

Yet, the development of system reliability analysis into a scientific discipline in itself needed a practical push, which came in the early 1900s with the rise of the concept of mass production for the manufacturing of large quantities of goods

E. Zio, *The Monte Carlo Simulation Method for System Reliability and Risk Analysis*, Springer Series in Reliability Engineering,
DOI: 10.1007/978-1-4471-4588-2_2, © Springer-Verlag London 2013

from standardized parts (rifle production at the Springfield armory, 1863 and Ford Model T car production, 1913) [3].

But actually, the catalyst for the actual emergence of system reliability analysis was the vacuum tube, specifically the triode invented by Lee de Forest in 1906, which at the onset of WWII initiated the electronic revolution, enabling a series of applications such as the radio, television, radar, and others.

The vacuum tube is by many recognized as the active element that allowed the Allies to win the so-called 'wizard war'. At the same time, it was also the main cause of equipment failure: tube replacements were required five times as often as all other equipments. After the war, this experience with the vacuum tubes prompted the US Department of Defense (DoD) to initiate a number of studies for looking into these failures.

A similar situation was experienced on the other side of the warfront by the Germans, where chief Engineer Lusser, a programme manager working in Peenemünde on the V1, prompted the systematic analysis of the relations between system failures and components faults.

These and other military-driven efforts eventually led to the rise of the new discipline of system reliability analysis in the 1950s, consolidated and synthesized for the first time in the Advisory Group on Reliability of Electronic Equipment (AGREE) report in 1957. The AGREE was jointly established in 1952 between the DoD and the American Electronics Industry, with the mission of [5]:

- Recommending measures that would result in more reliable equipment;
- Helping to implement reliability programs in government and civilian agencies;
- Disseminating a better education on reliability.

Several projects, still military-funded, developed in the 1950s from this first initiative [5–7]. Failure data collection and root cause analyses were launched with the aim of achieving higher reliability in components and devices. These led to the specification of quantitative reliability requirements, marking the beginning of the contractual aspect of reliability. This inevitably brought the problem of being able to estimate and predict the reliability of a component before it was built and tested: this in turn led in 1956 to the publication of a major report on reliability prediction techniques entitled 'Reliability Stress Analysis for Electronic Equipment' (TR-1100) by the Radio Corporation of America (RCA), a major manufacturer of vacuum tubes. The report presented a number of analytical models for estimating failure rates and can be considered the direct predecessor of the influential military standard MIL-HDBK-217F first published in 1961 and still used today to make reliability predictions.

Still from the military side, during the Korean war maintenance costs were found quite significant for some armed systems, thus calling for methods of reliability prediction and optimized strategies of component maintenance and renovation.

In the 1960s, the discipline of system reliability analysis proceeded along two tracks:

- Increased specialization in the discipline by sophistication of the techniques, e.g., redundancy modelling, Bayesian statistics, Markov chains, etc., and by the development of the concepts of reliability physics to identify and model the physical causes of failure and of structural reliability to analyze the integrity of buildings, bridges, and other constructions;
- Shift of the attention from component reliability to system reliability and availability, to cope with the increased complexity of the engineered systems, like those developed as part of military and space programs like the Mercury, Gemini, and Apollo ones.

Three broad areas characterized the development of system reliability analysis in the 1970s:

- The potential of system-level reliability analysis [8] motivated the rational treatment of the safety attributes of complex systems such as the nuclear power plants [9];
- The increased reliance on software in many systems led to the growth of focus on software reliability, testing, and improvement [10];
- The lack of interest on reliability programs that managers often showed already at that time, sparked the development of incentives to reward improvement in reliability on top of the usual production-based incentives.

With respect to methods of prediction reliability, no particular advancements were achieved in those years.

In the following years, the scientific and practicing community has witnessed an impressive increase of developments and applications of system reliability analysis, aimed at rationally coping with the challenges brought by the growing complexity of the systems and practically taking advantage of the computational power becoming available at reasonable costs [1].

The developments and applications of these years have been driven by a shift from the traditional industrial economy, valuing production, to the modern economy centered on service delivery: the fundamental difference is that the former type of economy gives value to the product itself whereas the latter gives value to the performance of the product in providing the service. The good is not the product itself but its service and the satisfaction of the customer in receiving it.

This change of view has led to an increased attention to service availability as a most important quality and to a consequent push in the development of techniques for its quantification. This entails consideration of the fact that availability is a property which depends on the combination of a number of interrelated processes of component degradation, of failure and repair, of diagnostics and maintenance, which result from the interaction of different systems including not only the hardware but also the software, the human, and the organizational and logistic systems.

In this scenario, we arrive at our times. Nowadays, system reliability analysis is a well-established, multidisciplinary scientific discipline which aims at providing

an ensemble of formal methods to investigate the uncertain boundaries around system operation and failure, by addressing the following questions [1, 11, 12]:

- Why systems fail, e.g., by using the concepts of reliability physics to discover causes and mechanisms of failure and to identify consequences;
- How to develop reliable systems, e.g., by reliability-based design;
- How to measure and test reliability in design, operation, and management;
- How to maintain systems reliable, by maintenance, fault diagnosis, and prognosis.

Operatively, the system reliability analysis which addresses the questions above is based on the quantitative definition of reliability in probabilistic terms: considering the continuous random variable *failure time* T, the reliability of the system at time t is the probability that the system does not fail up to time t, i.e., the probability that T takes on values larger than t.

Another quantity of interest is the system availability, which is used to characterize the ability of a system to fulfill the function for which it is operated. It applies to systems which can be maintained, restored to operation or renovated upon failure depending on the particular strategy adopted to optimally assure its function [1–6]:

- Off-schedule (corrective) maintenance, i.e., replacement or repair of the failed system;
- Preventive maintenance, i.e., regular inspections, and possibly repair, based on a structured maintenance plan;
- Condition-based maintenance, i.e., performance of repair actions upon detection of the degraded conditions of the system;
- Predictive maintenance, i.e., replacement of the system upon prediction of the evolution of the degradation conditions of the system.

The *instantaneous availability* is defined as the probability that the system is operating at time t. It differs from reliability, which is instead used to characterize the ability of the system of achieving the objectives of its specified mission within an assigned period of time, by the probability that the system functions with no failures up to time t.

Operatively, the time-dependent, instantaneous availability function of a system is synthesized by point values, e.g.:

- For units or systems under corrective maintenance, the *limiting* or *steady state availability* is computed as the mathematical limit of the instantaneous availability function in time as this latter grows to infinity. It represents the probability that the system is functioning at an arbitrary moment of time, after the transient of the failure and repair processes have stabilized. It is obviously undefined for systems under periodic maintenance, for which the limit does not exist;
- For systems under periodic maintenance, the average availability over a given period of time is introduced as indicator of performance. It represents the expected proportion of time that the system is operating in the considered period of time.

2.2 System Risk Analysis

This introduction to system risk analysis is based on [13]. The subject of risk nowadays plays a relevant role in the design, development, operation and management of components, systems, and structures in many types of industry. In all generality, the problem of risk arises wherever there exist a potential source of damage or loss, i.e., a hazard (threat), to a target, e.g., people or the environment. Under these conditions, safeguards are typically devised to prevent the occurrence of the hazardous conditions, and protections are emplaced to protect from and mitigate its associated undesired consequences. The presence of a hazard does not suffice itself to define a condition of risk; indeed, inherent in the latter there is the uncertainty that the hazard translates from potential to actual damage, bypassing safeguards and protections. In synthesis, the notion of risk involves some kind of loss or damage that might be received by a target and the uncertainty of its transformation in an actual loss or damage.

One classical way to defend a system against the uncertainty of its failure scenarios has been to: (i) identify the group of failure event sequences leading to credible worst-case accident scenarios $\{s^*\}$ (design-basis accidents), (ii) predict their consequences $\{x^*\}$, and (iii) accordingly design proper safety barriers for preventing such scenarios and for protecting from, and mitigating, their associated consequences [1].

Within this approach (often referred to as a *structuralist, defense-in-depth approach*), safety margins against these scenarios are enforced through conservative regulation of system design and operation, under the creed that the identified worst-case, credible accidents would envelope all credible accidents for what regards the challenges and stresses posed on the system and its protections. The underlying principle has been that if a system is designed to withstand all the worst-case credible accidents, then it is 'by definition' protected against any credible accident [14].

This approach has been the one classically undertaken, and in many technologies it still is, to protect a system from the uncertainty of the unknown failure behaviors of its components, systems, and structures, without directly quantifying it, so as to provide reasonable assurance that the system can be operated without undue risk. However, the practice of referring to 'worst' cases implies strong elements of subjectivity and arbitrariness in the definition of the accidental events, which may lead to the consideration of scenarios characterized by really catastrophic consequences, although highly unlikely. This may lead to the imposition of unnecessarily stringent regulatory burdens and thus excessive conservatism in the design and operation of the system and its protective barriers, with a penalization of the industry. This is particularly so for those high-consequence industries, such as the nuclear, aerospace, and process ones, in which accidents may lead to potentially large consequences.

For this reason, an alternative approach has been pushed forward for the design, regulation, and management of the safety of hazardous systems. This approach,

initially motivated by the growing use of nuclear energy and by the growing investments in aerospace missions in the 1960s, stands on the principle of looking quantitatively also at the reliability of the accident-preventing and consequence-limiting protection systems that are designed and implemented to intervene in protection against all potential accident scenarios, in principle with no longer any differentiation between credible and incredible, large, and small accidents [15]. Initially, a number of studies were performed for investigating the merits of a quantitative approach based on probability for the treatment of the uncertainty associated with the occurrence and evolution of accident scenarios [16]. The findings of these studies motivated the first complete and full-scale probabilistic risk assessment of a nuclear power installation [9]. This extensive work showed that indeed the dominant contributors to risk need not be necessarily the design-basis accidents, a 'revolutionary' discovery undermining the fundamental creed underpinning the structuralist, defense-in-depth approach to safety [14].

Following these lines of thought, and after several 'battles' for their demonstration and valorization, the probabilistic approach to risk analysis (Probabilistic Risk Analysis, PRA) has arisen as an effective way for analysing system safety, not limited only to the consideration of worst-case accident scenarios but extended to looking at all feasible scenarios and its related consequences, with the probability of occurrence of such scenarios becoming an additional key aspect to be quantified in order to rationally and quantitatively handle uncertainty [9, 17–24].

In this view, system risk analysis offers a framework for the evaluation of the risk associated to an activity, process, or system, with the final aim of providing decision support on the choice of designs and actions.

From the view point of safety regulations, this has led to the introduction of new criteria that account for both the consequences of the scenarios and their probabilities of occurrence under a now *rationalist, defense-in-depth approach*. Within this approach to safety analysis and regulation, system reliability analysis takes on an important role in the assessment of the probability of occurrence of the accident scenarios as well as the probability of the functioning of the safety barriers implemented to hinder the occurrence of hazardous situations and mitigate their consequences if such situations should occur [1].

2.2.1 The Framework of PRA

The basic analysis principles used in a PRA can be summarized as follows. A PRA systemizes the knowledge and uncertainties about the phenomena studied by addressing three fundamental questions [24]:

- Which sequences of undesirable events transform the hazard into an actual damage?
- What is the probability of each of these sequences?
- What are the consequences of each of these sequences?

This leads to a widely accepted, technical definition of risk in terms of a set of triplets [22] identifying the sequences of undesirable events leading to damage (the accident scenarios), the associated probabilities and the consequences. In this view, the outcome of a risk analysis is a list of scenarios quantified in terms of probabilities and consequences, which collectively represent the risk. On the basis of this information, the designer, the operator, the manager, and the regulator can act effectively so as to manage (and possibly reduce) risk.

In the PRA framework, knowledge of the problem and the related uncertainties are systematically manipulated by rigorous and repeatable probability-based methods to provide representative risk outcomes such as the expected number of fatalities (in terms of indices such as Potential Loss of Lives (PLL) and Fatal Accident Rate (FAR), the probability that a specific person shall be killed due to an accident (individual risk) and frequency-consequence (*f*-*n*) curves expressing the expected number of accidents (frequency *f*) with at least *n* fatalities.

In spite of the maturity reached by the methodologies used in PRA, a number of new and improved methods have been developed in recent years to better meet the needs of the analysis, in light of the increasing complexity of the systems and to respond to the introduction of new technological systems [1]. Many of the methods introduced allow increased levels of detail and precision in the modeling of phenomena and processes within an integrated framework of analysis covering physical phenomena, human and organisational factors as well as software dynamics (e.g., [25]). Other methods are devoted to the improved representation and analysis of the risk and related uncertainties, in view of the decision making tasks that the outcomes of the analysis are intended to support. Examples of newly introduced methods are Bayesian Belief Networks (BBNs), Binary Digit Diagrams (BDDs), multi-state reliability analysis, Petri Nets, and advanced MCS tools. For a summary and discussion of some of these models and techniques, see [1] and [20].

The probabilistic analysis underpinning PRA stands on two lines of thinking, the traditional frequentist approach and the Bayesian approach [19, 20]. The former is typically applied in case of large amount of relevant data; it is founded on well-known principles of statistical inference, the use of probability models, the interpretation of probabilities as relative frequencies, point values, confidence intervals estimation, and hypothesis testing.

The Bayesian approach is based on the use of subjective probabilities and is applicable also in case of scarce amount of data. The idea is to first establish adequate probability models representing the aleatory uncertainties, i.e., the variabilities in the phenomena studied, such as for example the lifetimes of a type of unit; then, the epistemic uncertainties (due to incomplete knowledge or lack of knowledge) about the values of the parameters of the models are represented by prior subjective probability distributions; when new data on the phenomena studied become available, Bayes' formula is used to update the representation of the epistemic uncertainties in terms of the posterior distributions. Finally, the predictive distributions of the quantities of interest (the observables, for example

the lifetimes of new units) are derived by applying the law of total probability. The predictive distributions are subjective but they also reflect the inherent variability represented by the underlying probability models.

2.2.2 Uncertainty Analysis

Uncertainty is an unavoidable component affecting the behaviour of systems and more so with respect to their limits of operation. In spite of how much dedicated effort is put into improving the understanding of systems, components and processes through the collection of representative data, the appropriate characterization, representation, propagation and interpretation of uncertainty remains a fundamental element of the risk analysis of any system. Following this view, uncertainty analysis is considered an integral part of PRA, although it can also exist independently in the evaluation of unknown quantities.

In the context of PRA, uncertainty is conveniently distinguished into two different types: randomness due to inherent variability in the system (i.e., in the population of outcomes of its stochastic process of behavior) and imprecision due to lack of knowledge and information on the system. The former type of uncertainty is often referred to as objective, aleatory or stochastic whereas the latter is often referred to as subjective, epistemic, or state-of-knowledge [26–29]. Probability models are introduced to represent the aleatory uncertainties, for example a Poisson model to represent the variation in the number of events occurring in a period of time. The epistemic uncertainties arise from a lack of knowledge of the parameters of the probability models. Whereas epistemic uncertainty can be reduced by acquiring knowledge and information on the system, the aleatory uncertainty cannot, and for this reason it is sometimes called irreducible uncertainty.

In all generality, the quantitative analyses of the phenomena occurring in many engineering applications are based on mathematical models that are then turned into operative computer codes for simulation. A model provides a representation of a real system dependent on a number of hypotheses and parameters. The model can be deterministic (e.g., Newton's dynamic laws or Darcy's law for groundwater flow) or stochastic (e.g., the Poisson model for describing the occurrence of earthquake events).

In practice, the system under analysis cannot be characterized exactly—the knowledge of the underlying phenomena is incomplete. This leads to uncertainty in both the values of the model parameters and on the hypotheses supporting the model structure. This defines the scope of the *uncertainty analysis*.

An uncertainty analysis aims at determining the uncertainty in analysis results that derives from uncertainty in analysis inputs [29–31]. We may illustrate the ideas of the uncertainty analysis by introducing a model $G(X)$, which depends on the input quantities X and on the function G; the quantity of interest Z is computed by using the model $Z = G(X)$. The uncertainty analysis of Z requires an assessment of the uncertainties of X and their propagation through the model G to produce a

characterization of the uncertainties of Z. Typically, the uncertainty related to the model structure G, e.g., uncertainty due to the existence of alternative plausible hypotheses on the phenomena involved, are treated separately [27, 32–34]; actually, while the first source of uncertainty has been widely investigated and more or less sophisticated methods have been developed to deal with it, research is still ongoing to obtain effective and accepted methods to handle the uncertainty related to the model structure [35]. See also [36] which distinguishes between model inaccuracies (the differences between Z and $G(X)$), and model uncertainties due to alternative plausible hypotheses on the phenomena involved.

The traditional tool used to express the uncertainties in PRA is (subjective) probabilities. In this context, the quantities X and Z could be chances representing fractions in a large (in theory infinite) population of similar items (loosely speaking, a chance is the Bayesian term for a frequentist probability, cf. the representation theorem of de Finetti [37], [38], p. 172). In this case, the assessment is consistent with the so-called *probability of frequency approach*, which is based on the use of subjective probabilities to express epistemic uncertainties of unknown frequencies, i.e., the chances [22]. The probability of frequency approach constitutes the highest level of uncertainty analysis according to a commonly referenced uncertainty treatment classification system [39].

Recently, many researchers have argued that the information commonly available in the practice of risk decision making does not provide a sufficiently strong basis for a specific probability assignment; the uncertainties related to the occurrence of the events and associated consequences are too large. Furthermore, in a risk analysis context there are often many stakeholders and they may not be satisfied with a probability-based assessment expressing the subjective judgments of the analysis group: again a broader risk description is sought.

Based on the above critiques, it is not surprising that alternative approaches for representing and describing uncertainties in risk assessment have been suggested, which produce epistemic-based uncertainty descriptions and in particular probability intervals.

Work has also been carried out to combine different approaches, for example probabilistic analysis and possibility theory. Here the uncertainties of some parameters are represented by probability distributions and those of some other parameters by means of possibilistic distributions. An integrated computational framework has been proposed for jointly propagating the probabilistic and possibilistic uncertainties [40]. This framework has been tailored to event tree analysis [41] and Fault Tree Analysis (FTA) [42], allowing for the uncertainties about event probabilities (chances) to be represented and propagated using both probability and possibility distributions.

References

1. Zio, E. (2009). Reliability engineering: Old problems and new challenges. *Reliability Engineering and System Safety, 94*, 125–141.
2. Coleridge, S. T. (1983). Biographia Literaria. In J. Engell & W. J. Bate (Eds.), *The collected works of Samuel Taylor Coleridge*. New Jersey: Princeton University Press.
3. Saleh, J. H., & Marais, K. (2006). Highlights from the early (and Pre-) history of reliability engineering. *Reliability Engineering and System Safety, 91*, 249–256.
4. Apostol, T. M. (1969). *Calculus* (2nd ed., Vol. 2). New York: Wiley.
5. Coppola, A. (1984). Reliability Engineering of electronic Equipment: an Historical Perspective. *IEEE Transactions on Reliability R-33* (1), 29–35.
6. Raymond Knight, C. (1991). Four decades of reliability progress. In *Proceedings of the Annual Reliability and Maintainability Symposium*, IEEE 1991, (pp. 156–160).
7. Denson, W. (1998). The History of Reliability Prediction. *IEEE Transactions on Reliability*, *47*(2-SP), 321–328.
8. Barlow, R. E., & Proschan, F. (1975). *Statistical theory of reliability and life testing*. Rinehart and Winston: Holt.
9. NRC (1975) *Reactor Safety Study, an Assessment of Accident Risks*, WASH-1400, Report NUREG-75/014. Washington, D.C., US Nuclear Regulatory Commission.
10. Moranda, P.B. (1975) Prediction of software reliability during debugging. In *Proceedings of Annua*L *Reliability and Maintainability Symposium* (pp. 327–332).
11. Cai, K. Y. (1996). System failure engineering and fuzzy methodology. *An Introductory Overview, Fuzzy Sets and Systems, 83*, 113–133.
12. Aven, T., Jensen, U. (1999). *Stochastic models in reliability*. Heidelberg: Springer.
13. Aven, T., & Zio, E. (2011). Some considerations on the treatment of uncertainties in risk assessment for practical decision making. *Reliability Engineering and System Safety, 96*, 64–74.
14. Apostolakis, G.E. (2006, 29–30 November). *PRA/QRA:* An historical perspective. In *2006 Probabilistic/Quantitative Risk Assessment Workshop*, Taiwan.
15. Farmer, F.R. (1964). *The growth of reactor safety criteria in the United Kingdom*, In *Anglo-Spanish Power Symposium*, Madrid.
16. Garrick, B.J., & Gekler, W.C. (1967). *Reliability analysis of nuclear power plant protective systems*, US Atomic Energy Commission, HN-190.
17. Breeding, R. J., Helton, J. C., Gorham, E. D., & Harper, F. T. (1992). Summary description of the methods used in the probabilistic risk assessments for NUREG-1150. *Nuclear Engineering and Design, 135*(1), 1–27.
18. NASA (2002). *Probabilistic Risk Assessment Procedures Guide for NASA Managers and Practitioners*.
19. Aven, T. (2003) *Foundations of risk analysis*, New Jersey: Wiley.
20. Bedford, T., Cooke, R. (2001). *Probabilistic risk analysis*, Cambridge: Cambridge University Press.
21. Henley, E. J., & Kumamoto, H. (1992). *Probabilistic risk assessment*. NY: IEEE Press.
22. Kaplan, S., & Garrick, B. J. (1981). On the quantitative definition of risk. *Risk Analysis, 1*, 1–11.
23. McCormick, N. J. (1981). *Reliability and risk analysis*. New York: Academic Press.
24. PRA (1983, January). *Procedures guide* (Vols. 1&2). NUREG/CR-2300.
25. Mohaghegh, Z., Kazemi, R., & Mosleh, A. (2009). Incorporating organizational factors into probabilistic risk assessment (PRA) of complex socio-technical systems: A hybrid technique formalization. *Reliability Engineering and System Safety, 94*, 1000–1018.
26. Parry, G., & Winter, P. W. (1981). Characterization and evaluation of uncertainty in probabilistic risk analysis. *Nuclear Safety, 22*(1), 28–42.
27. Apostolakis, G.E. (1990). The concept of probability in safety assessments of technological systems. *Science*, *250*, 1359–1364.

28. Hoffman, F. O., & Hammonds, J. S. (1994). Propagation of uncertainty in risk assessments: the need to distinguish between uncertainty due to lack of knowledge and uncertainty due to variability. *Risk Analysis, 14*(5), 707–712.
29. Helton, J.C. (2004) Alternative representations of epistemic uncertainty, *Special Issue of Reliability Engineering and System Safety*, *85*, 1–369.
30. Helton, J. C., Johnson, J. D., Sallaberry, C. J., & Storlie, C. B. (2006). Survey of sampling-based methods for uncertainty and sensitivity analysis. *Reliability Engineering & System Safety, 91*, 1175–1209.
31. Cacuci, D. G., & Ionescu-Bujor, M. A. (2004). Comparative review of sensitivity and uncertainty analysis of large-scale systems–II: statistical methods. *Nuclear Science and Engineering, 147*(3), 204–217.
32. Nilsen, T., & Aven, T. (2003). Models and model uncertainty in the context of risk analysis. *Reliability Engineering & Systems Safety, 79*, 309–317.
33. Devooght, J. (1998). Model uncertainty and model inaccuracy. *Reliability Engineering & System Safety, 59*, 171–185.
34. Zio, E., & Apostolakis, G. E. (1996). Two methods for the structured assessment of model uncertainty by experts in performance assessments of radioactive waste repositories. *Reliability Engineering & System Safety, 54*, 225–241.
35. Parry, G., Drouin, M.T. (2009). *Risk-Informed Regulatory Decision-Making at the U.S. NRC: Dealing with model uncertainty*, Nuclear Regulatory Commission, 2009.
36. Aven, T. (2010). Some reflections on uncertainty analysis and management. *Reliability Engineering & System Safety, 95*, 195–201.
37. de Finetti, B. (1930). Fondamenti logici del ragionamento probabilistico. *Bollettino dell'Unione Matematica Italiana, 9*, 258–261.
38. Bernardo, J. M., & Smith, A. F. M. (1994). *Bayesian theory*. Chichester: Wiley.
39. Paté-Cornell, M. E. (1996). Uncertainties in risk analysis: Six levels of treatment. *Reliability Engineering & System Safety, 54*(2–3), 95–111.
40. Baudrit, C., Dubois, D., & Guyonnet, D. (2006). Joint propagation of probabilistic and possibilistic information in risk assessment. *IEEE Transactions on Fuzzy Systems, 14*, 593–608.
41. Baraldi, P., & Zio, E. (2008). A combined Monte Carlo and possibilistic approach to uncertainty propagation in event tree analysis. *Risk Analysis, 28*(5), 1309–1325.
42. Flage, R., Baraldi, P., Ameruso, F., Zio, E. & Aven, T. (2009, September 7–10) Handling epistemic uncertainties in fault tree analysis by probabilistic and possibilistic approaches. In R.Bris, C. Guedes Soares & S. Martorell (Eds.), *Reliability, risk and safety: theory and applications*. *Supplement Proceedings of the European Safety and Reliability Conference 2009 (ESREL 2009)* (pp. 1761–1768). Prague: CRC Press London.

Chapter 3
Monte Carlo Simulation: The Method

3.1 Sampling Random Numbers

Let X be a random variable (rv) obeying a cumulative distribution function (cdf)

$$P(X \leq x) = F_X(x); \quad F_X(-\infty) = 0; \quad F_X(\infty) = 1 \tag{3.1}$$

In the following, if the rv X obeys a cdf we shall write $X \sim F_X(x)$. From the definition, it follows that $F_X(x)$ is a non-decreasing function and we further assume that it is continuous and differentiable at will. The corresponding probability density function (pdf) is then

$$f_X(x) = \frac{\mathrm{d}F_X(x)}{\mathrm{d}x}; \quad f_X(x) \geq 0; \quad \int_{-\infty}^{\infty} f_X(x)\mathrm{d}x = 1 \tag{3.2}$$

We now aim at sampling numbers from the cdf $F_X(x)$ A sequence of $N \gg 1$ values $\{X\} \equiv \{x_1, x_2, \ldots, x_N\}$ sampled from $F_X(x)$ must be such that the number n of sampled points falling within an interval $\Delta x \ll X_{\max} - X_{\min}$ (where $X_{\min}$ and $X_{\max}$ are the minimum and maximum values in $\{X\}$) is

$$\frac{n}{N} \simeq \int_{\Delta x} f_X(x)\mathrm{d}x \tag{3.3}$$

In other words, we require that the histogram of the sampled data approximates $f_X(x)$. Also, the x_i values should be uncorrelated and, if the sequence $\{X\}$ is periodic, the period after which the numbers start repeating should be as large as possible.

Among all the distributions, the uniform distribution in the interval [0,1), denoted as $U[0,1)$ or, more simply $U(0,1)$, plays a role of fundamental importance since sampling from this distribution allows obtaining rvs obeying any other distribution [1].

E. Zio, *The Monte Carlo Simulation Method for System Reliability and Risk Analysis*, Springer Series in Reliability Engineering,
DOI: 10.1007/978-1-4471-4588-2_3, © Springer-Verlag London 2013

3.2 The Uniform Random Number Generator: Sampling from the Uniform Distribution

The cdf and pdf of the distribution U [0,1) are

$$\begin{aligned} U_R(r) = r; \quad u_R(r) = 1 \quad &\text{for} \quad 0 \le r \le 1 \\ = 0 \qquad\quad = 0 \quad &\text{for} \quad r < 0 \\ = 1 \qquad\quad = 0 \quad &\text{for} \quad r > 1 \end{aligned} \tag{3.4}$$

The generation of random numbers R uniformly distributed in [0,1) has represented, and still represents, an important problem subject of active research. In the beginning, the outcomes of intrinsically random phenomena were used (e.g., throwing a coin or dice, spinning the roulette, counting of radioactive sources of constant intensity, etc.), but soon it was realized that, apart from the non-uniformity due to imperfections of the mechanisms of generation or detection, the frequency of data thus obtained was too low and the sequences could not be reproduced, so that it was difficult to find and fix the errors in the MCS codes in which the random numbers generated were used.

To overcome these difficulties, the next idea was to fill tables of random numbers to store in the computers (in 1955 RAND corporation published a table with 10^6 numbers), but the access to the computer memory decreased the calculation speed and, above all, the sequences that had been memorized were always too short with respect to the growing necessities.

Finally, in 1956, von Neumann proposed to have the computer directly generate the 'random' numbers by means of an appropriate function $g(\cdot)$ which should allow one to find the next number R_{k+1} from the preceding one R_k i.e.,

$$R_{k+1} = g(R_k) \tag{3.5}$$

The sequence thus generated is inevitably periodic: in the course of the sequence, when a number is obtained that had been obtained before, the subsequence between these two numbers repeats itself cyclically, i.e., the sequence enters a loop. Furthermore, the sequence itself can be reproduced so that it is obviously not 'random', rather deterministic. However, if the function $g(r)$ is chosen correctly, it can be said to have a pseudorandom character if it satisfies a number of randomness tests. In particular, Von Neumann proposed to obtain R_{k+1} by taking the central digits of the square of R_k. For example, for a computer with a four-digit word, if $R_k = 4,567$, then $R_k^2 = 20,857,489$ and $R_{k+1} = 8,574$, $R_{k+2} = 5,134$, and so on. This function turns out to be lengthy to be calculated and to give rise to rather short periods; furthermore, if one obtains $R_k = 0000$, then all the following numbers are also zero. Presently, the most commonly used methods for generating sequences $\{R\}$ of numbers from a uniform distribution are inspired from the Monte Carlo roulette game. In a real roulette game the ball, thrown with high initial speed, performs a large number of revolutions around the wheel and finally it comes to rest within one of the numbered compartments. In an ideal machine

nobody would doubt that the final compartment, or its associated number, is actually uniformly sampled among all the possible compartments or numbers.

In the domain of the real numbers within the interval [0,1), the game could be modeled by throwing a point on the positive x-axis very far from the origin with a method having an intrinsic dispersion much larger than unity: then, the difference between the value so obtained and the largest integer smaller than this value may be reasonably assumed as sampled from $U[0,1)$. In a computer, the above procedure is performed by means of a mixed congruential relationship of the kind

$$R_{k+1} = (aR_k + c) \bmod m \tag{3.6}$$

In words, the new number R_{k+1} is the remainder, modulo a positive integer m, of an affine transform of the old R_k with non-negative integer coefficients a and c. The above expression, in some way, resembles the uniform sampling in the roulette game, $aR_k + c$ playing the role of the distance travelled by the ball and m that of the wheel circumference. The sequence so obtained is made up of numbers $R_k < m$ and it is periodic with period $p < m$. For example, if we choose $R_0 = a = c = 5$ and $m = 7$, the sequence is $\{5,2,1,3,6,0,5,\ldots\}$, with a period $p = 6$. The sequences generated with the above described method are actually deterministic so that the sampled numbers are more appropriately called pseudo-random numbers. However, the constants a, c, m may be selected so that:

- The generated sequence satisfies essentially all randomness tests;
- The period p is very large.

Since the numbers generated by the above procedure are always smaller than m, when divided by m they lie in the interval [0,1).

Research to develop algorithms for generating pseudo-random numbers is still ongoing. Good statistical properties, low speed in numbers generation and reproducibility are central requirements for these algorithms to be suitable for MC simulation.

Other Pseudo-Random Number Generation (PRNG) algorithms include the Niederreiter [2], Sobol [3], and Mersenne Twister [4] algorithms. For example, this latter allows generating numbers with an almost uniform distribution in the range $[0, 2^k - 1]$, where k is the computer word length (nowadays, $k = 32$ or 64). Further details on other methods are given in [5–16], with wide bibliographies which we suggest to the interested reader.

Before leaving this issue, it is important to note that for the generation of pseudo-random numbers $U[0,1)$ many computer codes do not make use of machine subroutines, but use congruential subroutines which are part of the program itself. Thus, for example, it is possible that an excellent program executed on a machine with a word of length different from the one it was written for gives absurd results. In this case it should not be concluded that the program is 'garbage', but it would be sufficient to appropriately modify the subroutine that generates the random numbers.

3.3 Sampling Random Numbers from Generic Distributions

3.3.1 *Sampling by the Inverse Transform Method: Continuous Distributions*

Let $X \in (-\infty, +\infty)$ be a rv with cdf $F_X(x)$ and pdf $f_X(x)$, viz.,

$$F_X(x) = \int_{-\infty}^{x} f_X(x')\mathrm{d}x' = \mathrm{P}(X \leq x) \tag{3.7}$$

Since $F_X(x)$ is a non-decreasing function, for any $y \in [0, 1)$ its inverse may be defined as

$$F_X^{-1}(y) = \inf\{x : F_X(x) \geq y\} \tag{3.8}$$

With this definition, we take into account the possibility that in some interval $[x_s, x_d]$ $F_X(x)$ is constant (and $f_X(x)$ zero), that is

$$F_X(x) = \gamma \quad \text{for} \quad x_s < x \leq x_d \tag{3.9}$$

In this case, from definition (3.8) it follows that corresponding to the value γ, the minimum value x_s is assigned to the inverse function $F_X^{-1}(\gamma)$. This is actually as if $F_X(x)$ were not defined in $(x_s, x_d]$; however, this does not represent a disadvantage, since values in this interval can never be sampled because the pdf $f_X(x)$ is zero in that interval. Thus, in the following, we will suppose that the intervals $(x_s, x_d]$ (open to the left and closed to the right), in which $F_X(x)$ is constant, are excluded from the definition domain of the rv X. By so doing, the $F_X(x)$ will always be increasing (instead of non-decreasing). We now show that it is always possible to obtain values $X \sim F_X(x)$ starting from values R sampled from the uniform distribution $U_R[0,1)$. In fact, if R is uniformly distributed in [0,1), we have

$$\mathrm{P}(R \leq r) = U_R(r) = r \tag{3.10}$$

Corresponding to a number R extracted from $U_R(r)$, we calculate the number $X = F_X^{-1}(R)$ and wonder about its distribution. As it can be seen in Fig. 3.1, for the variable X we have

$$\mathrm{P}(X \leq x) = \mathrm{P}\left(F_X^{-1}(R) \leq x\right) \tag{3.11}$$

Because F_X is an increasing function, by applying it to the arguments at the right-hand side of Eq. (3.11), the inequality is conserved and from Eq. (3.10) we have

$$\mathrm{P}(X \leq x) = \mathrm{P}(R \leq F_X(x)) = F_X(x) \tag{3.12}$$

It follows that $X = F_X^{-1}(R)$ is extracted from $F_X(x)$. Furthermore, because $F_X(x) = r$

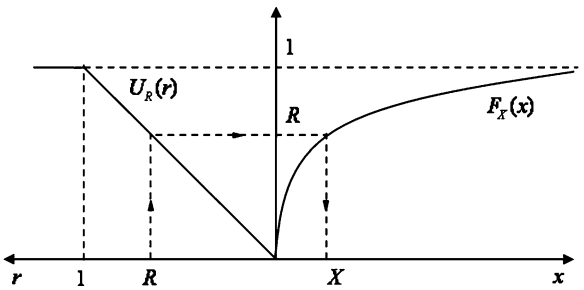

Fig. 3.1 Inverse transform method: continuous distributions

$$\mathrm{P}(X \leq x) = \mathrm{P}(R \leq r) \tag{3.13}$$

In terms of cdf

$$U_R(R) = F_X(x) \quad \text{and} \quad R = \int_{-\infty}^{x} f_X(x')\mathrm{d}x' \tag{3.14}$$

This is the fundamental relationship of the inverse transform method which for any R value sampled from the uniform distribution $U_R[0,1)$ gives the corresponding X value sampled from the $F_X(x)$ distribution (Fig. 3.1). However, it often occurs that the cdf $F_X(x)$ is noninvertible analytically, so that from Eq. (3.8) it is not possible to find $X \sim F_X(x)$ as a function of $R \sim U[0,1)$. An approximate procedure that is often employed in these cases consists in interpolating $F_X(x)$ with a polygonal function and in performing the inversion of Eq. (3.8) by using the polygonal. Clearly, the precision of this procedure increases with the number of points of $F_X(x)$ through which the polygonal passes. The calculation of the polygonal is performed as follows:

- If the interval of variation of x is infinite, it is approximated by the finite interval (x_a, x_b) in which the values of the pdf $f_X(x)$ are sensibly different from zero: for example, in case of the univariate normal distribution $N(\mu, \sigma^2)$ with mean value μ and variance σ^2, this interval may be chosen as $(\mu - 5\sigma, \mu + 5\sigma)$;
- The interval (0,1) in which both $F_X(x)$ and $U_R(r)$ are defined is divided in n equal subintervals of length $1/n$ and the points $x_0 = x_a, x_1, x_2, \ldots, x_n = x_b$ such that $F_X(x_i) = i/n$, $(i = 0,1,\ldots,n)$ are found, e.g., by a numerical procedure.

At this point the MC sampling may start: for each R sampled from the distribution $U_R[0,1)$, we compute the integer $i^* = Int(R \cdot n)$ and then obtain the corresponding X value by interpolating between the points x_{i^*}, i^*/n and x_{i^*+1}, $i^* + 1/n$. For example, in case of a linear interpolation we have

$$X = x_{i^*} + (x_{i^*+1} - x_{i^*})(R \cdot n - i^*) \tag{3.15}$$

For a fixed number n of points x_i upon which the interpolation is applied, the described procedure can be improved by interpolating with arcs of parabolas in place of line segments. The arcs can be obtained by imposing continuity conditions

of the function and its derivatives at the points x_i (cubic splines). The expression of X as a function of R is in this case more precise, but more burdensome and difficult to calculate. Currently, given the ease with which it is possible to increase the RAM memory of the computers, to increase the precision it is possibly preferable to increase the number n of points and to use the polygonal interpolation: as a rule of thumb, a good choice is often $n = 500$.

$$R : U_R(r) = r \text{ in } [0, 1) \Rightarrow X \sim F_X(x) \tag{3.16}$$

3.3.2 Sampling by the Inverse Transform Method: Discrete Distributions

Let X be a rv which can only have the discrete values x_k, $k = 0,1,\ldots$, with probabilities

$$f_k = \mathrm{P}(X = x_k) \geq 0,\ k = 0, 1, \ldots \tag{3.17}$$

Ordering the $\{x\}$ sequence so that $x_{k-1} < x_k$, the cdf is

$$F_k = \mathrm{P}(X \leq x_k) = \sum_{i=0}^{k} f_i = F_{k-1} + f_k \quad k = 0, 1, \ldots \tag{3.18}$$

where, by definition, $F_{-1} = 0$. The normalization condition of the cdf (Eq. 3.18) now reads

$$\lim_{k \to \infty} F_k = 1 \tag{3.19}$$

Following the scheme of the inverse transform method, given a value R sampled from the uniform distribution, the probability that R falls within the interval $(F_{k-1}, F_k]$ is in the discrete case

$$\mathrm{P}(F_{k-1} < R \leq F_k) = \int_{F_{k-1}}^{F_k} \mathrm{d}r = F_k - F_{k-1} = f_k = \mathrm{P}(X = x_k) \tag{3.20}$$

In words, for any $R \sim U[0,1)$, we get the realization $X = x_k$ where k is the index for which $F_{k-1} < R \leq F_k$ (Fig. 3.2).

In practice, a realization of X is sampled from the cdf F_k through the following steps:

1. Sample an $R \sim U[0,1)$;
2. Set $k = 0$; $F = f_o$;
3. If $R \leq F$, proceed to 5);

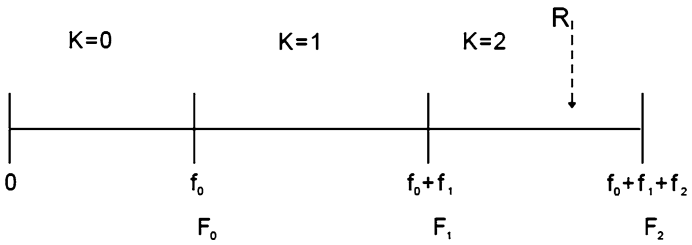

Fig. 3.2 Inverse transform method: discrete distributions, $k = 2 \Rightarrow X = x_2$

4. Viceversa, i.e., if $R > F$, set $k \leftarrow k + 1$ and then $F \leftarrow F + f_k$ and proceed to 3);
5. The required realization is $X = x_k$.

If the F_k values can be pre-computed, e.g., if their number is finite, the cycle (3–4) may be simplified by comparing R and F_k at step 3 and increasing only k at step 4.

Examples of Application of the Inverse Transform Sampling Method

Uniform Distribution in the interval (a,b)

A rv X is uniformly distributed in the interval (a,b) if

$$\begin{aligned} F_X(x) &= \frac{x-a}{b-a}; \quad & f_X(x) &= \frac{1}{b-a} \quad & \text{for} \quad & a \le x \le b \\ &= 0 & &= 0 & \text{for} \quad & x < a \\ &= 1 & &= 0 & \text{for} \quad & x > b \end{aligned} \tag{3.21}$$

Substituting in Eq. (3.18) and solving with respect to X yields

$$X = a + (b-a)R \tag{3.22}$$

As a first application, we show how it is possible to simulate Buffon's experiment, mentioned in the Introduction, with the aim of finding the probability P in Eq. (1.1). When the needle is thrown at random, the axis of the needle can have all possible orientations, with equal probability. Let φ be the angle between the needle's axis and the normal to the lines drawn on the floor. By symmetry, it is possible to consider the interval $(0, \pi/2)$ and from Eq. (3.21), with $a = 0$ and $b = \pi/2$, we have

$$F_\Phi(\phi) = \frac{\phi}{\frac{\pi}{2}}; \quad f_\Phi(\phi) = \frac{2}{\pi} \tag{3.23}$$

Corresponding to a random value Φ, the needle projection on the normal to the lines is $L\cos\Phi$ and thus the probability that the needle intercepts one of the lines is given by the ratio $L\cos\Phi/D$. Multiplying by $f_\Phi(\phi)$ and integrating, we obtain the value calculated by Buffon

$$P = \int_0^{\frac{\pi}{2}} \frac{L\cos\phi}{D}\frac{\pi}{2}d\phi = \frac{L/D}{\pi/2} \tag{3.24}$$

Operatively, for a given number of needle throws $N \gg 1$, e.g., $N = 10^3$, the procedure is as follows:

- Sample an $R_1 \sim U[0,1)$;
- Calculate from Eq. (3.22) $\Phi = R_1\pi/2$ then, the probability that the needle intercepts a line is $h = \frac{L\cos\Phi}{D}$;
- Sample an $R_2 \sim U[0,1)$ if $R_2 < h$, the needle has intercepted a line and thus we set $N_s = N_s + 1$, where N_s is the counter of the number of times the needle has intercepted a line.

At the end of this procedure, the estimate of the probability P is

$$P \cong \frac{N_s}{N}$$

A problem of, perhaps, more practical interest is that of sampling a direction $\underline{\Omega}$ from an isotropic angular distribution in space. This is, for example, a case of interest for the choice of an initial direction of flight for a neutron emitted by fission. In polar coordinates, the direction is identified by the angle $\vartheta \in (0,\pi)$ between $\underline{\Omega}$ and the z axis and by the angle $\varphi \in (-\pi, \pi)$ between the projection of $\underline{\Omega}$ on the xy plane and the x axis. Correspondingly,

$$\mathrm{d}\underline{\Omega} = \sin\vartheta \ \mathrm{d}\vartheta \ \mathrm{d}\phi = -\mathrm{d}\mu \ \mathrm{d}\phi \tag{3.25}$$

where, as usual, $\mu = \cos\vartheta$. The pdf of the isotropic distribution is then

$$f_{\underline{\Omega}}(\underline{\Omega})d\underline{\Omega} \equiv f_{\mu,\Phi}(\mu,\phi)\mathrm{d}\mu\mathrm{d}\phi = \frac{|d\underline{\Omega}|}{4\pi}f_1(\mu)\mathrm{d}\mu f_2(\phi)\mathrm{d}\phi \tag{3.26}$$

where

$$f_1(\mu) = \frac{1}{2}; \quad f_2(\phi) = \frac{1}{2\pi} \tag{3.27}$$

The required pdf is given by the product of two uniform pdfs, namely $f_1(\mu)$ and $f_2(\phi)$. If R_μ, R_Φ are two rvs $\sim U[0,1)$, we have

$$R_\mu = \int_{-1}^{\mu} f_1(\mu')\ \mathrm{d}\mu' = \frac{\mu+1}{2}; \quad R_\Phi = \int_{-\pi}^{\Phi} f_2(\phi)\ \mathrm{d}\phi = \frac{\Phi+\pi}{2\pi} \tag{3.28}$$

and finally

$$\mu = -1 + 2R_\mu; \quad \Phi = -\pi + 2\pi R_\Phi \tag{3.29}$$

In practice, the direction cosines u, v, w of $\underline{\Omega}$ are obtained through the following steps:

- Sampling of two rvs R_μ, $R_\Phi \sim U[0,1)$;
- Computation of $\mu = -1 + 2R_\mu$, $\Phi = -\pi + 2\pi R_\Phi$;
- Finally,

$$\begin{gathered} u = \underline{\Omega} \cdot \underline{i} = \sin\vartheta \cos\Phi = \sqrt{1-\mu^2}\cos\Phi \\ v = \underline{\Omega} \cdot \underline{j} = \sin\vartheta \sin\Phi = \sqrt{1-\mu^2}\sin\Phi = \sqrt{1-\mu^2-u^2} \\ w = \underline{\Omega} \cdot \underline{k} = \mu \end{gathered} \tag{3.30}$$

Note that a given value of μ pertains to two quadrants, so that care must be taken in selecting the proper one.

Exponential Distribution

Let us consider a two-state system whose transition probabilities from one state to the other only depend on the present state and not on the way in which this state was reached. Examples of such systems are:

- A radioactive nucleus: the two states are the nucleus at a given time, which we will call initial time, and the nucleus at the moment of disintegration; the rv in question, which is the argument of the transition pdf, is the time length between the initial time, at which we know that the nucleus is intact and the time at which the nucleus disintegrates.
- The path of a neutron in a medium: the two states are the neutron in a given position, which we will call initial, and the neutron in the position at which the collision occurs; the rv in consideration, which is the argument of the transition pdf, is the length of the flight path between the initial positions.
- A component of an industrial plant: the two states of the component are its nominal state and its failure state. The rv in consideration, which is the argument of the transition pdf, is the difference between the time at which we know that the component is in one of its two states, and the time at which the component moves to the other state.

Such systems, characterized by 'lack-of-memory', are said to be 'markovian', and they are said to be 'homogeneous' or 'inhomogeneous' according to whether the transitions occur with constant or variable-dependent (space- or time-dependent) rates, respectively. In the latter case, if the argument of the rate of leaving a given state is the sojourn time of the system in that state, the process is called 'semi-markovian'. Thus, a semi-markovian system is markovian only at the times of transition.

A rv $X \in [0, \infty)$ is said to be exponentially distributed if its cdf $F_X(x)$ and pdf $f_X(x)$ are

$$\begin{aligned} F_X(x) &= 1 - e^{-\int_0^x \lambda(u)du}; \quad f_X(x) = \lambda(x)e^{-\int_0^x \lambda(u)du} \quad \text{for} \quad 0 \le x \le \infty \\ &= 0 \qquad\qquad\qquad\qquad = 0 \qquad\qquad\qquad\qquad \text{otherwise} \end{aligned} \tag{3.31}$$

where $\lambda(\cdot)$is the transition rate, also called hazard function within the context of the last example mentioned above. In the following, we shall refer to an exponential distribution of a time variable, T. Corresponding to a realization of a rv $R \sim U[0,1)$, the realization t of the exponentially distributed rv T can be obtained by solving the equation

$$\int_0^t \lambda(u)\mathrm{d}u = -\log(1-R) \tag{3.32}$$

Let us first consider time-homogeneous systems, i.e., the case of constant λ. Correspondingly, Eq. (3.31) becomes

$$F_T(t) = 1 - e^{-\lambda t}; \quad f_T(t) = \lambda e^{-\lambda t} \tag{3.33}$$

The moments of the distribution with respect to the origin are

$$\mu'_k = \frac{k!}{\lambda^k} \; (k = 1, 2, \ldots) \tag{3.34}$$

Realizations of the associated exponentially distributed rv T are easily obtained from the inverse transform method. The sampling of a given number $N \gg 1$ of realizations is performed by repeating the following procedure:

- Sample a realization of $R \sim U[0,1)$;
- Compute $t = -\frac{1}{\lambda}\log(1-R)$.

An example of a time-homogeneous markovian process is the failure of a component, provided it is assumed that it does not age: such component, still good (state 1) at time t, has a probability $\lambda \mathrm{d}t$ of failing (entering state 2) between t and $t + \mathrm{d}t$; note that this probability does not depend neither on the time t nor on the age of the component at time t. The probability density per unit time that the component, still good at time t_0, will fail at time $t \ge t_0$ is

$$f_T(t) = e^{-\lambda(t-t_0)} \cdot \lambda \tag{3.35}$$

The collisions of a neutron with the nuclei of an homogeneous medium represent an example of a space-homogeneous markovian process: a neutron with energy E, traveling along a specified direction, say the x axis, at the point x has a probability $\Sigma_{\text{total}}(E)\mathrm{d}x$ of undergoing a collision between x and $x + \mathrm{d}x$, where $\Sigma_{\text{total}}(E)$ is the macroscopic total cross-section which plays the role of λ in the Eq. (3.31) for the exponential distribution; note that this probability does not depend neither on the point x where the neutron is, nor on the distance traveled by that neutron before arriving at x. The probability density per unit length that a neutron at point x_0 will make the first collision at point $x \ge x_0$ is

$$f(x,E) = e^{-\Sigma_{\text{total}}(E)(x-x_0)} \cdot \Sigma_{\text{total}}(E) \tag{3.36}$$

Returning to processes in the time domain, a generalization of the exponential distribution consists in assuming that the probability density of occurrence of an event, namely λ, is time dependent. As mentioned above, in this case we deal with non-homogeneous markovian processes. For example, although in the reliability and risk analyses of an industrial plant or system, one often assumes that the failures of the components occur following homogeneous Markov processes, i.e., exponential distributions with constant rates, it is more realistic to consider that the age of the system influences the failure probability, so that the transition probability density is a function of time. A case, commonly considered in practice is that in which the pdf is of the kind

$$\lambda(t) = \beta\,\alpha\,t^{\alpha-1} \tag{3.37}$$

with $\beta > 0$, $\alpha > 0$. The corresponding distribution, which constitutes a generalization of the exponential distribution, is called Weibull distribution and was proposed in the 1950s by W. Weibull in the course of its studies on the strength of materials. The cdf and the pdf of the Weibull distribution are

$$F_T(t) = 1 - e^{-\beta t^{\alpha}} \quad f_T(t) = \alpha\beta\, t^{\alpha-1} e^{-\beta t^{\alpha}} \tag{3.38}$$

The moments with respect to the origin are

$$\mu'_k = \beta^{-\frac{k}{\alpha}}\Gamma\left(\frac{k}{\alpha}+1\right) \quad k = 1,2,\ldots \tag{3.39}$$

In the particular case of $\alpha = 1$, the Weibull distribution reduces to the exponential distribution with constant transition rate $\lambda = \beta$. The importance of the Weibull distribution stems from the fact that the hazard functions of the components of most industrial plants closely follow this distribution in time, with different parameter values describing different phases of their life. In practice, a realization t of the rv T is sampled from the Weibull distribution through the following steps:

- Sampling of a realization of the rv $R \sim U[0,1)$;
- Computation of $t = \left(-\frac{1}{\beta}\ln(1-R)\right)^{\frac{1}{\alpha}}$.

Multivariate Normal Distribution

Let us consider a multivariate normal distribution of order k of the vector of rvs $\underline{Z} \equiv (k,1)$. The pdf is

$$f_{\underline{Z}}(\underline{z};\underline{a},\Sigma) = \frac{1}{(2\pi)^{\frac{k}{2}}|\Sigma|^{\frac{1}{2}}} e^{-\frac{1}{2}(\underline{z}-\underline{a})'\Sigma^{-1}(\underline{z}-\underline{a})} \tag{3.40}$$

where with the hyphen we indicate the transpose, $\underline{a} \equiv (k,1)$ is the vector of the mean values, and $\Sigma \equiv (k,k)$ is the symmetric covariance matrix, positive-defined and with determinant $|\Sigma|$ given by

$$\Sigma = E\left[(\underline{z}-\underline{a})(\underline{z}-\underline{a})'\right] = \begin{pmatrix} \sigma_1^2 & \sigma_{12}^2 & \cdots & \sigma_{1k}^2 \\ \sigma_{21}^2 & \sigma_2^2 & \cdots & \sigma_{2k}^2 \\ \vdots & \vdots & \ddots & \vdots \\ \sigma_{k1}^2 & \sigma_{k2}^2 & \cdots & \sigma_k^2 \end{pmatrix} \tag{3.41}$$

The generic term of Σ is

$$\sigma_{ij}^2 = E\left[(z_i - a_i)(z_j - a_j)\right] \tag{3.42}$$

and the elements σ_i^2, $i = 1,2,\ldots,k$ are the variances of the k normal variates. The pdf f in Eq. (3.40) is generally indicated as $N(\underline{a},\Sigma)$ and correspondingly a rv Z distributed according to f is indicated as $\underline{Z}(\underline{a},\Sigma)$.

The sampling from f of a random vector z, realization of $\underline{Z}$ can be done in the following way [17]:

1. $i = -1$;
2. $i \leftarrow i + 2$;
3. Sample two values u_i, u_{i+1} from the distribution $U[-1,1)$;
4. If $u_i^2 + u_{i+1}^2 > 1$ both values are rejected and we go back to 3. Otherwise, they are both accepted. Note that if the values are accepted, the point $P \equiv (u_i, u_{i+1})$ is uniformly distributed on the circle with center at the origin and radius 1;
5. Calculate the values

$$y_i = u_i \sqrt{-2\frac{\log(u_i^2 + u_{i+1}^2)}{u_i^2 + u_{i+1}^2}} \tag{3.43}$$

$$y_{i+1} = u_{i+1} \sqrt{-2\frac{\log(u_i^2 + u_{i+1}^2)}{u_i^2 + u_{i+1}^2}} \tag{3.44}$$

6. It can be shown that the variables y_i and y_{i+1} are independent and identically distributed (iid) standard normal variables $\sim N(0,1)$;
7 If k is even, and if $i + 1 \leq k$, we return to 2);
8. If k is odd and if $i \leq k$, we return to 2. In this last case, y_{k+1} is calculated but not used;
9. At this point, we have the random vector $\underline{y} \equiv (k,1)$ having iid components distributed as $N(0,1)$. By Cholesky's factorization of the matrix Σ into the product of a sub triangular matrix U and its transpose U', i.e., $\Sigma = U \cdot U'$, the random vector $\underline{z}$ is given by the expression

$$\underline{z} = \underline{a} + U\underline{y} \tag{3.45}$$

Because $E[\underline{y}] = 0$ and $Var[\underline{y}] = I$ we have

$$E[\underline{z}] = \underline{a} \tag{3.46}$$

$$Var[\underline{z}] = E[(\underline{z} - \underline{a})(\underline{z} - \underline{a})'] = E[U\underline{y}\underline{y}U'] = U\,Var[\underline{y}]U' = UU' = \Sigma \tag{3.47}$$

Determination of a conditioned pdf

In Eq. (3.40) let us partition $\underline{z}$ into two sub-vectors $\underline{z}_1$ and $\underline{z}_2$ relative to the first p and the remaining $q = k - p$ components, respectively. We then have

$$\underline{z} = \begin{bmatrix} \underline{z}_1 \\ \underline{z}_2 \end{bmatrix}; \quad \underline{a} = \begin{bmatrix} \underline{a}_1 \\ \underline{a}_2 \end{bmatrix} \tag{3.48}$$

Correspondingly, we partition Σ in sub matrices

$$\Sigma = \begin{bmatrix} \Sigma_{11} & \Sigma_{12} \\ \Sigma_{12}' & \Sigma_{22} \end{bmatrix} \tag{3.49}$$

We now write the pdf f in terms of the two groups of variables. We have

$$\Sigma^{-1} = \begin{bmatrix} \Sigma_p^{-1} & -\Sigma_p^{-1}\Sigma_{12}\Sigma_{22}^{-1} \\ -\Sigma_{22}^{-1}\Sigma_{12}'\Sigma_p^{-1} & -\Sigma_{22}^{-1} + \Sigma_{22}^{-1}\Sigma_{12}'\Sigma_p^{-1}\Sigma_{12}\Sigma_{22}^{-1} \end{bmatrix} \tag{3.50}$$

where

$$\Sigma_p = \Sigma_{11} - \Sigma_{12}\Sigma_{22}^{-1}\Sigma_{12}' \tag{3.51}$$

Furthermore, we have

$$|\Sigma| = |\Sigma_{22}|\left|\Sigma_p\right| \tag{3.52}$$

The exponent of $f_{\underline{Z}}(\underline{z}; \underline{a}, \Sigma)$ can be expressed in terms of the partitioned quantities

$$
\begin{aligned}
(\underline{z}-\underline{a})'\Sigma^{-1}(\underline{z}-\underline{a}) &= \left((\underline{z}_1-\underline{a}_1)'\ (\underline{z}_2-\underline{a}_2)'\right) \\
&\cdot \begin{bmatrix} \Sigma_p^{-1}\left[(\underline{z}_1-\underline{a}_1)-\Sigma_{12}\Sigma_{22}^{-1}(\underline{z}_2-\underline{a}_2)\right] \\ \Sigma_{22}^{-1}\left[-\Sigma_{12}'\Sigma_p^{-1}(\underline{z}_1-\underline{a}_1)+(I+\Sigma_{12}'\Sigma_p^{-1}\Sigma_{12}\Sigma_{22}^{-1})(\underline{z}_2-\underline{a}_2)\right] \end{bmatrix} \\
&=(\underline{z}_1-\underline{a}_1)'\Sigma_p^{-1}(\underline{z}_1-\underline{a}_1)+(\underline{z}_2-\underline{a}_2)'\Sigma_{22}^{-1}\left[(I+\Sigma_{12}'\Sigma_p^{-1}\Sigma_{12}\Sigma_{22}^{-1})(\underline{z}_2-\underline{a}_2)\right] \\
&\quad -(\underline{z}_1-\underline{a}_1)'\Sigma_p^{-1}\Sigma_{12}\Sigma_{22}^{-1}(\underline{z}_2-\underline{a}_2)-(\underline{z}_2-\underline{a}_2)'\Sigma_{22}^{-1}\Sigma_{12}'\Sigma_p^{-1}(\underline{z}_1-\underline{a}_1) \\
&=(\underline{z}_1-\underline{a}_1)'\Sigma_p^{-1}\left[(\underline{z}_1-\underline{a}_1)-\Sigma_{12}\Sigma_{22}^{-1}(\underline{z}_2-\underline{a}_2)\right]+(\underline{z}_2-\underline{a}_2)'\Sigma_{22}(\underline{z}_2-\underline{a}_2) \\
&\quad -(\underline{z}_2-\underline{a}_2)'\Sigma_{22}^{-1}\Sigma_{12}'\Sigma_p^{-1}\left[(\underline{z}_1-\underline{a}_1)-\Sigma_{12}\Sigma_{22}^{-1}(\underline{z}_2-\underline{a}_2)\right]
\end{aligned}
\tag{3.53}
$$

By putting

$$
\underline{a}_p=\underline{a}_1+\Sigma_{12}\Sigma_{22}^{-1}(\underline{z}_2-\underline{a}_2) \tag{3.54}
$$

we have

$$
(\underline{z}-\underline{a})'\Sigma^{-1}(\underline{z}-\underline{a})=(\underline{z}_2-\underline{a}_2)'\Sigma_{22}^{-1}(\underline{z}_2-\underline{a}_2)+(\underline{z}_1-\underline{a}_p)'\Sigma_p^{-1}(\underline{z}_1-\underline{a}_p) \tag{3.55}
$$

Correspondingly, $f_{\underline{Z}}(\underline{z};\underline{a},\Sigma)$ can be written as follows

$$
f_{\underline{Z}}(\underline{z}_1,\underline{z}_2)=\left[g(\underline{z}_1|\underline{z}_2)\right]\left[h(\underline{z}_2)\right] \tag{3.56}
$$

where

$$
g(\underline{z}_1|\underline{z}_2)=\frac{e^{-\frac{1}{2}(\underline{z}_1-\underline{a}_p)'\Sigma_p^{-1}(\underline{z}_1-\underline{a}_p)}}{(2\pi)^{\frac{p}{2}}\left|\Sigma_p\right|^{\frac{1}{2}}} \tag{3.57}
$$

$$
h(\underline{z}_2)=\frac{e^{-\frac{1}{2}(\underline{z}_2-\underline{a}_2)'\Sigma_{22}^{-1}(\underline{z}_2-\underline{a}_2)}}{(2\pi)^{\frac{q}{2}}|\Sigma_{22}|^{\frac{1}{2}}} \tag{3.58}
$$

It follows that $f(\underline{z};\underline{a},\Sigma)$ can be factored into the product of a q-variate multinormal $h(\underline{z}_2;\underline{a}_2,\Sigma_{22})$, having mean value $\underline{a}_2$ and covariance matrix Σ_{22}, and a conditioned p-variate multinormal $g(\underline{z}_1;\underline{a}_p,\Sigma_p|\underline{z}_2)$, which is also multinormal with mean value $\underline{a}_p$ depending on $\underline{z}_2$, and covariance matrix Σ_p Operatively, to sample a vector realization $\tilde{\underline{z}}\equiv(\tilde{\underline{z}}_1,\tilde{\underline{z}}_2)$ from $f(\underline{z}_1,\underline{z}_2)$, we first sample a vector $\tilde{\underline{z}}_2$ from $h(\underline{z}_2;\underline{a}_2,\Sigma_{22})$ and, then, a vector $\tilde{\underline{z}}_1$ from $g(\underline{z}_1;\underline{a}_p(\tilde{\underline{z}}_2),\Sigma_p|\tilde{\underline{z}}_2)$.

Multinomial Distribution

Let us consider a random process which can only have n possible outcomes, the probability of the kth one being f_k. Examples are the throwing of a dice, the kind of interaction that a neutron can have with a nucleus (scattering, absorption, fission, etc.), once it is known that the interaction has occurred, the kind of transition

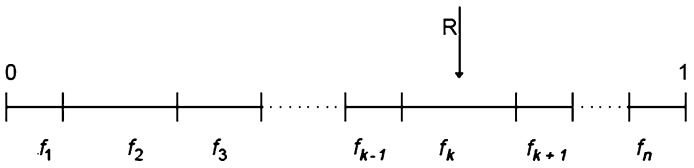

Fig. 3.3 Sampling the occurrence of an event from a multinomial distribution

(degradation, failure, repair, etc.) that a multi-state component may undergo from its current state to one of the other reachable ones, given that a transition is known to have occurred. The process is simulated by first dividing the interval [0,1) in n successive subintervals of amplitudes $f_1, f_2, \ldots, f_n$ and then performing a large number of trials in each of which a rv $R \sim U[0,1)$ is thrown on the interval [0,1) (Fig. 3.3). Every time a point falls within the kth subinterval, we say that out of the n possible ones the kth event has occurred: the probability of this event obeys the Bernoulli distribution, in which f_k is the probability of success and $\sum_{j=1 j\neq k}^{n} f_j = 1 - f_k$ is the complementary probability of the point falling elsewhere. The probability that in N trials, the point falls n_k times within the subinterval f_k is given by the binomial distribution

$$\binom{N}{n_k} f_k^{n_k} (1 - f_k)^{N - n_k} \tag{3.59}$$

The generalization of this distribution leads to the multinomial distribution which gives the probability that in N trials, the point falls n_1 times in the subinterval f_1, n_2 times in f_2,…, n_n times in f_n. Formally, the multinomial distribution is given by

$$\frac{N!}{n_1! n_2! \ldots n_n!} f_1^{n_1} f_2^{n_2} \ldots f_n^{n_n} \tag{3.60}$$

where, obviously, $n_1 + n_2 + \cdots + n_n = N$.

3.3.3 Sampling by the Composition Method

This method can be applied for sampling random numbers from a pdf that can be expressed as a mixture of pdfs.

Continuous Case

Let X be a rv having a pdf of the kind

$$f_X(x) = \int q(y) p(x, y) \mathrm{d}y \tag{3.61}$$

where $q(y) \geq 0$, $p(x,y) \geq 0$, $\forall x, y$ and where the integral is extended over a given domain of y. By definition of pdf, we have

$$\int f_X(x)\mathrm{d}x = \int\int \mathrm{d}x\mathrm{d}y q(y)p(x,y) = 1 \tag{3.62}$$

The pdf $f_X(x)$ is actually a mixture of pdfs. Indeed, the integrand function can be written as follows:

$$q(y)p(x,y) = q(y)\int p(x',y)\mathrm{d}x' \frac{p(x,y)}{\int p(x',y)\mathrm{d}x'} = h_Y(y)g(x|y) \tag{3.63}$$

where

$$h_Y(y) = q(y)\int p(x',y)\mathrm{d}x'; \quad g(x|y) = \frac{p(x,y)}{\int p(x',y)\mathrm{d}x'} \tag{3.64}$$

Let us show that $h_Y(y)$ is a pdf in y, and that $g(x|y)$ is a pdf in x. Because $p(x,y) \geq 0$, $h_Y(y) \geq 0$ and $g(x|y) \geq 0$. The normalization of $h_Y(y)$ can be derived immediately from that of $f_X(x)$ and the normalization of $g(x|y)$ is evident. Finally, the pdf $f_X(x)$ can be written as

$$f_X(x) = \int h_Y(y)g_X(x|y)\mathrm{d}y \tag{3.65}$$

where we have added the subscript X to the pdf $g(x|y)$ to indicate that it is a pdf of the rv X. Note that y plays the role of a parameter that is actually a random realization of the rv Y having a pdf $h_Y(y)$.

To sample a realization of X from $f_X(x)$ we proceed as follows:

- Sample a realization of Y from the univariate $h_Y(y)$;
- Sample a realization of X from the univariate $g_X(x|Y)$ (note that at this point Y has a known numerical value).

For example, let

$$f_X(x) = n\int_1^\infty y^{-n}e^{-xy}\mathrm{d}y \; (n > 1,\, 0 \leq x < \infty) \tag{3.66}$$

$$= ne^{-x}\sum_{k=1}^{n-1}\frac{(-x)^{k-1}}{(n-1)(n-2)\cdots(n-k)} + n\frac{(-x)^{n-1}}{(n-1)!}Ei(x) \tag{3.67}$$

where

$$Ei(x) = \int_x^\infty \frac{e^{-y}}{y}dy \tag{3.68}$$

is the integral Exponential function. Sampling from the explicit expression of the integral is too complicate, so that we prefer to resort to the composition method. Let us choose

$$q(y) = ny^{-n},\ p(x,y) = e^{-xy} \tag{3.69}$$

so that

$$\int_0^\infty p(x,y)\mathrm{d}x = \frac{1}{y} \tag{3.70}$$

and thus

$$h_Y(y) = ny^{n-1},\ g_X(x|y) = ye^{-xy} \tag{3.71}$$

The operative sequence for sampling a realization of X from $f_X(x)$ is thus

- We sample $R_1, R_2 \sim U[0,1)$;
- By using R_1, we sample a value of Y from $h_Y(y)$ with the inverse transform method

$$R_1 = \int_1^Y h_Y(y)\mathrm{d}y = 1 - Y^{-n} \tag{3.72}$$

We have

$$Y = (1 - R_1)^{-\frac{1}{n}} \tag{3.73}$$

- By substituting the value of Y in $g_X(x|y)$ we have

$$g_X(x|Y) = Ye^{-Yx} \tag{3.74}$$

Hence, $g_X(x|Y)$ is an exponential distribution with parameter Y. By using R_2 we finally sample the desired realization X from the $p_X(x|Y)$

$$X = -\frac{1}{Y}\ln(1 - R_2) = -(1 - R_1)^{\frac{1}{n}}\ln(1 - R_2) \tag{3.75}$$

For example, for $n = 3$ the rigorous expression for $f_X(x)$ is

$$f_X(x) = \frac{3}{2}[(1 - x)e^{-x} + x^2 Ei(x)] \tag{3.76}$$

In Fig. 3.4, we show the analytical form of $f_X(x)$ (full line) and the result of the MCS (indicated with the circles) with 10^5 random values sampled by the previously illustrated procedures. The values are calculated with the following *Matlab*® program:

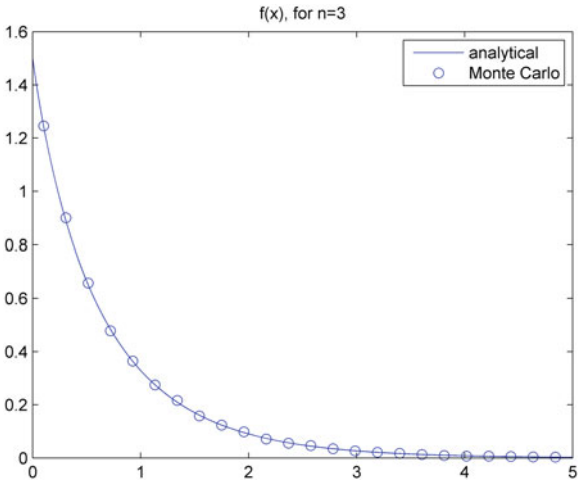

Fig. 3.4 Example of sampling from a continuous distribution, by the composition method. Analytical = *solid line*; MCS = *circle*

```
dx=.001;
x=dx:dx:10;
y=1.5*((1-x).*exp(-x)+x.^2.*expint(x));
l=1e5;
ymc=-rand(l,1).^0.33333.*log(rand(l,1));
dey=(max(ymc)-min(ymc))/50;
[h,xx]=hist(ymc,50);
hn=h/(l*dey);
plot(x,y);
hold;
plot(xx,hn,'o')
axis([0 5 0 1.6])
```

Discrete Case

Let X be a rv having pdf of the kind

$$f_X(x) = \sum_{k=0}^{\infty} q_k p(x, y_k) \tag{3.77}$$

where $q_k \geq 0$, $p(x, y_k) \geq 0 \quad \forall k, x, y_k$ and where

$$\int f_X(x)\mathrm{d}x = \sum_{k=0}^{\infty} q_k \int p(x, y_k)\mathrm{d}x = 1 \tag{3.78}$$

The pdf $f_X(x)$ is really a mixture of pdfs. Indeed, each term of the sum can be written as follows

$$q_k p(x, y_k) = q_k \int p(x', y_k)\mathrm{d}x' \frac{p(x, y_k)}{\int p(x', y_k)\mathrm{d}x'} = h_k g(x|y_k) \tag{3.79}$$

where

$$h_k = q_k \int p(x', y_k)\mathrm{d}x'; \quad g(x|y_k) = \frac{p(x, y_k)}{\int p(x', y_k)\mathrm{d}x'} \tag{3.80}$$

We show that in fact h_k is a probability, and that $g(x|y_k)$ is a pdf in x. Because $p(x, y_k) \geq 0$ and $q_k \geq 0$, it follows that $h_k \geq 0$ and $g(x|y_k) \geq 0$. The normalization of h_k follows immediately from that of $f_X(x)$

$$\sum_k h_k = \sum_k q_k \int p(x', y_k)\mathrm{d}x' = \int f_X(x')\mathrm{d}x' = 1 \tag{3.81}$$

The normalization of $g(x|y_k)$ is evident. Finally, the pdf $f_X(x)$ can be written as

$$f_X(x) = \sum_{k=0}^{\infty} h_k g_X(x|y_k) \tag{3.82}$$

where $g_X(x|y_k)$ is a pdf depending on the parameter y_k, which is a discrete rv having probability h_k.

To sample a value of X from $f_X(x)$ we proceed as follows:

- Sample a value Y_k from the distribution h_k ($k = 0,1,\ldots$);
- Sample a value of X from $g_X(x|Y_k)$.

For example let

$$f_X(x) = \frac{5}{12}[1 + (x-1)^4] \quad 0 \leq x \leq 2 \tag{3.83}$$

i.e.,

$$q_1 = q_2 = \frac{5}{12}; \quad p(x, y_1) = 1; \quad p(x, y_2) = (x-1)^4 \tag{3.84}$$

We have

$$h_1 = q_1 \int_0^2 p(x, y_1)\mathrm{d}x = \frac{5}{12} \times 2 = \frac{5}{6} \tag{3.85}$$

$$h_2 = q_2 \int_0^2 p(x, y_2)\mathrm{d}x = \frac{5}{12}\frac{2}{5} = \frac{1}{6} \tag{3.86}$$

$$g_X(x|y_1) = \frac{1}{2} \tag{3.87}$$

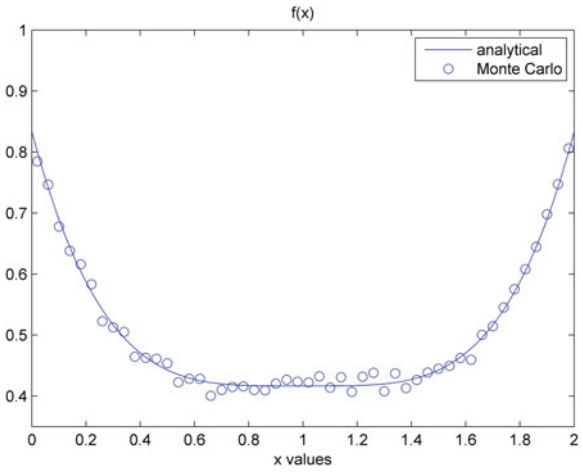

Fig. 3.5 Example of sampling from a discrete distribution, by the composition method. Analytical = *solid line*; MCS = *circles*

$$g_X(x|y_2) = \frac{(x-1)^4}{\frac{2}{5}} = \frac{5}{2}(x-1)^4 \tag{3.88}$$

Operatively, to sample a value of X from $f_X(x)$

- Sample $R_1, R_2 \sim U[0,1)$;
- If $R_1 \leq h_1 = \frac{5}{6}$, sample a value of X from $g_X(x|y_1)$, i.e.,

$$R_2 = \int_0^X g_X(x|y_1)\mathrm{d}x = \frac{1}{2}X \tag{3.89}$$

and thus

$$X = 2R_2 \tag{3.90}$$

- If $R_1 \geq h_1$, we extract a value of X from $g_X(x|y_2)$, i.e.,

$$R_2 = \frac{5}{2}\int_0^X (x-1)^4\mathrm{d}x = \frac{1}{2}\left[(X-1)^5 + 1\right] \tag{3.91}$$

and thus

$$X = 1 + (2R_2 - 1)^{1/5} \tag{3.92}$$

In Fig. 3.5, we show the analytical form of $f_X(x)$ (full line) and the result of the MCS (indicated with the circles) with 10^5 samplings. The values were calculated with the following *Matlab*® program:

```
dx=0.001;
x=0:dx:2;
y=0.41667*(1+(x-1).^4);
n=1e5;
c1=5/6;
c2=1/5;
r1=rand(n,1);
r2=rand(n,1);
X=zeros(n,1);
ip=find(r1<c1);
ig=find(r1>=c1);
X(ip)=2*r2(ip);
val=2*r2(ig)-1;
X(ig)=1+sign(val).*abs(val).^c2;
deX=(max(X)-min(X))/50;
[h,xx]=hist(X,50);
hn=h/(n*deX);
plot(x,y);
hold;
plot(xx,hn,'o')
```

3.3.4 Sampling by the Rejection Method

Let $f_X(x)$ be an analytically assigned pdf, in general quite complicated. The sampling of a realization of a rv X from its pdf with the rejection method consists in the tentative sampling of the realization of a rv X' from a simpler density function, and then testing the given value with a test that depends on the sampling of another rv. Then, $X = X'$ only if the test is passed; else, the value of X' is rejected and the procedure is restarted. The main disadvantage of this method can be the low efficiency of acceptance if many realizations of X' are rejected before one is accepted as X. In the following, when the sampling of a realization of Z from a pdf $g_Z(z)$, $z \in (z_1, z_2)$, can be easily done, for example by using one of the methods given in the previous paragraphs, we will simply say that we sample a $Z \sim G(z_1, z_2)$.

The von Neumann Algorithm

In its simplest version, the method of sampling by rejection can be summarized as follows: given a pdf $f_X(x)$ limited in (a, b) let

$$h(x) = \frac{f_X(x)}{\max\limits_x f_X(x)} \tag{3.93}$$

so that $0 \leq h(x) \leq 1$, $\forall x \in (a, b)$.

The operative procedure to sample a realization of X from $f_X(x)$ is the following:

1. Sample $X' \sim U(a, b)$, the tentative value for X, and calculate $h(X')$;
2. Sample $R \sim U[0, 1)$. If $R \leq h(X')$ the value X' is accepted; else start again from 1.

More generally, a given complicated $f_X(x)$ can be factored into the product of a density $g_{X'}(x)$, from which it is simple to sample a realization of X', and a residual function $H(x)$, i.e.,

$$f_X(x) = g_{X'}(x)H(x) \tag{3.94}$$

Note that $H(x)$ is not negative, being the ratio of two densities. We set

$$B_H = \max_x H(x) = \frac{\max_x(f_X(x))}{g_{X'}(x)} \tag{3.95}$$

and have

$$f_X(x) = \frac{g_{X'}(x)H(x)}{B_H} B_H = g_{X'}(x)h(x)B_H \tag{3.96}$$

where

$$h(x) = \frac{H(x)}{B_H} \quad \text{so that} \quad 0 \leq h(x) \leq 1 \tag{3.97}$$

Dividing by the integral of $f_X(x)$ over the entire domain, by hypothesis equal to one, we have

$$f_X(x) = \frac{g_{X'}(x)h(x)}{\int_{-\infty}^{\infty} g_{X'}(z)h(z)\mathrm{d}z} \tag{3.98}$$

Integrating Eq. (3.96) over the domain of x we have

$$\int_{-\infty}^{\infty} g_{X'}(z)h(z)\mathrm{d}z = \frac{1}{B_H} \tag{3.99}$$

From Eqs. (3.97) and (3.98), we also have

$$\int_{-\infty}^{\infty} g_{X'}(z)h(z)\mathrm{d}z \leq \int_{-\infty}^{\infty} g_{X'}(z)\mathrm{d}z = 1 \tag{3.100}$$

so that $B_H \geq 1$. The sampling of a random realization of X from $f_X(x)$ can be done in two steps:

1. Sample a realization of X' from the pdf $g_{X'}(x)$, which is simple by construction

$$\mathrm{P}(X' \leq x) = G_{X'}(x) = \int_{-\infty}^{x} g_{X'}(z)\mathrm{d}z \tag{3.101}$$

   and then compute the number $h(X')$;
2. Sample $R \sim U[0,1)$. If $R \leq h(X')$, the sampled realization of X' is accepted, i.e., $X = X'$; else the value of X' is rejected and we start again from 1. The acceptance probability of the sampled value X' is thus

$$\mathrm{P}(R \leq h(X')) = h(X') \tag{3.102}$$

We show that the accepted value is actually a realization of X sampled from $f_X(x)$. The probability of sampling a random value X' between z and $z + dz$ and accepting it, is given by the product of the probabilities

$$\mathrm{P}(z \leq X' < z + \mathrm{d}z)\mathrm{P}(R \leq h(z)) = g_{X'}(z)\mathrm{d}z h(z) \tag{3.103}$$

The corresponding probability of sampling a random value $X' \leq x$ and accepting it is

$$\mathrm{P}(X' \leq x \text{ AND } R \leq h(X')) = \int_{-\infty}^{x} g_{X'}(z)h(z)\mathrm{d}z \tag{3.104}$$

The probability that a sampled X' is accepted, i.e., the probability of success is given by the above expression for $x \to \infty$

$$\mathrm{P}(\text{success}) = \mathrm{P}(X' \leq x \text{ AND } R \leq h(X')) = \int_{-\infty}^{\infty} g_{X'}(z)h(z)\mathrm{d}z \tag{3.105}$$

The distribution of the accepted values (the others are rejected) is then

$$\begin{aligned} \mathrm{P}(X' \leq x|\text{success}) &= \frac{\mathrm{P}(X' \leq x \text{ AND } R \leq h(X'))}{\mathrm{P}(\text{success})} \\ &= \frac{\int_{-\infty}^{x} g_{X'}(z)h(z)\mathrm{d}z}{\int_{-\infty}^{\infty} g_{X'}(z)h(z)\mathrm{d}z} \end{aligned} \tag{3.106}$$

and the corresponding pdf is Eq. (3.97), i.e., the given $f_X(x)$.

The simple version of the rejection method by von Neumann is the case

$$g_{X'}(x) = \frac{1}{b-a} \tag{3.107}$$

The efficiency ε of the method is given by the probability of success, i.e., from Eq. (3.99)

$$\varepsilon = \mathrm{P}(\text{success}) = \int_{-\infty}^{\infty} g_{X'}(z)h(z)\mathrm{d}z = \frac{1}{B_H} \tag{3.108}$$

Let us now calculate the average number of trials that we must make before obtaining one success. The probability of having the first success at the kth trial is given by the geometric distribution

$$P_k = (1-\varepsilon)^{k-1}\varepsilon,\ k = 1, 2, \ldots \tag{3.109}$$

and the average number of trials to have the first success is

$$\begin{aligned} E(k) &= \sum_{k=1}^{\infty} kP_k = \varepsilon \sum_{k=1}^{\infty} k(1-\varepsilon)^{k-1} = -\varepsilon \tfrac{\mathrm{d}}{\mathrm{d}\varepsilon} \sum_{k=1}^{\infty} (1-\varepsilon)^k \\ &= -\varepsilon \tfrac{\mathrm{d}}{\mathrm{d}\varepsilon} \tfrac{1}{1-(1-\varepsilon)} = -\varepsilon \tfrac{\mathrm{d}}{\mathrm{d}\varepsilon} \tfrac{1}{\varepsilon} = \tfrac{1}{\varepsilon} = B_H \end{aligned} \tag{3.110}$$

For example, let the pdf

$$f_X(x) = \frac{2}{\pi(1+x)\sqrt{x}},\ 0 \le x \le 1 \tag{3.111}$$

For $x = 0$, $f_X(x)$ diverges and thus we cannot use the simple rejection technique. Note that the factor causing the divergence of $f_X(x)$, i.e.,$1/\sqrt{x}$, is proportional to the pdf of the rv R^2, with $R \sim U[0, 1)$. By the change of variables

$$X' = R^2 \tag{3.112}$$

the CDF of the rv X' is

$$G_{X'}(x) = \mathrm{P}(X' \le x) = \mathrm{P}\left(R^2 \le x\right) = \mathrm{P}\left(R \le \sqrt{x}\right) = \sqrt{x} \tag{3.113}$$

and the corresponding pdf is

$$g_{X'}(x) = \frac{\mathrm{d}G_{X'}(x)}{\mathrm{d}x} = \frac{1}{2\sqrt{x}} \tag{3.114}$$

Hence, $f_X(x)$ can be written as

$$f_X(x) = \frac{1}{2\sqrt{x}} \frac{4}{\pi} \frac{1}{1+x} = g_{X'}(x)H(x) \tag{3.115}$$

where

$$H(x) = \frac{4}{\pi} \frac{1}{1+x} \tag{3.116}$$

We have

$$B_H = \max_x H(x) = \frac{4}{\pi} \tag{3.117}$$

and thus

$$h(x) = \frac{H(x)}{B_H} = \frac{1}{1+x},\ 0 \le x \le 1 \tag{3.118}$$

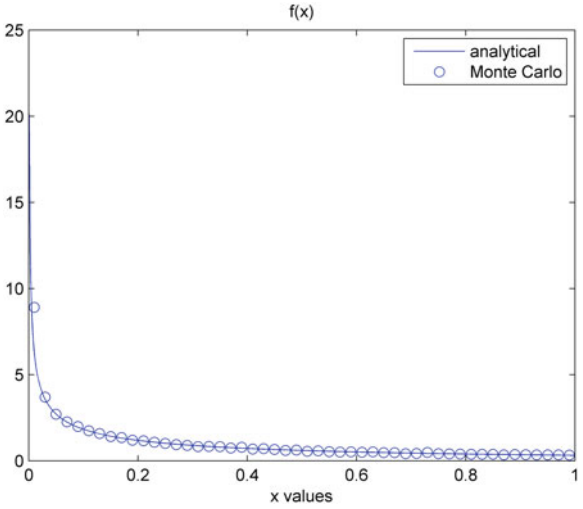

Fig. 3.6 Example of sampling by the rejection method. Analytical = *solid line*; MCS = *circles*

The operative procedure to sample a realization of the rv X from $f_X(x)$ is then:

1. Sample $R_1 \sim U[0,1)$ and then calculate:

$$X' = R_1^2 \text{ and } h(X') = \frac{1}{1+R_1^2} \tag{3.119}$$

2. Sample $R_2 \sim U[0,1)$. If $R_2 \leq h(X')$ accept the value of X', i.e., $X = X'$; else start again from 1.

The efficiency of the method, i.e., the probability that an extracted value of X' is accepted is

$$\varepsilon = \frac{1}{B_H} = \frac{\pi}{4} = 78.5\ \% \tag{3.120}$$

In Fig. 3.6, we show the analytical $f_X(x)$ (full line) and the result of the MCS (indicated by circles) with 10^5 trials.

The values were calculated with the following *Matlab*® program:

```
clear;dx=0.001;x=dx:dx:1;lx=length(x);u=ones(1,lx);
y=(2/pi)*u./((1+x).*sqrt(x));
n=1e5;r1=rand(1,n);r2=rand(1,n);v=ones(1,n);
h=v./(1+r1.^2);ip=find(r2<h);X=r1(ip).^2;
nn=length(X);deX=(max(X)-min(X))/50;
[h,xx]=hist(X,50);hn=h/(nn*deX);
disp(['Efficiency='num2str(nn/n)]),pause(10);
plot(x,y);hold;plot(xx,hn,'o');
xlabel('xvalues');title('f(x):–analytical;ooMonteCarlo') hold
```

In this case, the acceptance efficiency indeed turned out to be 78.5 %

3.4 The Solution of Definite Integrals by Monte Carlo Simulation

3.4.1 Analog Simulation

Let us consider the problem of obtaining an estimate of the n-dimensional definite integral

$$G = \int_D g(\underline{x}) f_{\underline{X}}(\underline{x}) \mathrm{d}\underline{x} \tag{3.121}$$

where $\underline{x}$ is an n-dimensional variable and the integration is extended to the domain $D \in \mathbb{R}^n$. We can always make the hypothesis that $f(\underline{x})$ has the characteristics of a pdf, i.e.,

$$f_{\underline{X}}(\underline{x}) > 0 \quad \forall \underline{x} \in D, \quad \int_D f_{\underline{X}}(\underline{x}) \mathrm{d}\underline{x} = 1 \tag{3.122}$$

If a factor $f_{\underline{X}}(\underline{x})$ having the above characteristics cannot be identified in the function to be integrated, it is always possible to set $f_{\underline{X}}(\underline{x})$ equal to a constant value to be determined from the normalization condition. From a statistical perspective, it is therefore possible to consider $\underline{x}$ as a random realization of a rv having pdf $f_{\underline{X}}(\underline{x})$. It then follows that $g(\underline{x})$ is also a rv and G can be interpreted as the expected value of $g(\underline{x})$, i.e.,

$$E[g(\underline{x})] = \int_D g(\underline{x}) f_{\underline{X}}(\underline{x}) \mathrm{d}\underline{x} = G \tag{3.123}$$

The variance of $g(\underline{x})$ is then

$$Var[g(\underline{x})] = \int_D [g(\underline{x}) - G]^2 f_{\underline{X}}(\underline{x}) \mathrm{d}\underline{x} = E\left[g^2(\underline{x})\right] - G^2 \tag{3.124}$$

The MCS estimation of G can be approached with a method known as that of the mean value estimation or of the 'dart game'.

Let us consider a dart game in $\mathbb{R}^n$ in which the probability of hitting a point $\underline{x} \in dx$ is $f_{\underline{X}}(\underline{x}) d\underline{x}$; we make the hypothesis that the dart throws are independent of each other and also that $f_{\underline{X}}(\underline{x})$ does not change as we proceed with the game. When a player hits point $\underline{x}$, he is given a prize $g(\underline{x})$. In a series of N throws in which the points $\underline{x}_1, \underline{x}_2, \ldots, \underline{x}_N$ are hit, the assigned prizes are $g(\underline{x}_1), g(\underline{x}_2), \ldots, g(\underline{x}_N)$. The average prize per throw is, then

$$G_N = \frac{1}{N} \sum_{i=1}^{N} g(\underline{x}_i) \tag{3.125}$$

Because the $g(\underline{x}_i)$'s are rvs, G_N is also a rv, having expected value and variance equal to

$$E[G_N] = \frac{1}{N}\sum_{i=1}^{N} E[g(\underline{x}_i)] \quad Var[G_N] = \frac{1}{N^2}\sum_{i=1}^{N} Var[g(\underline{x}_i)] \tag{3.126}$$

In Eq. (3.126), $E[g(\underline{x}_i)]$ and $Var[g(\underline{x}_i)]$ are the expected value and the variance of $g(\underline{x})$ computed at the point hit by the player on the ith throw. Each of these expected values is taken over an ensemble of $M \to \infty$ players who hit points $\underline{x}_{i_1}, \underline{x}_{i_2}, \ldots, \underline{x}_{i_M}$ at their ith throw. Because the probability distribution of these values does not depend on considering the particular ith throw, i.e., $f_{\underline{X}}(\underline{x})$ is independent of i, the process is stationary and

$$E[g(\underline{x}_i)] = \lim_{M\to\infty} \frac{1}{M}\sum_{j=1}^{M} g(\underline{x}_{i_j}) = E[g(\underline{x})] = G \tag{3.127}$$

Similarly

$$Var[g(\underline{x}_i)] = Var[g(\underline{x})] = E\left[g^2(\underline{x})\right] - G^2 \tag{3.128}$$

We thus obtain

$$E[G_N] = E[g(\underline{x})] = G \tag{3.129}$$

$$Var[G_N] = \frac{1}{N} Var[g(\underline{x})] = \frac{1}{N}\left[E\left[g^2(\underline{x})\right] - G^2\right] \tag{3.130}$$

In practical cases, $E[g^2(\underline{x})]$ and G are unknown (G is indeed the target of the present evaluation) and in their place we can use the estimates with $N \gg 1$. That is, we suppose that the process, in addition to being stationary, is also ergodic, and thus

$$E[g(\underline{x})] \approx \frac{1}{N}\sum_{i=1}^{N} g(\underline{x}_i) = \overline{g} \quad E[g^2(\underline{x})] \approx \frac{1}{N}\sum_{i=1}^{N} g^2(\underline{x}_i) = \overline{g^2} \tag{3.131}$$

Thus for $N \gg 1$, it follows that $G \approx G_N$ and

$$E[G_N] \approx G_N = \overline{g} \quad Var[G_N] \approx s^2_{G_N} = \frac{1}{N}\left(\overline{g^2} - \overline{g}^2\right) \tag{3.132}$$

In the last formula it is common to substitute $N - 1$ in place of N in the denominator, to account for the degree of freedom that is lost in the calculation of $\overline{g}$; generally, because $N \gg 1$, this correction is negligible.

3.4.2 Forced (Biased) Simulation

The evaluation of G by the analog method just illustrated yields poor results whenever $g(\underline{x})$ and $f_{\underline{X}}(\underline{x})$ are such that where one is large the other is small: indeed, in this case most of the sampled $\underline{x}_i$ values result in small $g(\underline{x}_i)$ values which give

scarce contribution to G_N, and few large $g(\underline{x}_i)$ values which 'de-stabilize' the sample average. This situation may be circumvented in the following manner, within a sampling scheme known under the name 'Importance Sampling' (see also Sect. 6.2). Eq. (3.121) can be written as

$$G = \int_D \frac{g(\underline{x}) f_{\underline{X}}(\underline{x})}{f_1(\underline{x})} f_1(\underline{x}) \mathrm{d}\underline{x} = \int_D g_1(\underline{x}) f_1(\underline{x}) \mathrm{d}\underline{x} \tag{3.133}$$

where $f_1(\underline{x}) \neq f_{\underline{X}}(\underline{x})$ is an appropriate function (typically called 'Importance Sampling Distribution', see Sect. 6.2) having the characteristics of a pdf as given in Eq. (3.122) and the prize of the dart game becomes

$$g_1(\underline{x}) = \frac{g(\underline{x}) f_{\underline{X}}(\underline{x})}{f_1(\underline{x})} \tag{3.134}$$

As we shall formally demonstrate later, the optimal choice of the pdf $f_1(\underline{x})$ is $f_1(\underline{x}) = k|g(\underline{x})| f_{\underline{X}}(\underline{x})$. Then, in correspondence of every value $\underline{x}_i$ extracted from $f_1(\underline{x})$ one would obtain always the same prize $g_1(\underline{x}_i) = 1/k$ and the variance of G_N would be actually zero: this means that just one sampling would suffice to obtain the *exact value* of G. However, we shall show that the determination of the constant k poses the exact same difficulties of computing G.

In view of (3.133), from a statistical point of view $\underline{x}$ can be interpreted as a rv distributed according to the pdf $f_1(\underline{x})$. As before, it follows that the prize $g_1(\underline{x})$ is also a rv and G can be interpreted as the expected value of $g_1(\underline{x})$. If E_1 and Var_1 denote the expected value and variance with respect to the pdf $f_1(\underline{x})$, we get

$$E_1[g_1(\underline{x})] = \int_D g_1(\underline{x}) f_1(\underline{x}) \mathrm{d}\underline{x} = G \tag{3.135}$$

$$Var_1[g_1(\underline{x})] = \int_D [g_1(\underline{x}) - G]^2 f_1(\underline{x}) \mathrm{d}\underline{x} = E_1\left[g_1^2(\underline{x})\right] - G^2 \tag{3.136}$$

As before, G can be estimated with the dart game method by sampling N values $\underline{x}_1, \underline{x}_2, \ldots, \underline{x}_N$ from the pdf $f_1(\underline{x})$, calculating the corresponding values of the prize $g_1(\underline{x}_i)$, and computing the sample mean by arithmetic averaging. The rv is thus

$$G_{1N} = \frac{1}{N} \sum_{i=1}^{N} g_1(\underline{x}_i) \tag{3.137}$$

and

$$\begin{aligned} E_1[G_{1N}] &= \tfrac{1}{N} \sum_{i=1}^{N} E_1[g_1(\underline{x}_i)] \\ Var_1[G_{1N}] &= \tfrac{1}{N^2} \sum_{i=1}^{N} Var_1[g_1(\underline{x}_i)] \end{aligned} \tag{3.138}$$

Similar to the analog case, we obtain

$$\begin{aligned} E_1[g_1(\underline{x}_i)] &= E_1[g_1(\underline{x})] = G \\ Var_1[g_1(\underline{x}_i)] &= Var_1[g_1(\underline{x})] = E_1\left[g_1^2(\underline{x})\right] - G^2 \end{aligned} \tag{3.139}$$

and

$$E_1[G_{1N}] = E_1[g_1(\underline{x})] = G \tag{3.140}$$

$$Var_1[G_{1N}] = \frac{1}{N} Var_1[g_1(\underline{x})] = \frac{1}{N}\left[E_1\left[g_1^2(\underline{x})\right] - G^2\right] \tag{3.141}$$

The estimates of the expected values from the corresponding averages are

$$\begin{aligned} E_1[g_1(\underline{x})] &\simeq \tfrac{1}{N}\sum_{i=1}^{N} g_1(\underline{x}_i) = \overline{g_1} \\ E_1\left[g_1^2(\underline{x})\right] &\simeq \tfrac{1}{N}\sum_{i=1}^{N} g_1^2(\underline{x}_i) = \overline{g_1^2} \end{aligned} \tag{3.142}$$

and finally, for $N \gg 1$

$$\begin{aligned} G_{1N} &= \overline{g_1} \simeq G \\ Var_1[G_{1N}] &= \tfrac{1}{N} Var_1[g_1(\underline{x})] = \tfrac{1}{N}\left[E_1\left[g_1^2(\underline{x})\right] - G^2\right] \simeq \tfrac{1}{N}\left(\overline{g_1^2} - \overline{g_1}^2\right) \end{aligned} \tag{3.143}$$

The variance $Var_1[G_{1N}]$ of the estimated value G_{1N} depends on the choice of $f_1(\underline{x})$. To minimize it amounts to finding the pdf $f_1(\underline{x})$ which minimizes $E_1\left[g_1^2(\underline{x})\right]$, with the imposition of the normalization condition that is required for $f_1(\underline{x})$ to be a pdf. By using the method of Lagrange multipliers, the optimal $f_1(\underline{x})$ is found by rendering stationary the functional

$$\begin{aligned} \ell\{f_1\} &= \int_D g_1^2(\underline{x}) f_1(\underline{x}) \mathrm{d}\underline{x} + \frac{1}{\lambda^2}\left[\int_D f_1(\underline{x})\mathrm{d}\underline{x} - 1\right] \\ &= \int_D \left[\frac{g^2(\underline{x}) f_{\underline{X}}^2(\underline{x})}{f_1(\underline{x})} + \frac{1}{\lambda^2} f_1(\underline{x})\right] \mathrm{d}\underline{x} - \frac{1}{\lambda^2} \end{aligned} \tag{3.144}$$

The pdf $f_1(\underline{x})$ is then the solution to $\frac{\partial \ell}{\partial f_1} = 0$. The condition is satisfied if

$$-\frac{g^2(\underline{x}) f_{\underline{X}}^2(\underline{x})}{f_1^2(\underline{x})} + \frac{1}{\lambda^2} = 0 \tag{3.145}$$

from which we obtain

$$f_1(\underline{x}) = |\lambda||g(\underline{x})| f_{\underline{X}}(\underline{x}) \tag{3.146}$$

The constant $|\lambda|$ can be determined from the normalization condition on $f_1(\underline{x})$, so that finally the best $f_1(\underline{x})$ is

$$f_1(x) = \frac{|g(\underline{x})| f_{\underline{X}}^2(\underline{x})}{\int_D |g(\underline{x}')| f_{\underline{X}'}(\underline{x}') \mathrm{d}\underline{x}'} \tag{3.147}$$

In correspondence to this optimal pdf, we have the value

$$\begin{aligned} \min_{f_1} E_1\left[g_1^2(\underline{x})\right] &= \int_D \frac{g^2(\underline{x}) f_{\underline{X}}^2(\underline{x})}{f_1(\underline{x})} \mathrm{d}\underline{x} \\ &= \int_D \frac{g^2(\underline{x}) f_{\underline{X}}^2(\underline{x})}{|g(\underline{x})| f_{\underline{X}}(\underline{x})} \mathrm{d}\underline{x} \int_D |g(\underline{x}')| f_{\underline{X}'}(\underline{x}') \mathrm{d}\underline{x}' \end{aligned} \tag{3.148}$$

Since independent of the sign of $g(\underline{x})$, $g^2(\underline{x})/g(\underline{x}) = |g(\underline{x})|$, we obtain

$$\min_{f_1} E_1\left[g_1^2(\underline{x})\right] = \left[\int_D |g(\underline{x})| f_{\underline{X}}(\underline{x}) \mathrm{d}\underline{x}\right]^2 \tag{3.149}$$

and correspondingly, from Eq. (3.141)

$$\min_{f_1} Var_1[G_{1N}] = \left\{\left[\int_D |g(\underline{x})| f_{\underline{X}}(\underline{x}) \mathrm{d}\underline{x}\right]^2 - G^2\right\} \tag{3.150}$$

In particular, if $g(\underline{x}) \geq 0$, the variance of G is equal to zero [18].

Figure 3.7 shows an example in which it is advantageous to use forced simulation: in fact, compared to what happens when using the natural pdf $f_{\underline{X}}(\underline{x})$, the maximum of the optimal pdf $f_1(\underline{x}) = f_{\underline{X}}^*(\underline{x})$ is shifted toward the maximum of $g(\underline{x})$, and the values sampled from that optimal pdf more frequently correspond to high values of the prize $g(\underline{x})$.

The described procedure for performing the optimal choice of $f_1(\underline{x})$, which would lead us to Eq. (3.147), is not operative because to calculate $f_1(\underline{x})$ one must know how to calculate the denominator of Eq. (3.147), and the difficulty of this operation is equivalent to the difficulty of calculating G.

This apparently surprising result could have been foreseen by examining Eq. (3.147) for $f_1(\underline{x})$. By following the dart game technique, to calculate G one must sample a sequence of values $\{\underline{x}_{1i}\}$ from $f_1(\underline{x})$ and then calculate the corresponding sequence of prizes $\{g(\underline{x}_{1i})\}$ with Eq. (3.134). Because by hypothesis we have $g(\underline{x}_{1i}) \geq 0$, for each $\underline{x}_{1i}$ we have

$$g(\underline{x}_{1i}) = \frac{g(\underline{x}_{1i}) f_{\underline{X}}(\underline{x}_{1i})}{\frac{g(\underline{x}_{1i}) f_{\underline{X}}(\underline{x}_{1i})}{\int_D g(\underline{x}) f_{\underline{X}}(\underline{x}) \mathrm{d}\underline{x}}} = \int_D g(\underline{x}) f_{\underline{X}}(\underline{x}) \mathrm{d}\underline{x} = G \tag{3.151}$$

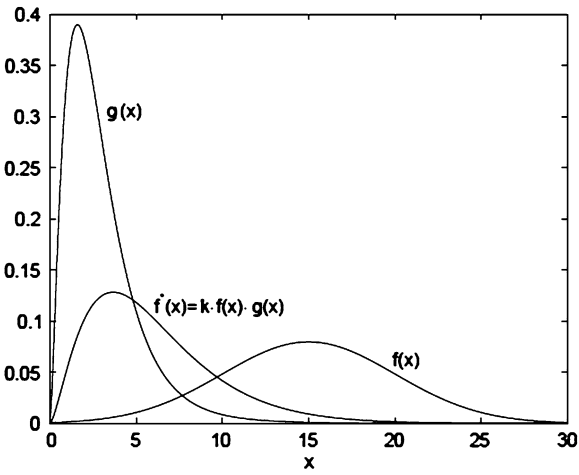

Fig. 3.7 An example in which it would be appropriate to resort to forced simulation

Then, it turns out that all the prizes $g(\underline{x}_{1i})$ are equal to each other and to G, so that the variance of the sequence $\{g(\underline{x}_{1i})\}$ is zero.

Operatively, one does not know how to calculate the denominator of Eq. (3.147), which is the value G of the integral (3.121) whose solution we are seeking. Then, in practice one chooses an $f_1^*(\underline{x})$ 'close' to $f_1(\underline{x})$ given by Eq. (3.147) and this allows estimating G with a considerably smaller variance than that which would be obtained by using the natural $f_{\underline{X}}(\underline{x})$ directly: sampling the values $\{\underline{x}_{1i}\}$ from a pdf $f_1^*(\underline{x})$ that approximates $f_1(\underline{x})$, the values of the sequence $\{g(\underline{x}_{1i})\}$ are *almost equal* to G and their variance is *small*.

The forced pdf $f_1^*(\underline{x})$ is usually assigned dependent on a vector $\underline{\alpha}$ of parameters, which are then determined so as to minimize the variance of the estimate. We clarify this with an example.

Let us estimate

$$G = \int_0^1 \cos\frac{\pi x}{2}\,\mathrm{d}x \tag{3.152}$$

The integral can be calculated analogically and we have $G = 2/\pi = 0.6366198$. Assuming that we are unable to perform the integration, we write the integral in the form of Eq. 3.121 by setting

$$g(x) = \cos\tfrac{\pi x}{2} \quad f(x) = 1 \tag{3.153}$$

Then

$$\begin{aligned} E[g^2(x)] &= \int_0^1 \cos^2\left(\tfrac{\pi x}{2}\right)\mathrm{d}x = \tfrac{1}{2} \\ Var[g(x)] &= \tfrac{1}{2} - \left(\tfrac{2}{\pi}\right)^2 = 9.47152 \cdot 10^{-2} \end{aligned} \tag{3.154}$$

Let us consider the two cases of estimating G by analog and optimally forced MCS.

The analog estimate given by Eq. (3.132) can be found with the following *Matlab*® program ($N = 10^4$histories)

N=1e4; *r=rand(N,1)*;*g=cos(pi*r/2)*;
GN=mean(g); *s2GN=var(g)/N*

The following values are obtained

$$\begin{gathered} G_N = 0.6342 \quad s^2_{G_N} = 9.6 \cdot 10^{-6} \\ \text{or} \\ G_N = (634.2 \pm 3.1) \cdot 10^{-3} \end{gathered} \tag{3.155}$$

The value G_N so obtained is consistent with the true value of G, from which it differs by 0.8 standard deviations.

In the case of the forced estimate of G, according to the optimal procedure we should calculate $f_1(x)$ with Eq. (3.147). Because $g(x) \geq 0$ for $0 \leq x \leq 1$, we know that in this case we would obtain $Var_1[G_{1N}] = 0$. We have $f_1(x) = \frac{g(x)}{k}$, where k is the constant denominator of Eq. (3.147). Let us suppose that we are unable to calculate k : to find $f_1^*(x)$ close to the optimal $f_1(x)$ we approximate $g(x)$ with the first two terms of the Taylor's expansion of the cosine function

$$f_1^*(x) \simeq \frac{\left[1 - \frac{1}{2}\left(\frac{\pi x}{2}\right)^2\right]}{k} \tag{3.156}$$

The pdf $f_1^*(x)$ is thus of the kind

$$f_1^*(x) = a - bx^2 \tag{3.157}$$

From the normalization condition, we have $a - \frac{b}{3} = 1$ and thus

$$f_1^*(x) = a - 3(a-1)x^2 \tag{3.158}$$

From the nonnegativity condition it follows that

$$\text{for } 0 \leq x < 1/\sqrt{3} \text{ it must be that } a > -\frac{3x^2}{1-3x^2} \text{ and thus } a > 0;$$

$$\text{For } 1/\sqrt{3} < x \leq 1 \text{ it must be that } a \leq \frac{3x^2}{3x^2-1} \text{ and thus } a \leq 3/2.$$

It follows that $f_1^*(x)$ has been determined with the exception of the parameter a, whose optimal value must be found inside the interval $\left(0, \frac{3}{2}\right)$.

From Eq. (3.134) we then have

$$g_1(x) = \frac{g(x) f_x(x)}{f_1(x)} = \frac{\cos\left(\frac{\pi x}{2}\right)}{a - 3(a-1)x^2} \tag{3.159}$$

In the ideal case, i.e., supposing we are able to evaluate the integrals, we would have

$$E_1\left[g_1^2(x)\right] = \int_0^1 \frac{g^2(x)}{f_1^*(x)}\mathrm{d}x = \int_0^1 \frac{\cos^2\left(\frac{\pi x}{2}\right)}{a-3(a-1)x^2}\mathrm{d}x \tag{3.160}$$

The minimum value for this expression is found for $a = 3/2$, and is equal to 0.406275. By substituting into Eq. (3.141) we have

$$Var_1[G_{1N}] = \frac{1}{N}\left[0.406275 - \left(\frac{2}{\pi}\right)^2\right] = \frac{1}{N}9.9026 \cdot 10^{-4} \tag{3.161}$$

By choosing for N the value 10^4, like in the analog case, we obtain a variance that is smaller by two orders of magnitude. In a real case, when we might be unable to evaluate the integrals, the value of the parameter a is determined by trial and error. For each trial value a, the $f_1^*(x)$ is given by Eq. (3.158) and is completely determined. From this $f_1^*(x)$ we sample N values x_i (i = 1,2,…,N), we calculate the corresponding values $g_1(x_i)$ with Eq. (3.159) and then $\overline{g_1}$ and $\overline{g_1^2}$ with Eq. (3.142); finally, we calculate $Var_1[G_{1N}]$ with Eq. (3.143). Among all the trial values a, the best choice is the one for which $Var_1[G_{1N}]$ is minimum. For this example, the determination of a was done by using the following *Matlab*® program ($N = 10^4$ histories) inside the interval [0,1.5] with steps equal to 0.05

```
clear; N=1e4; g=zeros(N,1); s2G1N=[];
a=0:0.05:1.5; la=length(a);
for k=1:la
        for n=1:N
                rr=zeros(1,3);r=zeros(1,3);
                c=[a(k)−1 0 −a(k) rand]; rr=roots(c);lrr=length(rr);
                j=0;
                for kk=1:lrr
                        r(kk)=−1;
                        if imag(rr(kk))==0
                        j=j+1;
                        r(j)=rr(kk);
                        end
                end
                i=find(r>0 && r<1); x=r(i);
                g(n)=cos(pi*x/2)/(a(k)−3*(a(k)−1)*x^2);
        end
        s2G1N=[s2G1N var(g)];
end
plot(a, s2G1N/N)
```

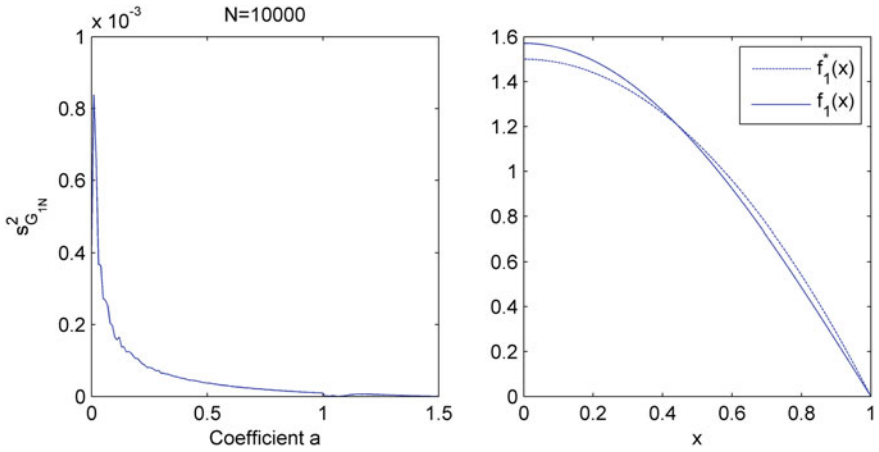

Fig. 3.8 Estimated variance as a function of parameter a (*left*); forced PDF $f_1(x)$and $f_1^*(x)$ (*right*)

Figure 3.8 reports the value $s^2_{G_{1N}}$ as a function of a (left) and the two pdfs $f_1(x)$ and $f_1^*(x)$ (right). This latter was calculated as a function of x, for the optimal value $a = 1.5$. From the Figure, it can be seen that $Var_1[G_{1N}]$ decreases monotonically as a increases, and reaches the same minimum $a = 3/2$, as in the theory. The corresponding estimate of G was obtained by using a forced MCS with the following *Matlab*® program

```
clear;
N=1e4; g=zeros(N,1); s2G1N=[]; a=1.5;
for n=1:N

        rr=zeros(1,3);r=zeros(1,3);
        c=[a-1 0 -a rand]; rr=roots(c);lrr=length(rr); j=0;
        for kk=1:lrr
        r(kk)=-1;

                if imag(rr(kk))==0
                j=j+1; r(j)=rr(kk);
                end

        end
        i=find(r>0 && r<1); x=r(i); g1(n)=cos(pi*x/2)/(a-3*(a-1)*x^2);

end
G1N=mean(g1); s2G1N=var(g1)/N;
```

The following values are obtained

$$\overline{g_{1N}} = 0.6366 \quad s^2_{G_{1N}} = 9.95 \cdot 10^{-8} \quad or \quad G_{1N} = (636.6 \pm .032) \cdot 10^{-3}$$

This result shows that choosing the optimal pdf $f_1^*(x)$ allows us to estimate G with a variance that is two orders of magnitude smaller than that of the analog computation.

Extension to the Multivariate Case

Let us consider the definite integral G of Eq. (3.121). The sampling of a rv vector $\underline{x}$ from $f_{\underline{X}}(\underline{x})$ can be done by starting from the following identity

$$f_{\underline{X}}(x_1, x_2, \ldots, x_n) = \left[\prod_{j=1}^{n-1} f_{j+1}(x_j | x_{j-1}, x_{j-2}, \ldots, x_1)\right] f(x_n | x_{n-1}, \ldots, x_1) \tag{3.162}$$

where

$$\begin{aligned} f_{j+1}(x_j | x_{j-1}, x_{j-2}, \ldots, x_1) &= \frac{\int \mathrm{d}x_{j+1} \mathrm{d}x_{j+2} \ldots \mathrm{d}x_n f_{\underline{X}}(\underline{x})}{\int \mathrm{d}x_j \mathrm{d}x_{j+1} \mathrm{d}x_{j+2} \ldots \mathrm{d}x_n f_{\underline{X}}(\underline{x})} \\ &= \frac{f_{\mathrm{marg}}(x_1, x_2, \ldots, x_j)}{f_{\mathrm{marg}}(x_1, x_2, \ldots, x_{j-1})} \end{aligned} \tag{3.163}$$

$$f(x_n | x_{n-1}, x_{n-2}, \ldots, x_1) = \frac{f_{\underline{X}}(\underline{x})}{\int \mathrm{d}x_n f(\underline{x})} \tag{3.164}$$

where $f_{marg}(x_1, x_2, \ldots, x_j)$ is the marginal pdf of $f_{\underline{X}}(\underline{x})$ with respect to the variables $x_1, x_2, \ldots, x_j$. From Eq. (3.162), it can be seen that we can sample $\underline{x}$ by sampling successively the x_j components from conditional univariate distributions, i.e.,

$$\begin{aligned} &[x_1 \text{ from } f_2(x_1)],\ [x_2 \text{ from } f_3(x_2 | x_1)], \ldots, \\ &[x_n \text{ from } f(x_n | x_{n-1}, \ldots, x_1)] \end{aligned} \tag{3.165}$$

In words, we sample x_1 from the marginal distribution of f with respect to all the variables except for x_1, x_2 from the conditional distribution with respect to the obtained value of x_1 and marginal with respect to all the remaining variables except for x_2, and so on.

3.5 Sensitivity Analysis by Monte Carlo Simulation

The definite integral G defined by (3.121) depends on the values of the parameters that appear in the function $g(\underline{x})$ and in the pdf $f_{\underline{X}}(\underline{x})$. Let us suppose, for simplicity, that those functions have in common a scalar parameter p: we want to make a MC estimate of the sensitivity of G with respect to a variation of the parameter p,

namely $\mathrm{d}G/\mathrm{d}p$. Thus, by including the parameter explicitly as an argument, we can write Eq. (3.121) as

$$G(p) = \int_D g(\underline{x};p) f_{\underline{X}}(\underline{x};p)\mathrm{d}\underline{x} \tag{3.166}$$

Of course, a special case of this formulation is the one in which only g or only f depends on p.

We present two procedures for estimating the sensitivity, both similar to the one described for forced simulation [19–23].

3.5.1 Correlated Sampling

Let us set, for brevity

$$\begin{aligned} g^* &\equiv g(\underline{x};p+\Delta p) \qquad & f^*_{\underline{X}} &\equiv f_{\underline{X}}(\underline{x};p+\Delta p) \\ g &\equiv g(\underline{x};p) & f_{\underline{X}} &\equiv f_{\underline{X}}(\underline{x};p) \end{aligned} \tag{3.167}$$

Further, let us indicate with $E[\cdot]$ and $E^*[\cdot]$ the expected values of the argument calculated with the pdfs $f_{\underline{X}}$ and $f^*_{\underline{X}}$, respectively. Corresponding to the value $p + \Delta p$ of the parameter, the definite integral defined by Eq. (3.121) becomes

$$G^* \equiv G(p+\Delta p) = \int_D g(\underline{x};p+\Delta p) f_{\underline{X}}(\underline{x};p+\Delta p)\mathrm{d}\underline{x} = E^*[g^*] \tag{3.168}$$

Also,

$$\begin{aligned} G^* \equiv G(p+\Delta p) &= \int_D g(\underline{x};p+\Delta p)\frac{f_{\underline{X}}(\underline{x};p+\Delta p)}{f_{\underline{X}}(\underline{x};p)} f_{\underline{X}}(\underline{x};p)\mathrm{d}\underline{x} \\ &= E^*\left[g^*\frac{f^*_{\underline{X}}}{f_{\underline{X}}}\right] \equiv E[h] \end{aligned} \tag{3.169}$$

where we set

$$h(\underline{x};p,\Delta p) = g(\underline{x};p+\Delta p)\frac{f_{\underline{X}}(\underline{x};p+\Delta p)}{f_{\underline{X}}(\underline{x};p)} \equiv g^*\frac{f^*_{\underline{X}}}{f_{\underline{X}}} \tag{3.170}$$

Corresponding to a given Δp (in general we choose $\Delta p/p \ll 1$). The MCS estimate of g^* can be done simultaneous to that of G with the described method of the dart game (Sect. 3.4.1): for each of the N values $\underline{x}_i$ sampled from $f_{\underline{X}}(\underline{x};p)$, we accumulate the value $g(\underline{x}_i;p)$ with the aim of calculating G_N to estimate G, and we also accumulate the value $h(\underline{x}_i;p,\Delta p)$ with the aim of calculating G^*_N as estimate of G^*. The values G_N and G^*_N, calculated by using the same sequence $\{\underline{x}_i\}$, are correlated. We have

$$G_N^* = \frac{1}{N}\sum_{i=1}^{N} h(\underline{x}_i; p, \Delta p) \tag{3.171}$$

But

$$\begin{aligned} E[h] &= G_N^* \\ Var[h] &= E[h^2] - (G^*)^2 \end{aligned} \tag{3.172}$$

Thus

$$\begin{aligned} E\left[G_N^*\right] &= G^* \\ Var\left[G_N^*\right] &= \tfrac{1}{N} Var[h] = \tfrac{1}{N}\left\{E[h^2] - (G^*)^2\right\} \end{aligned} \tag{3.173}$$

To compute the sensitivity of G with respect to the variation of the parameter from p to $p + \Delta p$, let us define

$$\Delta G_N^* = G_N^* - G_N = \frac{1}{N}\sum_{i=1}^{N} (h_i - g_i) \tag{3.174}$$

where, for brevity, we set

$$h_i \equiv h(\underline{x}_i; p + \Delta p) \text{ and } g_i \equiv g(\underline{x}_i; p) \tag{3.175}$$

We have

$$E[h_i - g_i] = E[h - g] = E[h] - E[g] = G^* - G \tag{3.176}$$

$$\begin{aligned} Var[h_i - g_i] = Var[h - g] &= E\left[\{(h - g) - G^* - G\}^2\right] \\ &= E\left[(h - G^*)^2\right] + E\left[(g - G)^2\right] - 2E[(h - G^*)(g - G)] \\ &= Var[h] + Var[g] - 2\{E[hg] - G^* G\} \end{aligned} \tag{3.177}$$

The sensitivity $\mathrm{d}G/\mathrm{d}p$ and its variance are estimated as

$$E\left[\frac{\Delta G_N}{\Delta p}\right] = \frac{1}{\Delta p} E[h_i - g_i] = \frac{1}{\Delta p}(G^* - G) \simeq \frac{1}{\Delta p}\left(\overline{h} - \overline{g}\right) \tag{3.178}$$

$$\begin{aligned} Var\left[\tfrac{\Delta G_N}{\Delta p}\right] &= \tfrac{1}{N}\left\{\tfrac{Var[h] + Var[g] - 2E[hg] + 2G^* G}{(\Delta p)^2}\right\} \simeq \\ &\tfrac{1}{N}\left\{\tfrac{\left(\overline{h^2} - \overline{h}^2\right) + \left(\overline{g^2} - \overline{g}^2\right) - 2E\left[\overline{hg} - \overline{h}\,\overline{g}\right]}{(\Delta p)^2}\right\} \end{aligned} \tag{3.179}$$

The value of G, with its variance, and the sensitivity $\mathrm{d}G/\mathrm{d}p$, with its variance, can be estimated by calculating, for each value $\underline{x}_i$ of the sequence $\{\underline{x}_i\}$ sampled from $f_{\underline{X}}(\underline{x}; p)$, the three values

$$g_i \equiv g(\underline{x}_i; p),\ g_i^* \equiv g(\underline{x}_i; p + \Delta p) \text{ and } f_i^* \equiv f_{\underline{X}}(\underline{x}_i; p + \Delta p) \tag{3.180}$$

and by accumulating the five quantities

$$g_i; \quad g_i^2; \quad h_i = g_i^* \frac{f_i^*}{f_i}; \quad h_i^2 \equiv \left(g_i^* \frac{f_i^*}{f_i} \right)^2; \quad h_i g_i = g_i^* \frac{f_i^*}{f_i} g_i \tag{3.181}$$

After the N accumulations, we calculate the arithmetic averages $\overline{g}, \overline{g^2}, \overline{h}, \overline{h^2}, \overline{hg}$ which, substituted in Eqs. (3.178) and (3.179), give the desired estimates.

3.5.2 *Differential Sampling*

By differentiating Eq. (3.166) with respect to the parameter of interest p, we obtain the expression for the first-order sensitivity of G with respect to a variation of p

$$\begin{aligned} \frac{\partial G}{\partial p} &= \int \left[\frac{\partial g(\underline{x}; p)}{\partial p} f_{\underline{X}}(\underline{x}; p) + g(\underline{x}; p) \frac{\partial f_{\underline{X}}(\underline{x}; p)}{\partial p} \right] \mathrm{d}\underline{x} \\ &= \int \left[\frac{\partial}{\partial p}(\underline{x}; p) + \frac{\partial}{\partial p_{\underline{X}}}(\underline{x}; p) \right] g(\underline{x}; p) f_{\underline{X}}(\underline{x}; p) \mathrm{d}\underline{x} \end{aligned} \tag{3.182}$$

The MC estimate of the first-order sensitivity can be obtained by sampling N values $\{\underline{x}_i\}$ from $f_{\underline{X}}(\underline{x}; p)$, and calculating the arithmetic average

$$\left(\frac{\partial G}{\partial p} \right)_N = \frac{1}{N} \sum_{i=1}^{N} \left[\frac{\partial}{\partial p} \ln g(\underline{x}_i; p) + \frac{\partial}{\partial p} \ln f_{\underline{X}}(\underline{x}_i; p) \right] g(\underline{x}_i; p) \tag{3.183}$$

The extension of this simple procedure to the calculation of the pure or mixed sensitivity of a generic nth order is straightforward.

3.6 Monte Carlo Simulation Error and Quadrature Error

Let us finally compare the statistical error made by estimating G by using the MCS method with N trials, and the numerical error derived by a quadrature formula in which the integrand function is calculated in N points [24, 25]. In any case, analog or biased, the MC error [see Eqs. (3.131) and (3.143)] varies with $N^{-\frac{1}{2}}$, i.e.,

$$\varepsilon_{MC} \sim N^{-\frac{1}{2}} \tag{3.184}$$

In the case of a fairly regular function, the error in any form of quadrature varies like Δ^k with Δ equal to the integration interval and k a small integer which depends

on the numerical method employed in the quadrature formula. In general, k increases with the complexity of the rule, but is at most $2 \div 3$.

In the case of a hypercube with n dimensions and side length 1, the number of points on one edge is Δ^{-1} so that the total number of points is $N = \Delta^{-n}$ and the numerical quadrature error is

$$\varepsilon_q \sim \Delta^k \sim N^{-\frac{k}{n}} \tag{3.185}$$

The MCS estimate is convenient, i.e., $\varepsilon_{MC} \leq \varepsilon_q$, if $n \geq 2k = 6$, i.e., if it is necessary to evaluate an integral in a domain that is at least 6-dimensional.

References

1. McGrath, E.J., Irving, D.C. (1975). *Techniques for Efficient Monte Carlo Simulation* (Vol. II, ORNL-RSIC-38).
2. Niederreiter, H. (1992). *Random Number Generation and Quasi-Monte Carlo Methods*, SIAM.
3. Sobol, I. M. (1967). The distribution of points in a cube and the approximate evaluation of integrals. *USSR Computational Mathematics and Mathematical Physics, 7*(4), 86–112.
4. Matsumoto, M., & Nishimura, T. (1998). Mersenne twister: a 623-dimensionally equidistributed uniform pseudo-random number generator. *ACM Transactions on Modeling and Computer Simulation, 8*(1), 3–30.
5. Rubinstein, R. Y. (1981). *Simulation and the Monte Carlo method*. NY: Wiley.
6. Kalos, M. H., & Whitlock, P. A. (2008). *Monte Carlo methods*. NY: Wiley.
7. Fang, K. T., Hickernell, F. J., & Niederreiter, H. (2002). *Monte Carlo and Quasi-Monte Carlo methods 2000*. Berlin: Springer.
8. Niederreiter, H., & Spanier, J. (1998). *Monte Carlo and Quasi-Monte Carlo methods*. Berlin: Springer.
9. Liu, J. S. (2001). *Monte Carlo strategies in scientific computing*., Springer Series in Statistics Berlin: Springer.
10. L'Ecuyer, P. (1994). Uniform random number generation. *Annals of Operational Research, 53*, 77–120.
11. L'Ecuyer, P. (2011). Uniform random number generators. In: M. Lovric (Ed.), *International Encyclopedia of Statistical Science Part 21*(pp. 1625–1630). Berlin: Springer.
12. Shortle, J. F., & L'Ecuyer, P. (2011). Introduction to rare-event simulation. In *Wiley Encyclopedia of Operations Research and Management Science*. New York: Wiley.
13. L'Ecuyer, P. (2011). Random number generators. In S. I. Gass & M. C. Fu (Eds.), *Wiley encyclopedia of operations research and management science* (3rd ed.). Berlin: Springer.
14. L'Ecuyer, P., Mandjes, M., Turn, B. (2009). Importance sampling and rare event simulation. In G. Rubino, B. Turn (eds.), Rare event simulation using Monte Carlo methods (pp. 17–38). New York: Wiley.
15. L'Ecuyer, P., (2010). Pseudorandom number generators. In R. Cont, (Ed.), *Wiley encyclopedia of quantitative finance* (pp. 1431–1437). New York: Wiley.
16. L'Ecuyer, P. (2004). Random number generation and Quasi-Monte Carlo. In J. Teugels, B. Sundt (Eds.), Wiley encyclopedia of actuarial science (Vol. 3, pp. 1363–1369). New York: Wiley.
17. Marsaglia G., Bray, T.A. (1964). A convenient method for generating normal variables. SIAM Review, *6*(3).

18. Booth, T. E. (1989). Zero-variance solutions for linear Monte Carlo. *Nuclear Science and Engineering, 102*, 332–340.
19. Hall, M. C. G. (1982). Cross-section adjustment with Monte Carlo sensitivities. *Application to the Winfrith Iron Benchmark, Nuclear Science and Engineering, 81*, 423–431.
20. Rief, H. (1984). Generalized Monte Carlo Perturbation algorithms for correlated sampling and a second-order series approach. *Annals of Nuclear Energy, 11*, 455–476.
21. Rief, H. (1987). Monte Carlo uncertainly analysis. In Y. Ronen (Ed.), *CRC handbook on uncertainty analysis*. Boca Raton: CRC press.
22. Rief, H. (1996). Stochastic perturbation analysis applied to neutral particle transfer. *Advances in Nuclear Science and Technology, 23*, 69–97.
23. Lux, I., & Koblinger, L. (1991). *Monte Carlo particle transport methods: Neutron and photon calculations*. Boca Raton: CRC Press.
24. Amster, H. J., & Djamehri, M. J. (1976). Prediction of statistical error in Monte Carlo transport calculations. *Nuclear Science and Engineering, 60*, 131–142.
25. Booth, T. E., & Amster, H. J. (1978). Prediction of Monte Carlo errors by a theory generalized to treat track-length estimators. *Nuclear Science and Engineering, 65*, 273–285.

Chapter 4
System Reliability and Risk Analysis by Monte Carlo Simulation

4.1 Introduction

System reliability analysis arouse has a scientific discipline in the 1950s, specialized in the 1960s, was integrated into risk assessment in the 1970s, and recognized as a relevant contributor to system analysis with the extensive methodological developments and practical applications of the 1980s and 1990s.

System reliability analysis aims at the quantification of the probability of failure of a system, through an ensemble of formal methods for investigating the uncertain boundaries between system operation and failure. This entails addressing the following questions:

- Why systems fail, e.g., by using the concepts of reliability physics to discover causes and mechanisms of failure and to identify consequences;
- How to develop reliable systems, e.g., by reliability-based design;
- How to measure and test reliability in design, operation, and management;
- How to maintain systems reliable, by fault diagnosis, prognosis, maintenance.

For a given system, the proper answers to these questions require to address the following issues:

- The representation and modeling of the system;
- The quantification of the system model;
- The representation, propagation, and quantification of the uncertainty in system behavior.

Nowadays, in its maturity, system reliability analysis is still confronted by these challenges, possibly sharpened by the increased complexity of the systems.

For complex systems made up of several components, it is important to analyze the possible mechanisms of failure and to evaluate their probabilities. Often, each such system is unique in the sense that there are no other identical systems (same components interconnected in the same way and operating under the same

E. Zio, *The Monte Carlo Simulation Method for System Reliability and Risk Analysis*, Springer Series in Reliability Engineering,
DOI: 10.1007/978-1-4471-4588-2_4, © Springer-Verlag London 2013

conditions) for which failure data have been collected; therefore, a statistical failure analysis is not possible.

Furthermore, it is not only the probability of system failure which is of interest but also the initiating causes and the combination of events which can lead to it.

The engineering way to tackle a problem of this nature, where many events interact to produce other events, is to relate these events using simple logical relationships (intersection, union, etc., see Appendix A) and to methodically build a logical structure which represents the system. Then, the logic model is solved in quantitative terms to provide the probability of system failure starting from the probabilities of failures of its components.

Actually, the reliability analysis of modern complex systems entails an integrated approach in which the hardware, software, organizational and human elements are treated in a combined frame which accounts for their dynamic interdependences in the complex related tasks of system production, maintenance, and emergency management. To cope with such complexity from a quantifiable point-of-view, computational methodologies are being advocated to provide a framework for simulating directly the response of a system to an initial perturbation, as the system hardware and software components and the operating crew interact with each other and with the environment. This can be achieved by embedding models of process evolution and human operator behavior within MCS procedures reproducing the stochastic occurrence of system failure and success state transitions.

4.2 Basic Principles of System Reliability Analysis

To characterize the failure behavior of a component in quantitative terms, let us consider the rv *time to failure, T*, whose cdf $F_T(t)$ and pdf $f_T(t)$ are typically called the failure probability and density functions at time t. The complementary cumulative function (ccdf) $R_T(t) = 1 - F_T(t) = P(T > t)$ is called *reliability* or *survival function* of the component at time t and gives the probability that the component survives up to time t with no failures.

Another information of interest for monitoring the failure evolution process of a component is given by the probability that it fails in an interval dt knowing that it has survived with no failures up to the time of beginning of the interval, t. This probability is expressed in terms of the product of the interval dt times a conditional probability density called *hazard function* or *failure rate* and usually indicated by the symbol $h_T(t)$

$$\begin{aligned} h_T(t)dt &= P(t < T \leq t + dt | T > t) \\ &= \frac{P(t < T \leq t + dt)}{P(T > t)} = \frac{f_T(t)dt}{R(t)} \end{aligned} \tag{4.1}$$

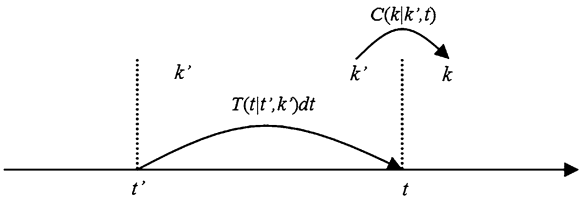

Fig. 4.1 Transition $(t', k') \Rightarrow (k, t)$

The hazard function $h_T(t)$ gives the same information of the pdf and cdf to whom it is univocally related by Eq. (4.1) and its integration

$$F_T(t) = 1 - e^{-\int_0^t h_T(s)ds} \tag{4.2}$$

In general, the hazard function follows the so-called 'bathtub' curve which shows three distinct phases in the life of a component: the first phase corresponds to a failure rate decreasing with time and it is characteristic of the *infant mortality* or *burn in* period whereupon the more the component survives, the lower becomes its probability of failure (this period is central for warranty analysis); the second period, called *useful life*, corresponds to a failure rate independent of time: during this period, failures occur at random times with no influence on the usage time of the component; finally, the last period sees an increase in the failure rate with time and corresponds to the development of irreversible aging processes which make the component more and more prone to fail as time goes by (this period is central for maintenance analysis).

4.3 The Transport Process of a Stochastic System

Let us consider a system made up of N_C physical components (pumps, valves, ducts, electronic circuitry, and so on). Each component can be in a number of states, e.g., working, failed, standby, etc. During its life, a component may move from one state to another by a transition which occurs stochastically in time and whose outcome (final state reached) is stochastic. The stochastic behavior of each component is then defined by a matrix of probabilities of transition between different states.

On the other hand, the full description of the system stochastic behavior in time is given by the pdf that the system makes a transition at a given time which leads it into a new configuration.

The configurations of the system (also termed 'states', in the following) can be numbered by an index that orders all the possible combinations of all the states of the components of the system. More specifically, let k_n denote the index that identifies the configuration reached by the plant at the n-th transition and t_n be the time at which the transition has occurred.

Consider the generic transition which has occurred at time t' with the system entering state k'. The probabilities which govern the occurrence of the next system transition at time t which lead the system into state k are (Fig. 4.1):

- $T(t|t',k')dt$ =conditional probability that the system makes the next transition between t and $t+dt$, given that the previous transition has occurred at time t' and that the system had entered in state k';
- $C(k|k',t)$ =conditional probability that the system enters in state k by effect of the transition occurring at time t with the system originally in state k'.

The probabilities above defined are normalized as follows

$$\int_{t'}^{\infty} T(t|t',k')dt \leq 1 \tag{4.3}$$

$$\sum_{k\in\Omega} C(k|k',t) = 1; \quad C(k|k,t) = 0 \tag{4.4}$$

where Ω is the set of all possible states of the system. In the following, unless otherwise stated, all the summations on the system states will be performed on all the values $k \in \Omega$. Note that $T(t|t',k')$ may not be normalized to one since with probability $1 - \int T(t|t',k')dt$ the system may fall at t' in a state k' from which it cannot exit, called absorbing state.

The two probability functions introduced form the so-called *probabilistic transport kernel* for the transition $(t',k') \rightarrow (t,k)$ [1–4]

$$K(t,k|t',k') = T(t|t',k')C(k|k',t) \tag{4.5}$$

4.4 System Reliability Analysis by Monte Carlo Simulation

In practice, the analysis of system reliability by MCS corresponds to performing a virtual experiment in which a large number of identical stochastic systems, each one behaving differently due to the stochastic character of the system behavior, are run for test during a given time and their failure occurrences are recorded [2]. This, in principle, is the same procedure adopted in the reliability tests performed on individual components to estimate their failure rates, mean times to failure, or other parameters characteristic of their failure behavior: the difference is that for components the tests can be actually done physically in laboratory, at reasonable costs and within reasonable testing times (possibly by resorting to accelerated testing techniques, when necessary) whereas for systems of components this is obviously impracticable for the costs and times involved in systems failures. Thus,

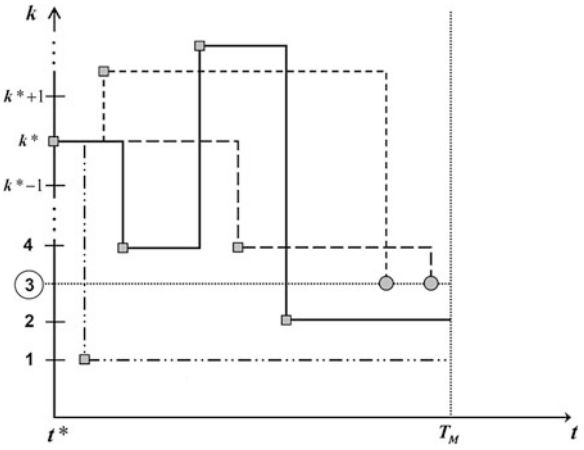

Fig. 4.2 System random walks in the system configuration versus time plane. System configuration *3 is circled* as a fault configuration. The *squares* identify points of transition; the *circle bullets* identify fault states. The *dashed lines* identify realizations leading to system failure before the mission time T_M

instead of making physical tests on a system, its stochastic process of transition among its states is modeled by defining its probabilistic transport kernel (Eq. 4.3) and a large number of realizations are generated by sampling from it the times and outcomes of the occurring transitions. Figure 4.2 shows a number of such realizations on the plane *system configuration versus time*: in such plane, the realizations take the form of random walks made of straight segments parallel to the time axis in-between transitions, when the system is in a given configuration, and vertical stochastic jumps to new system configurations at the stochastic times when transitions occur. In the following, we will use also the terms 'trial' and 'history' to refer to a random walk realization.

For the purpose of reliability analysis, a subset Γ of the system configurations is identified as the set of fault states. Whenever the system enters one such configuration, its failure is recorded together with its time of occurrence. With reference to a given time t of interest, an estimate $\hat{F}_T(t)$ of the probability of system failure before such time, i.e., of the unreliability $F_T(t)$, can be obtained by the frequency of system failures occurred before t, computed by dividing the number of random walk realizations which record a system failure before t by the total number of random walk realizations generated.

More specifically, from the point-of-view of the practical implementation into a computer code, the system mission time is subdivided in N_t intervals of length Δt and to each time interval an *unreliability* counter $C^R(t)$ is associated to record the occurrence of a failure: at the time τ when the system enters a fault state, a one is collected into all the unreliability counters $C^R(t)$ associated to times t successive to the failure occurrence time, i.e., $t \in [\tau, T_M]$ (Fig. 4.3). After simulating a large number of random walk trials M, an estimate of the system unreliability can be obtained by simply dividing by M the accumulated contents of the counters $C^R(t)$, $t \in [0, T_M]$.

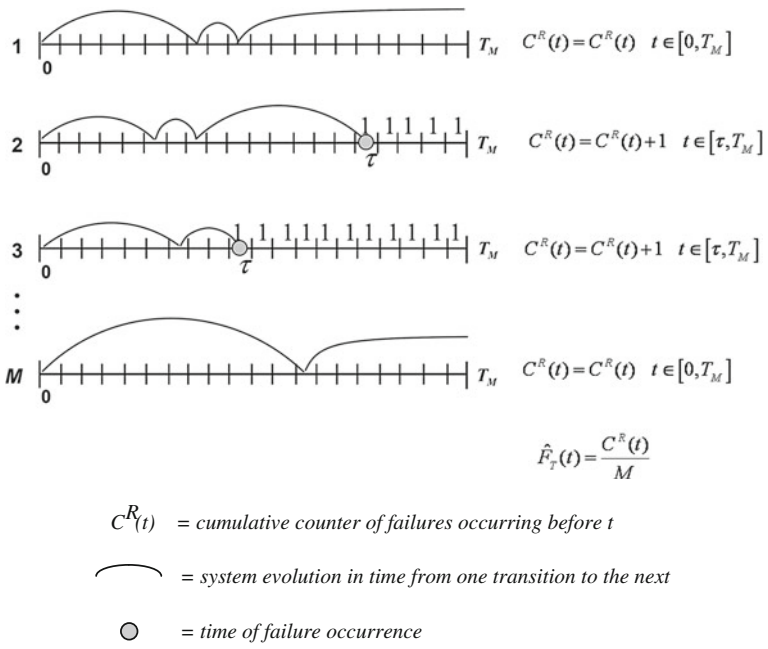

Fig. 4.3 MCS estimation procedure of unreliability $F_T(t)$. In the second and third simulated histories, the system enters a failed configuration at time τ; correspondingly, the failure occurrence is recorded by collecting ones in all cumulative counters $C^R(t)$, $t \in [\tau, T_M]$. In the end, the quantity $\hat{F}_T(t)$, frequency of failure occurrences before t, gives the MC estimate of the system unreliability at time t, $F_T(t)$

The MCS of one single system random walk (also called history or trial) entails the repeated sampling from the probabilistic transport kernel (Eq. 4.3) of the time of occurrence of the next transition and of the new configuration reached by the system as a consequence of the transition, starting from the current system configuration k' at t'. This can be done in two ways which give rise to the so-called *indirect* and *direct* MC approaches [5].

4.4.1 Indirect Simulation Method

The indirect method consists in sampling first the time t of a system transition from the corresponding conditional probability density $T(t|t', k')$ of the system performing at time t one of its possible transitions out of k' entered at the previous transition at time t'. Then, the transition to the new configuration k actually occurring is sampled from the conditional probability $C(k|t, k')$ that the system enters the new state k given that a transition has occurred at t starting from the system in state k'. The procedure then repeats to the next transition.

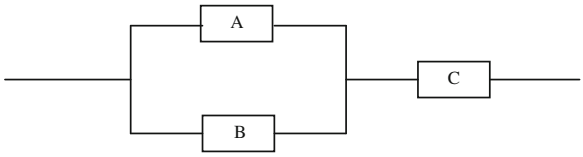

Fig. 4.4 A simple series–parallel logic

Table 4.1 Components transition rates

		Arrival			
Initial		1	2	3	
	1	–	$\lambda^{A(B)}_{1\to 2}$	$\lambda^{A(B)}_{1\to 3}$	
	2	$\lambda^{A(B)}_{2\to 1}$	–	$\lambda^{A(B)}_{2\to 3}$	
	3	$\lambda^{A(B)}_{3\to 1}$	$\lambda^{A(B)}_{3\to 2}$	–	

		Arrival			
		1	2	3	4
Initial	1	–	$\lambda^{C}_{1\to 2}$	$\lambda^{C}_{1\to 3}$	$\lambda^{C}_{1\to 4}$
	2	$\lambda^{C}_{2\to 1}$	–	$\lambda^{C}_{2\to 3}$	$\lambda^{C}_{2\to 4}$
	3	$\lambda^{C}_{3\to 1}$	$\lambda^{C}_{3\to 2}$	–	$\lambda^{C}_{3\to 4}$
	4	$\lambda^{C}_{4\to 1}$	$\lambda^{C}_{4\to 2}$	$\lambda^{C}_{4\to 3}$	–

Consider for example the system in Fig. 4.4, consisting of components A and B in active parallel followed by component C in series. Components A and B have two distinct modes of operation and a failure state whereas component C has three modes of operation and a failure state. For example, if A and B were pumps, the two modes of operation could represent the 50 and 100 % flow modes; if C were a valve, the three modes of operation could represent the 'fully open, 'half-open', and 'closed' modes.

For simplicity of illustration, let us assume that the components' times of transition between states are exponentially distributed and denote by $\lambda^{i}_{j_i\to m_i}$ the rate of transition of component i going from its state j_i to the state m_i. Table 4.1 gives the transition rates matrices in symbolic form for components A, B, and C of the example (the rate of self-transition $\lambda^{i}_{j_i\to j_i}$ of component i does not need to be assigned, since it can be retrieved from the probability equation stating that the sum of the probabilities i of making anyone of the transitions from state j_i to any reachable state m_i must be 1).

The components are initially ($t = 0$) in their nominal states which we label with the index 1 (e.g., pumps A and B at 50 % flow and valve C fully open), whereas the failure states are labeled with the index 3 for the components A and B and with the index 4 for component C.

The logic of operation is such that there is one minimal cut set (failure state) of order 1, corresponding to component C in state 4, and one minimal cut set (failure state) of order 2, corresponding to both components A and B being in their respective failed states 3.

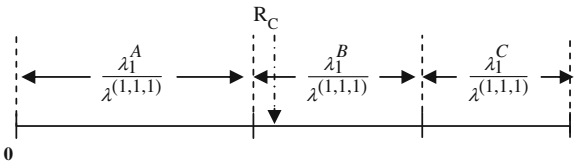

Fig. 4.5 Pictorial representation of the sampling of the component by the inverse transform method for discrete distributions

Let us consider one MC trial, starting at $t = 0$ with all components in their nominal states ($j_A = 1, j_B = 1, j_C = 1$). The rate of transition of component A(B) out of its nominal state 1 is simply

$$\lambda_1^{A(B)} = \lambda_{1\to 2}^{A(B)} + \lambda_{1\to 3}^{A(B)} \tag{4.6}$$

since the transition times are exponentially distributed and states 2 and 3 are the mutually exclusive and exhaustive arrival states of the transition.

Similarly, the transition rate of component C out of its nominal state 1 is

$$\lambda_1^{C} = \lambda_{1\to 2}^{C} + \lambda_{1\to 3}^{C} + \lambda_{1\to 4}^{C} \tag{4.7}$$

It follows, then, that the rate of transition of the system out of its current configuration $(j_A = 1, j_B = 1, j_C = 1)$ is

$$\lambda^{(1,1,1)} = \lambda_1^A + \lambda_1^B + \lambda_1^C \tag{4.8}$$

We are now in the position of sampling the first system transition time t_1, by applying the inverse transform method for continuous distributions (Sect. 3.3.1, Example 2)

$$t_1 = t_0 - \frac{1}{\lambda^{(1,1,1)}} \ln(1 - R_t) \tag{4.9}$$

where $R_t \sim U[0, 1)$ is a uniform rv.

Assuming that $t_1 < T_M$ (otherwise one would proceed to the successive trial of system simulation), one needs to determine which transition has occurred, i.e., which component has undergone the transition and to which arrival state. This can be done resorting to the inverse transform method for discrete distributions (Sect. 3.3.2). The probabilities of components A, B, C undergoing a transition out of their initial nominal states 1, given that a transition occurs at time t_1, are

$$\frac{\lambda_1^A}{\lambda^{(1,1,1)}}, \frac{\lambda_1^B}{\lambda^{(1,1,1)}}, \frac{\lambda_1^C}{\lambda^{(1,1,1)}} \tag{4.10}$$

respectively.

Figure 4.5 shows an example in which the sampled random number $R_C \sim U[0, 1)$ is such that component B undergoes the transition.

Given that at t_1 component B undergoes a transition, its arrival state can be sampled by applying again the inverse transform method for discrete distributions,

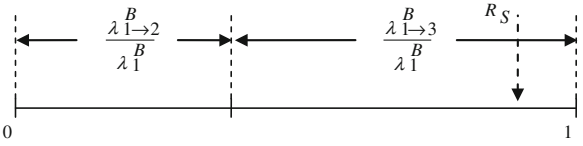

Fig. 4.6 Pictorial representation of the sampling of the arrival state of the transition by the inverse transform method for discrete distributions

this time to the set of discrete probabilities $\left\{\frac{\lambda^B_{1\to 2}}{\lambda^B_1}, \frac{\lambda^B_{1\to 3}}{\lambda^B_1}\right\}$ of the mutually exclusive and exhaustive arrival states of component B. In the example shown in Fig. 4.6, the sampled random number $R_S \sim U[0,1)$ is such that the occurring transition leads component B from state 1 to state 3, i.e., component B fails.

Note that for clarity of explanation, the procedure for sampling the transition $k'(1,1,1) \to k(1,3,1)$ from $C(k|k',t)$ was divided into two steps (component sampling followed by arrival state sampling) but one could have as well divided the interval [0,1) in $2+2+3$ subintervals proportional to $\lambda^A_{1\to 2}, \lambda^A_{1\to 3}, \lambda^B_{1\to 2}, \lambda^B_{1\to 3}, \lambda^C_{1\to 2}, \lambda^C_{1\to 3}, \lambda^C_{1\to 4}$ normalized to $\lambda^{(1,1,1)}$, and used a single random number $R_{CS} \sim U[0,1)$ to sample both the component and the arrival state, i.e., the whole transition, in one shot. The two procedures are statistically equivalent.

As a result of this first transition, at t_1 the system enters configuration (1,3,1). The simulation now continues with the sampling of the next transition time t_2, based on the updated system transition rate

$$\lambda^{(1,3,1)} = \lambda^A_1 + \lambda^B_3 + \lambda^C_1 \tag{4.11}$$

The next transition, then, occurs at

$$t_2 = t_1 - \frac{1}{\lambda^{(1,3,1)}} \ln(1 - R_t) \tag{4.12}$$

where $R_t \sim U[0,1)$.

Assuming again that $t_2 < T_M$, the component undergoing the transition and its arrival state are sampled as before by application of the inverse transform method to the appropriate discrete probabilities.

The trial simulation of the system random walk proceeds through the various transitions from one system configuration to another, until the mission time T_M. As explained earlier, when the system enters a failed configuration (*,*,4) or (3,3,*), where the * denotes any state of the component, its occurrence is recorded.

Finally, the following *Matlab*® program implements the indirect method to estimate the instantaneous unavailability of the considered system and its mean unavailability over a mission time T:

```
clear all
l_A=[0 1e-3 1e-3; 1e-4 0 1e-3; 1e-2 2e-2 0]; l_B=l_A;
l_C=[0 1e-4 1e-4 1e-3; 1e-4 0 1e-3 2e-3; 1e-3 2e-3 0 1e-5; 1e-2 2e-2 3e-2 0];
rates={l_A;l_B;l_C}; n_cmp=size(rates,1); nsim=1e5; bin_l=250; T=1e4;
time=0:bin_l:T; n_bins=length(time); Ca=zeros(1,n_bins);
downtime=zeros(1,nsim);
for i=1:nsim
   t=0;  state=ones(1,n_cmp); r=0; s=zeros(1,n_cmp); failure=0; repair=0;
   down=0; tempo=0;

   while t<=T
      for j=1:n_cmp
         l=rates{j,1};
         s(j)=sum(l(state(j),:));
      end
      r=sum(s); t=t+exprnd(1/r);
      cmp=find(cumsum(s)/r>rand,1,'first');
state(cmp)=find(cumsum(rates{cmp,1}(state(cmp),:))/s(cmp)>rand,1,'first');
      if ((state(1)==3 && state(2)==3) | state(3)==4) && down ==0
         failure=t; down=1;
      else
         repair=min([t T]);
      end
      if (repair >failure ) && down ==1
         failed_bins_m=find(time>failure,1,'first');
         failed_bins_M=find(time<=repair,1,'last');
         Ca(failed_bins_m:failed_bins_M)=Ca(failed_bins_m:failed_bins_M)+1;
         downtime(i)=downtime(i)+repair-failure;  down=0;
      end
   end
end
plot(time,Ca/nsim) mean_unav=mean(downtime)/T;
std_unav=std(downtime/T)/sqrt(nsim)
```

For the purpose of the example, the values of the transition rates of Table 4.1 have been set arbitrarily (Table 4.2) and the mission time has been assumed equal to 104 units of time. Figure 4.7 shows the instantaneous unavailability; the mean unavailability over the mission time is 0.01687.

4.4.2 Direct Simulation Method

The direct method differs from the indirect one in that the system transitions are not sampled by considering the kernel distributions for the whole system but rather by sampling directly the times of all possible transitions of all individual

Table 4.2 Numerical values of the transition rates (in arbitrary units of time $^{-1}$

		Arrival		
Initial		1	2	3
	1	0	$1e-3$	$1e-3$
	2	$1e-4$	0	$1e-3$
	3	$1e-2$	$2e-2$	0

		Arrival			
		1	2	3	4
Initial	1	0	$1e-4$	$1e-4$	$1e-3$
	2	$1e-4$	0	$1e-3$	$2e-3$
	3	$1e-3$	$2e-3$	0	$1e-5$
	4	$1e-2$	$2e-2$	$3e-2$	0

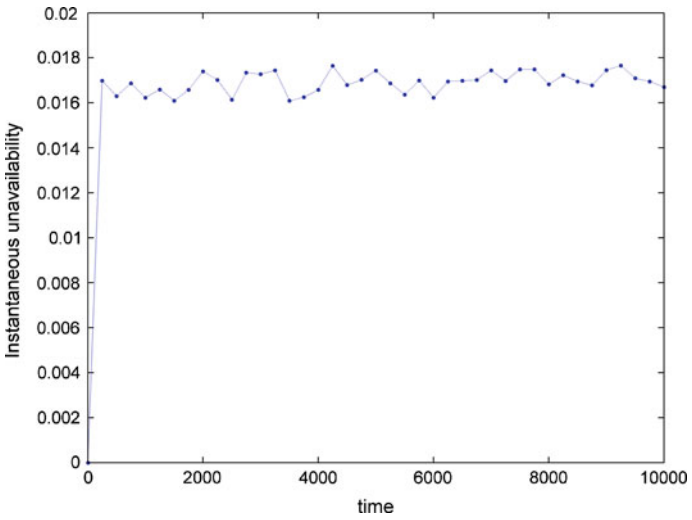

Fig. 4.7 Instantaneous unavailability over time

components of the system and then arranging the transitions along a timeline in increasing order, in accordance to their times of occurrence. The component which actually performs the transition is the one corresponding to the first transition in the timeline.

The timeline is updated after each transition occurs, to include the new possible transitions that the transient component can perform from its new state. In other words, during a system history starting from a given system configuration k' at t', we sample the times of transition $t^i_{j'_i \to m_i}$, $m_i = 1, 2, \ldots, N_{S_i}$, of each component i, $i = 1, 2, \ldots, N_C$ leaving its current state j'_i and arriving to the state m_i from the corresponding transition time probability distributions $f_T^{i,j'_i \to m_i}(t|t')$. The time instants $t^i_{j'_i \to m_i}$ obtained for all arrival states m_i are then arranged in ascending order

along a timeline from $t_{\min}$ to $t_{\max} \leq T_M$. The clock time of the trial is then moved to the first occurring transition time $t_{\min} = t^*$ in correspondence of which the system configuration is changed, i.e., the component i^* undergoing the transition is moved to its new state m_i^*. At this point, the new times of transition $t^{i^*}_{m_{i^*} \to l_i^*}, l_i* = 1, 2, \ldots, N_{S_{i^*}}$, of component i^* out of its current state m_i^* are sampled from the corresponding transition time probability distributions, $f_T^{i^*, m_{i^*} \to l_i^*}(t|t^*)$, and placed in the proper position of the timeline. The clock time and the system are then moved to the next first occurring transition time and corresponding new configuration, respectively, and the procedure repeats until the next first occurring transition time falls beyond the mission time, i.e., $t_{\min} > T_M$.

With respect to the previous example of Sect. 4.4.1, starting at $t = 0$ with the system in nominal configuration (1,1,1) one would sample the times of all possible components transitions

$$t^i_{1 \to m_i} = t_0 - \frac{1}{\lambda^i_{1 \to m_i}} \ln(1 - R^i_{t,1 \to m_i}) \quad \begin{matrix} i = A, B, C \\ m_i = 2, 3 \\ m_i = 2, 3, 4 \end{matrix} \quad \begin{matrix} \\ \text{for } i = A, B \\ \text{for } i = C \end{matrix} \tag{4.13}$$

where $R^i_{t,1 \to m_i} \sim U[0, 1)$.

These transition times would then be ordered in ascending order from $t_{\min}$ to $t_{\max} \leq T_M$. Let us assume that $t_{\min}$ corresponds to the transition of component A to state 3 of failure, i.e., $t_{\min} = t^A_{1 \to 3}$ (Fig. 4.8). The other sampled transition time relating to component A, namely $t^A_{1 \to 2}$, is canceled from the timeline and the current time is moved to $t_1 = t_{\min}$ in correspondence of which the system configuration changes, due to the occurring transition, to (3,1,1) still operational. The new transition times of component A toward the reachable arrival states $m_A = 1{,}2$ are then sampled

$$\begin{aligned} t^A_{3 \to m_A} &= t_1 - \frac{1}{\lambda^A_{3 \to m_A}} \ln(1 - R^A_{t,3 \to m_A}) \\ m_A &= 1, 2 \\ R^A_{t,3 \to m_A} &\sim U[0, 1) \end{aligned} \tag{4.14}$$

and placed at the proper position in the timeline of the succession of occurring transitions. The simulation then proceeds orderly to the successive times in the list, in correspondence of which a system transition occurs. After each transition, the timeline is updated by canceling the times of the transitions relating to the component which has undergone the last transition and by inserting the newly sampled times of the transitions of the same component from its new state to the reachable arrival states.

As with the indirect procedure explained above, when during the trial the system enters a fault configuration ones are collected in the system unreliability counters associated to the time intervals beyond that time, and in the end, after M trials, the unreliability estimate is computed, as previously shown (Fig. 4.3).

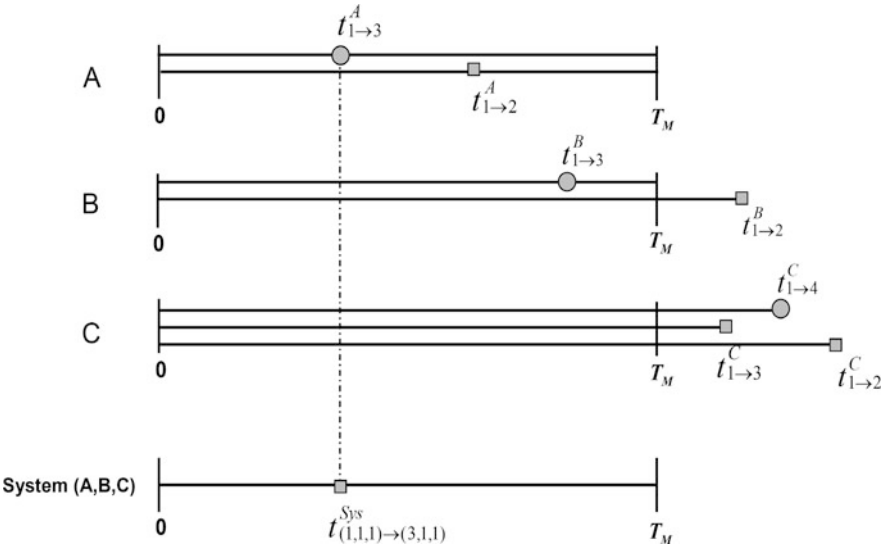

Fig. 4.8 Direct simulation method. The *squares* identify components transitions; the *bullets* identify fault states

Compared to the previous indirect method, the direct approach is more suitable for systems whose components failure and repair behaviors are represented by different stochastic distribution laws whose combination would lead to a complicated system transport kernel (Eq. 4.5) from which sampling of the system transition would be difficult and/or computationally burdensome.

On the other hand, it is important to point out that when dependences among components are present (e.g., due to load or standby configurations) the distribution of the next transition time of a component may be affected by the transition undergone by another component, in which case the next transition time of the affected component (and not only of the transient component) has also to be resampled after the transition. This can increase the burden, and thus reduce the performance, of the direct simulation approach.

In the example above, if the failure of component A changes the failure behavior of its companion component B (e.g., because it is required to carry all the load by itself and therefore is more stressed and prone to failure, which could, for example, translate in larger values of its transition rates out of the nominal state), then also the transition times of B would need to be resampled (with the real transition rates) upon occurrence of the failure of A.

Furthermore, the use of biasing techniques (Sect. 3.4.2) in the direct approach is not trivial, because the effects of introducing modified probability functions for one component have to be accounted for at the whole system level when setting up the modifications to the 'prizes' of the simulation (in the "dart game" view of Sect. 3.4.2).

Finally, the following *Matlab*® program implements the direct simulation method to estimate the instantaneous unavailability of the considered system and its mean unavailability over the mission time T. The lines of code different from the corresponding ones in the code for the indirect method presented at the end of Sect. 4.4.1 have been underlined:

```
clear all
l_A=[0 1e-3 1e-3; 1e-4 0 1e-3; 1e-2 2e-2 0]; l_B=l_A;
l_C=[0 1e-4 1e-4 1e-3; 1e-4 0 1e-3 2e-3; 1e-3 2e-3 0 1e-5; 1e-2 2e-2 3e-2 0];
rates={l_A;l_B;l_C}; n_cmp=size(rates,1); nsim=1e5; bin_l=250; T=1e4;
time=0:bin_l:T; n_bins=length(time); Ca=zeros(1,n_bins);
downtime=zeros(1,nsim);
for i=1:nsim
   t=0;  state=ones(1,n_cmp); t_times=zeros(1,n_cmp); s=zeros(1,n_cmp);
failure=0; repair=0;
   down=0; tempo=0;
   while t<=T
      for j=1:n_cmp
         l=rates{j,1};
         [t_times(j) s(j)]=min(exprnd(1./l(state(j),:)));
      end
      [tempo cmp]=min(t_times);
      state(cmp)=s(cmp);
      t=t+tempo;
      if ((state(1)==3 && state(2)==3) | state(3)==4) && down ==0
         failure=t; down=1;
      else
         repair=min([t T]);
      end
      if (repair >failure ) && down ==1
         failed_bins_m=find(time>failure,1,'first');
         failed_bins_M=find(time<=repair,1,'last');
         Ca(failed_bins_m:failed_bins_M)=Ca(failed_bins_m:failed_bins_M)+1;
         downtime(i)=downtime(i)+repair-failure;  down=0;
      end
   end
end
plot(time,Ca/nsim,'k.') mean_unav=mean(downtime)/T;
std_unav=std(downtime/T)/sqrt(nsim)
```

Figure 4.9 (top) compares the estimations of the system instantaneous unavailability provided by the direct and indirect simulation methods, with the transition rates data of Table 4.2 and $T = 10^4$ units of time. Figure 4.9 (bottom) reports the estimates of the mean unavailability over the mission time with the corresponding 68.3 % confidence intervals.

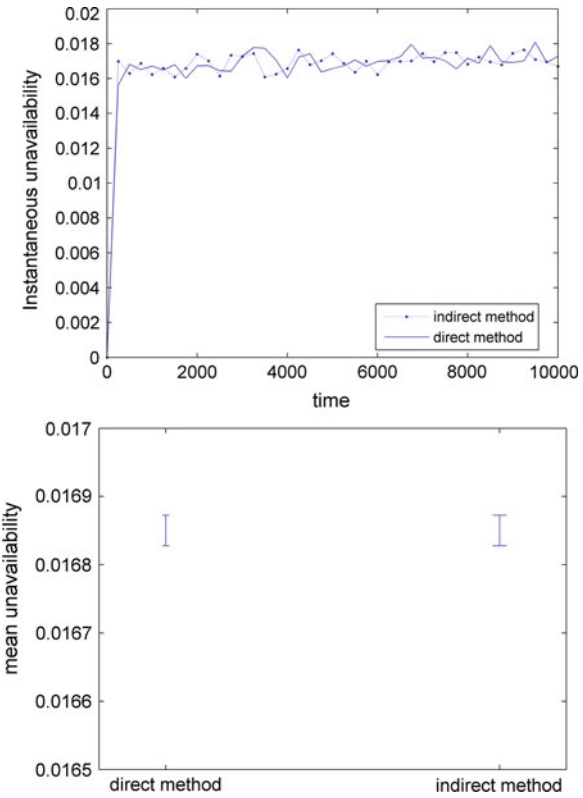

Fig. 4.9 Comparison of the results produced by the Direct and Indirect simulation methods applied to the system of Fig. 4.1, with the transition rate data of Table 4.2: *top*, instantaneous unavailability; *bottom*, mean unavailability over the mission time $T = 10^4$ and 68.3 % confidence intervals

4.5 Transport Theory for System Reliability

As mentioned above, the stochastic process of the system random walk of transitions in time from one configuration to another is governed by the *probabilistic transport kernel* (Eq. 4.5) which gives the probability density for the transition $(t', k') \to (t, k)$. The transport kernel provides a *local* description of the system stochastic process: starting from known time and outcome of the last transition (t', k'), it allows sampling the next time and outcome (t, k). Hence, knowledge of the transport kernel allows performing the simulation of the system random walks by sampling successively the times and outcomes of the transitions.

On the other hand, the full description of the system stochastic behavior in time is given by the pdf that the system makes a transition at a time between t and $t + dt$ leading to state k, independently of the time and outcome of the previous transition, i.e., integrating over all the times and outcomes of the previous transitions from which state k can be reached through a transition at time t (with all different probabilities). This pdf is denoted as $\psi(t, k)$ and can be constructed as the series of the partial probability densities $\psi^n(t, k)$ that the system enters state k at time t due to the n-th transition, $n = 0, 1, \ldots$

$$\psi(t,k) = \sum_{n=0}^{\infty} \psi^n(t,k) \tag{4.15}$$

Let us describe probabilistically the evolution of a random walk, in terms of the partial probability densities $\psi^n(t,k)$, $n = 0, 1, \ldots$. The system is known with certainty to be in state k^* (e.g., the nominal state) at the initial time t^* (e.g., 0). The stochastic evolution of the system proceeds from one transition to the next, $(t^*, k^*) \to (t_1, k_1) \to (t_2, k_2) \to \ldots \to (t_{n-1}, k_{n-1}) \to (t_n, k_n)$. The subsequent partial probability densities describing such stochastic process of evolution are

$$\begin{aligned}
&\psi^1(t_1,k_1) = K(t_1,k_1|t^*,k^*) \\
&\psi^2(t_2,k_2) = \sum_{k_1} \int_{t^*}^{t_2} dt_1 \psi^1(t_1,k_1) K(t_2,k_2|t_1,k_1) \\
&\ldots \\
&\psi^n(t_n,k_n) = \sum_{k_{n-1}} \int_{t^*}^{t_n} dt_{n-1} \psi^{n-1}(t_{n-1},k_{n-1}) K(t_n,k_n|t_{n-1},k_{n-1})
\end{aligned} \tag{4.16}$$

For example, the second equation defines the partial probability density $\psi^2(t_2,k_2)$ that the system makes its second transition at time t_2 which results in its entrance in state k_2. It is computed as the sum of the probability densities of all possible, mutually exclusive scenarios along which the system has a first transition in state k_1 at a time t_1 prior to t_2, i.e., $t_1 \in [t^*, t_2]$, with probability density $\psi^1(t_1,k_1)$ and from there it 'transports' to the next transition time t_2 and state k_2 with probability density $K(t_2,k_2|t_1,k_1)$. Note that the summation is actually such on the discrete rv describing the state of origin of the transition, k_1, whereas it is an integration over the continuous rv representing the previous transition time, t_1.

From the definition of the $\psi^n(t,k)$, $n = 0, 1, \ldots$, it is clear that they provide the desired *integral* description of the system stochastic process of transition with respect to the probability of making the n-th transition at a given time t_n leading the system to a given state k_n, which is given by the sum of the probabilities of all mutually exclusive random walks doing so. Note that in the situation described in which the initial time and state are known with certainty, the 0-th probability density is actually a Dirac delta in time located at t^* and a Kronecker delta in system state located at k^*, viz.,

$$\psi^0(t^*,k^*) = \delta(t-t^*)\delta_{kk^*} \tag{4.17}$$

Substituting in Eq. (4.16) t_n, k_n by t, k, and t_{n-1}, k_{n-1} by t' and k', the expression for ψ^n at the generic time t and state k becomes

$$\psi^n(t,k) = \sum_{k'} \int_{t^*}^{t} dt' \psi^{n-1}(t',k') K(t,k|t',k') \tag{4.18}$$

From Eq. (4.15), the probability density $\psi(t,k)$ of a transition at time t as a result of which the system enters state k is given by the series of all the possible partial transition densities, viz.,

$$\psi(t,k) = \sum_{n=0}^{\infty} \psi^n(t,k) = \psi^0(t,k) + \sum_{k'} \int_{t^*}^{t} dt' \psi(t',k') K(t,k|t',k') \tag{4.19}$$

This is the Boltzmann integral equation for the probability density of a system transition to state k occurring at time t. The solution to this equation can be obtained by standard analytical or numerical methods, under given simplifying assumptions, or with the MC method under realistic assumptions. In this latter case, a large number $M \gg 1$ of system life *histories* is performed (as explained in Sect. 4.4.1), each of which is a realization (random walk) of the system stochastic process of evolution in time. The ensemble of the random walks realized by the MC histories allows estimating the transition probability density $\psi(t,k)$.

To generate the random walks, the partial transition densities are first rewritten as follows, by successive substitutions

$$\begin{aligned}
\psi^1(t_1,k_1) &= K(t_1,k_1|t^*,k^*) \\
\psi^2(t_2,k_2) &= \sum_{k_1} \int_{t^*}^{t_2} dt_1 \psi^1(t_1,k_1) K(t_2,k_2|t_1,k_1) \\
&= \sum_{k_1} \int_{t^*}^{t_2} dt_1 K(t_1,k_1|t^*,k^*) K(t_2,k_2|t_1,k_1) \\
\psi^3(t_3,k_3) &= \sum_{k_2} \int_{t^*}^{t_3} dt_2 \psi^2(t_2,k_2) K(t_3,k_3|t_2,k_2) \\
&= \sum_{k_1,k_2} \int_{t^*}^{t_3} dt_2 \int_{t^*}^{t_2} dt_1 K(t_1,k_1|t^*,k^*) K(t_2,k_2|t_1,k_1) K(t_3,k_3|t_2,k_2) \\
&\dots \\
\psi^n(t,k) &= \\
&\sum_{k_1,k_2,\dots,k_{n-1}} \int_{t^*}^{t} dt_{n-1} \int_{t^*}^{t_{n-1}} dt_{n-2} \dots \int_{t^*}^{t_2} dt_1 K(t_1,k_1|t^*,k^*) K(t_2,k_2|t_1,k_1) \\
&\dots K(t,k|t_{n-1},k_{n-1})
\end{aligned} \tag{4.20}$$

Equation (4.20) shows that $\psi^n(t,k)$ can be calculated from the integration of the transport kernels over all possible random walks constituted of n intermediate transitions

$$(t^*, k^*) \rightarrow (t_1, k_1) \rightarrow (t_2, k_2) \rightarrow \ldots \rightarrow (t_{n-1}, k_{n-1}) \rightarrow (t_n, k_n) \rightarrow (t, k) \quad (4.21)$$

Conceptually, the MC estimation of the multidimensional integral defining $\psi^n(t,k)$ amounts to simulating a large number M of random walks and counting the number of these random walks whose n-th transition indeed occurs at time t, with the system indeed entering the state k: the frequency of these occurrences, i.e., the ratio of the number of occurrences over M, gives an estimate of $\psi^n(t,k)$. Actually, if during the simulation of the random walks the occurrence of a transition at time t which leads the system into state k is recorded independently of the order n of the transition, then the frequency of such occurrences over the M simulated histories gives directly an estimate of $\psi(t,k)$.

From the point of view of the implementation into a computer code, the system mission time is subdivided in N_t intervals of length Δt and to each time interval N counters are associated, one for each state of the system. Every time the system undergoes a transition of any order $n = 1,2,\ldots$, for which the system enters state k at time $t \in \Delta t_l$, the content C_{lk} of the lk-th counter is incremented by one. At the end of all the M MC histories, C_{lk} is equal to the number of occurrences of the system undergoing a transition (of any order) at time $t \in \Delta t_l$ which leads it into state k. An estimate of the transition probability density is then

$$\psi(t,k) \approx \frac{1}{\Delta t} \int_{\Delta t_l} \psi(\tau,k) d\tau \approx \frac{1}{\Delta t} \frac{C_{lk}}{M} \quad (4.22)$$

$$t \in \Delta t_l; \;\; l = 1,2,\ldots,N_t; \;\; k = 1,2,\ldots,N$$

With respect to the problem of estimating the system unreliability at time t, $F_T(t)$, let us recall that it is the probability that a system failure occurs before time t, i.e., that the system enters one of its fault states $k \in \Gamma$ prior to t. This probability is given by the sum of the probabilities of all mutually exclusive random walks which at a time τ prior to t, i.e., $\tau \in [0,t]$ lead the system into a fault state $k \in \Gamma$, i.e.,

$$F_T(t) = \sum_{k \in \Gamma} \int_0^t \psi(\tau,k) d\tau \quad (4.23)$$

where $\psi(\tau,k)$ is the probability density of undergoing a transition (of any order n) at time τ which leads the system into state k, i.e., of entering state k at time τ. Note that, it has been assumed that the system starts at time $t^* = 0$ and with respect to the continuous rv τ the summation becomes an integral, as explained before.

In Sect. 4.4, we have illustrated the practical procedure for estimating $F_T(t)$ by MCS (Fig. 4.3): (i) M random walks are sampled from the transport kernels; (ii) for each random walk in which the system enters a state $k \in \Gamma$ at time $\tau < t$, a one is cumulated in the counter associated to the time t; (iii) the estimate $\hat{F}_T(t)$ of the unreliability at time t is given by the cumulative value in the counter at the end of the M simulated random walks divided by M. Such procedure is actually a *dart*

game of the kind illustrated in Sect. 3.4.1. Indeed, Eq. (4.23) is an integral of the kind of Eq. (3.121) where $\underline{x}$ is the whole sequence of transition points, $(t^*, k^*; t_1, k_1; t_2, k_2, \ldots)$ (Fig. 4.2), the probability density function $f_{\underline{X}}(\underline{x})$ is $\psi(\tau, k)$ and the prize $g(\underline{x})$ is 1 and it is collected when the *dart* hits the target, i.e., the sequence of transition points, $(t^*, k^*; t_1, k_1; t_2, k_2, \ldots)$ ends in a fault state $k \in \Gamma$ at time $\tau < t$ (the circle bullets of Figs. 4.2 and 4.3). Note that for sampling the random walks of transition points $(t^*, k^*; t_1, k_1; t_2, k_2, \ldots)$ it is not necessary to know the probability density $\psi(\tau, k)$ since the random walks can be generated step-by-step by sampling from the probabilistic transport kernel of Eq. (4.5) (Fig. 4.1).

Similarly, the system unavailability at time t, $q(t)$, i.e., the probability that the system is in a fault state at time t (i.e. the complement to one of the system availability introduced in Sect. 2.1), is given by the sum of the probabilities of all mutually exclusive random walks which lead the system in a state $k \in \Gamma$ at a time τ prior to t and in which the system remains beyond time t, i.e.,

$$q(t) = \sum_{k \in \Gamma} \int_0^t \psi(\tau, k) R_k(\tau, t) d\tau \tag{4.24}$$

where $R_k(\tau, t)$ is the probability of the system not exiting before t from the failed state k entered at $\tau < t$.

An estimate of $q(t)$ may be obtained by MCS of the system random walks as was done for the unreliability estimation. Let us consider a single random walk and suppose that the system enters a failed state $k \in \Gamma$ at time τ_{in}, exiting from it at the next transition at time τ_{out}; as before, the time is suitably discretized in intervals of length Δt and cumulative counters $C^A(t)$ are introduced which accumulate the contributions to $q(t)$ in the time channels: in this case, we accumulate a unitary weight in the counters for all the time channels within $[\tau_{in}, \tau_{out}]$ during which the system is found in the unavailable state k. After performing all the M MC histories, the content of each counter divided by the number of histories M gives an estimate of the unavailability at that counter time (Fig. 4.10). This procedure corresponds to performing an ensemble average of the realizations of the stochastic process governing the system life.

The system transport formulation behind Eq. (4.24) suggests another analog MCS procedure. In a single MCS trial, the contributions to the unavailability at a generic time t are obtained by considering all the preceding entrances, during this trial, into failed states $k \in \Gamma$. Each such entrance at a time τ gives rise to a contribution in the counters of unavailability for all successsive time instants up to the mission time, represented by the probability $R_k(\tau, t)$ of remaining in that failed state at least up to t. In case of a system made up of components with exponentially distributed failure and repair times, we have

$$R_k(\tau, t) = e^{-\lambda^k (t - \tau)} \tag{4.25}$$

where λ^k is the sum of the transition rates (repairs or further failures) out of state k.

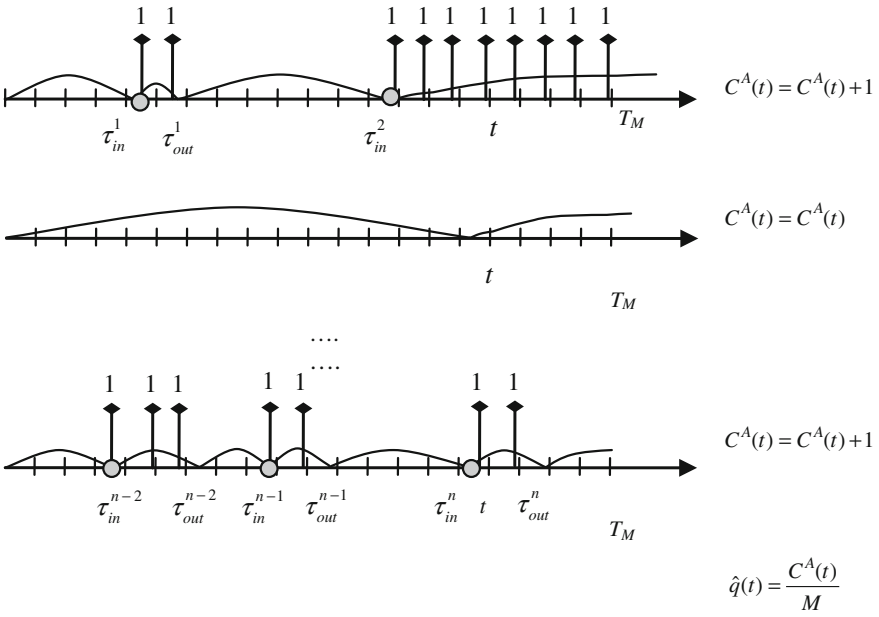

Fig. 4.10 MCS estimation procedure of unavailability $q(t)$. In the first history, the system enters the failed configuration at $\tau^1_{in} < t$ and exits at $\tau^1_{out} < t$; then it enters another, possibly different, failed configuration $k_2 \in \Gamma$ at $\tau^2_{in} < t$ and does not exit before the mission time T_M: for the estimation of the unavailability $q(t)$ the cumulative counter $C^A((t)$ is correspondingly updated by collecting a one in the counter. In the second history, no transitions at all occur before t; hence, the counter $C^A(t)$ remains unmodified. In the last history, the system enters a failed configuration, possibly different from the previous ones, at $\tau^n_{in} < t$ and exits from it after t; the cumulative counter $C^A(t)$ is again correspondingly updated by collecting a one in the counter. In the end, the quantity $\hat{q}(t)$, frequency of unavailability occurrences at time t, gives the MCS estimate of the system unavailability at time t, $q(t)$

Again, after performing all the MC histories, the contents of each unavailability counter are divided by the total number of histories M to provide an estimate of the mean time-dependent unavailability (Fig. 4.11).

The two analog MCS procedures presented above are equivalent and both lead to satisfactory estimates. Indeed, with reference to the underlying stochastic process, consider an entrance in state $k \in \Gamma$ at time τ, which occurs with probability density $\psi(\tau, k)$, and a subsequent generic time t: in the first procedure a one is scored in the counter pertaining to t only if the system has not left the state k before t and this

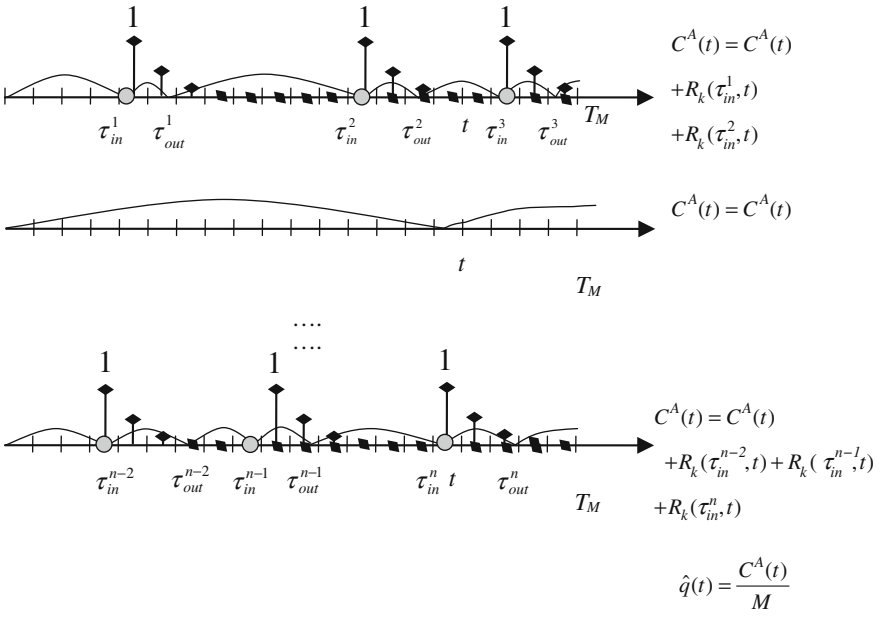

Fig. 4.11 MCS unavailability estimation procedure of collecting $R_k(\tau_{in}, t)$ contributions in all counters $C^A(t)$ associated to time t, following a failure to configuration $k \in \Gamma$ occurred at $\tau_{in} < t$. In the first history, the system enters three failed, possibly different configurations at $\tau_{in}^1 < t$, $\tau_{in}^2 < t$ and $\tau_{in}^3 > t$. For the estimation of the unavailability $q(t)$, the cumulative counter $C_A(t)$ is updated by collecting $R_k(\tau_{in}^1, t)$ and $R_k(\tau_{in}^2, t)$ in the counter, whereas the last failure does not contribute to $q(t)$ because the system has already passed the time of interest t. In the second history, no transitions at all occur before t; hence, the counter $C^A(t)$ remains unmodified. In the last history, the system fails three times; the cumulative counter $C^A(t)$ is correspondingly updated by adding the unavailability contributions brought by the three events. In the end, the quantity $\hat{q}(t)$, frequency of unavailability occurrences at time t, gives the MCS estimate of the system unavailability at time t, q(t)

occurs with probability $R_k(\tau, t)$. In this case, the collection of ones in t obeys a Bernoulli process with parameter $\psi(\tau, k) \cdot R_k(\tau, t)$ and after M trials the mean contribution to the unavailability counter at t is given by $M \cdot \psi(\tau, k) \cdot R_k(\tau, t)$. Thus, the process of collecting ones in correspondence of a given t over M MC trials and then dividing by M leads to estimating the quantity of interest $q(t)$. On the other hand, the second procedure leads, in correspondence of each entrance in state $k \in \Gamma$ at time τ, which again occurs with probability density $\psi(\tau, k)$, to scoring a contribution $R_k(\tau, t)$ in all the counters corresponding to $t > \tau$ so that the total accumulated contribution in all the M histories is again $M \cdot \psi(\tau, k) \cdot R_k(\tau, t)$. Dividing the accumulated score by M yields the estimate of $q(t)$. Thus, the two procedures lead to equivalent ensemble averages, even if with different variances. Here, we shall not discuss the subject of the variance.

The situation is quite different in case of a biased MCS in which all the transition rates are possibly varied. At any generic sampling of the rv X_n (which could be a transition time or state) in the biased, or forced, random walk when a biased $f_{X_n}{}^*(x_n)$ is used instead of the natural $f_{X_n}(x_n)$, the *weight* of the history is multiplied by $f_{X_n}(x_n)/f_{X_n}{}^*(x_n)$ and the prize is the weight accumulated in the trial up to that point. More specifically, in the biased MCS a weight is associated to each trial, it is initialized to unity and then updated by the factor $f_{X_n}(x_n)/f_{X_n}{}^*(x_n)$ every time a quantity x_n, with natural $f_{X_n}(x_n)$, is instead sampled from the biased $f_{X_n}{}^*(x_n)$. Note that the weight is in itself a rv depending, in each trial, on the number of times the biased probability has been used and on the values sampled from such probability.

In our specific application of system unreliability and unavailability calculations, biasing is used to artificially increase the probability of system trajectories in the phase space which lead the system toward entering a failed state $k \in \Gamma$. In case of exponential components, this objective may be achieved, for example, by properly modifying the components' natural transition rates λ to biased values λ^* which favor certain transitions [6].

With reference to the unavailability $q(t)$ of Eq. (4.24), following the lines of the previously presented analog simulation procedures, we may again conceive two approaches to estimation by a biased MCS of M trials; we anticipate that the first of them may lead to erroneous results:

1. The first approach closely adheres to the standard analog procedure of collecting unitary weights in the time-channeled counters when the system is in a failed state. Assume that in a given trial the biased probabilities are such to lead the system to enter a failed state $k \in \Gamma$ at time τ_{in} with weight w_{in}, and to exit from it at the next transition at time τ_{out}, sampled from the biased $R_k{}^*(\tau_{in}, t)$ which depends on the biased pdf $f_{X_n}{}^*(x_n)$ of the stochastic parameters X_n governing the possible transitions out of k. This time, as prize instead of a one we accumulate the current trial weight $w_{in} = \frac{\psi(\tau_{in},k)}{\psi^*(\tau_{in},k)}$ in the counters of all the time channels centered at $t \in [\tau_{in}, \tau_{out}]$. After performing all the M MCS trials, the accumulated weights contained in each counter are divided by the number of histories M to give an estimate of the unavailability at that time t. However, this procedure leads to erroneous results. Indeed, let us now switch our attention from the single trial to the ensemble of M trials. Considering a generic time t, the weight collected in t with the above procedure obeys a Bernoulli process with parameter $\psi^*(\tau, k) \cdot R_k{}^*(\tau, t)$, where $\psi^*(\tau, k)$ is the probability that the system enters a (failed) state $k \in \Gamma$ at time $\tau < t$ and $R_k{}^*(\tau, t)$ is the probability of the system remaining in state k at least up to time t. After M trials the overall contribution to the unavailability counter at t is given by $M \cdot \frac{\psi(\tau,k)}{\psi^*(\tau,k)} \cdot \psi^*(\tau, k) \cdot R_k^*(\tau, t)$, Thus, the process of collecting weights over M MCS trials and then dividing by M amounts to estimating $\sum_{k\in\Gamma} \int \psi(\tau, k) \cdot R_k{}^*(\tau, t) d\tau$, an erroneous result which differs, in general, from the quantity of interest $q(t)$ of Eq. (4.24).

2. According to the second procedure, in a given trial, the contributions to the unavailability at generic time t are obtained, in accordance to Eq. (4.24), by considering all the preceding entrances during this trial in failed states $k \in \Gamma$. In this biased case, such entrances depend on the biased probability density $\psi^*(\tau, k)$ and give rise to a contribution in the counters of unavailability for all successive times t up to the mission time. In this biased case, the contribution at time $t > \tau$ is represented by the product of the current trial weight $\frac{\psi(\tau,k)}{\psi^*(\tau,k)}$ times the natural probability $R_k(\tau, t)$ of remaining in that failed state at least up to t. Again, after performing all the MCS histories, the contents of each unavailability counter are divided by the total number of histories M to provide an estimate of $k \in \Gamma$ at time τ, which occurs with biased probability density $\psi^*(\tau, k)$, this procedure leads to scoring the prize $M \cdot \psi^*(\tau, k)$ times a contribution $\frac{\psi(\tau,k)}{\psi^*(\tau,k)} R_k(\tau, t)$ in the counter corresponding to $t > \tau$ so that the total accumulated contribution is $M \cdot \psi(\tau, k) \cdot R_k(\tau, t)$. Dividing the accumulated score by M yields the proper, unbiased estimate of the unavailability $q(t)$ of Eq. (4.24).

References

1. Cashwell, E. D., & Everett, C. J. (1959). *A practical manual of the monte carlo method for random walk problems*. New York: Pergamon Press.
2. Dubi, A. (1999). *Monte Carlo applications in systems engineering*. New York: Wiley.
3. Lux, I., & Koblinger, L. (1991). *Monte Carlo particle transport methods: neutron and photon calculations*. Boca Raton: CRC Press.
4. Rubinstein, R. Y. (1981). *Simulation and the Monte Carlo method*. New York: Wiley.
5. Labeau, P. E., & Zio, E. (2002). Procedures Of Monte Carlo transport simulation for applications in system engineering. *Reliability Engineering and System Safety, 77*, 217–228.
6. Marseguerra, M., & Zio, E. (1993). Nonlinear Monte Carlo reliability analysis with biasing towards top event. *Reliability Engineering and System Safety, 40*(1), 31–42.

Chapter 5
Practical Applications of Monte Carlo Simulation for System Reliability Analysis

In this chapter, we shall illustrate some applications of MCS applied to system reliability analysis. First, the power of MCS for realistic system modeling is shown with regard to a problem of estimating the production availability of an offshore plant, accounting for its operative rules and maintenance procedures [1]. Then, the application of MCS for sensitivity and importance analysis [1, 2] is illustrated.

5.1 Monte Carlo Simulation Estimation of the Production Availability of an Offshore Oil Plant

We consider the problem of determining the production availability of an offshore installation in which different kinds of production processes are carried out as shown in Fig. 5.1. The offshore installation is designed for the extraction of flow from a well and the successive separation of the incoming flow in three different components: gas, oil, and water [1].

The gas, separated by the separation unit from the water and oil coming from the well, is first compressed by two turbo-compressors (TCs), then dehydrated through a Tri-Ethylene Glycol (TEG) unit and finally exported. The nominal capacity of the gas exported is 3.0×10^6 Sm^3/d at the pressure of 60 bar. The gas capacity for the components is shown in Table 5.1. A flare is installed for safety purposes, to burn the gas when it cannot be exported.

The oil coming from the production well is separated by the separation unit and, after treatment, is exported through a pumping unit. In the perfect case of all units operating at their maximum capacity, 23,300 m^3/d of oil are exported. The capacities of the components for the oil production are summarized in Table 5.1.

E. Zio, *The Monte Carlo Simulation Method for System Reliability and Risk Analysis*, Springer Series in Reliability Engineering,
DOI: 10.1007/978-1-4471-4588-2_5, © Springer-Verlag London 2013

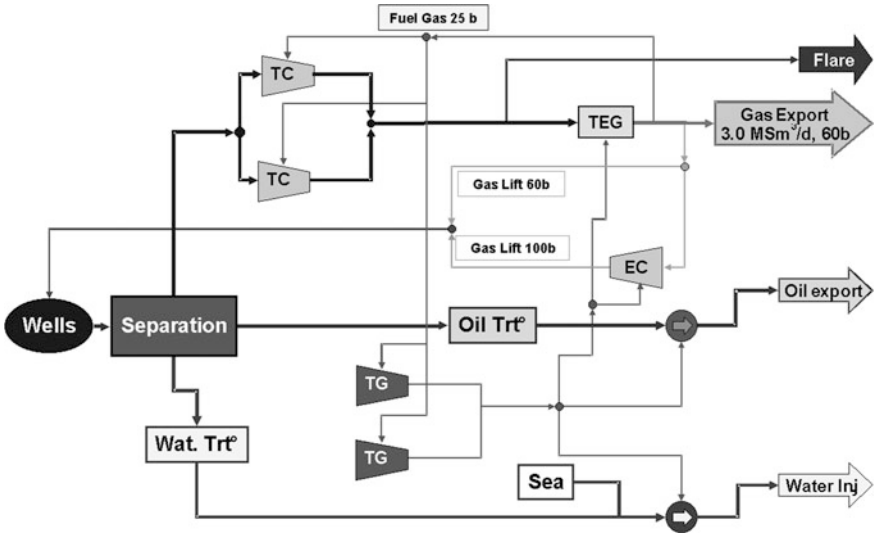

Fig. 5.1 Scheme of the offshore production plant

Table 5.1 Maximum capacities of the components of the gas, oil and water production processes

	Max capacity		
Component	Gas (Sm^3/d)	Oil (m^3/d)	Water (m^3/d)
Well	5.0×10^6	26,500	8,000
Separator unit	4.4×10^6	23,300	7,000
Oil treatment	–	23,300	–
Water treatment	–	–	7,000
Pumping unit	–	23,300	7,000
TC	2.2×10^6	–	–
TEG	4.4×10^6	–	–

As for the oil production, the water coming from the well is separated by the separation unit and, after treatment, is re-injected in the field in addition with seawater. The capacities of the components involved in the water production process are shown in Table 5.1.

To achieve the nominal level of production of the well, compressed gas is injected at the bottom in a so-called 'gas lift' configuration in which a fraction of the export gas (1.0×10^6 Sm^3/d) at the output of the TEG is diverted and compressed by an electro-compressor (EC) and finally injected, at a pressure of 100 bar, in the well. Alternatively, the gas lift can be injected directly in the well at a lower pressure (60 bar), but in this case the production level is reduced to 80 % of its maximum. When gas is not available for the gas lift, the production of the well is reduced to 60 % of its maximum. The gas lift creates a first operational loop in the plant because the input to the plant (i.e., the incoming flow of the well)

Table 5.2 Production of the well for different gas lift pressures

Gas lift		Gas	Oil	Water
Bar	Sm^3/d	Sm^3/d	m^3/d	m^3/d
100	1.0×10^6	5.0×10^6	26,500	8,000
60	1.0×10^6	4.0×10^6	21,200	6,400
0	0	3.0×10^6	15,900	4,800

Table 5.3 Electricity production and consumption of the components of the system

Component	Electricity production	Electricity consumption
	MW	MW
TG	13	–
EC	–	6
Export oil pumping unit	–	7
Water injection pumping unit	–	7
TEG	–	6

depends on the output (i.e., the export gas) of the plant itself. The production levels of the well are summarized in Table 5.2 as a function of the gas lift pressure.

A certain amount of gas also needs to be distributed to the two TCs and the two turbogenerators (TGs) used for the electricity production. Each individual TG and TC consumes 1.0×10^6 Sm^3/d. Such amount of 'fuel gas' is taken from the export gas at the output of the TEG unit. This establishes a second loop in the gas process scheme because the gas compressed by the two TCs is needed to run the TCs themselves.

The electricity produced by the two TGs is used to power the TEG unit, the EC, the oil export pumping unit, and the water injection pumping unit. In Table 5.3, the electric capacities of the components are summarized. Also here, there is a loop in the system because the gas produced by the TEG unit is used to produce, through the connection with the two TGs, the electricity consumed by the TEG unit itself.

For simplicity of illustration, only the failures of the TCs, TGs, EC, and TEG are taken into account. All the other components of the system are assumed to be always in their perfect state of functioning.

The TGs and TCs can be in three different states, indexed as follows: 0 = As good as new; 1 = Degraded; 2 = Failed. The EC and TEG can be in two states: 0 = As good as new; 2 = Failed. The 'Failed' state is such that the function of the component is lost. The 'Degraded' state is such that the function of the component is maintained but in this state the component has higher probability of going into the 'Failed' state: therefore, also when in this state the component needs to be repaired.

For simplicity, the times at which the degradation and failure transitions occur and the duration of the corrective maintenances (repairs) are assumed to be exponentially distributed, with values of the rates reported in Table 5.4. The failure rates are indicated with the Greek letter λ whereas the transitions of repair are indicated with the Greek letter μ.

Table 5.4 Failure and repair rates of the components

Transition	Rate (1/h)			
Component	TEG	EC	TG	TC
Number	1	2	3–4	5–6
$0 \rightarrow 1$	–	–	7.90×10^{-4}	6.70×10^{-4}
$1 \rightarrow 2$	–	–	1.86×10^{-3}	2.12×10^{-4}
$0 \rightarrow 2$	5.70×10^{-5}	1.70×10^{-4}	7.70×10^{-4}	7.40×10^{-4}
$1 \rightarrow 0$	–	–	3.20×10^{-2}	3.30×10^{-2}
$2 \rightarrow 0$	3.33×10^{-1}	3.20×10^{-2}	3.80×10^{-2}	4.80×10^{-2}

Table 5.5 Production components repair priority levels

Priority	Component	System conditions
1	TEG	–
1	TG	Other TG failed
1	TC	Other TC failed
2	EC	–
2	TC	Other TC not failed
3	TG	Other TG not failed

Only a single team is available for corrective maintenance, i.e., to perform repairs upon failures of the components of the system. This implies that only one component at a time can be repaired: when two or more components are failed at the same time, the maintenance team starts to repair the component which is most important with respect to system production. However, once a repair is started, it is brought to completion even if another component with higher repair priority were to fail.

The following priority of repair is introduced to handle the corrective maintenance dynamics:

- *Level* 1: utmost priority level. It pertains to components whose failures lead immediately to a total loss of the production process;
- *Level* 2: medium priority level. It applies to failures leading only to a partial loss of the export oil;
- *Level* 3: lower priority level. It pertains to failures which result in no loss of export oil.

With these rules, one can assign a priority of repair to each component, which is dependent on the system state, as shown in Table 5.5.

The TGs, TCs, and EC are subject to periodic preventive maintenance performed by a single team, different from the team for the corrective maintenance.

In order to maintain the production at a level as high as possible, preventive maintenance actions cannot be started if the system is not in a perfect state of operation, i.e., while some repair or other preventive maintenance action is taking place which limits the system production. While a preventive maintenance action is performed on a component, the other operating components can obviously fail

Table 5.6 Preventive maintenance strategy, in order of increasing period and mean duration

Type of maintenance	Component	Period (h)	Mean duration (h)
1	TC, TG	2,160	4
2	EC	2,666	113
3	TC, TG	8,760	120
4	TC, TG	43,800	672

and corresponding corrective maintenance actions are immediately undertaken. These failure and repair occurrences do not cause any disturbance on the preventive maintenance action, which goes on unaffected.

Four different types of preventive maintenance actions are considered for the test case, each one characterized by a different frequency and different mean duration (Table 5.6). For simplicity, the durations of the preventive maintenance are also assumed to be exponentially distributed variables.

When a failure occurs, the system is reconfigured in order to minimize, first of all, the impact on the export oil and then the impact on the exported gas. The impact on the water injection is considered as to not matter. Depending on these strategies of production reconfiguration, the different component failures have different effects on the three types of system production.

When only one TG fails, the 'export oil', 'fuel gas', and 'gas lift' are still served but the EC and the 'water injection' are stopped due to the lower level of electricity production. Indeed, the TG left running is unable to produce the electricity needed by the whole system and this requires that the EC and the pumping unit for the water injection be stopped. As a consequence, the 'export gas' and the 'export oil' decrease due to an overall lower production of the well caused by the unavailability of the 'gas lift' high pressure. When both TGs are lost, all productions are stopped because the TEG unit is not powered and it is not possible to use gas which has not been dehydrated.

When one TC is lost, 'export oil', 'export gas', 'fuel gas', and 'gas lift' are maintained. The non-compressed part of the gas is flared and therefore the quantity of 'export gas' is reduced. When both TCs are lost, all productions are stopped because without compressed gas it is not possible to produce fuel gas and, consequently, electricity to power the components.

When the TEG fails, the entire system is shutdown because it is not possible to use not dehydrated gas.

When the EC fails, the 'gas lift' pressure decreases and so do the well productions of 'export oil' and 'export gas'.

An analytic approach, e.g., by Markov modeling, to the evaluation of production availability is impractical for the complex system operational dynamics considered here. The number of possible configurations of the system, made of four components (two TCs and two TGs) that may be in three different states and two components (EC and TEG) that may be in two states, is not too large but a significant modeling complication derives from the fact that the periodic

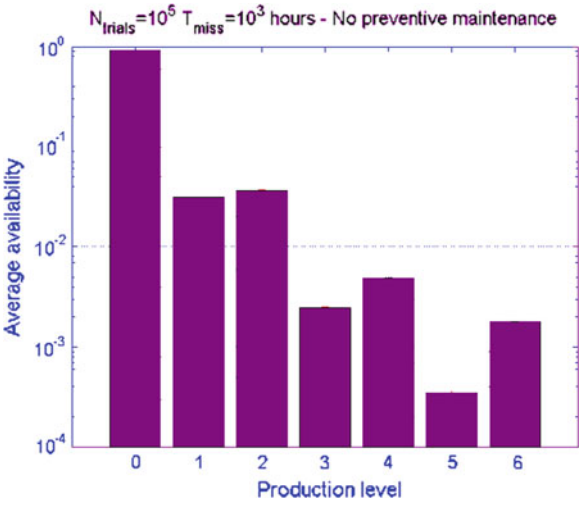

Fig. 5.2 Average plant availability over the mission time on the different production levels for the system without periodic preventive maintenance

maintenance actions are actually performed only if the system is in a perfect state, otherwise they are postponed. This implies that the maintenance periods are conditioned by the state of the plant.

On the contrary, the MCS approach can take into account the realistic aspects of system operation, without additional burden on the solution of the model. This has been here achieved by simulating with the indirect approach of Sect. 4.4.1 a large number of system random walks realized, one at a time, from the beginning of their operation to the end of their mission. This provides a sample of realizations of the system stochastic life process from which sample averages of the time-dependent oil, gas, and water production availabilities are performed.

To obtain the time-dependent production availabilities, the time is suitably discretized in intervals and counters are introduced to accumulate the contributions to production availability at different levels. It turns out that the system can be in seven different production levels of gas, oil, and water which can be automatically associated to the configuration of its components by extension of what is done for the unreliability and unavailability analyses of systems with two production levels (full production and no production) and N_C components with two states (working and failed). The details of this procedure can be found in [1].

First, the case in which the plant components do not undergo preventive maintenance has been considered. The system life evolution has been followed for a mission time T_M of 10^3 h, for a total computation time of 15 min on an Athlon@1400 MHz.

The average availability over the mission time of each production level is reported in Fig. 5.2. The plant is highly available (92.2 %) at the full production level (level 0). Figure 5.3 shows the time evolution of the expected values of the production of gas, oil, and water. After a short transient of about 140 h, the productions, as expected, reach their asymptotic values.

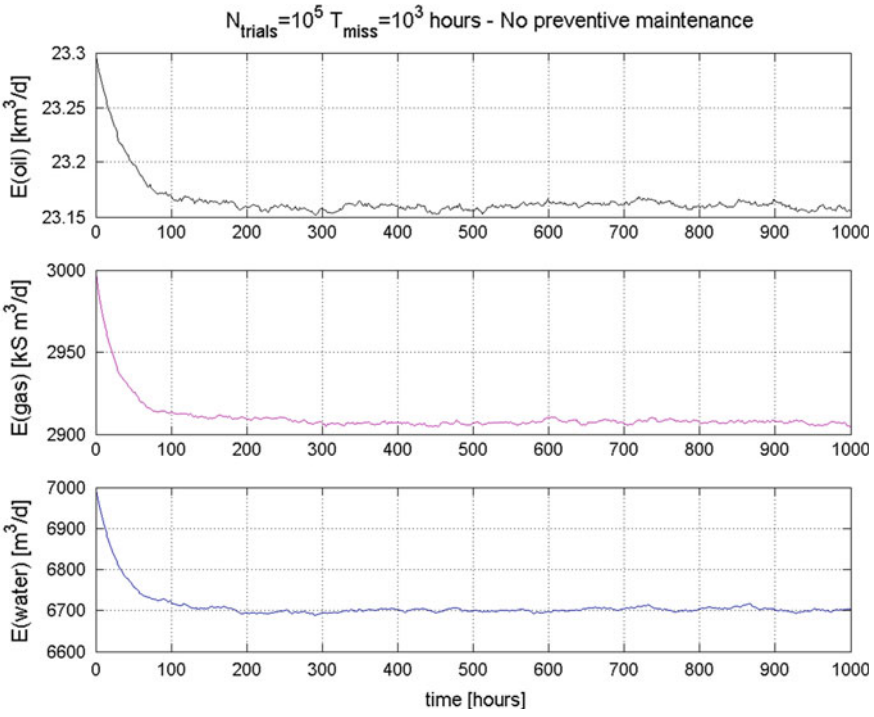

Fig. 5.3 Expected values of the gas (*top*), oil (*middle*) and water (*bottom*) production as a function of time for the system without preventive maintenance

Then, the behavior of the real system with periodic preventive maintenance has been analyzed. The mission time T_M for this case has been extended to 5×10^5 h, so as to capture the effects also of the maintenance action of type 4 which has a very long period. The computing time in this case increases to several hours, which would call for the implementation of some non-analog, biasing procedures to improve the simulation performance (Sect. 3.4.2).

The results of the average availability over the mission time of each production level of the plant are reported in Fig. 5.4. The plant production capacity appears reduced with respect to the case of no preventive maintenance of Fig. 5.2, with the plant having higher probabilities of performing at lower production levels. This is due to the fact that while some components are under maintenance, the plant is in a more critical state with respect to possible failures. For example the probability of no production (level 6) increases from 1.8×10^{-3} to 1.5×10^{-2}, due to the fact that when a TC is under preventive maintenance if the other one fails the system fails to no production. Figure 5.5 shows the time evolution of the expected values of the productions of gas, oil, and water.

Finally, Table 5.7 shows the effects of preventive maintenance by comparing the expected oil, gas, and water productions per year in the two cases, without and

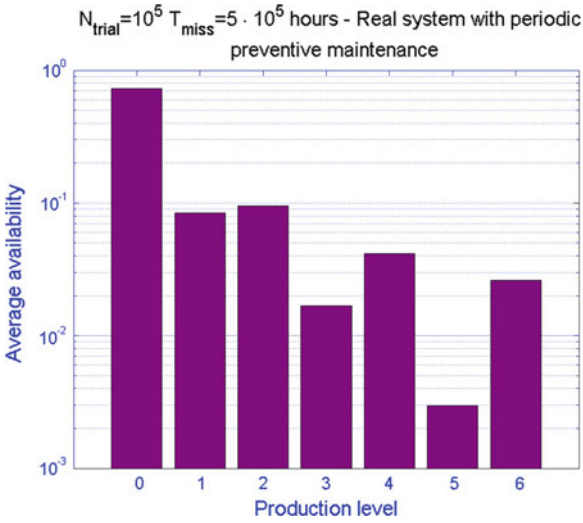

Fig. 5.4 Average plant availability over the mission time of the different production levels for the real system with periodic preventive maintenance

with preventive maintenance. Preventive maintenance appears to slightly decrease the production, as expected from the fact that it operates on components which are assumed not to age (constant failure rates) and thus has the sole effect of rendering them unavailable during maintenance, without mitigating their failure processes.

5.2 Monte Carlo Simulation for Sensitivity and Importance Analysis

In this section, we apply the MCS method for system transport analysis in order to perform a reliability/availability analysis, complete of the first-order sensitivity analysis presented in Sect. 3.5. For illustration purposes, we consider first a simple case study; then, we perform the analysis of the reactor protection system (RPS) of a nuclear power plant (NPP). The first-order sensitivity indexes computed by MCS are used to determine the values of the differential importance measure (DIM) of the system components, which relates to the effects of changes in the system performance due to changes in the properties of the system components [2].

In all generality, importance measures (IMs) are used for ranking the components of a system with respect to their contribution to the considered metric of risk, unreliability or unavailability. For example, in the nuclear field, the calculation of IMs is a relevant outcome of the PRA of NPPs [3–5]. In this framework, IMs evaluate the importance of components (or more generally, events) with respect to their impact on a risk metric G, usually the Core Damage Frequency or the Large Early Release Frequency. In other system engineering applications, such as aerospace and transportation, the impact of components is considered on the system unreliability or, for renewal systems, such as the manufacturing production and power generation ones, on the system unavailability.

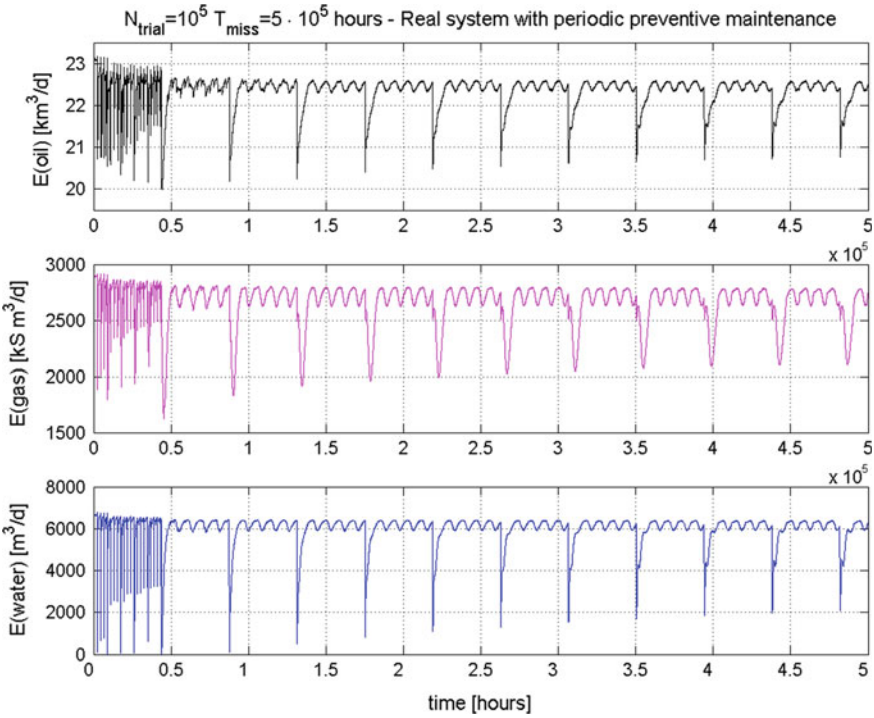

Fig. 5.5 Expected values of the gas (*top*), oil (*middle*) and water (*bottom*) production as a function of time for the real system with preventive periodic maintenance with a mission time T_M of 5×10^5 h

Table 5.7 Comparison of the expected productions per year between case A (real system without preventive maintenance) and B (real system with preventive maintenance)

	Oil ($10^6 \times m^3$ year	Gas ($10^6 \times Sm^3$ year)	Water ($10^6 \times m^3$ year)
Case A	8.482	1,065	2.447
Case B	8.154	969.8	2.446

In what follows, we briefly recall the concepts underlying the definition of the DIM introduced in [6], which the reader should consult for further details.

Consider a generic system performance metric G. In general, the metric can be expressed as a function $G(p_1, p_2, \ldots, p_{Np})$ of the parameters p_i, $i = 1,2,\ldots N_p$ of the underlying stochastic model (components failure rates, repair rates, aging rates, maintenance intervals, human error probabilities, etc.). The total variation of the function of interest due to small variations in its parameters, one at a time, is given by the differential

$$dG = \frac{\partial G}{\partial p_1} \cdot dp_1 + \frac{\partial G}{\partial p_2} \cdot dp_2 + \cdots + \frac{\partial G}{\partial p_{N_P}} \cdot dp_{N_P} \tag{5.1}$$

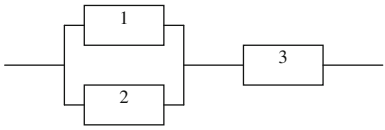

Fig. 5.6 A simple series–parallel system

The DIM of parameter p_i is then defined as the fraction of total change in G that is due to a change in the parameter value

$$\mathrm{DIM}(p_i) = \frac{\mathrm{d}G_{p_i}}{\mathrm{d}G} = \frac{\frac{\partial G}{\partial p_i} \cdot \mathrm{d}p_i}{\frac{\partial G}{\partial p_1} \cdot \mathrm{d}p_1 + \frac{\partial G}{\partial p_2} \cdot \mathrm{d}p_2 + \cdots + \frac{\partial G}{\partial p_{N_P}} \cdot \mathrm{d}p_{N_P}} \tag{5.2}$$

Because of its definition, once all the individual sensitivities $\frac{\partial G}{\partial p_i}$, $i = 1,2,\ldots N_p$ have been computed, the DIM enjoys the additivity property, i.e., the DIM of a subset of parameters p_i, p_j,…,p_k, is the sum of the DIMs of the individual parameters

$$\begin{aligned}\mathrm{DIM}(p_i, p_j, \ldots, p_k) &= \frac{\frac{\partial G}{\partial p_i} \cdot \mathrm{d}p_i + \frac{\partial G}{\partial p_j} \cdot \mathrm{d}p_j + \cdots + \frac{\partial G}{\partial p_k} \cdot \mathrm{d}p_k}{dG} \\ &= \mathrm{DIM}(p_i) + \mathrm{DIM}(p_j) + \cdots + \mathrm{DIM}(p_k)\end{aligned} \tag{5.3}$$

Viewing the definition of DIM in Eq. (5.2) in terms of a limit for the parameter variation going to zero, allows defining the operational steps for its computation. Two different hypotheses can be considered: H1, all the parameters change by the same small value (uniform changes); H2, the parameters are changed by the same percentage (uniform percentage changes). Under H1, $\mathrm{DIM}(p_i)$ measures the importance of parameter p_i with respect to a small equal change in all parameters; under H2, $\mathrm{DIM}(p_i)$ measures the importance of parameter p_i when all the parameters are changed by the same fraction of their nominal values. Clearly the two assumptions address different situations and should lead to different importance values. The conditions under which to apply one hypothesis or the other depend on the problem and risk metric model at hand. In particular, when investigating the effects of changes at the parameter level, H1 cannot be used since the parameters may have different dimensions (e.g., failure rates have inverse-time units, maintenance intervals have time units and human error probabilities are dimensionless numbers).

5.2.1 Case Study 1: Simple System

We consider the simple series–parallel system structure of Fig. 4.4 which, for ease of consultation, we represent again in Fig. 5.6, with the components numbered 1, 2 and 3. The unavailability $U_A(t)$ is the risk metric of interest G, and we want to estimate its first-order sensitivity with respect to variations in the parameters of the underlying stochastic failure-repair processes that the components undergo.

Table 5.8 Transition rates

i	λ_i (h^{-1})	μ_i (h^{-1})
1	0.005	0.02
2	0.005	0.02
3	0.0005	0.03

Concerning the model which governs the stochastic transitions of the system components, the following simplifying assumptions are made, so as to allow validation against analytical results:

- The components are binary, with one functioning state (state 1) and one faulty state (state 2);
- The time of transition of component i from state j_i to state m_i is a stochastic variable which follows an exponential distribution with constant rate $\lambda^i_{j_i \to m_i}$, $i = 1, 2, 3$ j_i, $m_i = 1, 2$ (i.e., no aging effects are considered). Correspondingly, in this case of a system made up of components with exponentially distributed transition times, the function of interest reads $R_k(\tau, t) = e^{-\lambda^k (t-\tau)}$ where $\lambda^k = \sum_{i=1}^{3} \lambda^i_{j_k}$ is the sum of the components transition rates out of their respective states j_k attained when the system entered the state indexed k;
- There are no dependencies of any kind (e.g., load-sharing, standbys, etc.);
- Repair starts immediately upon failure of the unit;
- There is a sufficient number of repair teams to act simultaneously on all components;
- Repairs are always successful and lead the component to its perfect functioning conditions (e.g., *as good as new*).

The mission time of the system is $T_M = 1{,}000$ h and the values of the transition rates of the components are those reported in Table 5.8, where for simplicity of notation we have identified with λ_i the failure rates $\lambda^i_{1\to 2}$ and with μ_i the repair rates $\lambda^i_{2\to 1}$, $i = 1, 2, 3$.

Figure 5.7 shows the evolution in time of the system unavailability $U_A(t)$, as computed analytically (solid line) and estimated by a MCS with 10^6 trials (dots with one standard deviation error bars).

In the simple example considered, we know the explicit analytical form of the unavailability function which can be differentiated with respect to the transition rates parameters to obtain the first-order sensitivities. The analytical results can then be compared with the MCS estimates. Figures 5.8 and 5.9 report the sensitivities obtained with respect to the failure rate λ_1 and the repair rate μ_1 of component 1. Similar results are obtained for the sensitivities with respect to the transition rates of components 2 and 3. The MCS estimates are in good agreement with the analytical results. Obviously, in the MCS, the simultaneous calculation of the unavailability estimate and of its sensitivities leads to an increased computational burden with respect to the estimation of the unavailability only. In this case, this turned out to be a factor of about three.

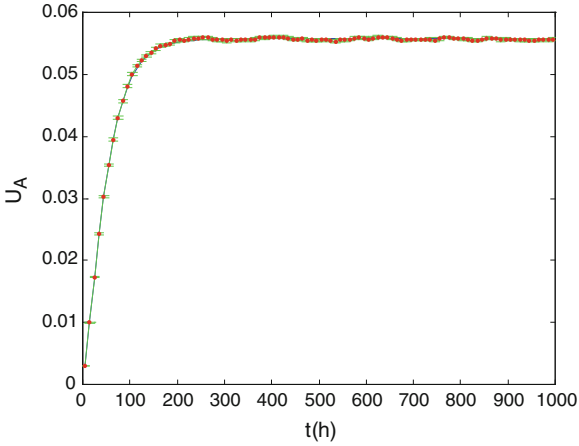

Fig. 5.7 Unavailability $U_A(t)$. Analytic computation (*solid line*); MCS estimate with 10^6 trials (*dotted line* with one standard deviation error bar)

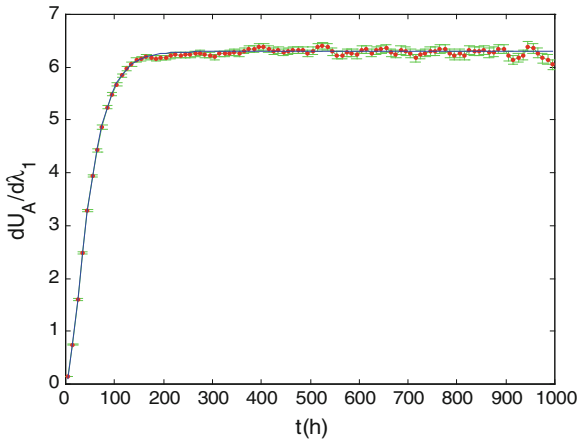

Fig. 5.8 First-order sensitivity of the unavailability $U_A(t)$ with respect to the failure rate λ_1 of the component 1. Analytic computation (*solid line*); MCS estimate with 10^6 trials (*dotted line* with one standard deviation error bar)

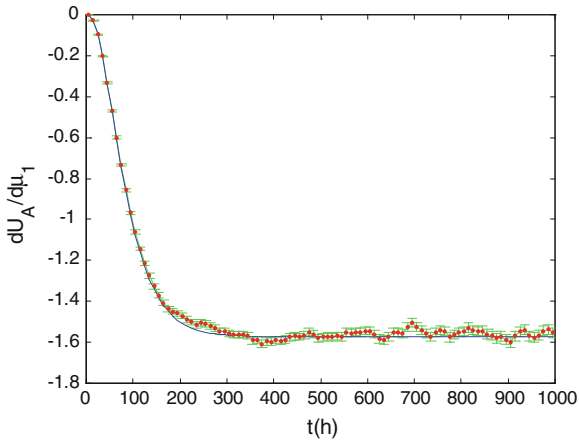

Fig. 5.9 First-order sensitivity of the unavailability $U_A(t)$ with respect to the repair rate μ_1 of the component 1. Analytic computation (*solid line*); MCS estimate with 10^6 trials (*dotted line* with one standard deviation error bar)

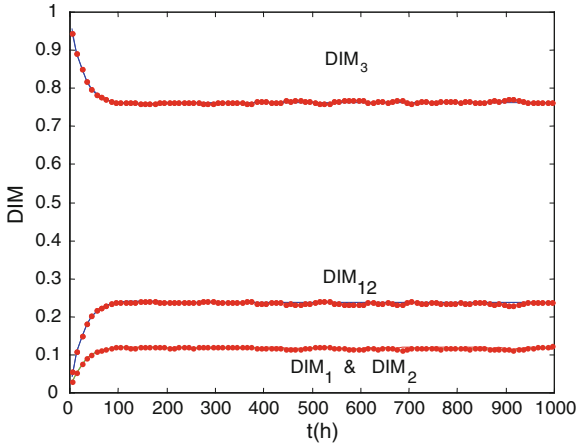

Fig. 5.10 DIMs of the three components and of the parallel block. Analytic computation (*solid line*); MCS estimate with 10^6 trials (*dotted line*)

Given the first order sensitivities with respect to the failure and repair rates of each component, it is possible to compute the DIMs of each component by exploiting the additivity property

$$\mathrm{DIM}_i = \frac{\frac{\partial U_A}{\partial \lambda_i} \cdot \mathrm{d}\lambda_i + \frac{\partial U_A}{\partial \mu_i} \cdot \mathrm{d}\mu_i}{\sum_{j=1}^{3} \frac{\partial U_A}{\partial \lambda_j} \cdot \mathrm{d}\lambda_j + \sum_{j=1}^{3} \frac{\partial U_A}{\partial \mu_j} \cdot \mathrm{d}\mu_j} \tag{5.4}$$

for $i = 1, 2, 3$, and the DIM of the parallel block

$$\mathrm{DIM}_{12} = \mathrm{DIM}_1 + \mathrm{DIM}_2 \tag{5.5}$$

Note that given the homogeneity of the units of measure of λ and μ, both operative hypotheses H1 and H2 can be employed.

Figure 5.10 shows the results computed analytically (solid line) and estimated by MCS with 10^6 trials (dots), under hypothesis H1 and with $\Delta\lambda_i = \Delta\mu_i, i = 1, 2, 3$, chosen sufficiently small for the convergence of the incremental ratios involved in the DIM definition [6]. The results obtained show that component 3 is more important than components 1 and 2, because of its series logic position. Although not reported here, this ranking was verified to be in good agreement with those obtained on the basis of the Birnbaum importance and the risk reduction worth measures [3–5], whereas they are in disagreement with the rankings obtained on the basis of the Fussel-Vesely and risk achievement worth measures [3–5] due to the relevance given in the latter to the unavailabilities of the individual components.

DIM_1 and DIM_2 start from a value close to zero whereas DIM_3 starts from a value close to unity. At short times, approximating the exponential functions with the first term of Mac Laurin series we have

$$\begin{aligned} U_A(t) &\cong (1 - (1 + \lambda_1 \cdot t) \cdot (1 + \lambda_2 \cdot t)) \cdot (1 - (1 + \lambda_3 \cdot t)) \\ &= \lambda_1 \cdot \lambda_3 \cdot t^2 + \lambda_2 \cdot \lambda_3 \cdot t^2 + \lambda_1 \cdot \lambda_2 \cdot \lambda_3 \cdot t^3 \end{aligned} \tag{5.6}$$

Thus, at short times, the derivatives of the unavailability with respect to the μ_i's are negligible and the DIM of the generic ith component is only governed by the derivative of the unavailability with respect to its failure rate, λ_i

$$\begin{aligned}\frac{\partial U_A(t)}{\partial \lambda_1} &\cong \lambda_3 \cdot t^2 + \lambda_2 \cdot \lambda_3 \cdot t^3 \\ \frac{\partial U_A(t)}{\partial \lambda_2} &\cong \lambda_3 \cdot t^2 + \lambda_1 \cdot \lambda_3 \cdot t^3 \\ \frac{\partial U_A(t)}{\partial \lambda_3} &\cong \lambda_1 \cdot t^2 + \lambda_2 \cdot t^2 + \lambda_1 \cdot \lambda_2 \cdot t^3\end{aligned} \tag{5.7}$$

At long times, once the transients have vanished, the DIMs stabilize on asymptotic values.

In practice, it is important to account for the aging processes of the components and the corresponding countermeasures of maintenance. These phenomena introduce additional parameters which the system unavailability turns out to be dependent upon. Information on the sensitivity of the system unavailability with respect to these parameters is of relevance to establish optimal maintenance strategies.

Let us consider the same system of Fig. 5.6 and let us assume that its generic component now ages in time according to a linear model for the failure rate $\lambda(t)$ [7]

$$\lambda(t) = \lambda_0 + at \tag{5.8}$$

where λ_0 is the constant failure rate in absence of aging and a is the aging rate.

The corresponding mean time to failure (MTTF) is equal to

$$\overline{t_f} = \frac{1}{2}\sqrt{\frac{2\pi}{a}} e^{\frac{\lambda_0^2}{2a}} \left[1 - \Phi\left(\frac{\lambda_0}{\sqrt{2a}}\right)\right] \tag{5.9}$$

where $\Phi(x) = \frac{2}{\sqrt{\pi}} \int_0^x e^{-u^2} \mathrm{d}u$ is the error function.

The effects of aging are mitigated through preventive maintenance actions, performed with period τ, which rejuvenate the component. The period τ is chosen sufficiently small that the failure rate $\lambda(t)$ increases only slightly. In order to simplify the calculations, we approximate the matter by substituting the underlying cdf of the time to failure with the simpler exponential distribution, whose parameter λ^* is determined by imposing that the two cdfs give the same failure probability within [0, τ]. It follows that the failure rate of the exponential distribution must have the effective value (constant throughout the maintenance period)

$$\lambda^* = \lambda_0 + \frac{1}{2}a\tau \tag{5.10}$$

which is the average of the λ(t) function over the period τ. Note that this effective failure rate of a component, λ^*, is strictly linked to the maintenance period τ. Within this approximation, the MTTF becomes $\overline{t_f^*} = \frac{1}{\lambda^*}$.

Table 5.9 Aging rates and maintenance periods

i	a_i (h^{-2})	τ_i (h)	λ_i^* (h^{-1})
1	1.3×10^{-5}	131.4	5.85×10^{-3}
2	1.3×10^{-5}	131.4	5.85×10^{-3}
3	8×10^{-5}	132.5	5.82×10^{-3}

Obviously, the exponential approximation is good for small values of the aging rate, i.e., for slowly varying failure rates, whereas for large values of the aging rate the discrepancy between the underlying true cdf and the exponential approximation becomes significant as they coincide only at $t = \tau$. In this latter case, in the limit of zero repair times, the probability of a failure within the period $[0, \tau]$ is the same by construction but the failure occurs at very different times: the exponential distribution somewhat favors early failures whereas the distribution with linear aging shifts the failures to later times, closer to the end of the period τ.

As for the maintenance scheduling, we assume that for each component the period between maintenances is a fraction $1/\alpha_\tau$ of its MTTF, i.e.,

$$\tau = \frac{1}{\alpha_\tau} \bar{t}_f^* = \frac{1}{\alpha_\tau} \frac{1}{\lambda^*} = \frac{1}{\alpha_\tau} \cdot \frac{1}{\lambda_0 + a \cdot \frac{\tau}{2}} \tag{5.11}$$

We then obtain the explicit expression for the maintenance period

$$\tau = \frac{\lambda_0}{a} \left[\sqrt{1 + \frac{1}{\alpha_\tau \frac{\lambda_0^2}{2a}}} - 1 \right]. \tag{5.12}$$

By doing so, the maintenance period τ of each component is linked to the values of (λ_0, a) characterizing its failure behavior.

Concerning the repair process, we maintain the initial assumption of constant repair rate, μ.

For our numerical example, the values of λ_0 for the various components are taken equal to the failure rates of Table 5.8 and the same is done for the repair rates. Table 5.9 reports for each component $i = 1, 2, 3$ the value of the aging rate a_i, the maintenance period τ_i (corresponding to a value $\alpha_\tau = 1.3$ chosen such as to obtain similar values of the maintenance periods for all components) and the value of the mean failure rate over the maintenance period, λ_i^* (which also turns out to be very similar for all components). The effect on the system unavailability is a reduction of a factor of four on its steady state value.

Figure 5.11 reports the results of the sensitivity of the unavailability $U_A(t)$ with respect to the aging rate a_1 of component 1. Similar results are obtained for the sensitivities with respect to the aging rates of the other components 2 and 3. The analytical results are obtained by resorting to the equivalent system of components with constant failure rates λ_i^*, $i = 1, 2, 3$. Thus, the variation Δa_1 of the aging rate a_1 translates in a variation of the associated failure rate λ_1^* and the sensitivity of the unavailability is computed as the incremental ratio $\frac{U_A(t;\lambda_1^*(a_1+\Delta a_1)) - U_A(t;\lambda_1^*(a_1))}{\lambda_1^*(a_1+\Delta a_1) - \lambda_1^*(a_1)}$. Again,

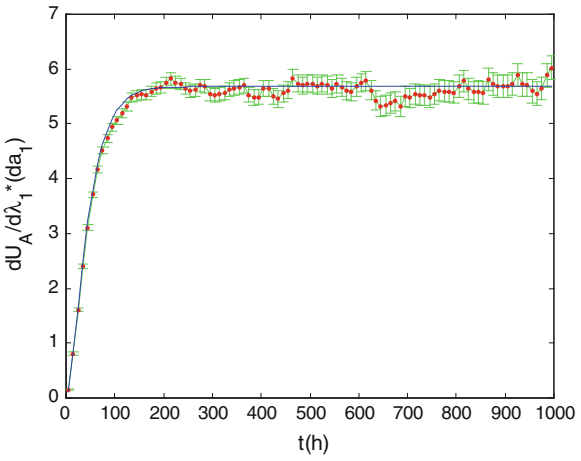

Fig. 5.11 First-order sensitivity of the unavailability $U_A(t)$ with respect to the aging rate a_1 of component 1. Analytic computation (*solid line*); MCS estimate with 10^6 trials (*dotted line* with one standard deviation error bar) estimated by MCS)

the MCS estimates turn out to be in good agreement with the analytical results, despite the approximations introduced.

The DIMs of the individual components are computed by resorting to the additivity property

$$\mathrm{DIM}_i = \frac{\frac{\partial U_A}{\partial \lambda_i} \cdot \mathrm{d}\lambda_i + \frac{\partial U_A}{\partial \mu_i} \cdot \mathrm{d}\mu_i + \frac{\partial U_A}{\partial a_i} \cdot \mathrm{d}a_i}{\sum_{j=1}^{3} \frac{\partial U_A}{\partial \lambda_j} \cdot \mathrm{d}\lambda_j + \sum_{j=1}^{3} \frac{\partial U_A}{\partial \mu_j} \cdot \mathrm{d}\mu_j + \sum_{j=1}^{3} \frac{\partial U_A}{\partial a_j} \cdot \mathrm{d}a_j} \tag{5.13}$$

In this case, the unit of measure of λ_i and μ_i (h^{-1}) differs from that of a_1 (h^{-2}), $i = 1, 2, \ldots, 3$, so that only hypothesis H2 could be applied. However, as just explained, the variation on a_i is actually modeled in terms of its effects on λ_i^* (Eq. 5.10) which has the same units (h^{-1}) of λ_i and μ_i so that hypothesis H1 can also be used. Figure 5.12 shows the results for this latter case; again, the variations to the parameters of component 3 turn out to be the most relevant.

In Fig. 5.13, the DIMs found in the cases with (dotted lines) or without (solid lines) aging and maintenance are compared. The effects of aging and maintenance are shown to increase the relevance of components 1 and 2, and correspondingly to decrease that of component 3. This is due to the fact that in the case of aging and maintenance, given the model assumed, the differences $\left|\lambda_1^* - \lambda_3^*\right| = \left|\lambda_2^* - \lambda_3^*\right|$ are reduced of two orders of magnitude with respect to the values $|\lambda_1 - \lambda_3| = |\lambda_2 - \lambda_3|$ of the case without aging and maintenance.

5.2.2 Case Study 2: The Reactor Protection System

We consider a nuclear RPS, also known as the reactor control rod scram system, for the case of a small loss of coolant accident (LOCA), as described in [8]. The reader is referred to such reference for an accurate description of the system

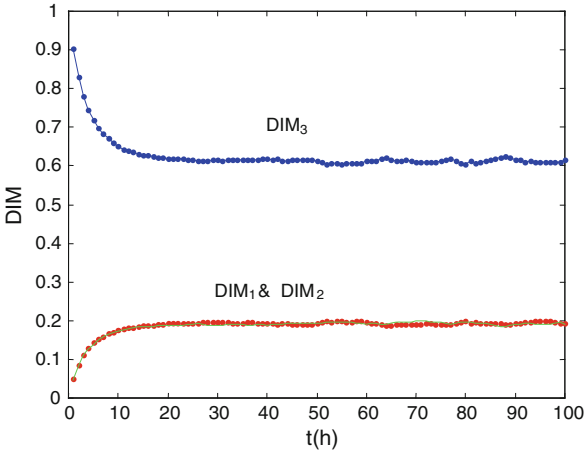

Fig. 5.12 DIMs of the three components for the case of aging and preventive periodic maintenance. Analytic computation (*solid line*); MCS estimate with 10^6 trials (*dotted line*)

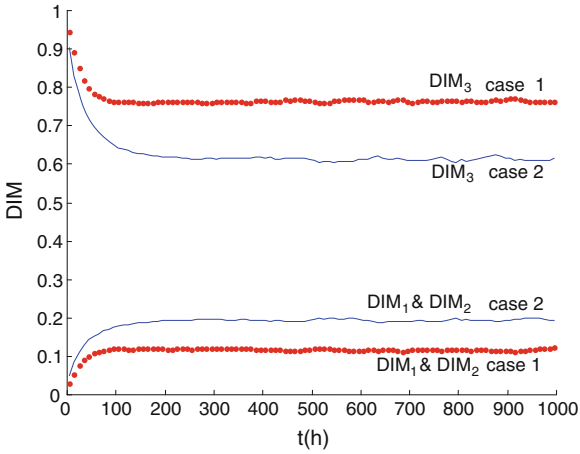

Fig. 5.13 Comparison of the DIMs of the three components for the case with (*dotted line*) and without (*solid line*) aging and preventive periodic maintenance

components and of their mechanics of operation. During normal control of the reactor, the rods are raised or lowered into the core by the use of magnetic jacks.

When during accident the shutdown of the reactor (reactor scram or trip) is required, the control rods are rapidly dropped into the core by removing the voltage to the magnetic jacks. More precisely, the control rod assemblies are dropped by removal of power through the opening of either the reactor trip breaker RTA, controlled by RPS Train A or the reactor trip breaker RTB, controlled by RPS Train B.

We refer to the analysis and model assumptions of [8] with respect to the assessment of the probability of the top event that at least two out of 48 rods fail to enter the core when conditions following a small LOCA exist, which require a reactor scram: this probability is, then, the system performance metric G. The focus

Table 5.10 Minimal cut sets for the reactor protection system [8]

Minimal cut sets (mcs)	mcs code	mcs order
{Core distortion}	{'IEDCOREF'}	1
{Rod drop failure}	{'IED0001F'}	1
{Wire failure}	{'IWR0001Q'}	1
{Common mode failure}	no code	1
{RTA,RTB}	{'ICB0005D','ICB0004D'}	2
{RTA,BYB}	{'ICB0005D','ICB0005C'}	2
{RTA,Train B}	{'ICB0005D','**'}	2
{BYA,RTB}	{'ICB0004C','ICB0004D'}	2
{BYA,BYB}	{'ICB0004C','ICB0005C'}	2
{BYA,Train B}	{'ICB0004C','* *'}	2
{Train A,RTB}	{'*','ICB0004D'}	2
{Train A,BYB}	{'*','ICB0005C'}	2
{Train A,Train B}	{'*','**'}	2
{Train A, Test RTB}	{'*','ICB0002X'}	2
{Train B, Test RTA}	{'**','ICB0003X'}	2

'*':IWR0007Q + ITM0009Q + ITM0011Q + ITM0013Q + ITM0015Q + ITM0017-Q + ITM0019Q + ITM0021Q + ITM0023Q + ITM0025Q
'**' IWR0006Q + ITM0008Q + ITM0010Q + ITM0012Q + ITM0014Q + ITM0016Q + ITM0018Q + ITM0020Q + ITM0022Q + ITM0024Q

of the analysis is concerned with the failures of the electronic control system of the trip circuit breakers. Twelve failure events are considered. The rods and jacks components are considered only with respect to their mechanical fault events. The two trip breakers connected in series control the power provided by two motor generators connected in parallel. Each of them is bypassed by a special test breaker of the same type of the trip breakers. These are called bypass A (BYA) and B, for RTA and RTB respectively. BYA is tripped by the reactor Train B and BYB is tripped by the reactor train A. The tripping signals which trip the various breakers come from two logic trains which are identical in design. Each one is composed of a relay logic for combining various transducer bistable signals into a single command to trip the reactor. The initiating bistable signals are combined into eight functional signals called RT1-RT7 and manual trip. Each of the eight functional signals is capable of initiating a trip by itself.

The details of the fault tree, the modeling assumptions and the detailed data for the quantitative analysis are contained in [8]. The system minimal cut sets (mcs) and the relevant unavailability data are recalled in Tables 5.10 and 5.11 below, where the events which cause them are reported with the original coding employed in [8].

Here we report the results of the importance analysis carried out based on the DIM computed by MCS. In Fig. 5.14, we report the time-dependent DIM for each failure event considered in the analysis, computed by analog MCS with 10^8 trials under hypothesis H1 of uniform variation. The additional burden in the simulation due to the computation of the 12 (number of parameters) $\times$ 100 (time points) first-order sensitivities was of a factor of 5 in the CPU time.

Table 5.11 Unavailability data of the failure events of the reactor protection system [8]

Event/component	Code	Occurrence rate $\lambda\,(h^{-1})$	Unavailability	
Rod drop failure	IED0001F	4.72×10^{-8}	1.7×10^{-5}	
Wire failure	IWR0001Q	2.0×10^{-9}	1.0×10^{-7}	
Core distortion	IEDCOREF	2.0×10^{-9}	1.0×10^{-7}	
Common mode failure	No code	6.33×10^{-8}	3.0×10^{-5}	
Test of RTB	ICB0002X	6.50×10^{-6}	6.1×10^{-3}	
Test of RTA	ICB0003X	6.50×10^{-6}	6.1×10^{-3}	
BYA	ICB0004C	1.0×10^{-6}	3.6×10^{-4}	
RTB	ICB0004D	2.78×10^{-6}	1.0×10^{-3}	
BYB	ICB0005C	1.0×10^{-6}	3.6×10^{-4}	
RTA	ICB0005D	2.78×10^{-6}	1.0×10^{-3}	
Train A				
Terminal board short circuit	ITM0009Q	3.0×10^{-7}	1.08×10^{-4}	
Terminal board short circuit	ITM0011Q	3.0×10^{-7}	1.08×10^{-4}	
Terminal board short circuit	ITM0013Q	3.0×10^{-7}	1.08×10^{-4}	
Terminal board short circuit	ITM0015Q	3.0×10^{-7}	1.08×10^{-4}	
Terminal board short circuit	ITM0017Q	3.0×10^{-7}	1.08×10^{-4}	
Terminal board short circuit	ITM0019Q	3.0×10^{-7}	1.08×10^{-4}	
Terminal board short circuit	ITM0021Q	3.0×10^{-7}	1.08×10^{-4}	
Terminal board short circuit	ITM0023Q	3.0×10^{-7}	1.08×10^{-4}	
Terminal board short circuit	ITM0025Q	3.0×10^{-7}	1.08×10^{-4}	
Wire failure	IWR0007Q	1.0×10^{-8}	3.6×10^{-6}	
Train A		2.71×10^{-6}	360	9.7×10^{-4}
Train B				
Terminal board short circuit	ITM0008Q	3.0×10^{-7}	360	1.08×10^{-4}
Terminal board short circuit	ITM0010Q	3.0×10^{-7}	360	1.08×10^{-4}
Terminal board short circuit	ITM0012Q	3.0×10^{-7}	360	1.08×10^{-4}
Terminal board short circuit	ITM0014Q	3.0×10^{-7}	360	1.08×10^{-4}
Terminal board short circuit	ITM0016Q	3.0×10^{-7}	360	1.08×10^{-4}
Terminal board short circuit	ITM0018Q	3.0×10^{-7}	360	1.08×10^{-4}
Terminal board short circuit	ITM0020Q	3.0×10^{-7}	360	1.08×10^{-4}
Terminal board short circuit	ITM0022Q	3.0×10^{-7}	360	1.08×10^{-4}
Terminal board short circuit	ITM0024Q	3.0×10^{-7}	360	1.08×10^{-4}
Wire failure	IWR0006Q	1.0×10^{-8}	360	3.6×10^{-6}
Train B		2.71×10^{-6}	360	9.7×10^{-4}

We can distinguish four groups of importance. The first group, characterized by the largest values of DIMs includes the following four events: failure of a sufficient number of control rods to enter the core due to core distortions; failure of a sufficient number of control rods to drop due to mechanical faults; wire faults to the trip bus resulting in no loss of power when the trip breakers are opened; common mode human errors. Each one of these events constitutes a minimal cut set of first order and for this reason they are characterized by values of DIM, under hypothesis H1, two orders of magnitude larger than the ones of the next group, in spite of having probability values two orders of magnitude lower. The two logic

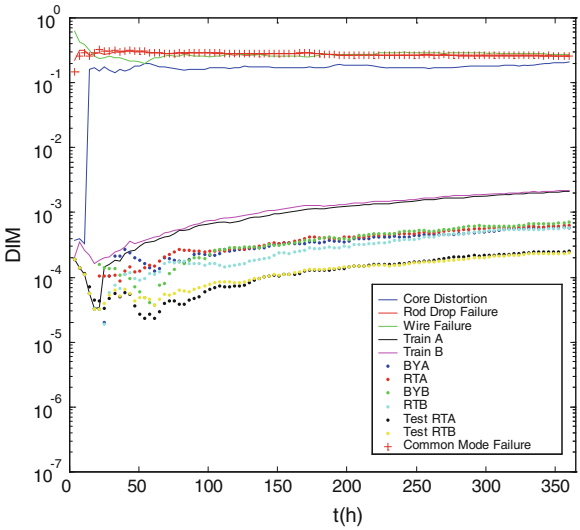

Fig. 5.14 DIMs of the RPS components under hypothesis H1

trains A and B form the second group of importance in the RPS due to the fact that they contribute to most of the second-order mcs of the system. The third group of importance is made of the bypass breakers, BYA and BYB, and trip breakers RTA and RTB: these events make up a smaller number of mcs of order two than the events of the previous group. Finally, the last group in order of importance is characterized by the unavailabilities of RTA and RTB due to testing and maintenance. These events also form mcs of order two but in a small number. In synthesis, under the hypothesis H1 the DIM gives indications on the relevance of an event with respect to its logical role in the system whereas the probability of the event does not contribute significantly. This viewpoint is similar to that characterizing the definition of Birnbaum importance and indeed similar results can be found with respect to this latter measure, as shown in Fig. 5.15.

In Fig. 5.16, we report the time-dependent DIM for each failure event of the RPS, computed by analog MCS with 10^8 trials under hypothesis H2 of uniform percentage variation. The additional burden due to the perturbation analysis for the computation of the first-order sensitivities was of a factor of 5.

We can distinguish five groups of importances. The first group, of largest DIM values, comprises the common mode human errors and the failure of a sufficient number of control rods to drop due to mechanical faults. These events, already in the first group of importance under hypothesis H1, are responsible for two mcs of order one with probability values which are low, in an absolute sense, but high relative to the four mcs of order one (i.e., considering also the events of failure of a sufficient number of control rods to enter the core due to core distortions and of wire faults to the trip bus resulting in no loss of power when the trip breakers are opened). It is evident how under the hypothesis H2 the DIM, besides the significance of the logical structure, also reflects the quantitative relevance related to the probability of the events.

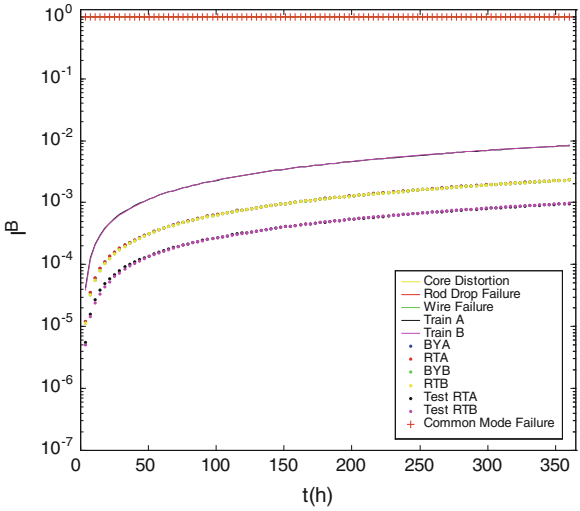

Fig. 5.15 Birnbaum measures of the RPS components computed with 10^8 MCS trials

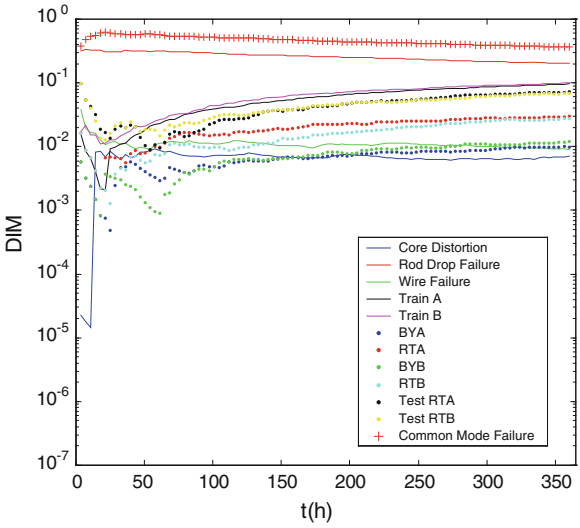

Fig. 5.16 DIMs of the RPS components under hypothesis H2

As in the previous case of hypothesis H1, the two logic trains A and B form the second group of importance in the RPS due to the fact that they contribute to most of the second-order mcs of the system with rates of occurrence which are among the largest in value.

The events of unavailability due to inspection and maintenance of RTA (*Test RTA*) and RTB (*Test RTB*) constitute the third important group, close to the second one. These events contribute to a smaller number of second-order cut sets but their

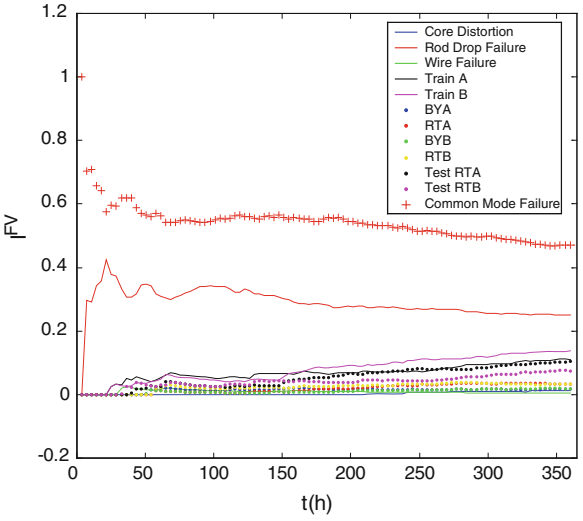

Fig. 5.17 Fussel-Vesely measures of the RPS components computed with 10^8 MCS trials

probability of occurrence is the highest among the 12 events considered: the effect of these two characteristics is such to put them in the third group of importance, whereas under hypothesis H1 they were in the least important group.

The events included in the fourth group of importance, the failures to open the trip breakers RTA and RTB, participate to few mcs and with small probability.

Finally, the last group of importance contains the events of failure of a sufficient number of control rods to enter the core due to core distortions, of wire faults to the trip bus resulting in no loss of power when the trip breakers are opened and of failure to close the bypass breakers, BYA and BYB. The first two events are cut sets of order one, and thus belong to the first group of importance under hypothesis H1, but they occur with negligible probability; the latter two events have the same logical relevance of the events of failure to open the trip breakers RTA and RTB in the fourth group but they occur with a smaller probability.

In synthesis, under the hypothesis H2 the DIM gives indications on the relevance of an event with respect to both its logical role in the system and its probability of occurrence. As mentioned before, this viewpoint is similar to that characterizing the definition of Fussel-Vesely importance and indeed similar results can be found with respect to this latter measure, as shown in Fig. 5.17.

The computed IMs identify possible weaknesses in the system design and management, with reference to the logic of the system or to the reliability/availability characteristics of the components and events involved. The situations identified as critical can be tackled with improvement actions, e.g., the introduction of a redundancy or of a more reliable component, aiming at reducing the criticality degree of the identified situation. The actual effectiveness of a proposed system modification must be evaluated within a risk-informed point of view to verify the net gains and losses in terms of risk and cost. This aspect will however, not be considered here.

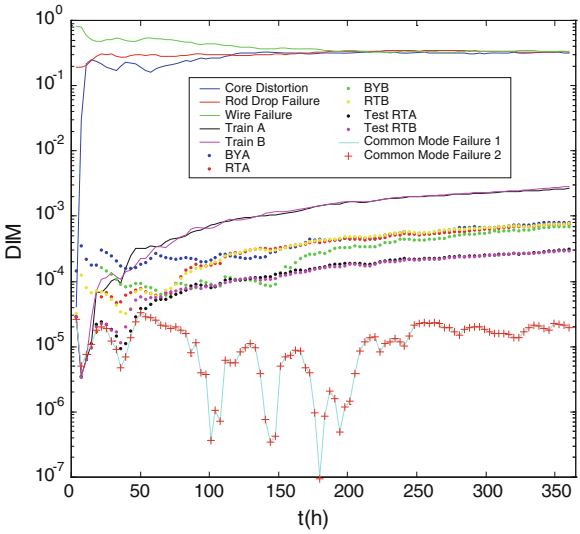

Fig. 5.18 DIMs of the RPS components under hypothesis H1, with two independent testing teams

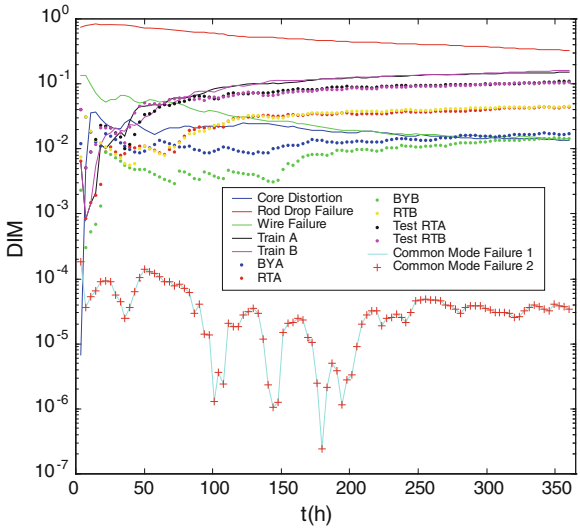

Fig. 5.19 DIMs of the RPS components under hypothesis H2, with two independent testing teams

The results of the DIM for the RPS, under both hypotheses H1 and H2, suggest the introduction of corrective measures to limit the criticality of the events of common mode failures due to human errors. The importance of such event can be mitigated, for example, by having two independent teams performing the operations of testing and calibration of the instruments of Trains A and B: by so doing, the previous *Common Mode Event* is splitted into two independent human error events (here denoted *Common Mode Failure* 1 and 2 to maintain the association with the previous common mode event), each one occurring with the same probability given in Table 5.11 for this type of event. Thus, we basically substitute

a cut set of order one with one of order two. This modification leads to a reduction of a factor of three in the system unavailability.

Figure 5.18 shows the behavior of the DIMs of the components, under hypothesis H1, in the new situation with redundant teams for the testing of Trains A and B. The splitted human error events now bear the smaller values of the IM (the corresponding two lines obviously coincide in the graph) because of their new redundant position in the logical structure of the system. The large fluctuations of the DIM values are obviously due to the very low occurrence probability of the second-order cut sets.

Figure 5.19 shows the behavior of the DIMs of the components, under hypothesis H2, in the new situation with redundant teams for the testing of Trains A and B. The two human error events, *Common Mode Failure* 1 and 2, still have the smaller values of the IM because of their new redundant position in the logical structure of the system; these values, however, are larger than under hypothesis H1 because of the small probability of occurrence associated to this second-order cut set.

In summary, the corrective action on the *Common Mode Failure* was successful in reducing significantly the DIM relevance of the event.

We also analyzed the case that the Common Mode Failure event can be detected immediately upon occurrence and consider the possibility of as good as new corrective repair interventions to re-establish the proper situation. We took, for simplicity, a constant repair rate of arbitrary value $\mu = 2.0 \times 10^{-2}\,\mathrm{h}^{-1}$. This approach differs from the previous one in that the logical structure of the system is not changed, the Common Mode Failure still constituting a cut set of order one, whereas the reliability/availability characteristics of the event are improved due to the introduced repair actions. The modification introduced has been chosen such as to lead again to a reduction of a factor of two in the system unavailability.

For the sake of brevity, we do not report here the details of this case but simply synthesize its results. Under hypothesis H1, the DIM values show that in the new situation, with corrective repairs upon common mode failures during testing and calibration of the instrumentation of Trains A and B, the importance of the Common Mode Failure event is reduced, but not significantly due to the fact that hypothesis H1 gives emphasis to the role of the event in the logical structure of the system (which is left unchanged by the modification introduced) while it does not give significant account to the probability of the events. On the contrary, under hypothesis H2, in spite of the fact that the Common Mode Failure event still constitutes a cut set of order one, its importance tends to values comparable to those of other events contributing to cut sets of order two, due to the significantly improved reliability/availability characteristics related to this event.

Summarizing, in light of the obtained results it seems that with the assumptions and numerical values used in our example, the first action of introducing two distinct and independent teams for the testing and calibration of the instrumentation of Trains A and B is more effective in reducing the importance of the Common Mode Failure event than the second action of corrective repairs.

References

1. Zio, E., Baraldi, P., & Patelli, E. (2006). Assessment of the availability of an offshore installation by Monte Carlo simulation. *International Journal of Pressure Vessel and Piping, 83*, 312–320.
2. Marseguerra, M., & Zio, E. (2004). Monte Carlo estimation of the differential importance measure: Application to the protection system of a nuclear reactor. *Reliability Safety and System Safety, 86*, 11–24.
3. Cheok, M. C., Parry, G. W., & Sherry, R. R. (1998). Use of importance measures in risk informed regulatory applications. *Reliability Engineering and System Safety, 60*, 213–226.
4. Henley, E. J., & Kumamoto, H. (1991). *Probabilistic risk assessment*. New York: IEEE Press.
5. Wall, I. B., Worledge, D. H. (1996, September 29–October 3). Some perspectives on risk importance measures. In *Proceedings of PSA'96*, Park City, Utah.
6. Borgonovo, E., & Apostolakis, G. E. (2001). A new importance measure for risk-informed decision making. *Reliability Engineering and System Safety, 72*, 193–212.
7. NUREG/CR. (1987, April). *Risk evaluations of aging phenomena: The linear aging reliability model and its extension*. US Nuclear Regulatory Commission.
8. Wash-1400 (NUREG75/014). (1975). *Reactor safety study. An assessment of accidents risk in U.S. commercial nuclear power plants*. Appendix 2: Fault trees.

Chapter 6
Advanced Monte Carlo Simulation Techniques for System Failure Probability Estimation

6.1 General Remarks

In mathematical terms, the probability of the event F of system failure can be expressed as a multidimensional integral of the form

$$P(F) = P(\underline{x} \in F) = \int I_F(\underline{x}) q_{\underline{X}}(\underline{x}) \mathrm{d}\underline{x} \tag{6.1}$$

where $\underline{X} = (X_1, X_2, \ldots, X_j, \ldots, X_n) \in \mathbb{R}^n$ is the vector of the uncertain input parameters/variables of the model describing the system behavior, $q_{\underline{X}} : \mathbb{R}^n \to [0, \infty)$ is the multidimensional pdf, $F \subset \mathbb{R}^n$ is the failure region and $I_F : \mathbb{R}^n \to \{0, 1\}$ is an indicator function such that $I_F(\underline{x}) = 1$, if $\underline{x} \in F$ and $I_F(\underline{x}) = 0$, otherwise. The failure domain F is commonly defined by a so-called performance function (PF) or limit state function (LSF) $g_{\underline{X}}(\underline{x})$ which is lower than or equal to zero if $\underline{x} \in F$ and greater than zero, otherwise.

In practical cases, the multidimensional integral Eq. (6.1) cannot be easily evaluated by analytical methods nor by numerical schemes. On the other hand, MCS offers an effective means for estimating the integral, because the method does not suffer from the complexity and dimension of the domain of integration, albeit it implies the non-trivial task of sampling from the multidimensional pdf. The MCS solution to Eq. (6.1) entails that a large number of samples of the values of the uncertain parameters $\underline{x}$ be drawn from $q_{\underline{X}}(\underline{x})$ and that these be used to compute an unbiased and consistent estimate of the system failure probability as the fraction of the number of samples that lead to failure. However, a large number of samples (inversely proportional to the failure probability) are necessary to achieve an acceptable estimation accuracy: in terms of the integral in Eq. (6.1) this can be seen as due to the high dimensionality n of the problem and the large dimension of the relative sample space compared to the failure region of interest [1]. This calls for simulation techniques that allow performing robust estimations

E. Zio, *The Monte Carlo Simulation Method for System Reliability and Risk Analysis*, Springer Series in Reliability Engineering,
DOI: 10.1007/978-1-4471-4588-2_6, © Springer-Verlag London 2013

Table 6.1 List of notation

	Section 3.4.2	Chapter 6
F	cdf	Failure region
Γ	Failure region (set of failure states)	
g	Prize function	Performance function/Limit state function
f	pdf	
f_I	Importance sampling distribution	
q		pdf
$\tilde{q}$		ISD

with a limited number of input samples (and associated low computational time), somewhat along the lines of Sect. 3.4.2.

Note that in the present chapter a different notation than that used in Sect. 3.4.2 (and Chap. 3 in general) is used, to remain as close as possible to the notation used in the literature specialized on the subject content of the chapter. For reader's convenience, Table 6.1 lists the main notation adopted in the two chapters.

6.2 Importance Sampling

In the framework of the "Forced simulation" scheme for solving definite integrals (Sect. 3.4.2), the importance sampling (IS) method amounts to replacing the original pdf $q_{\underline{X}}(\underline{x})$ with an importance sampling distribution (ISD) $\tilde{q}_{\underline{X}}(\underline{x})$ arbitrarily chosen by the analyst so as to generate a large number of samples in the "important region" of the sample space, i.e., the failure region F [1, 2].

The IS algorithm proceeds as follows [2]:

1. Identify a proper ISD, $\tilde{q}_{\underline{X}}(\cdot)$, in order to increase the probability of occurrence of the failure samples;
2. Express the failure probability $P(F)$ in Eq. (6.1) as a function of the ISD $\tilde{q}_{\underline{X}}(\cdot)$

$$\begin{aligned} P(F) &= \int I_F(\underline{x}) q_{\underline{X}}(\underline{x}) \mathrm{d}\underline{x} \\ &= \int \left[\frac{I_F(\underline{x}) q_{\underline{X}}(\underline{x})}{\tilde{q}_{\underline{X}}(\underline{x})} \right] \tilde{q}_{\underline{X}}(\underline{x}) \mathrm{d}\underline{x} \\ &= E_{\tilde{q}} \left[\frac{I_F(\underline{x}) q(\underline{x})}{\tilde{q}(\underline{x})} \right] \end{aligned} \tag{6.2}$$

3. Draw N_T iid samples $\left\{ \underline{x}^k : k = 1, 2, \ldots, N_T \right\}$ from the ISD $\tilde{q}_{\underline{X}}(\cdot)$; if a good choice for the ISD $\tilde{q}_{\underline{X}}(\cdot)$ is made, the samples $\left\{ \underline{x}^k : k = 1, 2, \ldots, N_T \right\}$ concentrate in the failure region F of interest;

4. Compute an estimate $\hat{P}(F)$ for the failure probability $P(F)$ in Eq. (6.1) by resorting to the last expression in Eq. (6.2)

$$\hat{P}(F) = \frac{1}{N_T} \sum_{k=1}^{N_T} \frac{I_F(\underline{x}^k) q_{\underline{X}}(\underline{x}^k)}{\tilde{q}_{\underline{X}}(\underline{x}^k)} \tag{6.3}$$

5. The variance $V\left[\hat{P}(F)\right]$ of the estimator $\hat{P}(F)$ in Eq. (6.3) is given by

$$\begin{aligned} V\left[\hat{P}(F)\right] &= \frac{1}{N_T} V_{\tilde{q}}\left[\frac{I_F(\underline{x}) q_{\underline{X}}(\underline{x})}{\tilde{q}_{\underline{X}}(\underline{x})}\right] \\ &= \frac{1}{N_T}\left(\int \frac{I_F(\underline{x}) q_{\underline{X}}^2(\underline{x})}{\tilde{q}_{\underline{X}}^2(\underline{x})} \tilde{q}_{\underline{X}}(\underline{x}) \mathrm{d}\underline{x} - P(F)^2\right) \end{aligned} \tag{6.4}$$

As shown in Sect. 3.4.2, the quantity in Eq. (6.4) becomes zero when

$$\tilde{q}_{\underline{X}}(\underline{x}) = \tilde{q}_{\underline{X}}^{\mathrm{opt}}(\underline{x}) = \frac{I_F(\underline{x}) q_{\underline{X}}(\underline{x})}{P(F)} \tag{6.5}$$

As pointed out earlier, this represents the optimal choice for the IS density, but it is practically unfeasible since it requires the a priori knowledge of $P(F)$. Several techniques have been developed in order to approximate the optimal sampling density Eq. (6.5) or to at least find one giving small variance of the estimator in Eq. (6.3). Recent examples include the use of engineering judgment [3], design points [2] and kernel density estimators [1].

6.3 The Cross-Entropy Method

The cross-entropy (CE) method is a simulation-based technique for solving rare-event probability estimation problems and complex, multi-extrema optimization problems [3, 4]. It provides a simple adaptive procedure for estimating the optimal values of the set of parameters of the biasing probability distributions and also enjoys asymptotic convergence properties under certain circumstances. Recently, the method has been successfully applied to the estimation of rare-event probabilities in queuing models [5] and Markovian reliability models [6].

The CE method is based on an iterative procedure in which each iteration is composed of two stages:

1. Generate a random data sample (trajectories, vectors, etc.) according to a specified mechanism;
2. Update the parameters of the random mechanism based on the generated data, in order to produce an improved sample in the next iteration.

The importance of the method stems not only from its efficiency but also from the fact that it defines a precise mathematical framework for deriving fast and optimal updating rules, based on advanced simulation.

Although the focus of this book is on simulation, it is interesting to note that the CE method can also be applied to solve complex, multicriteria optimization problems, both deterministic and stochastic (noisy). In the former, the objective function to be optimized is completely known (e.g., like in the traveling salesman, quadratic assignment, and max-cut problems), whereas in the latter it is itself random or to be estimated via simulation (e.g., like in the buffer allocation, stochastic scheduling, flow control, and routing of data networks problems). In the case of deterministic optimization, the problem is translated into a related stochastic optimization problem which is solved by rare-event simulation techniques.

The CE optimization method is based on ideas which are quite different from those of other well-known random search algorithms for global optimization, e.g., simulated annealing, tabu search, guided local search, ant colony, and genetic algorithms. Indeed, in general, these are local heuristics which exploit the local neighborhood structures within a randomized search procedure, whereas CE performs a global random search procedure by reconstructing the initial probability distribution to make occurrence of events more likely in the proximity of a global extremum. Tabu search and guided local search methods are based on a completely different mechanism of iterative generation of solutions, driven by a penalization of the neighborhood of previously examined solutions. Instead, in principle, the CE method and genetic algorithms share the idea of sampling random solutions and improving the way the samples are generated in successive iterations (generations). In both methods, the goodness of the solutions is computed with respect to a score or PF (fitness). On the other hand, the encoding of the solution in the genetic algorithms is problem specific and may require significant efforts, and a number of parameters can be critical for the algorithms, e.g., the crossover and mutation probabilities, the sample (population) size. On the contrary, the way the CE method samples the solutions in the next iteration (generation) is less heuristic, as the updating of the parameters of the sample distribution is optimal in the Kullback–Leibler sense. Also the ant colony optimization method bears some similarities with the CE method; a difference is in the way the next sample of solutions is generated because in the former method a problem-dependent heuristic is implemented such that good solutions in the previous iteration increase the probability that solutions in the future iterations follow a similar path whereas in the latter method, the future solutions are sampled from probability distributions whose parameters are updated based on a principled calculation.

A flourishing literature of works which employ the CE optimizer method seems to demonstrate its potentials. Applications include: buffer allocation [7]; static simulation models [8], queuing models of telecommunication systems [9, 10]; neural computation [11]; control and navigation [12]; DNA sequence alignment [13]; scheduling [14]; vehicle routing [15]; reinforcement learning [16]; project management [17]; heavy tail distributions [18]; network reliability [19, 20]; max-cut and bipartition problems [21]; HIV spread control [22, 23].

6.3.1 The Cross-Entropy Method for the Estimation of Rare-Event Probabilities

Let, $\underline{X} = (X_1, \ldots, X_n)$ be a vector of rvs describing the behavior of a stochastic system and $q_{\underline{X}}(\underline{x}; \underline{\lambda})$ the corresponding joint pdf of real-valued parameter vector $\underline{\lambda}$. For example, assuming that the rvs $X_1, \ldots, X_n$ are independent of each other and exponentially distributed with means $\frac{1}{\lambda_1}, \ldots, \frac{1}{\lambda_n}$, respectively, the pdf $q_{\underline{X}}(\underline{x}; \underline{\lambda})$ reads

$$q_{\underline{X}}(\underline{x}; \underline{\lambda}) = \prod_{j=1}^{n} \lambda_j \cdot \exp\left(- \sum_{j=1}^{n} \lambda_j x_j \right) \tag{6.6}$$

The problem of interest regards the evaluation of the expected performance $P(F)$ of a stochastic system, in the following expressed in terms of the probability that a real-valued function $Y(\underline{X})$ is greater than or equal to some threshold value α_Y

$$P(F) = P(Y(\underline{X}) \geq \alpha_Y) = E_{f_{\underline{X}}}\left[I_{\{Y(\underline{X}) \geq \alpha_Y\}} \right] \tag{6.7}$$

where the subscript $q_{\underline{X}}$ specifies that the expectation is taken with respect to the pdf $q_{\underline{X}}(\cdot)$ and $I_{\{Y(\underline{X}) \geq \alpha_Y\}}$ is an indicator function equal to 1 if $Y(\underline{X}) \geq \alpha_Y$ and 0 otherwise; in relation to the original failure probability estimation problem of Eq. (6.1), this means that $X \in F$ when $Y(\underline{X}) \geq \alpha_Y$.

If the probability in Eq. (6.7) is very small, say of the order of 10^{-5}, the event $Y(\underline{X}) \geq \alpha_Y$ is called a rare event. Classical examples of rare events are the failures of a redundant system made of highly reliable components, the occurrence of earthquakes of large magnitude and the release of radionuclides from a safe waste repository.

The estimation of the probability in Eq. (6.7) entails the solution of the multidimensional integral of the expectation operator. As seen in Sect. 3.4, MCS can be used for estimating such an integral [24–26]; this requires drawing a large number N of samples $\underline{x}_1, \ldots, \underline{x}_N$ of the random vector $\underline{X}$ from the multidimensional joint pdf $q_{\underline{X}}(\cdot)$, which in general may not be a trivial task [1]; then, an estimator $\hat{P}(F)$ of the probability in Eq. (6.7) is obtained by dividing the number of times that $I_{\{Y(\underline{x}_i) \geq \alpha_Y\}} = 1$ by the total number of samples drawn N, viz.,

$$\hat{P}(F) = \frac{1}{N} \sum_{i=1}^{N} I_{\{Y(\underline{x}_i) \geq \alpha_Y\}} \tag{6.8}$$

This estimator is unbiased, i.e., as N approaches infinity, the probability in Eq. (6.8) approaches the true value in Eq. (6.7). For rare events, given the high dimensionality of the random vector $\underline{X}$ and the large dimension of the sample space relatively to the region of occurrence of the rare events, a large number of samples $\underline{x}$ are necessary, in practice to achieve an acceptable estimation accuracy, i.e., a small relative error or a narrow confidence interval. This may lead to very

large computing times, especially if the calculation of $Y(\underline{x})$ is done by long-running computer codes (one code run for each sample $\underline{x}$).

We have seen that an alternative to circumvent this problem is to utilize the forced simulation of Sect. 3.4.2 as developed in the IS procedure explained in Sect. 6.2 [24, 25], in which the random samples $\underline{x}_1, \ldots, \underline{x}_N$ are drawn from a different pdf $\tilde{q}_{\underline{X}}(\cdot)$ and the likelihood ratio estimator of $P(F)$ is computed

$$\hat{P}(F) = \frac{1}{N} \sum_{i=1}^{N} I_{\{Y(\underline{x}) \geq \alpha_Y\}} W(\underline{x}; \underline{\lambda}) \tag{6.9}$$

where

$$W(\underline{x}; \underline{\lambda}) = \frac{q_{\underline{X}}(\underline{x}; \underline{\lambda})}{\tilde{q}_{\underline{X}}(\underline{x})} \tag{6.10}$$

is the likelihood ratio. For example, considering again independent rvs $X_1, \ldots, X_n$ exponentially distributed with means $\frac{1}{\lambda_1}, \ldots, \frac{1}{\lambda_n}$, respectively, and restricting the functional form of the IS density $\tilde{q}_{\underline{X}}(\cdot)$ to an exponential function of parameter vector $\underline{\upsilon}$, the likelihood ratio in Eq. (6.10) becomes

$$W(\underline{x}; \underline{\lambda}, \underline{\upsilon}) \equiv \frac{q_{\underline{X}}(\underline{x}; \underline{\lambda})}{\tilde{q}_{\underline{X}}(\underline{x}; \underline{\upsilon})} = \prod_{j=1}^{n} \frac{\lambda_j}{\upsilon_j} \cdot \exp\left(- \sum_{j=1}^{n} (\lambda_j - \upsilon_j) x_j \right) \tag{6.11}$$

The question then arises on which IS density $\tilde{q}_{\underline{X}}(\cdot)$ to use for minimizing the error of the estimator. As shown in Sect. 3.4.2, the optimal choice is to use [24–26]

$$\tilde{q}^*_{\underline{X}}(\underline{x}) = \frac{I_{\{Y(\underline{x}) \geq \alpha_Y\}} f_{\underline{X}}(\underline{x}, \underline{\lambda})}{P(F)} \tag{6.12}$$

because by so doing the elements in the sum of Eq. (6.9) are all equal to $P(F)$

$$I_{\{Y(\underline{x}_i) \geq \alpha_Y\}} \frac{q_{\underline{X}}(\underline{x}_i; \underline{\lambda})}{\tilde{q}^*_{\underline{X}}(\underline{x}_i)} = P(F) \quad i = 1, 2, \cdots, N \tag{6.13}$$

and one single sample $\underline{x}$ drawn from $q^*_{\underline{X}}(\cdot)$ would allow to obtain the exact value of the probability of interest [Eq. (6.7)].

As explained in Sect. 3.4.2, the optimal IS density $\tilde{q}^*_{\underline{X}}(\cdot)$ cannot be used in practice because one needs to know the value of the unknown $P(F)$ to calculate it, and then, one chooses a functional form of $\tilde{q}_{\underline{X}}(\underline{x}; \underline{\upsilon})$ dependent on a vector of parameters $\underline{\upsilon}$ whose values are determined so as to minimize the variance of the estimator (6.9) [24–26].

An alternative way to proceed is to choose a $\tilde{q}_{\underline{X}}(\cdot)$ of the same functional form $q_{\underline{X}}(\cdot)$ of the original pdf but dependent on a different vector of parameters $\underline{\upsilon}$ (the reference or tilting parameter vector), whose values are determined so as to

minimize the distance between the densities $\tilde{q}^*_{\underline{X}}(\cdot)$ [Eq. (6.12)] and the chosen $\tilde{q}_{\underline{X}}(\cdot)$.

A particularly convenient form of distance between two pdfs $p_{\underline{X}}(\cdot)$ and $h_{\underline{X}}(\cdot)$ is the Kullback–Leibler distance, also called CE

$$D\left(p_{\underline{X}}, h_{\underline{X}}\right) = E_{p_{\underline{X}}}\left[\ln \frac{p_{\underline{X}}(\underline{x})}{h_{\underline{X}}(\underline{x})}\right] = \int p_{\underline{X}}(\underline{x}) \ln p_{\underline{X}}(\underline{x}) \mathrm{d}\underline{x} - \int p_{\underline{X}}(\underline{x}) \ln h_{\underline{X}}(\underline{x}) \mathrm{d}\underline{x} \quad (6.14)$$

Notice that Eq. (6.14) is not a distance metric in the strict mathematical sense; for example, it does not satisfy the symmetry property.

The idea behind the CE method is to choose the IS density $\tilde{q}_{\underline{X}}(\underline{x}) = q_{\underline{X}}(\underline{x}; \underline{v})$ such that its Kullback–Leibler distance from the optimal IS density $\tilde{q}^*_{\underline{X}}(\cdot)$ is minimal. Minimizing the Kullback–Leibler distance between the densities $\tilde{q}_{\underline{X}}(\underline{x}) = q_{\underline{X}}(\underline{x}; \underline{v})$ and $\tilde{q}^*_{\underline{X}}(\cdot)$ amounts to finding the values of the parameters $\underline{v}$ of $\tilde{q}_{\underline{X}}(\cdot)$ such that the second quantity in Eq. (6.14) $-\int \tilde{q}^*_{\underline{X}}(\underline{x}) \ln q_{\underline{X}}(\underline{x}; \underline{v}) \mathrm{d}\underline{x}$ is minimized. This is equivalent to solving the maximization problem

$$\max_{\underline{v}} \int \tilde{q}^*_{\underline{X}}(\underline{x}) \ln q_{\underline{X}}(\underline{x}; \underline{v}) \mathrm{d}\underline{x} \quad (6.15)$$

Substituting Eq. (6.12) for $\tilde{q}^*_{\underline{X}}(\cdot)$

$$\max_{\underline{v}} \int \frac{I_{\{Y(\underline{x}) \geq \alpha_Y\}} q_{\underline{X}}(\underline{x}; \underline{\lambda})}{P(F)} \ln q_{\underline{X}}(\underline{x}; \underline{v}) \mathrm{d}\underline{x} \quad (6.16)$$

which is equivalent to

$$\max_{\underline{v}} E_{f_{\underline{X}}(\underline{X}; \underline{\lambda})}\left[I_{\{Y(\underline{X}) \geq \alpha_Y\}}\right] \ln q_{\underline{X}}(\underline{x}; \underline{v}) \quad (6.17)$$

Applying again IS with a different density $q_{\underline{X}}(\underline{x}; \underline{\omega})$ to effectively tackle the computation of the expectation value for rare-event problems, the maximization problem in Eq. (6.17) can be rewritten as:

$$\max_{\underline{v}} E_{f_{\underline{X}}(\underline{X}; \underline{\omega})}\left[I_{\{Y(\underline{X}) \geq \alpha_Y\}}\right] W(\underline{x}; \underline{\lambda}, \underline{\omega}) \ln q_{\underline{X}}(\underline{x}; \underline{v}) \quad (6.18)$$

for any reference parameter ω, where $W(x, \lambda, \omega)$ is the likelihood ratio in Eq. (6.11) between $q_{\underline{X}}(\underline{x}; \underline{\lambda})$ and $q_{\underline{X}}(\underline{x}; \underline{\omega})$.

The optimal reference vector $\underline{v}^*$ solution of Eq. (6.18) can be estimated by solving its stochastic, simulated counterpart

$$\max_{\underline{v}} \frac{1}{N}\sum_{i=1}^{N} I_{\{Y(\underline{x}_i)\geq \alpha_Y\}} W(\underline{x}_i;\underline{\lambda},\underline{\omega}) \ln q_{\underline{X}}(\underline{x}_i;\underline{v}) \tag{6.19}$$

where the vector values $\underline{x}_1,\ldots,\underline{x}_N$ are drawn from $q_{\underline{X}}(\underline{x};\underline{\omega})$.

In typical applications, the function to be maximized in Eq. (6.19) is convex and differentiable with respect to $\underline{v}$, and thus the solution to Eq. (6.19) may be readily obtained by solving for $\underline{v}$ the following system of equations

$$\frac{1}{N}\sum_{i=1}^{N} I_{\{Y(\underline{x}_i)\geq \alpha_Y\}} W(\underline{x}_i;\underline{\lambda},\underline{\omega}) \nabla \ln q_{\underline{X}}(\underline{x}_i;\underline{v}) = 0 \tag{6.20}$$

where the gradient is with respect to $\underline{v}$.

Operatively, the algorithm for the CE method would proceed as follows:

1. $k = 0$; choose an initial reference vector $\underline{v}^{(0)}$, e.g., $\underline{v}^{(0)} = \underline{\lambda}$;
2. $k = k + 1$;
3. Draw a random sample of vector values $\underline{x}_1,\ldots,\underline{x}_N$ from $q_{\underline{X}}\left(\underline{x};\underline{v}^{(k-1)}\right)$;
4. Find the solution $\underline{v}^k$ to the maximization problem in Eq. (6.19)

$$\underline{v}^{(k)} = \arg\max_{\underline{v}} \frac{1}{N}\sum_{i=1}^{N} I_{\{Y(\underline{x}_i)\geq \alpha_Y\}} W\left(\underline{x}_i;\underline{\lambda},\underline{v}^{(k-1)}\right) \ln q_{\underline{X}}(\underline{x}_i;\underline{v}) \tag{6.21}$$

5. Return to Eq. (6.7) unless convergence is achieved.

A possible stopping criterion demands to stop the iterations when all the parameters have ceased to increase or decrease monotonously. Letting K_j be the iteration at which the sequence of iterated values $v_j^{(0)}, v_j^{(1)}, v_j^{(2)}, \ldots$ of the jth component of $\underline{v}$ starts fluctuating, i.e., $v_j^{(0)} \leq v_j^{(1)} \leq v_j^{(2)} \ldots \leq v_j^{(K_j-1)} > v_j^{(K_j)}$ or $v_j^{(0)} \geq v_j^{(1)} \geq v_j^{(2)} \ldots \geq v_j^{(K_j-1)} < v_j^{(K_j)}$, the criterion requires to stop at the iteration $K = \max_j K_j$.

The advantage of the CE method with respect to the variance minimization one of Sect. 3.4.2 is that $\underline{v}^k$ can often be calculated analytically. In particular, this is true if the distributions involved are exponential or discrete with finite support [27].

However, as presented up to now the method is of little practical use when rare events are involved, i.e., when the probability $P(F)$ in Eq. (6.7) is less than, say, 10^{-5}. Indeed, due to the rarity of the target event $\{Y(\underline{X}) \geq \alpha_Y\}$, most of the sampled values of the binary indicator variable $I_{\{Y(\underline{x}_i)\geq \alpha_Y\}}$ $i = 1,\ldots,N$ will be zero for practical sample dimension N. In this case, the difficult problem of estimating the very small probability $P(F)$ can be broken down into a sequence of simple problems involving larger probabilities which are solved by an iterative two-phase procedure each time generating a sequence of pairs of estimates of the reference parameter $\underline{v}$ and the level α_Y, in a way to avoid that the indicator

variable takes a value of zero too many times while estimating the optimal value $\underline{v}^*$ of the reference parameter vector. The iterative sequencing of $\underline{v}$ and α_Y estimation is regulated by introducing the rarity parameter ρ usually of the order of 0.01.

Starting as before from an initial reference parameter vector $\underline{v}^{(0)}$, e.g., equal to $\underline{\lambda}$, at each iteration the two phases proceed as follows:

- *Update* of $\alpha_Y^{(k)}$: Given the reference parameter vector estimate $\underline{v}^{(k-1)}$ at the previous iteration, the updated value $\alpha_Y^{(k)}$ is taken as the $(1-\rho)$-quantile of $Y(\underline{X})$ when the density is $q_{\underline{X}}\left(\underline{x};\underline{v}^{(k-1)}\right)$, i.e., $\alpha_Y^{(k)}(<\alpha_Y)$ such that under the current density $q_{\underline{X}}\left(\underline{x};\underline{v}^{(k-1)}\right)$ the probability $l_k = E_{q_{\underline{X}}\left(\underline{x};\underline{v}^{(k-1)}\right)}\left[I_{\left\{Y\left(\underline{X}\right)\geq\alpha_Y^{(k)}\right\}}\right]$ is at least equal to ρ

$$P\left[Y(\underline{X})\geq\alpha_Y^{(k)}\right]\geq\rho \tag{6.22}$$

  where $\underline{X}\sim q_{\underline{X}}\left(\underline{x};\underline{v}^{(k-1)}\right)$; a simple estimator of $\alpha_Y^{(k)}$ can be obtained from the random sample of values $Y(\underline{x}_1), Y(\underline{x}_2), \ldots, Y(\underline{x}_N)$ ordered from the smallest to the largest, taking the $(1-\rho)$ sample quantile, i.e., the $(1-\rho)N$ order statistic of the sequence $Y(\underline{x}_1), Y(\underline{x}_2), \ldots, Y(\underline{x}_N)$

$$\alpha_Y^{(k)} = Y_{[(1-\rho)N]} \tag{6.23}$$

  Note that updating the procedure in this way is feasible because the value $\alpha_Y^{(k)}$ is such that the event $\left\{Y(\underline{X})\geq\alpha_Y^k\right\}$ is not so rare (it has a probability of around ρ);
- *Update* of $\underline{v}^{(k)}$: The updated value $\underline{v}^{(k)}$ of the reference parameter vector is found as the optimal value for estimating l_k, i.e., the solution of [see Eq. (6.18)]

$$\max_{\underline{v}} E_{q_{\underline{X}}\left(\underline{x};\underline{v}^{(k-1)}\right)}\left[I_{\left\{Y\left(\underline{X}\right)\geq\alpha_Y^{(k)}\right\}}\right] W\left(\underline{x};\underline{\lambda},\underline{v}^{(k-1)}\right)\ln q(\underline{x};\underline{v}) \tag{6.24}$$

  which from the stochastic simulated counterpart gives [see Eq. (6.19)]

$$\underline{v}^{(k)} = \arg\max_{\underline{v}}\frac{1}{N}\sum_{i=1}^{N} I_{\left\{Y\left(\underline{x}_i\right)\geq\alpha_Y^{(k)}\right\}} W\left(\underline{x}_i;\underline{\lambda},\underline{v}^{(k-1)}\right)\ln q_{\underline{X}}(\underline{x}_i;\underline{v}) \tag{6.25}$$

As before, the optimal solution $\underline{v}^{(k)}$ can often be found analytically, particularly when $q_{\underline{X}}(\underline{x};\underline{v})$ is exponential or discrete with finite support.

Operatively, the algorithm for the CE method for rare-event probability estimation becomes:

1. $k = 0$; choose an initial reference vector $\underline{v}^{(0)}$, e.g., $\underline{v}^{(0)} = \underline{\lambda}$, and a value of ρ, e.g., 10^{-2};
2. $k = k + 1$; (iteration = level counter);
3. Draw a random sample of vector values $\underline{x}_1, \ldots, \underline{x}_N$ from $q_{\underline{X}}\left(\underline{x}; \underline{v}^{(k-1)}\right)$ and compute the corresponding sample $Y(\underline{x}_1), Y(\underline{x}_2), \ldots, Y(\underline{x}_N)$;
4. Find the $(1 - \rho)$ sample quantile $\alpha_Y^{(k)}$ [Eq. (6.23)];
5. With the same sample $\underline{x}_1, \ldots, \underline{x}_N$ determine the solution $\underline{v}^{(k)}$ in Eq. (6.25)

$$\underline{v}^{(k)} = \arg\max_{\underline{v}} \frac{1}{N} \sum_{i=1}^{N} I_{\left\{Y\left(\underline{x}_i\right) \geq \alpha_Y^{(k)}\right\}} W\left(\underline{x}_i; \underline{\lambda}, \underline{\omega}\right) \ln q_{\underline{X}}\left(\underline{x}_i; \underline{v}\right) \tag{6.26}$$

6. If the value of $\alpha_Y^{(k)}$ in step 4 above is less than α_Y, return to step 2; otherwise
7. Estimate the rare-event probability $P(F)$ as

$$P(F) = \frac{1}{N} \sum_{i=1}^{N} I_{\left\{Y\left(\underline{x}_i\right) \geq \alpha_Y\right\}} W\left(\underline{x}_i; \underline{\lambda}, \underline{v}^K\right) \tag{6.27}$$

where K is the number of iteration levels.

Thus, starting with $\underline{v}^{(0)}$ at the first iteration, a good estimate of the updated reference parameter vector $\underline{v}^{(1)}$ is sought by making the target event $\{Y(\underline{X}) \geq \alpha_Y\}$ less rare by temporarily using a level $\alpha_Y^{(1)} (< \alpha_Y)$. The value $\underline{v}^{(1)}$ thereby obtained will hopefully make the target event $\{Y(\underline{X}) \geq \alpha_Y\}$ less rare in the following iteration, so that a threshold $\alpha_Y^{(2)} (< \alpha_Y)$ can be used, which is closer to α_Y itself. The algorithm proceeds in this way until at some iteration K the threshold level reached is at least α_Y, and thus the original value of α_Y can be used without getting too few samples.

Note that in practice the sample size N_1 used in steps 3–5 for the updating of the pair α_Y and $\underline{v}$ can be significantly smaller than the one used in step 7 for the estimation of the probability $P(F)$.

Also, to obtain a more accurate estimate of the optimal reference parameter vector $\underline{v}^*$ it is sometimes useful, especially with small sample sizes, to repeat the iterative loop of steps 2–6 for some additional iterations after the threshold α_Y has been reached.

6.3.2 The Cross-Entropy Method for Combinatorial Optimization

The CE method previously introduced can be transformed into a randomized algorithm for solving combinatorial optimization problems. The main idea is to associate a rare-event probability estimation problem (the so-called associated

stochastic problem) to the combinatorial optimization problem and then to tackle the former with an iterative algorithm similar to the one illustrated earlier, in which at each iteration two stages are performed:

1. Generation of a random sample of data (trajectories, vectors, etc.) according to a specified mechanism;
2. Updating of the parameters of the random mechanism (typically parameters of pdfs) based on the generated data, in order to produce an improved sample in the next iteration.

Without loss of generality, consider the problem of maximizing the PF $Y(\underline{x})$ over all possible values $\underline{x} \in \Omega$. Let Y^* denote the value of the maximum, i.e.,

$$Y^* = \max_{\underline{x} \in \Omega} Y(\underline{x}) \tag{6.28}$$

To the maximization problem (6.28), one associates the stochastic problem of probability estimation in Eq. (6.7), which is rewritten here as follows:

$$P(\alpha_Y) = P(Y(\underline{X}) \geq \alpha_Y) = E_{q_{\underline{X}}}\left[I_{\{Y(\underline{X}) \geq \alpha_Y\}}\right] \tag{6.29}$$

where the random vector $\underline{X} \sim q_{\underline{X}}(\cdot; \underline{\lambda})$ and the dependence of the expected performance on the known or unknown threshold α_Y is rendered explicit. Note that one may know α_Y and want to estimate $P(F)$ or viceversa.

To explain how Eq. (6.29) is associated to Eq. (6.28), suppose for example that $\alpha_Y = Y^*$ and that $q_{\underline{X}}(\cdot; \underline{\lambda}) = \frac{1}{|\Omega|}$, i.e., uniform; then, typically $P(Y^*) = q_{\underline{X}}(\underline{x}^*; \underline{\lambda}) = \frac{1}{|\Omega|}$ is a very small number and a natural way to estimate it is to use the likelihood ratio estimator in Eq. (6.27) with reference parameter υ^* estimated by

$$\underline{\upsilon}^* = \arg\max_{\underline{\upsilon}} \frac{1}{N} \sum_{i=1}^{N} I_{\{Y(\underline{x}_i) \geq \alpha_Y\}} \ln q_{\underline{X}}(\underline{x}_i; \underline{\upsilon}) \tag{6.30}$$

where the random samples $\underline{x}_i$ are drawn from the pdf $q_{\underline{X}}(\cdot; \underline{\lambda})$.

In general, let us consider the problem of estimating $P(F)$ for a certain α_Y close to Y^*; then, it is plausible that $q_{\underline{X}}(\cdot; \underline{\upsilon}^*)$ assigns most of the probability mass close to the optimal vector value $\underline{x}^*$, and thus can be used to generate an approximate solution to the maximization problem (6.28). However, the event $\{Y(\underline{X}) \geq \alpha_Y\}$ is a rare event: the (nontrivial) problem of estimating the value of $P(F)$ can then be tackled with the previously introduced CE method, by making adaptive changes to the pdf, i.e., to its reference parameter vector $\underline{\upsilon}$, according to Kullback–Leibler distance (CE), and thus creating a sequence $q_{\underline{X}}\left(\cdot; \underline{\upsilon}^{(0)}\right)$, $q_{\underline{X}}\left(\cdot; \underline{\upsilon}^{(1)}\right)$, ... of pdfs that are steered toward the optimal density.

A two phase, multilevel procedure, analogous to the one devised for the rare-event simulation problem, is adopted to construct a sequence of levels $\alpha_Y^{(1)}, \alpha_Y^{(2)}, \ldots, \alpha_Y^{(K)}$ and corresponding optimal parameter vectors $\underline{\upsilon}^{(1)}, \underline{\upsilon}^{(2)}, \ldots, \underline{\upsilon}^{(K)}$

such that the convergence value $\alpha_Y^{(K)}$ is close to the optimal value Y^* and $\underline{v}^{(K)}$ is such that the corresponding density assigns high probability mass to the vector values $\underline{x}$ that give a high performance $Y(\underline{x})$.

Starting from an initial reference parameter vector $\underline{v}^{(0)}$, e.g., equal to $\underline{\lambda}$, and a value of the rarity parameter ρ not too small, e.g., equal to 10^{-2}, at each iteration the two phases proceed as follows:

- *Update* of $\alpha_Y^{(k)}$: Given the reference parameter vector estimate $\underline{v}^{(k-1)}$ at the previous iteration, the updated value $\alpha_Y^{(k)}$ is taken as the $(1-\rho)$-quantile of $Y(\underline{X})$ where $\underline{X} \sim q_{\underline{X}}\left(\underline{x}; \underline{v}^{(k-1)}\right)$; a simple estimator of $\alpha_Y^{(k)}$ can be obtained from the random sample of values $Y(\underline{x}_1), Y(\underline{x}_2), \ldots, Y(\underline{x}_N)$ ordered from the smallest to the largest, taking the $(1-\rho)$ sample quantile, i.e., the $(1-\rho)N$ order statistic of the sequence $Y(\underline{x}_1), Y(\underline{x}_2), \ldots, Y(\underline{x}_N)$ as in Eq. (6.23);
- *Update* of $\underline{v}^{(k)}$: The updated value $\underline{v}^{(k)}$ of the reference parameter vector is found as the optimal value for estimating $P_k(F)$, i.e., as the solution to the optimization problem

$$\max_{\underline{v}} E_{q_{\underline{X}}\left(\underline{X}; \underline{v}^{(k-1)}\right)} \left[I_{\left\{Y(\underline{X}) \geq \alpha_Y^{(k)}\right\}} \right] \ln q(\underline{x}; \underline{v}) \tag{6.31}$$

whose stochastic simulated counterpart is

$$\max_{\underline{v}} \frac{1}{N} \sum_{i=1}^{N} I_{\left\{Y(\underline{x}_i) \geq \alpha_Y^{(k)}\right\}} \ln q_{\underline{X}}(\underline{x}_i; \underline{v}) \tag{6.32}$$

Note that differently from Eqs. (6.24) and (6.25), Eqs. (6.31) and (6.32) do not contain the likelihood ratio term W. This is because while in the rare-event simulation problem the initial (nominal) parameter vector $\underline{\lambda}$ is specified in advance and it is an essential element of the rare-event probability estimation problem, in the combinatorial optimization problem the initial reference vector parameter $\underline{\lambda}$ is arbitrarily introduced to define the associated stochastic problem and it is redefined at each iteration. Indeed, at each iteration the optimal reference parameter vector $\underline{v}^{(k)}$ is determined with respect to the problem of estimating $P(Y(\underline{X}) \geq \alpha_Y)$ with $\underline{X} \sim q_{\underline{X}}\left(\underline{x}; \underline{v}^{(k-1)}\right)$ and not $\underline{X} \sim q_{\underline{X}}(\underline{x}; \underline{\lambda})$. Consequently, the likelihood ratio term W that plays a crucial role in the rare-event estimation problem does not appear in the combinatorial optimization problem. Of course, it is possible to include the W term in the solution to the combinatorial optimization problem but numerical results suggest that this may often lead to less reliable (i.e., noisy) estimates $\underline{v}^{(K)}$ of $\underline{v}^*$.

Finally, the following smoothed updating procedure is often conveniently applied

$$\hat{\underline{v}}^{(k)} = \alpha \underline{v}^{(k)} + (1-\alpha)\hat{\underline{v}}^{(k-1)} \tag{6.33}$$

where $\underline{v}^{(k)}$ is the reference parameter vector obtained from the solution of Eq. (6.32) and $0.7 \leq \alpha \leq 1$ is a smoothing parameter. The reason for using the smoothing procedure is twofold: (1) to smooth out the values of $\hat{\underline{v}}^{(k)}$ and (2) to reduce the probability that some components of the reference parameter vector will be zero or one at the first few iterations: once such entries become zero or one, they remain so forever, which is undesirable in a vector or matrix of probabilities.

Operatively, the algorithm for the CE method for combinatorial optimization becomes:

1. $k = 0$; choose an initial reference vector $\underline{v}^{(0)}$, e.g., $\underline{v}^{(0)} = \underline{\lambda}$, and a value of ρ, e.g., 10^{-2};
2. $k = k + 1$; (iteration = level counter);
3. Draw a random sample of vector values $\underline{x}_1, \ldots, \underline{x}_N$ from $q_{\underline{X}}\left(\underline{x}; \underline{v}^{(k-1)}\right)$ and compute the corresponding sample $Y(\underline{x}_1), Y(\underline{x}_2), \ldots, Y(\underline{x}_N)$;
4. Find the $(1 - \rho)$ sample quantile $\alpha_Y^{(k)}$ [Eq. (6.23)];
5. With the same sample $\underline{x}_1, \ldots, \underline{x}_N$ determine the solution $\underline{v}^{(k)}$ of Eq. (6.32);
6. Smooth out the reference parameter vector $\underline{v}^{(k)}$ by computing $\hat{\underline{v}}^{(k)}$ with Eq. (6.33);
7. If the value of $\alpha_Y^{(k)}$ does not change for a number of iteration steps, say five, then stop; otherwise, reiterate from step 2.

The stopping criterion, the sample size N, the reference parameter vector $\underline{v}^{(0)}$, and the rarity parameter ρ for initializing the associated stochastic problem, and the smoothing parameter α need to be specified in advance by the analyst. Numerical studies suggest to take values of ρ of the order of 10^{-2}, the smoothing parameter around 0.7 and $N = CR$ where C is a constant, e.g., equal to 5, and R is the number of auxiliary distribution parameters introduced into the associated stochastic problem. The above suggestions are rules of thumb; in practice, it may be useful to run a number of small test problems derived from the original one, in order to tune the parameters.

The main advantage of the CE method for combinatorial optimization problems is that in many cases the updating of $\underline{v}^{(k)}$ can be done analytically, with no need for numerical optimization. Note that in general there are many ways to generate the samples of $\underline{X}$ while estimating the rare-event probability $P(\alpha_Y)$ of the associated stochastic problem and it is not always clear which yields the best results and/or easiest updating formulas.

6.4 Latin Hypercube Sampling

Latin hypercube sampling (LHS) is a method for efficiently generating a distribution of plausible realizations of values from a multidimensional distribution. The technique was first described in [28] and has been further developed for different purposes by several researchers [29–31].

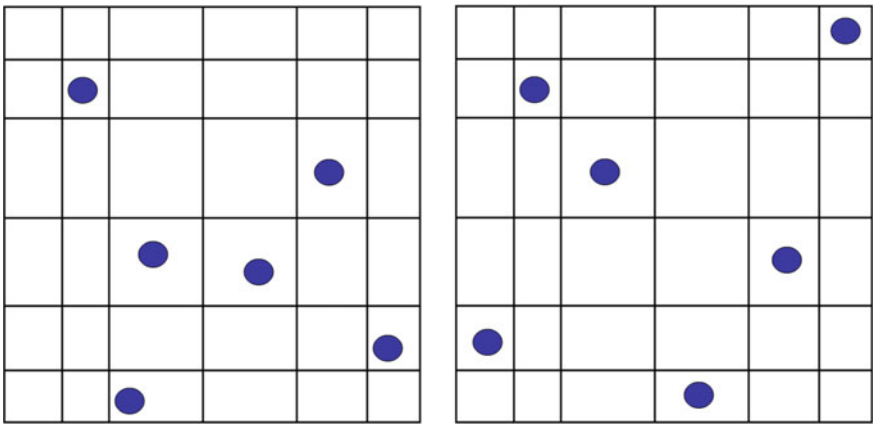

Fig. 6.1 Examples of a *square grid* containing sample positions generated at random without any constraint (*left*) and of a *Latin square* where only one sample is contained in each row and each column (*right*)

In the context of statistical sampling, a square grid containing sample positions is a Latin square if and only if there is only one sample in each row and each column (Fig. 6.1). A Latin hypercube is the generalization of this concept to an arbitrary number of dimensions, whereby each sample is the only one in each axis-aligned hyperplane containing it [32].

The LHS procedure for drawing N_T samples from n independent random variables $\{X_j : j = 1, 2, \ldots, n\}$ with distributions $\{q_j(\cdot) : j = 1, 2, \ldots, n\}$ is detailed below [31].

The range of each variable is divided into N_T disjoint intervals of equal probability and one value is selected at random from each interval, in consistency with the corresponding distributions $\{q_j(\cdot) : j = 1, 2, \ldots, n\}$. The N_T values x_1^k, $k = 1, 2, \ldots, N_T$ thus obtained for X_1 are paired at random, without replacement, with the N_T values x_2^k, $k = 1, 2, \ldots, N_T$ obtained for X_2 to produce the N_T ordered pairs of values $\{x_1^k, x_2^k\}$, $k = 1, 2, \ldots, N_T$. These N_T ordered pairs are combined at random without replacement with the N_T values x_3^k, $k = 1, 2, \ldots, N_T$ of X_3 to form the N_T ordered triplets $\{x_1^k, x_2^k, x_3^k\}$, $k = 1, 2, \ldots, N_T$. The process is repeated for all the n variables until a set of N_T n-tuples is obtained. These n-tuples are of the form

$$\underline{x}^k = \left\{x_1^k, x_2^k, \ldots, x_j^k, \ldots, x_n^k\right\}, \quad k = 1, 2, \ldots, N_T \tag{6.34}$$

and constitute the Latin hypercube samples [31].

For illustration, consider a simple example where it is desired to generate a Latin hypercube sample of size $N_T = 4$ from two rvs $\{X_1, X_2\}$. It is assumed that

X_1 has a standard normal distribution (i.e., with zero mean and unit standard deviation) and X_2 has a uniform distribution on the interval (0, 1) (Fig. 6.2, top, left, and right, respectively). The ranges of X_1 and X_2 are subdivided into $N_T = 4$ intervals each of probability equal to $1/N_T = 1/4 = 0.25$; these intervals are identified by the solid lines that originate at 0.25, 0.5, and 0.75 on the ordinates of Fig. 6.2, middle, left, and right, extend horizontally on the cdfs and then drop vertically to the abscissas to produce the four indicated intervals. Random values $x_1^1, x_1^2, \ldots, x_1^4$ and $x_2^1, x_2^2, \ldots, x_2^4$ are then sampled from these intervals for the two rvs X_1 and X_2, respectively. The sampling of these random realizations is performed as follows [30]: (1) sample u_1^1 and u_2^1 from a uniform distribution on (0, 0.25), u_1^2 and u_2^2 from a uniform distribution on (0.25, 0.5), …, u_1^4 and u_2^4 from a uniform distribution on (0.75, 1.0); (2) use the cdfs to identify (i.e., sample) the corresponding X_1 and X_2 values by means of the inverse transform method [25]: this identification is represented by the dashed lines that originate on the ordinates of Fig. 6.2, middle, left and right, in correspondence of $u_1^1, u_1^2, \ldots, u_1^4$ and $u_2^1, u_2^2, \ldots, u_2^4$, respectively, and then drop vertically to the abscissas to produce $x_1^1, x_1^2, \ldots, x_1^4$ and $x_2^1, x_2^2, \ldots, x_2^4$, respectively. The generation of the LHS is then completed by randomly pairing without replacement the resulting values for X_1 and X_2. Since this pairing is not unique, many different LHSs are possible, with the LHS in Fig. 6.2, bottom, left, resulting from the pairings $\{x_1^1, x_2^2\}$, $\{x_1^2, x_2^3\}$, $\{x_1^3, x_2^4\}$, $\{x_1^4, x_2^1\}$ and the LHS in Fig. 6.2, bottom, right, resulting from the pairings $\{x_1^1, x_2^3\}$, $\{x_1^2, x_2^1\}$, $\{x_1^3, x_2^2\}$, $\{x_1^4, x_2^4\}$ (dots).

The effectiveness of LHS, and hence its popularity, derives from the fact that it provides a dense stratification over the range of each uncertain variable with a relatively small sample size while preserving the desirable probabilistic features of simple random sampling, i.e., standard MCS [30].

A drawback of the LHS technique is that its highly structured form makes it difficult to increase the size of an already existing Latin Hypercube Sample while preserving its stratification properties. Unlike simple random sampling, the size of a Latin hypercube sample cannot be increased simply by generating additional sample elements as the new sample containing the original Latin hypercube sample and the additional sample elements will no longer have the structure of a Latin hypercube sample. For the new sample to also be a Latin hypercube sample, the additional sample elements must be generated with a procedure that takes into account the existing Latin hypercube sample that is being increased in size and the definition of LHS [31]. Moreover, it has been experimentally shown that LHS, which is very efficient for estimating mean values and standard deviations in complex reliability problems [29], is only slightly more efficient than standard MCS for estimating small failure probabilities [33].

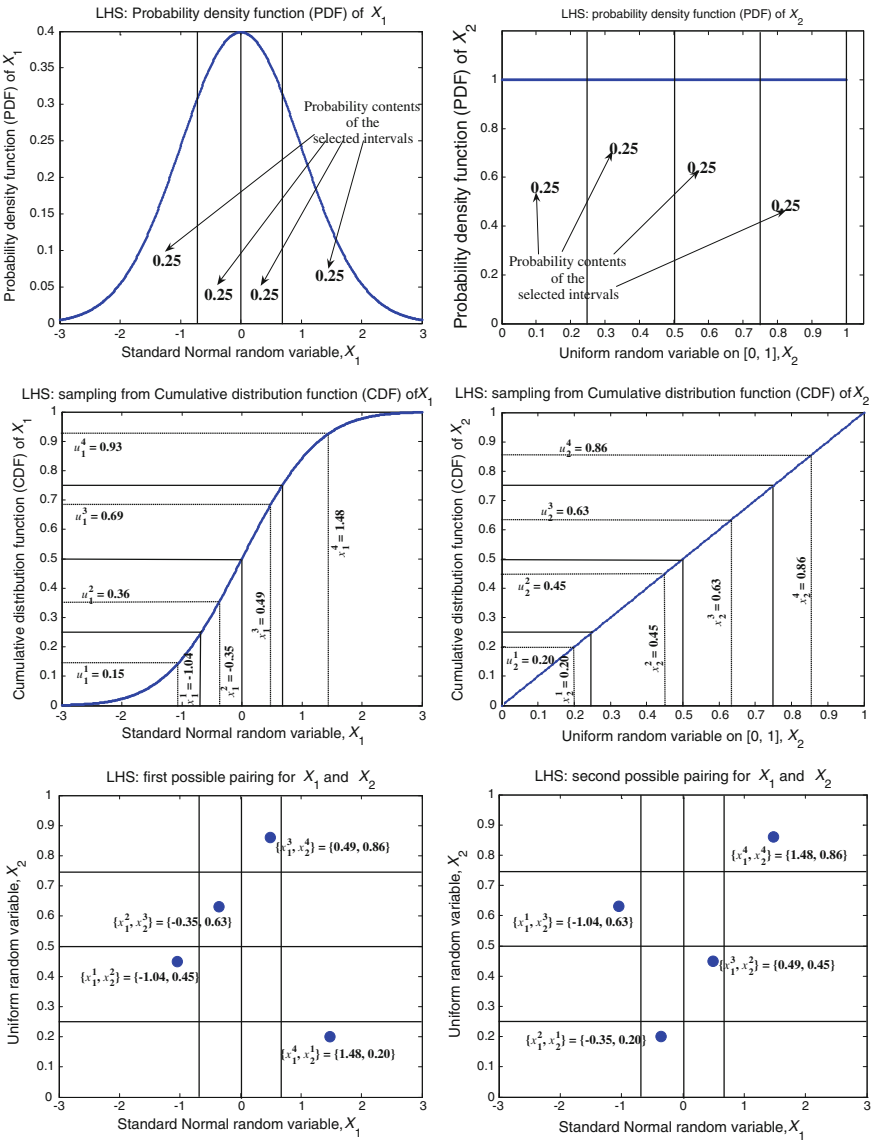

Fig. 6.2 Examples of LHS for the generation of a sample of size $N_T = 4$ from two rvs $\{X_1, X_2\}$ with X_1 standard normal (*first*) and X_2 uniform on (0, 1) (*second*). *Top* pdfs (*thick solid lines*); *third* and *fourth* cdfs (*thick solid lines*) and corresponding disjoint intervals of equal probability (*thin solid lines*); *fifth* and *sixth* two possible Latin hypercube samples of size $N_T = 4$ originating from two different possible random pairings (*dots*)

6.5 Orthogonal Axis

The orthogonal axis (OA) method combines the first-order reliability method (FORM) approximation [34] and MCS in a sort of IS around the "design point" of the problem.

The OA algorithm proceeds as follows [35, 36]:

1. Transform $\underline{X} = (X_1, X_2, \ldots, X_j, \ldots, X_n) \in \mathbb{R}^n$, i.e., the vector of uncertain parameters/values defined in the original physical space $\underline{X} \in \mathbb{R}^n$, into the vector $\underline{\theta} \in \mathbb{R}^n$, where each element of the vector θ_j, $j = 1, 2, \ldots, n$, is associated with a central unit Gaussian standard distribution [2]. Thus, the joint pdf of $\underline{\theta}$ can simply be written as

$$\phi_n(\underline{\theta}) = \prod_{j=1}^{n} \varphi(\theta_j) \tag{6.35}$$

   where $\varphi(\theta_j) = (1/\sqrt{2\pi}) e^{-(\theta_j^2/2)}$, $j = 1, 2, \ldots, n$;
2. With reference to the LSF $g_{\underline{X}}(\underline{x})$ of the given problem (Sect. 6.1), find the "design point" $\underline{\theta}^*$ of the problem (see Sect. 6.8.2.1 for the definition of the design point);
3. Rotate the coordinate system (i.e., by means of a proper rotation matrix R) so that the new coordinate θ_n is in the direction of the axis defined by the design point $\underline{\theta}^*$;
4. Define a new failure function $g_{axis}(\underline{\theta})$ as

$$g_{axis}(\underline{\theta}) = g_{\underline{X}}(R\underline{\theta}) \tag{6.36}$$

5. Writing $\underline{\theta}$ as $\left(\underline{\tilde{\theta}}, \theta_n\right)$, where $\underline{\tilde{\theta}} = (\theta_1, \theta_2, \ldots, \theta_{n-1})$, express the failure probability $P(F)$ as follows:

$$\begin{aligned} P(F) &= P\left[g_{\text{axis}}\left(\underline{\tilde{\theta}}, \theta_n\right) \le 0\right] \\ &= \int P\left[g_{\text{axis}}\left(\underline{\tilde{\theta}}, \theta_n\right) \le 0 \middle| \underline{\tilde{\theta}}\right] \phi_{n-1}\left(\underline{\tilde{\theta}}\right) \mathrm{d}\underline{\tilde{\theta}} \\ &= E_{\tilde{\theta}}\left\{P\left[g_{\text{axis}}\left(\underline{\tilde{\theta}}, \theta_n\right) \le 0\right]\right\} \end{aligned} \tag{6.37}$$

6. Generate N_T iid $(n-1)$-dimensional samples $\left\{\underline{\tilde{\theta}}^k : k = 1, 2, \ldots, N_T\right\}$, where $\underline{\tilde{\theta}}^k = \left(\theta_1^k, \theta_2^k, \ldots \theta_{n-1}^k\right)$;
7. Compute an estimate $\hat{P}(F)$ for the failure probability $P(F)$ as follows:

$$\hat{P}(F) = \frac{1}{N_T} \sum_{k=1}^{N_T} P\left[g_{\text{axis}}\left(\underline{\tilde{\theta}}^k, \theta_n\right) \le 0\right] \tag{6.38}$$

The terms $P\left[g_{\text{axis}}\left(\underline{\tilde{\theta}}^k, \theta_n\right) \leq 0\right]$, $k = 1, 2, \ldots, N_T$, are evaluated with an iterative algorithm which searches for the roots of the equation $g_{\text{axis}}\left(\underline{\tilde{\theta}}^k, \theta_n\right) = 0$ [35, 36]. It is worth noting that the idea underlying the OA method is essentially the same as that of LS. However, in OA the "important direction" is forced to coincide with that of the design point of the problem; moreover, OA employs a rotation of the coordinate system, which can be difficult to define in very high-dimensional problems.

6.6 Dimensionality Reduction

Objective of the dimensionality reduction (DR) method is to reduce the variance associated to the failure probability estimates by exploiting the property of conditional expectation [35, 36]. In extreme synthesis, the LSF $g_{\underline{X}}(\underline{x}) \leq 0$ is re-expressed in such a way as to highlight one of the n uncertain input variables of $\underline{X}$ (say, X_j); then, the failure probability estimate is computed as the expected value of the cdf of X_j conditional on the remaining $(n - 1)$ input variables. By so doing, the zero values contained in the standard MCS estimator (i.e., $I_F(\underline{x}) = 0$, if $\underline{x} \in F$) are removed: this allows to (1) reach any level of probability (even very small) and (2) reduce the variance of the failure probability estimator [35, 36].

The DR algorithm proceeds as follows [35, 36]:

1. Write the failure event $g_{\underline{X}}(\underline{x}) = g_{\underline{X}}\left(x_1, x_2, \ldots, x_j, \ldots, x_n\right) \leq 0$ in such a way as to highlight one of the n uncertain input variables (e.g., X_j)

$$x_j \leq h_{\underline{X}}\left(\underline{x}_{-j}\right), \quad j = 1, 2, \ldots, n \tag{6.39}$$

   where $h_{\underline{X}}(\cdot)$ is a function defined on $\mathbb{R}^{n-1}$ which takes values on the set of all (measurable) subsets of $\mathbb{R}$ and $\underline{x}_{-j}$ is a vector containing values of all the uncertain input variables except the value x_j of X_j, i.e., $\underline{x}_{-j} = \left(x_1, x_2, \ldots, x_{j-1}, x_{j+1}, \ldots, x_n\right)$;
2. Write the failure probability $P(F)$ as follows

$$\begin{aligned} P(F) &= P\left[g_{\underline{X}}(\underline{x}) \leq 0\right] \\ &= P\left[x_j \leq h_{\underline{X}}\left(\underline{x}_{-j}\right)\right] \\ &= E_{\underline{X}_{-j}}\left\{F_{\underline{X}_j|\underline{X}_{-j}}\left[h_{\underline{X}}\left(\underline{x}_{-j}\right)\right]\right\} \end{aligned} \tag{6.40}$$

   where $F_{\underline{X}_j|\underline{X}_{-j}}(\cdot)$ is the cdf of X_j conditional on $\underline{X}_{-j}$;

3. Draw N_T samples $\left\{\underline{x}_{-j}^k : k = 1, 2, \ldots, N_T\right\}$, where $\underline{x}_{-j}^k = \left(x_1^k, x_2^k, \ldots, x_{j-1}^k, x_{j+1}^k, \ldots, x_n^k\right)$, from the $(n-1)$-dimensional marginal pdf $q_m\left(\underline{x}_{-j}\right)$, i.e., $q_m\left(\underline{x}_{-j}\right) = q_m\left(x_1, x_2, \ldots, x_{j-1}, x_{j+1}, \ldots, x_n\right) = \int_{x_j} q\left(x_1, x_2, \ldots, x_j, \ldots, x_n\right) \mathrm{d}x_j$;
4. Using the last expression in Eq. (6.39), compute an unbiased and consistent estimate $\hat{P}(F)$ for the failure probability $P(F)$ as follows

$$\hat{P}(F) = \frac{1}{N_T} \sum_{k=1}^{N_T} F_{\underline{X}_j|\underline{X}_{-j}}\left[h_{\underline{X}}\left(\underline{x}_{-j}^k\right)\right] \tag{6.41}$$

It is worth noting that in Eq. (6.40) the failure probability estimate is computed as the expected value of the cdf $F_{\underline{X}_j|\underline{X}_{-j}}(\cdot)$ of X_j conditional on the remaining $(n-1)$ uncertain variables. Since this quantity takes values between 0 and 1, the zero values contained in the standard MCS estimator (i.e., $I_F(\underline{x}) = 0$, if $\underline{x} \in F$) are removed: this allows to (1) reach any level of failure probability (even very small) and (2) reduce the variance of the failure probability estimator. However, such method cannot always be applied: first, the PF $g_{\underline{X}}(\cdot)$ must be known analytically; second, it must have the property that one of the uncertain input variables can be separated from the others to allow rewriting the failure condition $g_{\underline{X}}(\underline{x}) \leq 0$ in the form of Eq. (6.39) [35, 36].

Finally, notice that DR can be considered a very special case of line sampling (LS, Sect. 6.8) where the PF $g_{\underline{X}}(\cdot)$is analytically known and the important direction $\underline{\alpha}$ coincides with the "direction" of the variable X_j, i.e., $\underline{\alpha} = \left(0, 0, \ldots, x_j, \ldots, 0, 0\right)$.

6.7 Subset Simulation

Subset simulation (SS) is an adaptive stochastic simulation method for efficiently computing small failure probabilities, originally developed for the reliability analysis of structural systems [37]. The underlying idea is to express the (small) failure probability as a product of (larger) probabilities conditional on some intermediate failure events. This allows converting a rare-event simulation into a sequence of simulations of more frequent events. During simulation, the conditional samples are generated by means of a Markov chain designed so that the limiting stationary distribution is the target conditional distribution of some adaptively chosen failure event; by so doing, the conditional samples gradually populate the successive intermediate failure regions up to the final target (rare) failure region [1].

For a given target failure event F of interest, [i.e., the failure region $F \subset \mathbb{R}^n$, see Eq. (6.1)] let $F_1 \supset F_2 \supset \cdots \supset F_m = F$ be a sequence of intermediate failure

events (sets in $\mathbb{R}^n$), so that $F_k = \cap_{i=1}^{k} F_i$, $k = 1, 2, \ldots, m$. By sequentially conditioning on the event F_i, the failure probability $P(F)$ can be written as:

$$P(F) = P(F_m) = P(F_1) \prod_{i=1}^{m-1} P(F_{i+1}|F_i) \tag{6.42}$$

Notice that even if $P(F)$ is small, the conditional probabilities involved in Eq. (6.42) can be made sufficiently large by appropriately choosing m and the intermediate failure events $\{F_i, i = 1, 2, \ldots, m - 1\}$.

The original idea of SS is to estimate the failure probability $P(F)$ by estimating $P(F_1)$ and $\{P(F_{i+1}|F_i) : i = 1, 2, \ldots, m-1\}$. Considering for example $P(F) \approx 10^{-5}$ and choosing $m = 5$ intermediate failure events such that $P(F_1)$ and $\{P(F_{i+1}|F_i) : i = 1, 2, 3, 4\} \approx 0.1$, the conditional probabilities can be evaluated efficiently by simulation of the relatively frequent failure events [37].

Standard MCS can be used to estimate $P(F_1)$. On the contrary, computing the conditional failure probabilities in Eq. (6.42) by MCS entails the nontrivial task of sampling from the conditional distributions of $\underline{X}$ given that it lies in F_i, $i = 1, 2, \ldots, m - 1$, i.e., from $q_{\underline{X}}(\underline{x}|F_i) = q_{\underline{X}}(\underline{x}) I_{F_i}(\underline{x}) / P(F)$. In this regard, Markov Chain Monte Carlo (MCMC) simulation provides a powerful method for generating samples conditional on the failure region F_i, $i = 1, 2, \ldots, m - 1$ [1, 37]. The related algorithm is presented in Sect. 6.7.1.

6.7.1 Markov Chain Monte Carlo Simulation

MCMC simulation comprises a number of powerful simulation techniques for generating samples according to any given probability distribution [38–40].

In the context of the failure probability assessment of interest here, MCMC simulation provides an efficient way for generating samples from the multidimensional conditional pdf $q_{\underline{X}}(\underline{x})$. The distribution of the samples thereby generated tends to the multidimensional conditional pdf $q_{\underline{X}}(\underline{x}|F)$ as the length of the Markov chain increases. In mathematical terms, letting $\{\underline{x}^u : u = 1, 2, \ldots, N_s\}$ be the set of MCMC samples, then $\underline{x}^{N_s}$ tends to be distributed as $q_{\underline{X}}(\underline{x}|F)$ as $N_s \to \infty$. In the particular case of the initial sample $\underline{x}^1$ being distributed exactly as the multidimensional conditional pdf $q_{\underline{X}}(\underline{x}|F)$, then so are the subsequent samples and the Markov chain are always stationary [37].

Furthermore, since in practical applications dependent rvs may often be generated by some transformation of independent rvs, in the following it is assumed without loss of generality that the components of $\underline{X}$ are independent, that is, $q_{\underline{X}}(\underline{x}) = \prod_{j=1}^{n} q_j(x_j)$, where $q_j(x_j)$ denotes the 1-D pdf of x_j [37].

To illustrate the MCMC simulation algorithm with reference to a generic failure region F_i, let $\underline{\tilde{x}}^u = \left\{\tilde{x}_1^u, \tilde{x}_2^u, \ldots, \tilde{x}_j^u, \ldots, \tilde{x}_n^u\right\}$ be the uth Markov chain sample drawn and let $p_j^*(\xi_j|x_j^u)$, $j = 1, 2, \ldots, n$, be a one-dimensional 'proposal pdf' for ξ_j, centered at the value x_j^u and satisfying the symmetry property $p_j^*(\xi_j|x_j^u) = p_j^*(x_j^u|\xi_j)$. Such distribution, arbitrarily chosen for each element x_j of $\underline{x}$, allows generating a "precandidate value" ξ_j based on the current sample value x_j^u. The following algorithm is then applied to generate the next Markov chain sample $\underline{\tilde{x}}^{u+1} = \left\{\tilde{x}_1^{u+1}, \tilde{x}_2^{u+1}, \ldots, \tilde{x}_j^{u+1}, \ldots, \tilde{x}_n^{u+1}\right\}$, $u = 1, 2, \ldots, N_s - 1$ [37]:

1. Generation of a candidate sample $\underline{\tilde{x}}^{u+1} = \left(\tilde{x}_1^{u+1}, \tilde{x}_2^{u+1}, \ldots, \tilde{x}_j^{u+1}, \ldots, \tilde{x}_n^{u+1}\right)$: for each parameter x_j, $j = 1, 2, \ldots, n$:
   (a) Sample a precandidate value ξ_j^{u+1} from $p_j^*(\cdot|x_j^u)$;
   (b) Compute the acceptance ratio

$$r_j^{u+1} = \frac{q_j(\xi_j^{u+1})}{q_j(x_j^u)} \tag{6.43}$$

   (c) Set the new value $\tilde{x}_j^{u+1}$ of the jth element of $\underline{\tilde{x}}^{u+1}$ as follows:

$$\tilde{x}_j^{u+1} = \begin{cases} \xi_j^{u+1} & \text{with probability } \min(1, r_j^{u+1}) \\ x_j^u & \text{with probability } 1 - \min(1, r_j^{u+1}) \end{cases} \tag{6.44}$$

2. Acceptance/rejection of the candidate sample vector $\underline{\tilde{x}}^{u+1}$:
   If $\underline{\tilde{x}}^{u+1} = \underline{x}^u$ (i.e., no precandidate values have been accepted), set $\underline{\tilde{x}}^{u+1} = \underline{x}^u$. Otherwise, check whether $\underline{\tilde{x}}^{u+1}$ is a system failure configuration, i.e., $\underline{\tilde{x}}^{u+1} \in F_i$: if it is, then accept the candidate $\underline{\tilde{x}}^{u+1}$ as the next state, i.e., set $\underline{x}^{u+1} = \underline{\tilde{x}}^{u+1}$; otherwise, reject the candidate $\underline{\tilde{x}}^{u+1}$ and take the current sample as the next one, i.e., set $\underline{x}^{u+1} = \underline{x}^u$.

In synthesis, a candidate sample $\underline{\tilde{x}}^{u+1}$ is generated from the current sample $\underline{x}^u$ and then either the candidate sample $\underline{\tilde{x}}^{u+1}$ or the current sample $\underline{x}^u$ is taken as the next sample $\underline{x}^{u+1}$, depending on whether the candidate $\underline{\tilde{x}}^{u+1}$ lies in the failure region F_i or not. For clarity, a pictorial representation of the MCMC simulation algorithm is provided in Fig. 6.3.

Step 1 above can be viewed as a "local" random walk in the neighborhood of the current state $\underline{x}^u$, while step 2 above ensures that the next sample always lies in F_i so as to produce the correct conditioning in the samples. Thus, step 2 is, in principle, similar to the standard MCS approach in that both are based on accepting samples that lie in F_i. However, the acceptance rate for the Metropolis algorithm should be considerably higher than for standard MCS, because the candidate state $\underline{\tilde{x}}^{u+1}$ is

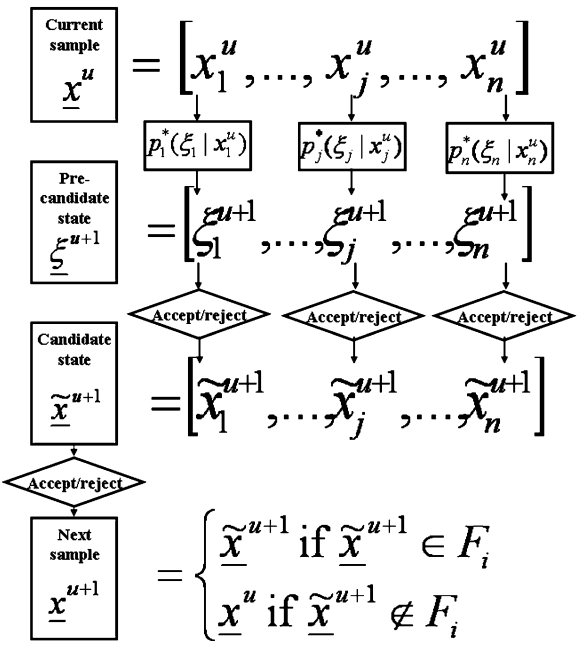

Fig. 6.3 Illustration of the MCMC simulation algorithm [37]

simulated in the neighborhood of the current state $\underline{\tilde{x}}^u \in F_i$ if the proposal pdfs $\left\{p_j^* : j = 1, 2, \ldots, n\right\}$ are sufficiently local and so $\underline{\tilde{x}}^{u+1}$ should have a high probability of lying in F_i. Thus, Markov chain simulation accelerates the efficiency of exploring the failure region. The higher acceptance rate, however, is gained at the expense of introducing dependence between successive samples, which inevitably reduces the efficiency of the conditional failure probability estimators [1].

Proof of Stationary Distribution of the Markov Chain

In this section, we show that the next sample $\underline{x}^{u+1}$ of the Markov chain is distributed as $q_{\underline{X}}(\cdot|F_i)$ if the current sample $\underline{x}^u$ is, and hence $q_{\underline{X}}(\cdot|F_i)$ is the stationary distribution of the Markov chain. Since all the Markov chain samples lie in F_i, it is sufficient to consider the transition between the states in F_i, which is governed by step 1 of the MCMC Simulation algorithm described in Sect. 6.7.1.

According to step 1 above, the transition of the individual components of $\underline{x}^u$ is independent, so the transition pdf of the Markov chain between any two states in F_i can be expressed as a product of the component transition pdfs

$$p(\underline{x}^{u+1}|\underline{x}^u) = \prod_{j=1}^{n} p_j(x_j^{u+1}|x_j^u) \tag{6.45}$$

where $p_j(\cdot|x_j^u)$ is the transition pdf for the jth component of $\underline{x}^u$.

For $x_j^{u+1} \neq x_j^u$

$$p_j(x_j^{u+1}|x_j^u) = p_j^*(x_j^{u+1}|x_j^u)\min\left\{1, \frac{q_j(x_j^{u+1})}{q_j(x_j^u)}\right\} \tag{6.46}$$

Using Eq. (6.46), together with the symmetry property of $p_j^*(\cdot|x_j^u)$ and the identity $\min\{1,\ a/b\}b = \min\{1,\ b/a\}a$ for any positive numbers a and b, it is straightforward to show that $p_j(\cdot|x_j^u)$ satisfies the 'reversibility' condition with respect to $q_j(\cdot)$

$$p_j(x_j^{u+1}|x_j^u)q_j(x_j^u) = p_j(x_j^u|x_j^{u+1})q_j(x_j^{u+1}) \tag{6.47}$$

Combining Eqs. (6.45) and (6.47) and the fact that all the states lie in F_i, the transition pdf for the whole state $\underline{x}^u$ also satisfies the following reversibility condition with respect to $q(\cdot|F_i)$

$$p\left(\underline{x}^{u+1}|\underline{x}^u\right)q_{\underline{X}}(\underline{x}^u|F_i) = p\left(\underline{x}^u|\underline{x}^{u+1}\right)q_{\underline{X}}\left(\underline{x}^{u+1}|F_i\right) \tag{6.48}$$

Thus, if the current sample $\underline{x}^u$ is distributed as $q(\cdot|F_i)$, then

$$\begin{aligned} p\left(\underline{x}^{u+1}\right) &= \int p\left(\underline{x}^{u+1}|\underline{x}^u\right)q_{\underline{X}}(\underline{x}^u|F_i)\mathrm{d}\underline{x}^u \\ &= \int p\left(\underline{x}^u|\underline{x}^{u+1}\right)q_{\underline{X}}\left(\underline{x}^{u+1}|F_i\right)\mathrm{d}\underline{x}^u \\ &= q_{\underline{X}}\left(\underline{x}^{u+1}|F_i\right)\int p\left(\underline{x}^u|\underline{x}^{u+1}\right)\mathrm{d}\underline{x}^u \\ &= q_{\underline{X}}\left(\underline{x}^{u+1}|F_i\right) \end{aligned} \tag{6.49}$$

since $\int p\left(\underline{x}^u|\underline{x}^{u+1}\right)\mathrm{d}\underline{x}^u = 1$. This shows that the next Markov chain sample $\underline{x}^{u+1}$ will also be distributed as $q_{\underline{X}}(\cdot|F_i)$, and so the latter is indeed the stationary distribution for the generated Markov chain.

6.7.2 The Subset Simulation Procedure

Utilizing the MCMC Simulation method described in Sect. 6.7.1, SS proceeds as follows. First, N vectors $\left\{\underline{x}_0^k : k = 1, 2, \ldots, N\right\}$ are simulated by standard MCS to compute an estimate $\tilde{P}_1$ for $P(F_1)$ by

$$P(F_1) \approx \tilde{P}_1 = \frac{1}{N}\sum_{k=1}^{N} I_{F_1}(\underline{x}_0^k) \tag{6.50}$$

where $\left\{\underline{x}_0^k : k = 1, 2, \ldots, N\right\}$ are iid samples drawn from the original multidimensional pdf $q_{\underline{X}}(\cdot)$. The subscript "0" denotes the fact that these samples

correspond to "Conditional Level 0". Among the iid samples $\{\underline{x}_0^k : k = 1, 2, \ldots, N\}$, those lying in F_1 can be readily identified: these samples are at "Conditional level 1" and are distributed as $q_{\underline{X}}(\cdot|F_1)$. Starting from each of these samples, additional conditional samples lying in F_1 are generated using MCMC simulation: as shown in Sect. 6.7.1, these samples will also be distributed as $q_{\underline{X}}(\cdot|F_1)$ because the Markov chain is in stationary state. These samples can be used to estimate $P(F_2|F_1)$ using an estimator $\tilde{P}_2$ similar to Eq. (6.49). Notice that the Markov chain samples which lie in F_2 are at "Conditional level 2" and distributed as $q_{\underline{X}}(\cdot|F_2)$; thus, they provide seeds for simulating more samples according to $q_{\underline{X}}(\cdot|F_2)$ to estimate $P(F_3|F_2)$. Repeating the process, the conditional failure probabilities can be computed for the higher conditional levels until the failure region of interest F ($\equiv F_m$) is reached. At the ith conditional level, $i = 1, 2, \ldots, m-1$, let $\{\underline{x}_i^k : k = 1, 2, \ldots, N\}$ be the Markov chain samples with distribution $q_{\underline{X}}(\cdot|F_i)$, possibly coming from different chains generated by different seeds; then

$$P(F_{i+1}|F_i) \approx \tilde{P}_{i+1} = \frac{1}{N}\sum_{k=1}^{N} I_{F_{i+1}}(\underline{x}_i^k) \tag{6.51}$$

Finally, combining Eqs. (6.42), (6.50) and (6.51), the failure probability estimator is

$$\tilde{P}_F = \prod_{i=1}^{m} \tilde{P}_i \tag{6.52}$$

Notice that the total number of samples generated during the SS procedure is roughly $N_T = mN$ where m is the number of levels and N is the number of samples generated for each level $i = 1, 2, \ldots, m$.

6.7.3 Statistical Properties of Estimators

In this section, results are presented about the statistical properties of the estimators $\tilde{P}_i$, $i = 1, 2, \ldots, m$, and $\tilde{P}_F$. The detailed derivation of these results can be found in [37].

Monte Carlo Simulation Estimator $\tilde{P}_1$

As it is well known, the MCS estimator $\tilde{P}_1$ in Eq. (6.50), computed using the iid samples $\{\underline{x}_0^k : k = 1, 2, \ldots, N\}$ converges almost surely to P_1 (Strong Law of Large Numbers), is unbiased, consistent, and normally distributed as $N \to \infty$

(Central Limit Theorem). The coefficient of variation (c.o.v., defined as the ratio of the standard deviation to the mean of the estimate) of $\tilde{P}_1$, δ_1, is given by

$$\delta_1 = \sqrt{\frac{1 - P(F_1)}{NP(F_1)}} \tag{6.53}$$

Conditional Probability Estimator $\tilde{\mathrm{P}}_i, \mathbf{i} = 2, 3, \ldots, \mathbf{m}$

Since the Markov chains generated at each conditional level are started with samples distributed as the corresponding target conditional pdf, the Markov chain samples used for computing the conditional probability estimators based on Eq. (6.51) are all identically distributed as the target conditional pdf. It follows that the conditional probability estimators $\tilde{P}_i$, $i = 2, 3, \ldots, m$, are unbiased. The c.o.v. of $\tilde{P}_i$, δ_i, is given by

$$\delta_i = \sqrt{\frac{1 - P(F_i|F_{i-1})}{NP(F_i|F_{i-1})}(1 + \gamma_i)} \tag{6.54}$$

where

$$\gamma_i = 2 \sum_{\tau=1}^{N/N_c - 1} \left(1 - \frac{\tau N_c}{N}\right) \rho_i(\tau) \tag{6.55}$$

is a correlation factor. It has been assumed that at each simulation level there are N_c Markov chains developed, each having N/N_c samples, so that the total number of samples generated at each simulation level is $N_c \times N/N_c = N$ (the question of how to maintain a fixed number of chains N_c will be discussed later). In Eq. (6.55)

$$\rho_i(\tau) = R_i(\tau)/R_i(0) \tag{6.56}$$

is the correlation coefficient at lag τ of the stationary sequence $\left\{I_{F_i}(\underline{x}_{i-1}^{c,u}) : u = 1, 2, \ldots, N/N_c\right\}$., where $\underline{x}_{i-1}^{c,u}$ denotes the uth sample along the cth chain (started from the cth seed) at the $(i-1)$th simulation level. In Eq. (6.56)

$$\begin{aligned} R_i(\tau) &= E\left\{\left[I_{F_i}(\underline{x}_{i-1}^{c,u}) - P(F_i|F_{i-1})\right] \cdot \left[I_{F_i}(\underline{x}_{i-1}^{c,u+\tau}) - P(F_i|F_{i-1})\right]\right\} \\ &= E\left[I_{F_i}(\underline{x}_{i-1}^{c,u}) I_{F_i}(\underline{x}_{i-1}^{c,u+\tau})\right] - P(F_i|F_{i-1})^2 \end{aligned} \tag{6.57}$$

is the covariance between $I_{F_i}(\underline{x}_{i-1}^{c,u})$ and $I_{F_i}(\underline{x}_{i-1}^{c,u+\tau})$, for any $u = 1, 2, \ldots, N/N_c$, and it is independent of u due to stationarity. It is also independent of the chain index c since all chains are probabilistically equivalent.

The covariance sequence $\{R_i(\tau) : \tau = 1, 2, \ldots, N/N_c - 1\}$ can be estimated using the Markov chain samples $\left\{\underline{x}_{i-1}^{c,u} : c = 1, 2, \ldots, N_c; u = 1, 2, \ldots, N/N_c\right\}$ at the $(i-1)$th conditional level by

$$R_i(\tau) \approx \tilde{R}(\tau) = \left(\frac{1}{N - \tau N_c} \sum_{c=1}^{N_c} \sum_{\tau=1}^{N/N_c - 1} I_{F_i}(\underline{x}_{i-1}^{c,u}) I_{F_i}(\underline{x}_{i-1}^{c,u+\tau}) \right) - \tilde{P}_i \tag{6.58}$$

from which the correlation sequence $\{\rho_i(\tau) : \tau = 1, 2, \ldots, N/N_c - 1\}$ and hence the correlation factor γ_i in Eq. (6.55) can also be estimated. Consequently, the c.o.v. δ_i for the conditional estimator $\tilde{P}_i$ can be estimated by Eq. (6.54), where $P(F_i|F_{i-1})$ is approximated by $\tilde{P}_i$ using Eq. (6.51).

Failure Probability Estimator $\tilde{P}_F$

Due to the correlation among the estimators $\left\{\tilde{P}_i : i = 1, 2, \ldots, m\right\}$, $\tilde{P}_F$ given by Eq. (6.52) is biased for every N. This correlation is due to the fact that the samples used for computing $\tilde{P}_i$ which lie in F_i are used to start the Markov chains to compute $\tilde{P}_{i+1}$. It can be shown that the fractional bias of $\tilde{P}_F$ is bounded by

$$\left| E\left[\frac{\tilde{P}_F - P(F)}{P(F)} \right] \right| \leq \sum_{i>j} \delta_i \delta_j + o(1/N) = O(1/N) \tag{6.59}$$

which means that $\tilde{P}_F$ is asymptotically unbiased and the bias is $O(1/N)$.

On the other hand, the c.o.v. δ of $\tilde{P}_F$ may be bounded above by using

$$\delta^2 = E\left[\frac{\tilde{P}_F - P(F)}{P(F)} \right] \leq \sum_{i,j=1}^{m} \delta_i \delta_j + o(1/N) = O(1/N) \tag{6.60}$$

showing that $\tilde{P}_F$ is a consistent estimator and its c.o.v. δ is $O(1/\sqrt{N})$. Note that the c.o.v. δ in Eq. (6.60) is defined through the expected deviation about the target failure probability $P(F)$ instead of $E\left[\tilde{P}_F\right]$ so that the effects of the bias are accounted for. The upper bound corresponds to the case when the conditional probability estimators $\left\{\tilde{P}_i : i = 2, 3, \ldots, m\right\}$ are fully correlated. The actual c.o.v. depends on the correlation between the $\tilde{P}_i$'s. If all the $\tilde{P}_i$'s were uncorrelated, then

$$\delta^2 = \sum_{i=1}^{m} \delta_i^2 \tag{6.61}$$

Although the $\tilde{P}_i$'s are generally correlated, simulations show that δ^2 may be well approximated by Eq. (6.61). This will be illustrated in the applications of the Sects. 7.1 and 7.2.

6.7.4 Implementation Issues

Choice of the Proposal Pdfs

The proposal pdfs $\left\{P_j^* : j = 1, 2, \ldots, n\right\}$ affect the deviation of the candidate sample from the current one, thus controlling the efficiency of the Markov chain samples in populating the failure region. Simulations show that the efficiency of the method is almost insensitive to the *type* of the proposal pdfs, and hence those which can be manipulated most easily may be used. For example, the uniform pdf centered at the current sample with a proper width is a good candidate for $\left\{P_j^* : j = 1, 2, \ldots, n\right\}$, and thus it will be used in the applications of the Sects. 7.1 and 7.2.

On the other hand, the *spreads* of the proposal pdfs affect the size of the region covered by the Markov chain samples, and consequently they control the efficiency of the method. Small spreads tend to increase the correlation between successive samples due to their proximity to the conditioning central value, thus slowing down the convergence of the failure probability estimators. Indeed, as it has been shown in Sects. 6.7.3.2 and 6.7.3.3, the c.o.v. of the failure probability estimates, increases as the correlation between the successive Markov chain samples increases. On the other hand, excessively large spreads may reduce the acceptance rate, increasing the number of repeated Markov chain samples, still slowing down convergence [1]. The optimal choice of the spread of the proposal pdfs $\left\{P_j^* : j = 1, 2, \ldots, n\right\}$ is therefore a tradeoff between acceptance rate and correlation due to proximity of the MCMC samples. Roughly speaking, the spread of p_j^* may be chosen as some fraction of the standard deviation of the corresponding parameter x_j, $j = 1, 2, \ldots, n$, as specified by the original pdf $q(\underline{x})$, although the optimal choice depends on the particular type of the problem [1].

Choice of Intermediate Failure Events

The choice of the intermediate failure regions $\{F_i : i = 1, 2, \ldots, m-1\}$ plays a key role in the SS procedure. Two issues are basic to their choice. The first is a parameterization of the target failure region F which allows the generation of intermediate failure regions by varying the value of the defined parameter. The second issue concerns the choice of the specific sequence of values of the defined parameter which affects the values of the conditional failure probabilities $\{P(F_{i+1}|F_i) : i = 1, 2, \ldots, m-1\}$ and hence the efficiency of the SS procedure [37].

Generic Representation of Failure Regions

Many failure regions encountered in engineering applications are a combination of the union and intersection of failure regions of components. In particular, consider a failure region of the following form

$$F = \bigcup_{b=1}^{n} \bigcap_{j=1}^{n_b} \{\underline{x} : O_{bj}(\underline{x}) < D_{bj}(\underline{x})\} \tag{6.62}$$

where $O_{bj}(\underline{x})$ and $D_{bj}(\underline{x})$ may be viewed as the output performance and demand variables of the component (b, j) of the system, respectively. The failure region F in Eq. (6.62) can be considered as the failure of a system with η subsystems connected in series, where the bth subsystem consists of n_b components connected in parallel.

In order to apply SS, it is requested to parameterize F with a single parameter so that the sequence of intermediate failure regions $\{F_i : i = 1, 2, \ldots, m-1\}$ can be generated by varying that parameter. This can be accomplished as follows. For the failure region F in Eq. (6.62), the "critical output-to-demand ratio" (CODR) $Y(\underline{x})$ is defined as

$$Y(\underline{x}) = \max_{b=1,2,\ldots,n} \min_{j=1,2,\ldots nb} \frac{O_{bj}(\underline{x})}{D_{bj}(\underline{x})} \tag{6.63}$$

Then, it can be easily verified that

$$F = \{\underline{x} : Y(\underline{x}) < 1\} \tag{6.64}$$

and so the sequence of intermediate failure regions can be generated as

$$F_i = \{\underline{x} : Y(\underline{x}) < y_i\} \tag{6.65}$$

where $y_1 > y_2 > \cdots > y_i > \cdots > y_m = y > 0$ is a decreasing sequence of (normalized) intermediate threshold values.

It is straightforward to generalize to failure regions consisting of multiple stacks of unions and intersections. Essentially, Y is defined using "max" and "min" in the same order corresponding to each occurrence of union ($\cup$) and intersection ($\cap$) in F, respectively [1].

Choice of Intermediate Threshold Levels

The choice of the sequence of intermediate threshold values $\{y_i, i = 1, 2, \ldots, m\}$ appearing in the parameterization of intermediate failure regions affects the values of the conditional failure probabilities, and hence the efficiency of the SS procedure. If the sequence decreases slowly, then the conditional probabilities will be large, and so their estimation requires a low number of samples N. A slow sequence, however, requires more simulation levels m to reach the target failure

region, increasing the total number of samples $N_T = mN$ in the whole procedure. Conversely, if the sequence increases so rapidly that the conditional failure events become rare, it will require a high number of samples N to obtain an accurate estimate of the conditional failure probabilities in each simulation level, which again increases the total number of samples N_T. Thus, it can be seen that the choice of the intermediate threshold values is a tradeoff between the number N of samples required in each simulation level and the number m of simulation levels required to reach the target failure region [37].

One strategy for the choice of the intermediate threshold values is to select the y_i's a priori; unfortunately, in this case it is difficult to control the values of the conditional probabilities $\{P(F_{i+1}|F_i) : i = 1, 2, \ldots, m-1\}$. For this reason, in the applications of the Sects. 7.1 and 7.2 the y_i's are chosen "adaptively" so that the estimated conditional probabilities $\{P(F_{i+1}|F_i) : i = 1, 2, \ldots, m-1\}$ are equal to a fixed value $p_0 \in (0, 1)$. This can be accomplished by choosing the intermediate threshold level y_i, $i = 1, 2, \ldots, m$, as the $(1 - p_0)N$th smallest value (i.e., an order statistics) among the CODRs $\left\{Y\left(\underline{x}_{i-1}^k\right) : k = 1, 2, \ldots, N\right\}$ where the $\underline{x}_{i-1}^k$'s are the Markov chain samples generated at the $(i-1)$th conditional level for $i = 2, 3, \ldots, m-1$, and the $\underline{x}_0^k$'s are the samples from the initial standard MCS. This choice of the intermediate threshold levels implies that they are dependent on the conditional samples and will vary in different simulation runs. For a target failure probability level of 10^{-3}–10^{-6}, choosing $p_0 = 0.1$ is found to yield good efficiency [37].

Computational Flow of Subset Simulation

According to the considerations made in Sect. 6.7.4.2, in the actual SS implementation it is assumed, with no loss of generality, that the failure event of interest can be defined in terms of the value of a critical response variable Y of the system under analysis being lower than a specified threshold level y, i.e., $F = \{Y < y\}$. The sequence of intermediate failure events $\{F_i : i = 1, 2, \ldots, m\}$ can then be correspondingly defined as $\{F_i\{Y < y_i\}, i = 1, 2, \ldots, m\}$, where $y_1 > y_2 > \cdots > y_i > \cdots > y_m = y > 0$ is a decreasing sequence of intermediate threshold values [1, 37].

Moreover, the intermediate threshold values are chosen adaptively in such a way that the estimated conditional failure probabilities are equal to a fixed value p_0 [1, 37].

The SS algorithm proceeds as follows (Fig. 6.4). First, N vectors $\left\{\underline{x}_0^k : k = 1, 2, \ldots, N\right\}$ are sampled by standard MCS, i.e., from the original pdf function $q_{\underline{X}}(\cdot)$. The subscript '0' denotes the fact that these samples correspond to "Conditional Level 0". The corresponding values of the response variable $\left\{Y\left(\underline{x}_0^k\right) : k = 1, 2, \ldots, N\right\}$ are then computed and the first intermediate threshold value y_1 is chosen as the $(1 - p_0)N$th value in the decreasing list of values $\left\{Y\left(\underline{x}_0^k\right) : k = 1, 2, \ldots, N\right\}$. By so doing, the sample estimate of $P(F_1) = P(Y < y_1)$ is equal to p_0 (note that it has been implicitly assumed that $p_0 N$ is an integer value).

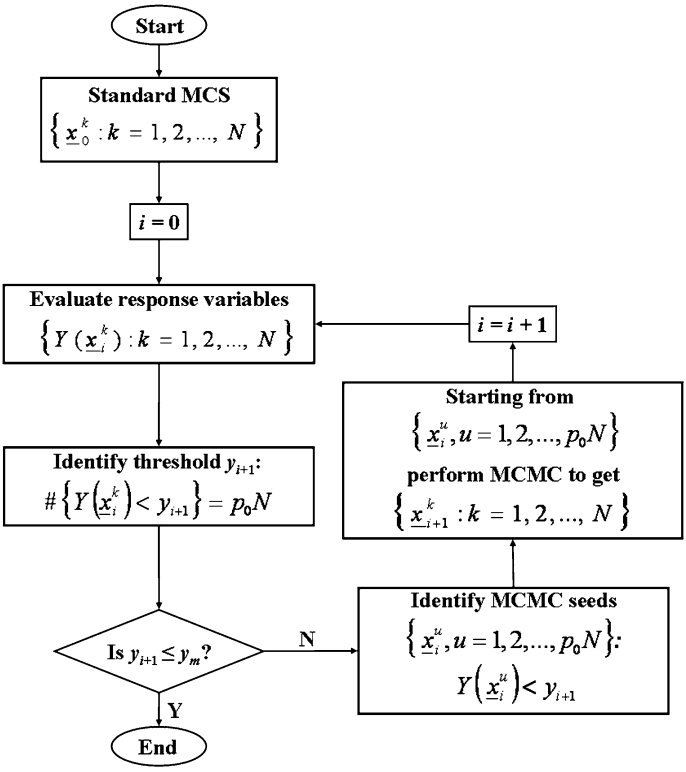

Fig. 6.4 Flow diagram of the SS algorithm

With this choice of y_1, there are now p_0N samples among $\{\underline{x}_0^k : k = 1, 2, \ldots, N\}$ whose response Y lies in $F_1 = \{Y < y_1\}$. These samples are at "Conditional level 1" and distributed as $q_{\underline{X}}(\cdot|F_1)$. Starting from each one of these samples, MCMC simulation is used to generate $(1 - p_0)N$ additional conditional samples distributed as $q_{\underline{X}}(\cdot|F_1)$, so that there are a total of N conditional samples $\{\underline{x}_0^k : k = 1, 2, \ldots, N\} \in F_1$, at "Conditional level 1". Then, the intermediate threshold value y_2 is chosen as the $(1 - p_0)N$th value in the descending list of $\{Y(\underline{x}_1^k) : k = 1, 2, \ldots, N\}$ to define $F_2 = \{Y < y_2\}$ so that, again, the sample estimate of $P(F_2|F_1) = P(Y < y_2|Y < y_1)$ is equal to p_0. The p_0N samples lying in F_2 are conditional values from $q_{\underline{X}}(\cdot|F_2)$ and function as "seeds" for sampling $(1 - p_0)N$ additional conditional samples distributed as $q_{\underline{X}}(\cdot|F_2)$, making up a total of N conditional samples $\{\underline{x}_2^k : k = 1, 2, \ldots, N\}$ at "Conditional level 2". This procedure is repeated for the remaining conditional levels until the samples at "Conditional level $(m - 1)$" are generated to yield $y_m < y$ as the $(1 - p_0)N$th value in the descending list of $\{Y(\underline{x}_{m-1}^k) : k = 1, 2, \ldots, N\}$, so that there are enough samples for estimating $P(Y < y)$.

In the end, with this procedure the exact total number of samples generated is equal to $N + (m - 1)(1 - p_0)N$ [41].

For clarity sake, a step-by-step illustration of the procedure for Conditional levels 0 and 1 is provided in Fig. 6.5 by way of an example.

Notice that the procedure is such that the response values $\{y_i, i = 1, 2, \ldots, m\}$ at the specified probability levels $P(F_1) = p_0$, $P(F_2) = p(F_2|F_1)P(F_1) = p_0^2$, …, $P(F_m) = p_0^m$ are estimated, rather than the failure probabilities $P(F_1)$, $P(F_2|F_1)$, …, $P(F_m|F_{m-1})$, which are a priori fixed at p_0. In this view, SS is a method for generating samples whose response values correspond to specified probability levels, rather than for estimating probabilities of specified failure events. As a result, it produces information about $P(Y < y)$ versus y at all the simulated values of Y rather than at a single value of y. This feature is important because the whole trend of $P(Y < y)$ versus y obviously provides much more information than a point estimate [42].

For a threshold value y of interest that does not coincide with the simulated values of Y, the following formula may be used for estimating $P(F) = P(Y < y)$, which follows directly from the Theorem of Total Probability (Appendix A.4)

$$P(F) \sum_{i=0}^{m} P(F|B_i)P(B_i) \tag{6.66}$$

where

$$\begin{aligned} B_0 &= \bar{F}_1 = \{Y \geq y_1\} \\ B_i &= F_i - F_{i+1} = \{y_{i+1} \leq Y < y_i\}, \quad i = 1, 2, \ldots, m-1 \\ B_m &= F_m = \{Y < y_m\} \end{aligned} \tag{6.67}$$

are "bins" derived from the intermediate failure events $\{F_i : i = 1, 2, \ldots, m\}$.

Note that $\{B_i : i = 0, 1, \ldots, m\}$ form a partition of the uncertain parameter space, i.e., $p(B_i \cap B_j) = 0$ for $i \neq j$ and $\sum_{i=0}^{m} P(B_i) = 1$. In fact

$$\begin{aligned} p(B_0) &= 1 - p_0 \\ p(B_i) &= p_0^i - p_0^{i+1}, \quad i = 1, 2, \ldots, m-1 \\ p(B_m) &= p_0^m \end{aligned} \tag{6.68}$$

The conditional probability $P(F|B_i)$ in Eq. (6.66) is simply estimated as the fraction of samples in B_i that lie in F (i.e., with corresponding $Y < y$), whereas the samples conditional on each bin B_i can be readily obtained from those in SS. Basically, the $(1 - p_0)N$ samples at Conditional Level 0 that do not lie in Conditional Level 1 are collected in B_0; for $i = 1, 2, \ldots, m - 1$, the $(1 - p_0)N$ samples at Conditional Level i (with corresponding $Y < y_i$) that do not lie in Conditional Level $(i + 1)$ (i.e., with $Y \geq y_{i+1}$) are collected in B_i; the samples in F_m (i.e., with $Y < y_m$) are collected in B_m [42].

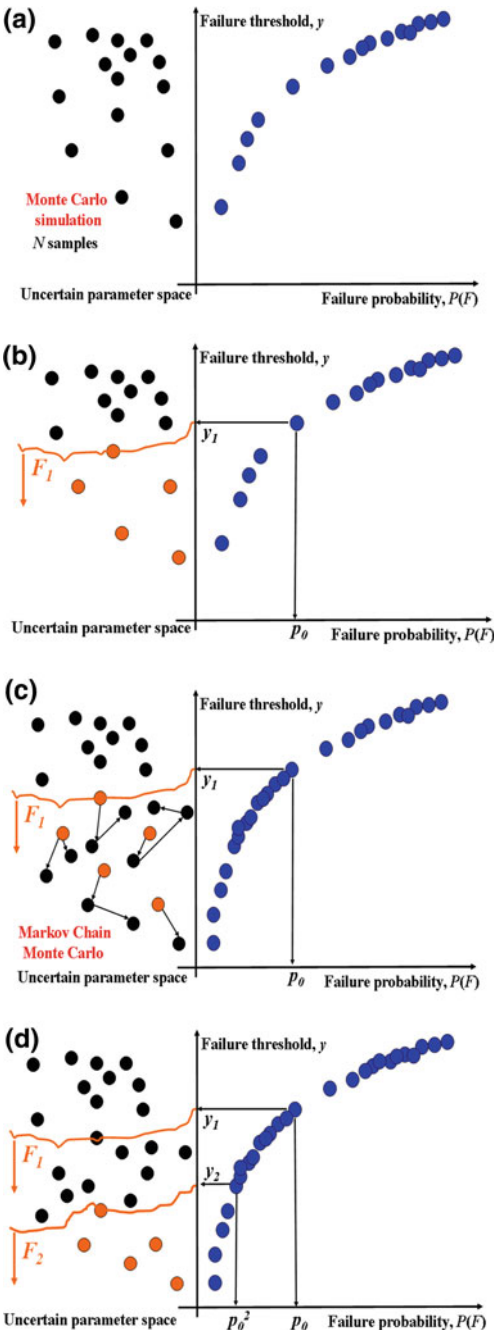

Fig. 6.5 Illustration of the SS procedure: **a** conditional level 0: standard Monte Carlo simulation; **b** conditional level 0: adaptive selection of y_1; **c** conditional level 1: MCMC simulation; **d** conditional level 1: adaptive selection of y_2

Computational Efficiency

The computational efficiency of SS relative to standard MCS increases with decreasing failure probability to be estimated; in fact, the computational effort depends roughly on the logarithm of $P(F)$ and so grows more slowly as $P(F)$ decreases than for standard MCS [37].

To get an idea of the number of samples required to achieve a given accuracy in $\tilde{P}_F$, consider the case where $P(F_1) = P(F_{i+1}|F_i) = p_0$ and the same number of samples N is used in the simulation at each level. Then, from Eq. (6.54) the c.o.v. δ_i of the estimator for a failure probability $P(F_i)$, $i = 2, 3, \ldots, m$, could be obtained by

$$\bar{\delta}_i^2 = \frac{(1-p_0)(1+\bar{\gamma})}{Np_0}, \quad i = 2, 3, \ldots, m \tag{6.69}$$

where $\bar{\gamma}$ is a suitable average value of the correlation parameters γ_i defined in Eq. (6.55) for the simulated samples at each level; by so doing, the δ_i's are assumed to be the same for all conditional levels $i = 2, 3, \ldots, m$ [37]. Using Eqs. (6.54) and (6.61) and noting that the number of simulation levels m necessary to reach the target failure probability $P(F) = p_0^m$ is $m = \log P(F)/\log p_0$, it can be concluded that in order to achieve a given c.o.v. of $\bar{\delta}$ in the estimate $\tilde{P}_F$, the total number of samples required is roughly

$$N_T \approx mN = (\log P(F))^2 \frac{(1-p_0)(1+\bar{\gamma})}{(\log p_0)^2 p_0 \bar{\delta}^2} \tag{6.70}$$

Thus, for a fixed p_0 and $\bar{\delta}$, $N_T \propto (\log P(F))^2$. Compared with standard MCS, where $N_T \propto 1/P(F)$, this implies a substantial improvement in efficiency when estimating small probabilities. In particular, for standard MCS, the minimum number of samples required to give a c.o.v. of $\bar{\delta}$ is $N_0 = (1 - P(F))/P(F)\bar{\delta}^2$. A measure of the efficiency of SS relative to standard MCS is then given by

$$\frac{N_0}{N_T} = \frac{p_0(1-P(F))(\log p_0)^2}{P(F)(\log P(F))^2(1-p_0)(1+\bar{\gamma})} \tag{6.71}$$

It is noted that the computational overhead required for SS, beyond that due to the system analysis for each sample that is also required in standard MCS, is negligible. Taking $p_0 = 0.1$, for target failure probabilities of $P(F) = 10^{-3}$ and 10^{-6} (that correspond to $m = 3$ and six conditional levels, respectively), the above equation gives $N_0/N_T = 4$ and 1,030, respectively (since $\bar{\gamma}$ is about 2) [37]. This shows that SS becomes more efficient than standard MCS for smaller values of $P(F)$. This gain in efficiency is based on $\bar{\gamma}$, which can be achieved if the proposal distribution is chosen properly [1].

6.8 Line Sampling

Line sampling (LS) has been originally developed for the reliability analysis of complex structural systems with small failure probabilities [43]. The underlying idea is to employ *lines* instead of random *points* in order to probe the failure domain of the high-dimensional system under analysis [44].

The problem of computing the multidimensional failure probability integral (Sect. 6.1) in the original "physical" space is transformed into the so-called "standard normal space", where each rv is represented by an independent central unit Gaussian distribution. In this space, a *unit* vector $\underline{\alpha}$ (hereafter also called "important unit vector" or "important direction") is determined, possibly pointing toward the failure domain F of interest (for illustration purposes, two plausible important unit vectors, $\underline{\alpha}^1$ and $\underline{\alpha}^2$, pointing toward two different failure domains, F^1 and F^2, are visually represented in Fig. 6.6, left and right, respectively, in a two-dimensional uncertain parameter space). The problem of computing the high-dimensional failure probability integral in Eq. (6.1) is then reduced to a number of conditional 1-D problems, which are solved along the "important direction" $\underline{\alpha}$ in the standard normal space. The conditional 1-D failure probabilities (associated to the conditional 1-D problems) are readily computed by using the standard normal cdf [44].

6.8.1 Transformation of the Physical Space into the Standard Normal Space

Let $\underline{X} = \left(X_1, X_2, \ldots, X_j, \ldots, X_n\right) \in \mathbb{R}^n$ be the vector of uncertain parameters defined in the original physical space $\underline{X} \in \mathbb{R}^n$. For problems where the dimension n is not so small, the parameter vector $\underline{X}$ can be transformed into the vector $\underline{\theta} \in \mathbb{R}^n$, where each element of the vector θ_j, $j = 1, 2, \ldots, n$, is associated with a central unit Gaussian standard distribution [2]. The joint pdf of the random parameters $\left\{\theta_j : j = 1, 2, \ldots, n\right\}$ is, then

$$\varphi(\underline{\theta}) = \prod_{j=1}^{n} \phi_j(\theta_j) \tag{6.72}$$

where $\varphi_j(\theta_j) = \left(1/\sqrt{2\pi}\right)e^{-x_j^2/2}$, $j = 1, 2, \ldots, n$.

The mapping from the original, physical vector of rvs $\underline{X} \in \mathbb{R}^n$ to the standard normal vector $\underline{\theta} \in \mathbb{R}^n$ is denoted by $T_{X\theta}(\cdot)$ and its inverse by $T_{\theta X}(\cdot)$, i.e.,

$$\underline{\theta} = T_{X\theta}(\cdot) \tag{6.73}$$

$$\underline{X} = T_{\theta X}(\cdot) \tag{6.74}$$

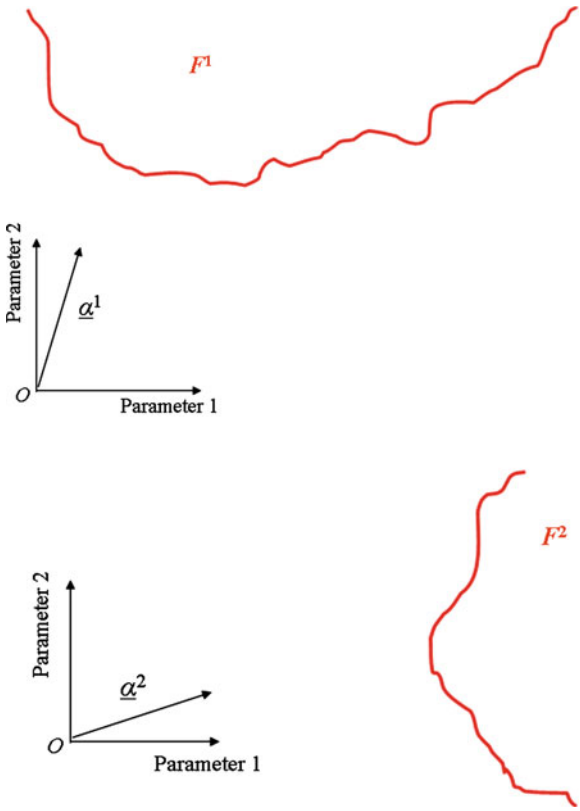

Fig. 6.6 Examples of possible important unit vectors $\underline{\alpha}^1$ (*left*) and $\underline{\alpha}^2$ (*right*) pointing toward the corresponding failure domains F^1 (*left*) and F^2 (*right*) in a two-dimensional uncertain parameter space

Transformations [Eq. (6.73) and (6.74)] are in general nonlinear and are obtained by applying Rosenblatt's or Nataf's transformations, respectively [45–47]; they are linear only if the random vector $\underline{X}$ is jointly Gaussian distributed. By transformation [Eq. (6.73)], also the PF $g_{\underline{X}}(\cdot)$ defined in the physical space can be transformed into $g_\theta(\cdot)$ in the standard normal space

$$g_\theta(\underline{\theta}) = g_{\underline{X}}(\underline{x}) = g_{\underline{X}}(T_{\theta X}(\underline{\theta})) \tag{6.75}$$

Since in most cases of practical interest the function $g_\theta(\underline{\theta})$ is not known analytically, it can be evaluated only point wise. According to Eq. (6.75), the evaluation of the system PF $g_\theta(\cdot)$ at a given point $\underline{\theta}^k$, $k = 1, 2, \ldots, N_T$, in the standard normal space requires (1) a transformation into the original space, (2) a complete simulation of the system response, and (3) the computation of the system performance from the response. The computational cost of evaluating the failure probability is governed by the number of system performance analyses that have to be carried out [2].

6.8.2 The Important Direction $\underline{\alpha}$ for Line Sampling: Interpretation and Identification

In this section, (1) three methods proposed in the open literature to identify the LS important direction $\underline{\alpha}$ are summarized, (2) the interpretation of the important unit vector $\underline{\alpha}$ as the direction of the "design point" in the standard normal space is given, (3) the interpretation of $\underline{\alpha}$ as the normalized gradient of the PF in the standard normal space is presented, (4) a method for calculating the important unit vector $\underline{\alpha}$ as the normalized "center of mass" of the failure domain F of interest is provided.

Design Point Direction

A plausible selection of $\underline{\alpha} = \left(\alpha_1, \alpha_2, \ldots, \alpha_j, \ldots, \alpha_n\right)$ could be the direction of the "design point" in the standard normal space [43]. According to a geometrical interpretation, the "design point" is defined as the point $\underline{\theta}^*$ *on* the limit state surface $g_\theta(\underline{\theta}) = 0$ in the standard normal space, which is closest to the origin [2] (Fig. 6.7). It can be computed by solving the following constrained minimization problem

$$\text{Find } \underline{\theta}^* : ||\underline{\theta}^*||_2 = \min_{g_\theta(\underline{\theta})=0} \left\{||\underline{\theta}||_2\right\} \tag{6.76}$$

where $||\cdot||_2$ is the well-known Euclidean norm.

It can be demonstrated that $\underline{\theta}^*$ in Eq. (6.76) is also the point of maximum likelihood [48]; as such, it is the best choice unless additional information about the true limit state surface is available [49]. Then, the unit important vector $\underline{\alpha}$ can be easily obtained by normalizing $\underline{\theta}^*$, i.e., $\underline{\alpha} = \underline{\theta}^* / ||\underline{\theta}^*||_2$.

However, the design points, and their neighborhood, do not always represent the most important regions of the failure domain, especially in high-dimensional spaces [2]. Moreover, the computational cost associated with the resolution of the constrained minimization problem in Eq. (6.76) can be quite high, in particular, if long-running numerical codes are required to simulate the response of the system to its uncertain input parameters.

Gradient of the Performance Function in the Standard Normal Space

Since the unit vector $\underline{\alpha} = \left(\alpha_1, \alpha_2, \ldots, \alpha_j, \ldots, \alpha_n\right)$ points toward the failure domain F, it can be used to draw information about the relative importance of the random parameters $\left\{\theta_j := j = 1, 2, \ldots, n\right\}$ with respect to the failure probability $P(F)$; actually, the more relevant a rv in determining the failure of the system is the larger the corresponding component of the unit vector $\underline{\alpha}$ will be [44].

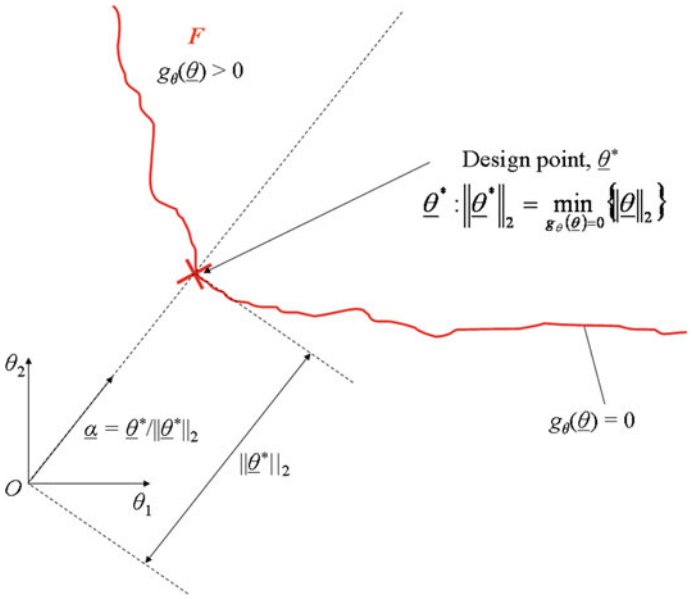

Fig. 6.7 Interpretation of the LS important direction $\underline{\alpha}$ as the direction of the design point in the standard normal space [43]

Such quantitative information can be easily obtained from the gradient of the PF $g_\theta(\underline{\theta})$ in the standard normal space, $\nabla g_\theta(\underline{\theta})$

$$\nabla g_\theta(\underline{\theta}) = \left[\frac{\partial g_\theta(\underline{\theta})}{\partial \theta_1} \frac{\partial g_\theta(\underline{\theta})}{\partial \theta_2} \cdots \frac{\partial g_\theta(\underline{\theta})}{\partial \theta_j} \cdots \frac{\partial g_\theta(\underline{\theta})}{\partial \theta_n}\right]^T \tag{6.77}$$

The gradient measures in a unique way the relative importance of a particular rv with respect to the failure probability $P(F)$; actually, the larger the (absolute) value of a component of Eq. (6.77) is, the greater the "impact" of the corresponding rv will be on the PF $g_\theta(\underline{\theta})$ in the standard normal space. In other words, given a specified finite variation $\Delta\underline{\theta}$ in the parameter vector $\underline{\theta}$, the PF $g_\theta(\underline{\theta})$ will change most if this variation is taken in the direction of Eq. (6.77). Thus, it is reasonable to identify the LS important direction with the direction of the gradient Eq. (6.77) and compute the corresponding unit vector $\underline{\alpha}$ as the *normalized* gradient of the PF $g_\theta(\cdot)$ in the standard normal space, i.e., $\underline{\alpha} = \nabla g_\theta(\underline{\theta}) / ||\nabla g_\theta(\underline{\theta})||_2$ [44].

For clarity sake, Fig. 6.8 shows this procedure with reference to a 2-Dimensional problem: the important unit vector $\underline{\alpha} = (\alpha_1, \alpha_2)$ associated to the 2-Dimensional PF $g_\theta(\theta_1, \theta_2)$ is computed at a proper (selected) point $\underline{\theta}^0 = (\theta_1^0, \theta_2^0)$ (e.g., the nominal point of the system under analysis). Notice that since component

$\alpha_1 = \frac{\partial g_\theta(\underline{\theta})}{\partial \theta_1}\Big|_{\underline{\theta}^0} \Big/ \left\|\nabla g_\theta(\underline{\theta})|_{\underline{\theta}^0}\right\|_2$ (Fig. 6.8, top) is significantly larger than

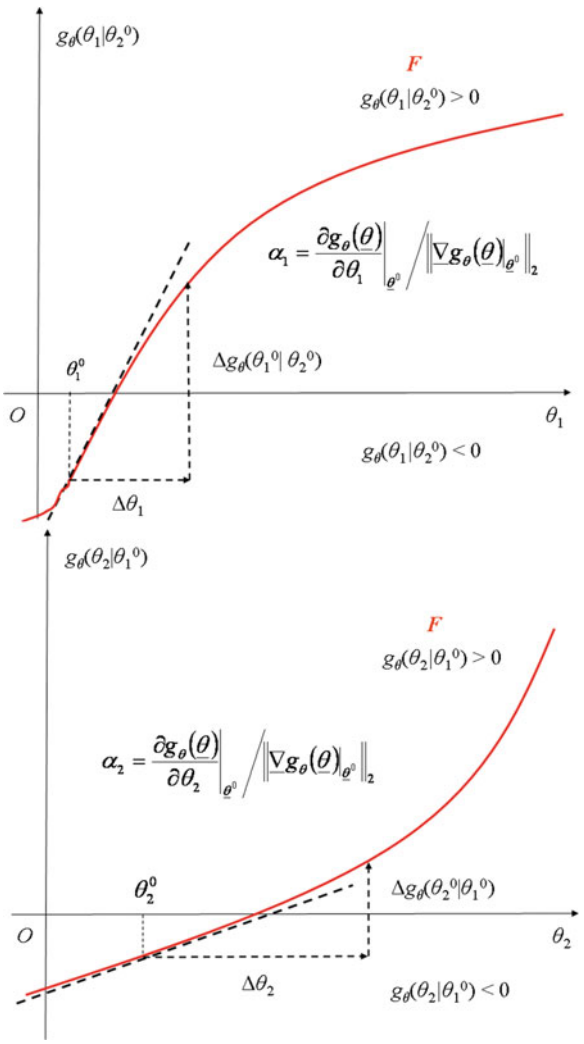

Fig. 6.8 Interpretation of the LS important unit vector $\underline{\alpha}$ as the normalized gradient of the PF $g_\theta(\cdot)$ computed at proper point $\underline{\theta}^0$ (e.g., the nominal point) in the standard normal space (a two-dimensional case is considered for simplicity). *Top* determination of component α_1; *bottom* determination of component α_2. Since $\alpha_1 > \alpha_2$, rv θ_1 is "more important" than θ_2 in determining the failure of the system [44]

component $\alpha_2 = \left.\frac{\partial g_\theta(\underline{\theta})}{\partial \theta_2}\right|_{\underline{\theta}^0} \Big/ \left\|\underline{\nabla} g_\theta(\underline{\theta})|_{\underline{\theta}^0}\right\|_2$ (Fig. 6.8 bottom), then rv θ_1 will be far more important than θ_2 in leading the system to failure.

It is worth noting that thanks to the transformation into dimensionless standard normal variables, the relative importance of the uncertain parameters in terms of the impact on the PF can be compared directly in the standard normal space. On the contrary, the importance of the physical rvs cannot be directly compared using the gradient $\underline{\nabla} g_{\underline{X}}(\underline{x})$ in the original space: this is evident by considering that the components of $\underline{X}$ have different, not commensurable physical units [44].

When the PF is defined on a high-dimensional space, i.e., when many parameters of the system under analysis are random, the computation of the gradient $\underline{\nabla} g_\theta(\underline{\theta})$ in Eq. (6.77) becomes a numerically challenging task. Actually, as the function $g_\theta(\underline{\theta})$ is known only implicitly through the response of a numerical code, for a given vector $\underline{\theta} = \left(\theta_1, \theta_2, \ldots, \theta_j, \ldots, \theta_n\right)$ at least n system performance analyses are required to determine accurately the gradient at a given point $\underline{\theta}^0$ of the PF $g_\theta(\cdot)$ by straightforward numerical differentiation, e.g., the secant method [50, 51]. In order to reduce the computational effort required by the gradient computation, an efficient iterative procedure is proposed in [44] based on a linear approximation of the PF $g_\theta(\cdot)$ in the neighborhood of the point $\underline{\theta}^0$. In particular, the procedure aims at obtaining an approximate estimate for the gradient $\underline{\nabla} g_\theta(\underline{\theta})|_{\underline{\theta}^0}$ by imposing the condition that as many components of the gradient vector as possible are set to 0: this obviously reduces the number of system performance analyses necessary for the calculation. The above simplification is based on the practical observation that in most engineering systems there is often a large subset of rvs with comparatively less effect on the PF $g_\theta(\cdot)$: this assumption is found to be particularly true for high-dimensional systems, i.e., those with a large number n of rvs, say $n > 100$ [44].

Normalized "Center of Mass" of the Failure Domain F

The important unit vector $\underline{\alpha}$ can also be computed as the normalized "center of mass" of the failure domain F of interest [43].

A point $\underline{\theta}^0$ is chosen which belongs to the failure domain F: the latter can be determined with standard MCS or by engineering judgment when it is possible. Subsequently, $\underline{\theta}^0$ is used as the initial point of a Markov chain which lies entirely in the failure domain F. For that purpose a Metropolis–Hastings algorithm can be employed, with which a sequence of N_s points $\{\underline{\theta}^u, u = 1, 2, \ldots, N_s\}$ lying in the failure domain F is obtained [38]. The unit vectors $\underline{\theta}^u / \|\underline{\theta}^u\|$, $u = 1, 2, \ldots, N_s$, are then averaged in order to obtain the LS important unit vector as $\underline{\alpha} = \frac{1}{N_s} \cdot \sum_{u=1}^{N_s} \underline{\theta}^u / \|\underline{\theta}^u\|$ (Fig. 6.9). The latter is by no means optimal, but it is clear that it provides a good approximation of the important regions of the failure domain (at least as the sample size N_s increases). On the down side, it should be noticed that this procedure implies N_s additional system analyses, which substantially increase the computational cost associated to the simulation method.

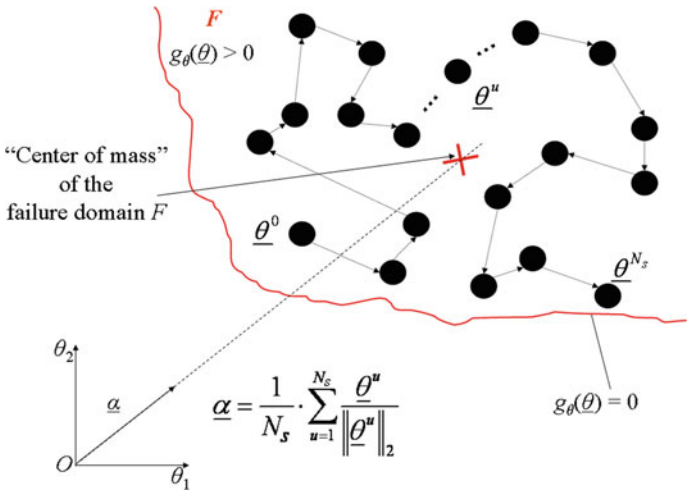

Fig. 6.9 Interpretation of the LS important unit vector $\underline{\alpha}$ as the normalized "center of mass" of the failure domain F in the standard normal space. The "center of mass" of F is computed as an average of N_s failure points generated by means of a Markov chain starting from an initial failure point $\underline{\theta}^0$ [43]

6.8.3 *Minimization of the Variance of the LS Failure Probability Estimator*

A more efficient way to identify the *optimal* important direction $\underline{\alpha}^{\text{opt}}$ for LS is to take the one minimizing the variance $\sigma^2\left[\hat{P}(F)^{N_T}\right]$ of the LS failure probability estimator $\hat{P}(F)^{N_T}$. Notice that $\underline{\alpha}^{\text{opt}}$ can be expressed as the normalized version of a proper vector $\underline{\theta}^{\text{opt}}$ in the standard normal space, i.e., $\underline{\alpha}^{\text{opt}} = \underline{\theta}^{\text{opt}} / \left\|\underline{\theta}^{\text{opt}}\right\|_2$. Thus, in order to search for a physically meaningful important unit vector $\underline{\alpha}^{\text{opt}}$ (i.e., a vector that optimally points toward the failure domain F of interest), $\underline{\theta}^{\text{opt}}$ should belong to the failure domain F of interest, i.e., $\underline{\theta}^{\text{opt}} \in F$ or, equivalently, $g(\underline{\theta}^{\text{opt}}) > 0$.

In mathematical terms, the optimal LS important direction $\underline{\alpha}^{\text{opt}}$ is obtained by solving the following nonlinear constrained minimization problem

$$\begin{aligned} \text{Find } \underline{\alpha}^{\text{opt}} = \underline{\theta}^{\text{opt}} / \left\|\underline{\theta}^{\text{opt}}\right\|_2 : \ \sigma^2\left[\hat{P}(F)^{N_T}\right] = \min_{\underline{\alpha}=\underline{\theta}/\|\underline{\theta}\|_2} \left\{\sigma^2\left[\hat{P}(F)^{N_T}\right]\right\} \\ \text{subject to } \underline{\theta} \in F (\text{i.e., } g(\underline{\theta}) > 0). \end{aligned} \tag{6.78}$$

The conceptual steps of the procedure for solving Eq. (6.78) are schematized in (Fig. 6.10):

1. An optimization algorithm proposes a candidate solution $\underline{\alpha} = \underline{\theta}/\|\underline{\theta}\|_2$ to Eq. (6.78);

2. The LS failure probability estimator $\hat{P}(F)^{N_T}$ and the associated variance $\sigma^2\left[\hat{P}(F)^{N_T}\right]$ are calculated using the unit vector $\underline{\alpha} = \underline{\theta}/\|\underline{\theta}\|_2$ proposed as important direction in step 1 above; notice that $2{\cdot}N_T$ or $3{\cdot}N_T$ system performance analyses (i.e., runs of the system model code) have to be carried out in this phase;
3. The variance $\sigma^2\left[\hat{P}(F)^{N_T}\right]$ obtained in step 2 above is the objective function to be minimized; it measures the quality of the candidate solution $\underline{\alpha} = \underline{\theta}/\|\underline{\theta}\|_2$ proposed by the optimization algorithm in step 1 above;
4. The feasibility of the proposed solution $\underline{\alpha} = \underline{\theta}/\|\underline{\theta}\|_2$ is checked by evaluating the system PF $g_\theta(\cdot)$ (i.e., by running the system model code) in correspondence of $\underline{\theta}$: if the proposed solution $\underline{\alpha} = \underline{\theta}/\|\underline{\theta}\|_2$ is not feasible (i.e., if $\underline{\theta} \notin F$ or, equivalently, $g_\theta(\underline{\theta}) \leq 0$), it is *penalized* by *increasing* the value of the corresponding objective function $\sigma^2\left[\hat{P}(F)^{N_T}\right]$ through an *additive* factor;
5. Steps 1–4 are repeated until a predefined stopping criterion is met and the optimization algorithm identifies the *optimal* unit vector $\underline{\alpha}^{\text{opt}} = \underline{\theta}^{\text{opt}}/\left\|\underline{\theta}^{\text{opt}}\right\|_2$.

Notice that (1) the optimization search requires the iterative evaluation of hundreds or thousands of possible solutions $\underline{\alpha} = \underline{\theta}/\|\underline{\theta}\|_2$ to Eq. (6.78) and (2) $2\ N_T$ or $3\ N_T$ system performance analyses (i.e., runs of the system model code) have to be carried out to calculate the objective function $\sigma^2\left[\hat{P}(F)^{N_T}\right]$ for *each* proposed solution; as a consequence, the computational effort associated to this technique could be absolutely prohibitive with a system model code requiring hours or even minutes to run a single simulation. Hence, it is often unavoidable, for practical applicability, to resort to a simplified model or a regression model (e.g., based on artificial neural networks, ANNs, as in [52]) as a fast-running approximator of the original system model for performing the calculations in steps 2 and 4 above, to make the computational cost acceptable.

To sum up, the characteristics of the main methods for the definition of the LS important direction $\underline{\alpha}$ are summarized in Table 6.2.

6.8.4 Theoretical Formulation of the LS Method

Without loss of generality, let us assume for the moment that the standard normal rv θ_1 points in the direction of the important unit vector $\underline{\alpha}$: this can always be assured by a suitable rotation of the coordinate axes. Then, the failure domain F can be alternatively expressed as

$$F = \left\{\underline{\theta} \in \mathbb{R}^n : \theta_1 \in F_1(\theta_1, \theta_2, \ldots, \theta_j \ldots, \theta_n)\right\} \tag{6.79}$$

where F_1 is a function defined in $\mathbb{R}^{n-1}$. For example, if the failure domain corresponds to a PF of the form $g_\theta(\underline{\theta}) = g_{\theta,-1}(\underline{\theta}_{-1}) - \theta_1 \geq 0$, where $\underline{\theta}_{-1}$ is the $(n-1)$-dimensional vector $\left(\theta_2, \theta_3, \ldots, \theta_j, \ldots, \theta_n\right)$, then $F_1(\underline{\theta}_{-1})$ is simply the

Table 6.2 Summary of the methods employed in this work for estimating the LS important direction $\underline{\alpha}$

Concept	Evaluations to be performed
Design point	Minimization of the distance $\|\underline{\theta}\|_2$ in Eq. (6.76)
	Evaluation of the PF $g_\theta(\underline{\theta})$ to verify if $\underline{\theta}$ is a feasible solution to Eq. (6.77) i.e., if $\underline{\theta}$ belongs to the failure surface $g_\theta(\underline{\theta}) = 0$
Gradient	Evaluation of the PF $g_\theta(\underline{\theta})$ to estimate the gradient $\nabla g_\theta(\underline{\theta})$ in Eq. (6.77) by numerical differentiation
Variance minimization	Minimization of the variance $\sigma^2\left[\hat{P}(F)^{N_T}\right]$ of the LS failure probability estimator $\hat{P}(F)^{N_T}$
	Calculation of the variance $\sigma^2\left[\hat{P}(F)^{N_T}\right]$ of the LS failure probability estimator $\hat{P}(F)^{N_T}$
	Evaluation of the PF $g_\theta(\underline{\theta})$ for the estimation of the failure probability $\hat{P}(F)^{N_T}$ and its variance $\sigma^2\left[\hat{P}(F)^{N_T}\right]$ during the LS simulation
	Evaluation of the PF $g_\theta(\underline{\theta})$ to verify if $\underline{\theta}$ is a feasible solution to Eq. (6.78), i.e., if $\underline{\theta}$ belongs to the failure domain F (where $g_\theta(\underline{\theta}) > 0$)

half-open interval $\left[g_{\theta,-1}(\underline{\theta}_{-1}), \infty\right)$. Notice that functions similar to F_1 in Eq. (6.79) can be defined in all generality with respect to *any direction* in the random parameter space.

Using Eqs. (6.1) and (6.72) the probability of failure $P(F)$ can be expressed as follows

$$\begin{aligned} P(F) &= \int_n \ldots \int I_F(\underline{\theta}) \prod_{j=1}^{n} \phi_j(\theta_j) \mathrm{d}\underline{\theta} \\ &= \int_{n-1} \ldots \int \left(\int I_F(\underline{\theta}_{-1}) \phi_1(\theta_1) \mathrm{d}\theta_1 \right) \prod_{j=2}^{n} \phi_j(\theta_j) \mathrm{d}\underline{\theta}_{-1} \\ &= \int_{n-1} \ldots \int \Phi(F_1(\underline{\theta}_{-1})) \prod_{j=2}^{n} \phi_j(\theta_j) \mathrm{d}\underline{\theta}_{-1} \\ &= E_{\underline{\theta}_{-1}}[\Phi(F_1(\underline{\theta}_{-1}))] \end{aligned} \tag{6.80}$$

where $\Phi(A) = \int I_A(x)\varphi(x)\mathrm{d}x$ is the so-called Gaussian measure of A [43]. In contrast to standard MCS, where $P(F)$ is expressed as expectation of the discrete rv $I_F(\underline{\theta})$ as in Eq. (6.1), in Eq. (6.80) it is written as the expectation, with respect to $\underline{\theta}_{-1}$, of the continuous rv $\Phi(F_1(\underline{\theta}_{-1}))$.

An unbiased MC estimator $\hat{P}(F)$ of the last integral in Eq. (6.80) can be computed as

$$\hat{P}(F) = \frac{1}{N_T} \cdot \sum_{k=1}^{N_T} \Phi\left(F_1\left(\underline{\theta}_{-1}^k\right)\right) \tag{6.81}$$

where $\underline{\theta}^k_{-1}$, $k = 1, 2, \ldots, N_T$, are iid samples in the standard normal space. The variance of the estimator in Eq. (6.81) is thus determined by the variance of $\Phi(F_1(\underline{\theta}_{-1}))$; specifically $\sigma^2\left(\hat{P}(F)\right) = \sigma^2[\Phi(F_1(\underline{\theta}_{-1}))]/N_T$. It is interesting to observe that $\Phi(F_1(\underline{\theta}_{-1}))$ takes values in (0, 1), which means that $\Phi(F_1(\underline{\theta}_{-1})) \leq 1$ and $\Phi^2(F_1(\underline{\theta}_{-1})) \leq \Phi(F_1(\underline{\theta}_{-1}))$, $\forall \underline{\theta}_{-1} \in \mathbb{R}^{n-1}$. As a consequence

$$\begin{aligned}
&\sigma^2[\Phi(F_1(\underline{\theta}_{-1}))] \\
&\quad = E_{\underline{\theta}_{-1}}\left[\Phi^2(F_1(\underline{\theta}_{-1}))\right] - E^2_{\underline{\theta}_{-1}}[\Phi(F_1(\underline{\theta}_{-1}))] \\
&\quad \leq E_{\underline{\theta}_{-1}}[\Phi(F_1(\underline{\theta}_{-1}))] - E^2_{\underline{\theta}_{-1}}[\Phi(F_1(\underline{\theta}_{-1}))] \\
&\quad = P(F)(1 - p(F)) = \sigma^2(I_F(\underline{\theta}))
\end{aligned} \tag{6.82}$$

Hence, the c.o.v. $\delta = \sqrt{\sigma^2\left(\hat{P}(F)\right)}\Big/P(F)$ of the estimator in Eq. (6.81) is always smaller than that of standard MCS; this implies that the convergence rate attained by the LS scheme in Eq. (6.81) is always faster than that of standard MCS.

Moreover, for a linear limit state surface, two extreme cases can be observed. In the first case, where the boundary of the failure domain F is perpendicular to the sampling direction, it is evident that $\sigma^2\left(\hat{P}(F)\right) = 0$ and $\delta = 0$. In the second case, the boundary of F is parallel to the LS important direction and consequently $\Phi(F(\underline{\theta}_{-1})) = I_F(\underline{\theta})$ thus, the c.o.v. is the same as that of standard MCS [43].

Finally, notice that in the derivation of Eqs. (6.80), (6.81), and (6.82), for ease of notation, it has been assumed without loss of generality that the direction of the unit vector $\underline{\alpha}$ (i.e., the vector pointing to the important region of the failure domain) coincides with that of θ_1; this can always be assured by a suitable rotation of the coordinate axes. In the following, the important direction will be always referred to as $\underline{\alpha}$.

6.8.5 The Line Sampling Algorithm

The LS algorithm proceeds as follows [44]:

1. Determine the *unit* important direction $\underline{\alpha} = \left(\alpha_1, \alpha_2, \ldots, \alpha_j, \ldots, \alpha_n\right)$. Any of the methods summarized in Sect. 6.8.2 can be employed to this purpose. Notice that the computation of $\underline{\alpha}$ implies additional system analyses, which substantially increase the computational cost associated to the simulation method;
2. From the original multidimensional joint pdf $q(\cdot) : \mathbb{R}^n \rightarrow [0, +\infty)$, sample N_T vectors $\left\{\underline{x}^k : k = 1, 2, \ldots, N_T\right\}$, with $\underline{x}^k = \left(\underline{x}^k_1, \underline{x}^k_2, \ldots, \underline{x}^k_j, \ldots, \underline{x}^k_n\right)$ by standard MCS;
3. Transform the N_T sample vectors $\left\{\underline{x}^k : k = 1, 2, \ldots, N_T\right\}$ defined in the original (i.e., physical) space of possibly dependent, non-normal rvs (step 2 above) into N_T samples $\left\{\underline{\theta}^k : k = 1, 2, \ldots, N_T\right\}$ defined in the standard normal space where

each component of the vector $\underline{\theta}^k = \left(\underline{\theta}_1^k, \underline{\theta}_2^k, \ldots, \underline{\theta}_j^k, \ldots, \underline{\theta}_n^k\right)$, $k = 1, 2, \ldots, N_T$, is associated with an independent central unit Gaussian standard distribution;

4. Estimate N_T conditional "one-dimensional" failure probabilities $\left\{\hat{P}^k(F) : k = 1, 2, \ldots, N_T\right\}$, corresponding to each one of the standard normal samples $\left\{\underline{\theta}^k : k = 1, 2, \ldots, N_T\right\}$ obtained at step 3 above. In particular, for each random sample $\underline{\theta}^k$, $k = 1, 2, \ldots, N_T$, perform the following steps (Fig. 6.11) [2, 44, 53, 54]:

   (a) Define the sample vector $\tilde{\underline{\theta}}^k$, $k = 1, 2, \ldots, N_T$, as the sum of a deterministic multiple of $\underline{\alpha}$ and a vector $\underline{\theta}^{k,\perp}$, $k = 1, 2, \ldots, N_T$, perpendicular to the direction $\underline{\alpha}$, i.e.

$$\tilde{\underline{\theta}}^k = c^k \underline{\alpha} + \underline{\theta}^{k,\perp} \tag{6.83}$$

   where c^k is a real number in $(-\infty, +\infty)$, $k = 1, 2, \ldots, N_T$ and

$$\underline{\theta}^{k,\perp} = \underline{\theta}^k - \left\langle \underline{\alpha}, \underline{\theta}^k \right\rangle \underline{\alpha} \tag{6.84}$$

   In Eq. (6.84), $\underline{\theta}^k$, $k = 1, 2, \ldots, N_T$, denotes a random realization of the input variables in the standard normal space of dimension n and $\left\langle \underline{\alpha}, \underline{\theta}^k \right\rangle$ is the scalar product between $\underline{\alpha}$ and $\underline{\theta}^k$, $k = 1, 2, \ldots, N_T$. Finally, it is worth noting that since the standard Gaussian space is isotropic, both the scalar c^k and the vector $\underline{\theta}^{k,\perp}$ are also standard normally distributed [53, 54];

   (b) Compute the value c^{-k} as the intersection between the LSF $g_\theta\left(\tilde{\underline{\theta}}^k\right) = g_\theta(c^k \underline{\alpha} + \underline{\theta}^{k,\perp}) = 0$ and the line $l^k\left(c^k, \underline{\alpha}\right)$ passing through $\underline{\theta}^k$ and parallel to $\underline{\alpha}$ (Fig. 6.11). The value of c^{-k} can be approximated by evaluating the PF $g_\theta(\cdot)$ at two or three different values of c^k (e.g., c_1^k, c_2^k and c_3^k in Fig. 6.10), fitting a first- or second-order polynomial and determining its root (Fig. 6.11). Hence, for each standard normal random sample $\underline{\theta}^k$, $k = 1, 2, \ldots, N_T$, two or three system performance evaluations are required;

   (c) Solve the conditional 1-D reliability problem associated to each random sample $\underline{\theta}^k$, $k = 1, 2, \ldots, N_T$, in which the only (standard normal) rv is c^k. The associated conditional failure probability $\hat{P}^k(F)$, $k = 1, 2, \ldots, N_T$, is given by

$$\begin{aligned} \hat{P}^k &= P[N(0,1) > \overline{c}^k] = 1 - P[N(0,1) > \overline{c}^k] \\ &= 1 - \Phi(\overline{c}^k) = \Phi(\overline{-c}^k) \end{aligned} \tag{6.85}$$

   where $\Phi(\cdot)$ denotes the standard normal cdf;

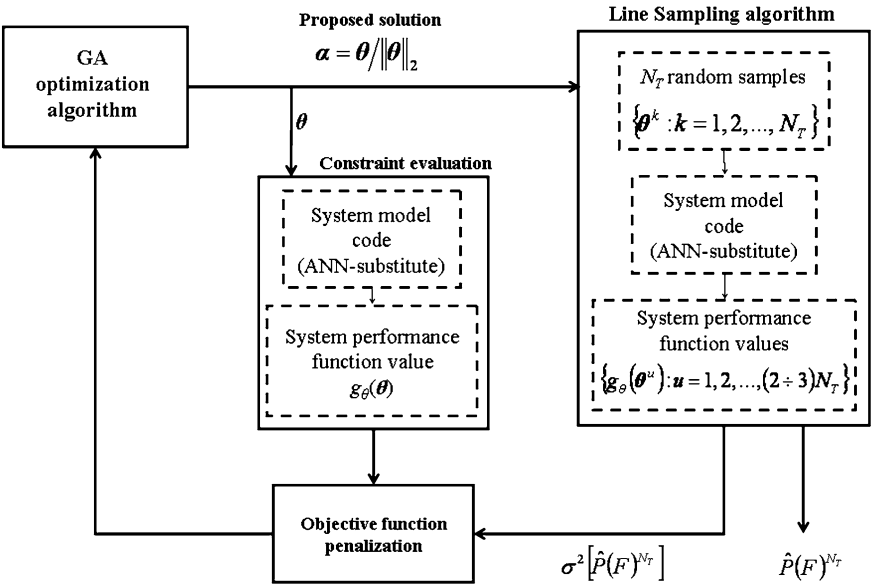

Fig. 6.10 Method for estimating the LS important direction $\underline{\alpha}$ by minimization of the variance $\sigma^2\left[\hat{P}(F)^{N_T}\right]$ of the LS failure probability estimator. The system model code is assumed to be substituted by, e.g., an ANN for fast calculations

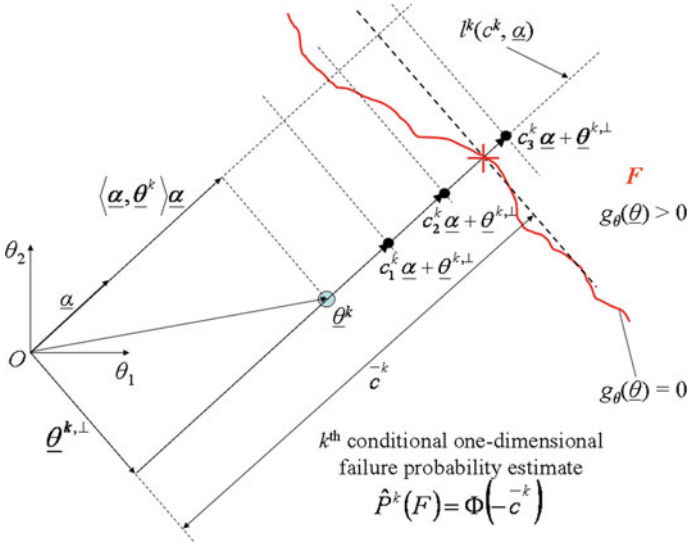

Fig. 6.11 The line sampling procedure [44]

5. Using the independent conditional "one-dimensional" failure probability estimates $\{\hat{P}^k(F) : k = 1, 2, \ldots, N_T\}$ in Eq. (6.85) (step 4.c. above), compute the unbiased estimator $\hat{P}(F)$ for the failure probability $P(F)$ as

$$\hat{P}(F) = \frac{1}{N_T} \sum_{k=1}^{N_T} \hat{P}^k(F) \tag{6.86}$$

Comparing Eq. (6.86) to (6.81), it is evident that the "Gaussian measures" of the failure domain F, i.e., $\{\Phi(F_1(\underline{\theta}^k_{-1})) : k = 1, 2, \ldots, N_T\}$ in Eq. (6.80), are nothing but the conditional 1-D failure probability estimates $\{\hat{P}(F) : k = 1, 2, \ldots N_T\}$ in Eq. (6.86).

The variance of the estimator in Eq. (6.85) is

$$\sigma^2\left(\hat{P}(F)\right) = \frac{1}{N_T(N_T - 1)} \sum_{k=1}^{N_T} \left(\hat{P}^k(F) - \hat{P}(F)\right)^2 \tag{6.87}$$

With the described approach, the variance of the estimator $\hat{P}(F)$ of the failure probability $P(F)$ is considerably reduced. In general, a relatively low number N_T of simulations has to be carried out to obtain a sufficiently accurate estimate. A single evaluation would suffice for the ideal case in which the LSF is linear and a LS direction $\underline{\alpha}$ perpendicular to it has been identified [43].

References

1. Schueller, G. I. (2007). On the treatment of uncertainties in structural mechanics and analysis. *Computers and Structures, 85*, 235–243.
2. Schueller, G. I., Pradlwarter, H. J., & Koutsourelakis, P. S. (2004). A critical appraisal of reliability estimation procedures for high dimensions. *Probabilistic Engineering Mechanics, 19*, 463–474.
3. Pagani, L., Apostolakis, G. E., & Hejzlar, P. (2005). The impact of uncertains on the performance of passive system. *Nuclear Technology, 149*, 129–140.
4. Rubinstein, R. Y. (1999). The cross-entropy method for combinatorial and continuous optimization. *Methodology and Computing in Applied Probability, 2*, 127–190.
5. De Boer, P. T., Kroese, D. P., & Rubinstein, R. Y. (2004). A fast cross-entropy method for estimating buffer overflows in queueing networks. *Management Science, 50*(7), 883–895.
6. Ridder, A. (2005). Importance sampling simulations of Markovian reliability systems using cross-entropy. *Annuals of Operations Research, 134*, 119–136.
7. Allon, G., Kroese, D. P., Raviv, T., & Rubinstein, R. Y. (2004). Application of the cross-entropy method to the buffer allocation problem in a simulation-based environment. *Annals of Operations Research, 134*, 137–151.
8. Homem de Mello, T., & Rubinstein, R. Y. (2002). *Rare event probability estimation for static models via cross-entropy and importance sampling*. Submitted. New York: Wiley.
9. De Boer, P. T. (2000). *Analysis and efficient simulation of queueing models of telecommunication systems*. PhD thesis, University of Twente.

10. De Boer, P. T. (2005). Rear-event simulation of non-Markovian queueing networks using a state-dependent change of measure determined using cross-entropy. *Annals of Operations Research, 134*, 69–100.
11. Dubin, U. (2002). *The cross-entropy method for combinatorial optimization with applications*. The Technion, Israel Institute of Technology, Haifa, Master's thesis.
12. Helvik, E., & Wittner, O. (2001). *Using the cross-entropy method to guide/govern mobile agent's path finding in networks*. In 3rd International Workshop on Mobile Agents for Telecommunication Applications—MATA'01.
13. Kroese, D. P., & Keith, J. M. (2002). *Sequence alignment by rare event simulation.* In Proceedings of the 2002 Winter Simulation Conference, San Diego, U.S. 2002 (pp, 320–327).
14. Margolin, L. (2005). On the convergence of the cross-entropy method. *Annuals of Operations Research, 134*, 201–214.
15. Chepuri, K., & Homem de Mello, T. (2005). Solving the vehicle routing problem with stochastic demands using the cross entropy method. *Annals of Operations Research, 134*, 153–181.
16. Menache, I., Mannor, S., & Shimkin, N. (2005). Basis function adaption in temporal difference reinforcement learning. *Annals of Operations Research, 134*, 215–238.
17. Cohen, I., Golany, B., & Shtub, A. (2005). Managing stochastic finite capacity multi-project systems through the cross-entropy method. *Annals of Operations Research, 134*, 183–199.
18. Kroese, D. P., & Rubinstein, R. Y. (2004). The transform likelihood ratio method for rare event simulation with heavy tails. *Queueing Systems, 46*, 317–351.
19. Hui, K. P., Bean, N., Kraetzl, M., & Kroese, D. P. (2004). The cross-entropy method for network reliability estimation. *Annals of Operations Research, 134*, 101–118.
20. Kroese, D. P., Nariai, S., & Hui, K.-P. (2007). Network reliability optimization via the cross-entropy method. *IEEE Transactions on Reliability*, *56*(2), 275–287.
21. Rubinstein, R. Y. (2002). The cross-entrophy method and rare-events for maximal cut and bipartition problems. *ACM Transactions on modelling and Computer Simulation, 12*(1), 27–53.
22. Sani, A., & Kroese, D. P. (2008). Controling the number of HIV infectives in a mobile population. *Mathematical Biosciences, 213*(2), 103–112.
23. Sani, A., & Kroese, D. P. (2007). *Optimal Epidemic Intervention of HIV Spread Using the Cross-Entropy Method*. In Proceedings of the International Congress on Modelling and Simulation (MODSIM), Modelling and Simulation Society of Australia and New Zealand (pp. 448–454).
24. Rubistein, R. Y., (1981). *Simulation and the Monte Carlo method*. New York: Wiley.
25. Kalos, M. H., & Whitlock, P. A. (1986). *Monte Carlo methods* (Vol. 1: Basic). New York: Wiley.
26. Zio, E. (2009). *Computational methods for reliability and risk analysis*, Chapter 2. Singapore: World Scientific.
27. Rubinstein, Y., & Kroese, D. P. (2004). *The cross-entropy method: A unified approach to Monte Carlo simulation, randomized optimization and machine learning*. New York: Springer.
28. MacKay, M. D., Beckman, R. J., & Conover, W. J. (1979). A comparison of three methods for selecting values of input variables in the analysis of output from a computer code. *Technometrics, 21*(2), 239–245.
29. Olsson, A., Sabdberg, G., & Dahlblom, O. (2003). On Latin hypercube sampling for structural reliability analysis. *Structural Safety, 25*, 47–68.
30. Helton, J. C., & Davis, F. J. (2003). Latin hypercube sampling and the propagation of uncertainty in analyses of complex systems. *Reliability Engineering and System Safety, 81*, 23–69.
31. Sallaberry, C. J., Helton, J. C., & Hora, S. C. (2008). Extension of Latin hypercube samples with correlated variables. *Reliability Engineering and System Safety, 93*(7), 1047–1059.
32. Liefvendahl, M., & Stocki, R. (2006). A study on algorithms for optimization of Latin hypercubes. *Journal of Statistical Planning and Inference, 136*, 3231–3247.

33. Pebesma, E. J., & Heuvelink, G. B. M. (1999). Latin hypercube sampling of Gaussian random fields. *Technometrics, 41*(4), 203–212.
34. Der Kiureghian, A. (2000). The geometry of random vibrations and solutions by FORM and SORM. *Probabilistic Engineering Mechanics, 15*(1), 81–90.
35. Gille. A. (1998). *Evaluation of failure probabilities in structural reliability with Monte Carlo methods*. In Proceeedings of ESREL, Throndheim, Norway.
36. Gille. A. (1999). *Probabilistic numerical methods used in the applications of the structural reliability domain*. PhD Thesis, Universitè Paris 6, Paris.
37. Au, S. K., & Beck, J. L. (2001). Estimation of small failure probabilities in high dimensions by subset simulation. *Probabilistic Engineering Mechanics, 16*(4), 263–277.
38. Metropolis, N., Rosenbluth, A. W., Rosenbluth, M. N., & Taller, A. H. (1953). Equations of state calculations by fast computing machines. *Journal of Chemical Physics, 21*(6), 1087–1092.
39. Hastings, W. K. (1970). Monte Carlo sampling methods using Markov chains and their applications. *Biometrika, 57*, 97–109.
40. Fishman, G. S. (1996). *Monte Carlo: Concepts, algorithms, and applications*. New York: Springer.
41. Au, S. K., Ching, J., & Beck, J. L. (2007). Application of subset simulation methods to reliability benchmark problems. *Structural Safety, 29*, 183–193.
42. Au, S. K. (2005). Reliability-based design sensitivity by efficient simulation. *Computers and Structures, 83*, 1048–1061.
43. Koutsourelakis, P. S., Pradlwarter, H. J., & Schueller, G. I. (2004). Reliability of structures in high dimensions, Part I: Algorithms and application. *Probabilistic Engineering Mechanics, 19*, 409–417.
44. Pradwarter, H. J., Pellisetti, M. F., Schenk, C. A., Schueller, G. I., Kreis, A., Fransen, S., et al. (2005). Realistic and efficient reliability estimation for aerospace structures. *Computer Methods in Applied Mechanics and Engineering, 194*, 1597–1617.
45. Rosenblatt, M. (1952). Remarks on multivariate transformations. *The Annals of Mathematical Statistics, 23*(3), 470–472.
46. Nataf, A. (1962). Determination des distribution dont les marges sont donnees. *Comptes Rendus de l'Academie des* Sciences, *225*, 42–43.
47. Huang, B., & Du, X. (2006). A robust design method using variable transformation and Gauss-Hermite integration. *International Journal for Numerical Methods in Engineering, 66*, 1841–1858.
48. Freudenthal, A. M. (1956). Safety and the probability of structural failure. *ASCE Transactions, 121*, 1337–1397.
49. Schueller, G. I., & Stix, R. (1987). A critical appraisal of method to determine failure probabilities. *Structural Safety, 4*(4), 293–309.
50. Ahammed, M., & Malchers, M. E. (2006). Gradient and parameter sensitivity estimation for systems evaluated using Monte Carlo analysis. *Reliability Engineering and System Safety, 91*, 594–601.
51. Fu, M. (2006). Stochastic gradient estimation. In S. G. Henderson & B. L. Nelson (Eds.), *Handbook on operation research and management science: Simulation*. Amsterdam: Elsevier.
52. Zio, E., & Pedroni, N. (2010). An optimized line sampling method for the estimation of the failure probability of nuclear passive systems. *Reliability Engineering and System Safety, 95*(12), 1300–1313.
53. Pradlwarter, H. J., Schueller, G. I., Koutsourelakis, P. S., & Charmpis, D. C. (2007). Application of line sampling simulation method to reliability benchmark problems. *Structural Safety, 29*, 208–221.
54. Au, S. K., & Beck, J. L. (2003). Importance sampling in high dimensions. *Structural Safety, 25*, 139–163.

Chapter 7
Practical Applications of Advanced Monte Carlo Simulation Techniques for System Failure Probability Estimation

7.1 Subset Simulation Applied to a Series–Parallel Continuous-State System

In this chapter, SS (Sect. 6.7) is applied for performing the reliability analysis of a series–parallel multistate system of literature [1]. The original system, characterized by multiple discrete states, is extended to have continuous states.

Let us consider the simple series–parallel system of Fig. 5.6. For each component $j = 1, 2, 3$ we assume that there is an infinite set of continuous states, each one corresponding to a different hypothetical level of performance, v_j. Each component can randomly occupy the continuous states, according to properly defined pdfs $q_j(v_j)$, $j = 1, 2, 3$. Table 7.1 gives the ranges of variability $[v_{j,\min}, v_{j,\max}]$ of the performances v_j (in arbitrary units) of the three components $j = 1, 2, 3$.

In all generality, the output performance $O_{\underline{v}}$ associated to the system state $\underline{v} = (v_1, v_2, \ldots, v_j, \ldots, v_n)$ is obtained on the basis of the performances v_j of the components $j = 1, 2, \ldots, n$ constituting the system. More precisely, we assume that the performance of each node constituted by n_o elements in parallel logic, is the sum of the individual performances of the components and that the performance of the node series system is that of the node with the lowest performance, which constitutes the 'bottleneck' of the system [1–3]. For example, with reference to the system configuration $\underline{v}^* = (v_1^*, v_2^*, v_3^*)$, with $v_1^* = 80$, $v_2^* = 40$ and $v_3^* = 75$, the first node is characterized by a value of the performance equal to $v_1^* + v_2^* = 120$, whereas the second node has performance $v_3^* = 75$. This latter node determines the value of the system performance $O_{\underline{v}^*} = 75$.

The system is assumed to fail when its performance O falls below some specified threshold value o, so that its probability of failure $P(F)$ can be expressed as $P(O < o)$. During simulation, the intermediate failure events $\{F_i : i = 1, 2, \ldots, m\}$

E. Zio, *The Monte Carlo Simulation Method for System Reliability and Risk Analysis*, Springer Series in Reliability Engineering,
DOI: 10.1007/978-1-4471-4588-2_7, © Springer-Verlag London 2013

Table 7.1 Performance data of the components of the continuous-state system of Fig. 5.6

Component index, j	Performance range, $[v_{j,\min}, v_{j,\max}]$
1	[0, 80]
2	[0, 80]
3	[0, 100]

Table 7.2 Parameters of the pdfs of the components' performances

		Pdf parameters	
Component index, j	Performance range, $[v_{j,\min}, v_{j,\max}]$	Mean, $\bar{v}_j$	Standard deviation, σ_{v_j}
1	[0, 80]	40	10
2	[0, 80]	40	10
3	[0, 100]	50	12.5

are adaptively generated as $F_i = \{O < o_i\}$, where $o_1 > o_2 > \ldots > o_i > \ldots > o_n = o$ are the intermediate threshold values for the SS procedure.

The pdfs $q_j(v_j)$ of the performances v_j, $j = 1, 2, 3$, of the components constituting the system are assumed Normal, with the parameters (i.e., the mean $\bar{v}_j$ and the standard deviation σ_{v_j}, $j = 1, 2, 3$) reported in Table 7.2. These values have been obtained by proper manipulation of the original discrete-state probabilities in [2].

In the application of SS, the conditional failure regions are chosen such that a conditional failure probability of $p_0 = 0.1$ is attained at all conditional levels. The simulations are carried out for $m = 4$ conditional levels, thus covering the estimation of failure probabilities as small as 10^{-4}.

At each conditional level, $N = 500$ samples are generated. The total number of samples is thus $N_T = 500 + 450 + 450 + 450 = 1850$, because $p_0 N = 50$ conditional samples from one conditional level are used to start the next conditional level and generate the missing $(1 - p_0)N = 450$ samples at that level. The failure probability estimates corresponding to the intermediate thresholds $\{o_i : i = 1, 2, 3, 4\}$, i.e., 10^{-1}, 10^{-2}, 10^{-3}, and 10^{-4}, are computed using a total number of samples equal to $N_T = 500$, 950, 1400 and 1850, respectively.

For each component performance v_j, $j = 1, 2, 3$, the one-dimensional 'proposal pdf' $p_j^*(\xi_j|v_j)$ adopted to generate by MCMC simulation the random 'pre-candidate value' ξ_j based on the current sample component v_j, is chosen as a symmetric uniform distribution

$$p_j^*(\xi_j|v_j) = \begin{cases} 1/(2l_j) & |\xi_j - v_j| \le l_j \\ 0 & \text{otherwise} \end{cases}, \quad j = 1, 2, 3 \tag{7.1}$$

where l_j is the maximum step length, i.e., the maximum allowable distance that the next sample can depart from the current one. The choice of l_j is such that the standard deviation of $p_j^*(\xi_j|v_j)$ is equal to that of $q_j(v_j)$, $j = 1, 2, 3$.

The results of the application of SS to the performance analysis of the system in Fig. 5.6 are now illustrated. First, the percentiles of the system performance are determined; then, the probabilities of failure of the system are estimated for different threshold levels of performance o; finally, the sensitivity of the performance of the system to the performances of the constituting components is studied by examination of the conditional sample distributions at different failure probability levels.

The α^{th} percentile of the rv O is defined as the value o^{α} such that

$$P(O \leq o^{\alpha}) = \alpha. \tag{7.2}$$

Figure 7.1 shows the empirical cdf of the system performance O for different confidence levels $\alpha = 0.1$, 0.01, 0.001 and 0.0001. The results produced by SS with a total of 1850 samples (i.e., four simulation levels, each with $N = 500$ samples) are shown in solid lines, whereas those produced by standard MCS with the same number of samples (i.e., 1850) are shown in dashed lines. The dot-dashed lines correspond to the results obtained by standard MCS with 500,000 samples, which produce reliable results for benchmarking up to a confidence level $\alpha = 0.0001$ (Fig. 7.1, bottom). It can be seen that the results from SS are reasonably close to the benchmark solution for all confidence levels, except in the upper regime of Fig. 7.1, bottom, where the error in the standard MCS solution in this probability regime also contributes to the observed discrepancy. On the other hand, the results of the standard MCS with 1850 samples fail to reproduce reliable results for small values of α (Fig. 7.1, middle, right and Fig. 7.1, bottom). This is due to the fact that with 1850 samples there are on average only $1850 \cdot 0.001 \sim 0.2$ failure samples in Fig. 7.1, middle, right, and $1850 \cdot 0.0001 \sim 0.2$, i.e., less than one failure sample, in Fig. 7.1, bottom. In contrast, for SS, due to successive conditioning, it is guaranteed that there are 1850, 1400, 950, 500, and 50 conditional failure samples in Fig. 7.1, top, left and right, middle, left and right, and bottom, respectively, providing sufficient information for efficiently estimating the cdf.

Notice that for the standard MCS with 500,000 samples, there are on average 50 samples in Fig. 7.1, bottom, i.e., the same number as produced by SS, but this is achieved at a much higher computational effort.

Table 7.3 reports the values of the percentiles $o^{0.1}, o^{0.01}, o^{0.001}$ and $o^{0.0001}$ of the output performance O of the series–parallel distribution system: for α equal to 0.1 and 0.01, both SS and MCS with 1850 samples produce results similar to those of the benchmark simulation approach (i.e., MCS with 500,000 samples), whereas for α equal to 0.001 and 0.0001, only SS achieves reliable results.

Figure 7.2 shows the system failure probability estimates for different threshold levels o, obtained in a single simulation run. Note that a single SS run yields failure probability estimates for all threshold levels o up to the smallest one (10^{-4}) considered (solid lines). For comparison, the results using standard MCS with 100,000 samples are shown in the same Figures (dot-dashed lines). The results of the SS are shown to approximate well the estimates obtained by standard MCS.

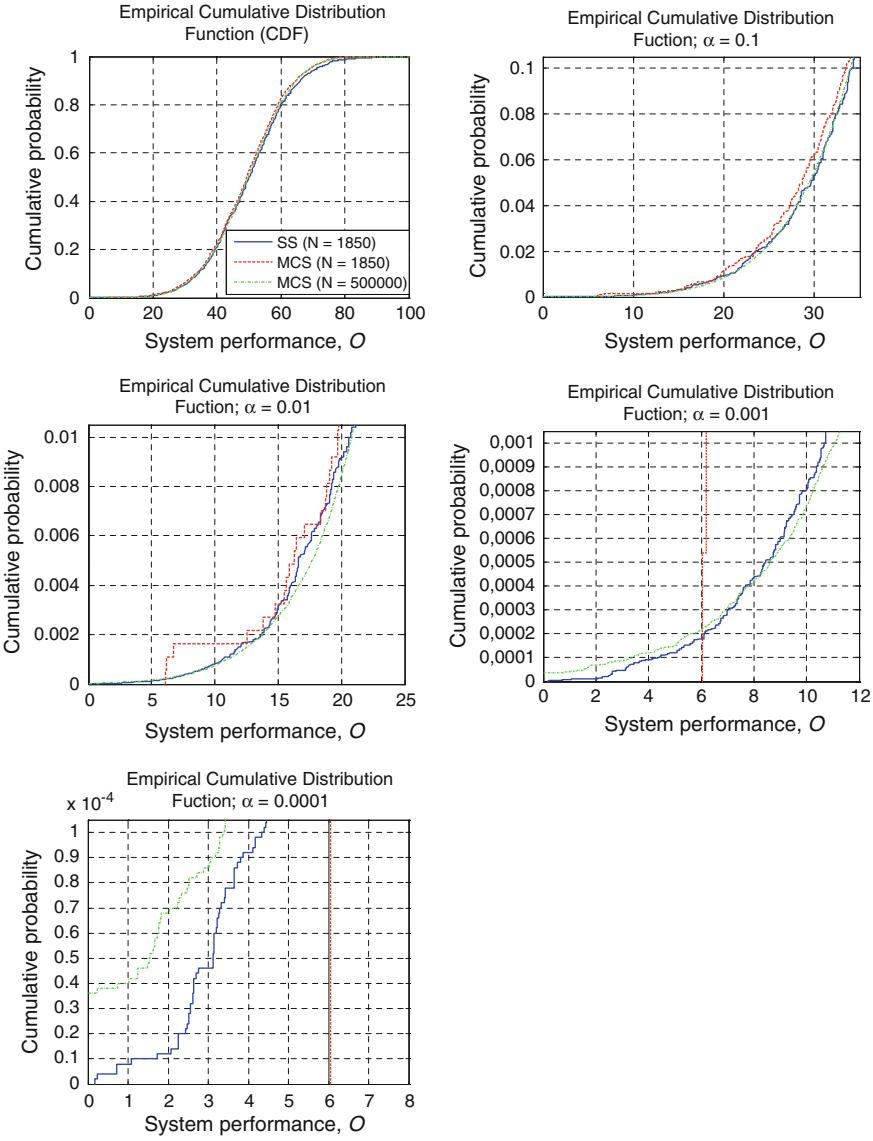

Fig. 7.1 Empirical cdf of the performance O of the series–parallel, continuous-state system, at different confidence levels: $\alpha = 1$ (*top*, *left*), $\alpha = 0.1$ (*top*, *right*), $\alpha = 0.01$ (*middle*, *left*), $\alpha = 0.001$ (*middle*, *right*) and $\alpha = 0.0001$ (*bottom*). *Solid lines* SS with 1850 samples; *dashed lines* standard MCS with 1850 samples; *dot-dashed lines* standard MCS with 500000 samples

To assess quantitatively the statistical properties of the failure probability estimates produced by SS, 50 independent runs have been carried out and the sample mean and sample c.o.v. of the failure probability estimates thereby

Table 7.3 Percentiles of the performance O of the series–parallel, continuous-state system, determined by SS with 1850 samples and by standard MCS with 1850 and 500,000 samples, at different confidence levels $\alpha = 0.1, 0.01, 0.001, 0.0001$

Simulation approach	Number of samples	Percentile values			
		$o^{0.1}$	$o^{0.01}$	$o^{0.001}$	$o^{0.0001}$
SS	1850	34.09	20.62	10.63	4.33
MCS	1850	33.43	19.69	6.19	6.06
MCS	500000	33.97	20.81	11.06	3.40

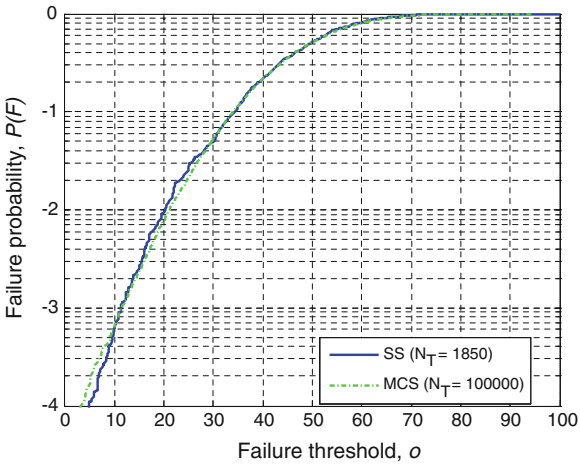

Fig. 7.2 SS (*solid lines*) and standard MCS (*dot-dashed lines*) estimates of the system failure probabilities for different values of the failure threshold o

obtained have been computed. Figure 7.3 shows the sample means of the system failure probability estimates obtained by SS (solid lines); a comparison with the estimates computed by direct MCS using 100,000 samples is also given (dot-dashed lines). The sample means of the failure probability estimates almost coincide with the standard MCS results, except at small failure probabilities, near 10^{-4}, where the error in the MCS estimates becomes significant. This leads to conclude that the bias due to the correlation between the conditional probability estimators at different levels is negligible, so that the failure probability estimates obtained by SS can be taken as practically unbiased [4, 5].

The c.o.v. of the failure probability estimate is plotted versus different failure probability levels $P(F)$ (solid line) in Fig. 7.4. In the Fig. 7.4, the dashed line shows a lower bound on the c.o.v. which would be obtained if the conditional probability estimates at different simulation levels were uncorrelated; on the contrary, the dot-dashed line provides an upper bound on the c.o.v. which would be obtained in case of full correlation among the conditional probability estimates. From the Figure, it can be seen that the trend of the actual c.o.v. estimated from 50 runs follows more closely the lower bound, confirming that the conditional failure probability estimates are almost completely uncorrelated. A detailed theoretical analysis of these statistical aspects can be found in [4–6].

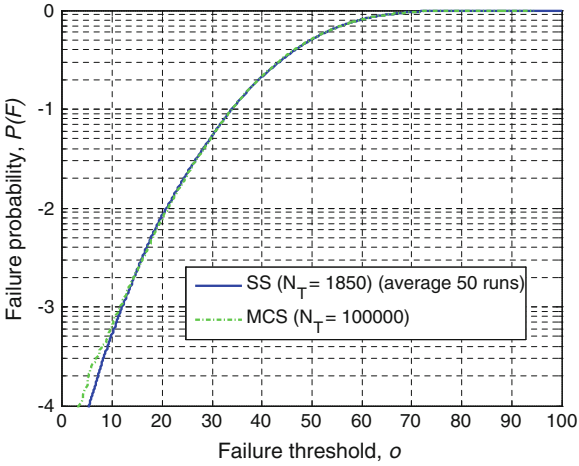

Fig. 7.3 Sample averages of the failure probability estimates over 50 SS runs (*solid lines*) and standard MCS estimates (*dot-dashed lines*) for different values of the failure threshold o

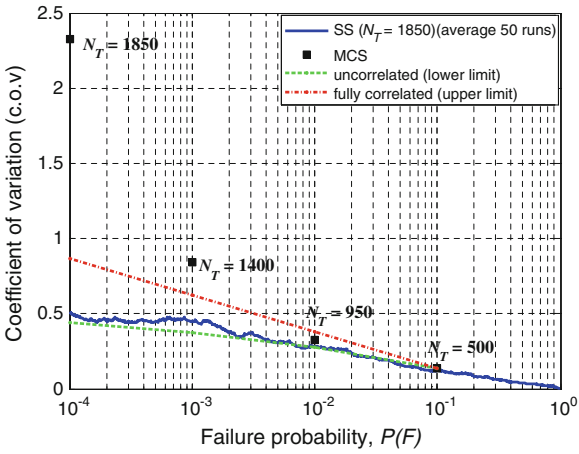

Fig. 7.4 c.o.v. versus different failure probability levels $P(F)$. *Solid line* sample average over 50 SS runs; dashed lines: sample average of the lower bound over 50 SS runs; *dot-dashed lines* sample average of the upper bound over 50 SS runs; *squares* standard MCS (iid samples)

The computational efficiency of SS can be compared with that of a standard MCS in terms of the c.o.v. of the failure probability estimates computed from the same number of samples. Recall that the number of samples required by SS at the probability levels 10^{-1}, 10^{-2}, 10^{-3} and 10^{-4} are $N_T = 500$, 950, 1400 and 1850, respectively, as explained above. The exact c.o.v. of the MC estimator using the same number of samples at probability levels $P(F) = 10^{-1}$, 10^{-2}, 10^{-3} and 10^{-4} are computed using $\sqrt{(1 - P(F))/P(F)N_T}$, which holds for N_T iid samples: the results are shown as squares in Fig. 7.4. It can be seen that while the c.o.v. of the standard MCS grows exponentially with decreasing failure probability, the c.o.v. of the SS estimate only grows in a logarithmic manner: this empirically proves that SS can lead to a substantial improvement in efficiency over standard MCS when estimating small failure probabilities. These results agree with several theoretical analyses which can be found in the open literature [4–7].

The Markov chain samples generated by SS can be used not only for estimating the conditional probabilities but also to infer the probable scenarios that will occur in the case of failure [8]. In all generality, from the comparison of the pdf $q(x_j|F)$ of the uncertain parameter x_j, $j = 1, 2, \ldots, n$, conditional to the occurrence of failure F, with the unconditional pdf $q(x_j)$, an indication can be obtained on how important is the parameter x_j in affecting the system failure.

Formally, for any given value of x_j the Bayes' theorem reads

$$P(F|x_j) = \frac{q(x_j|F)}{q(x_j)} P(F) \quad j = 1, 2, \ldots, n \tag{7.3}$$

so that $P(F|x_j)$ is insensitive to x_j when $q(x_j|F) \sim q(x_j)$, i.e., when the conditional pdf $q(x_j|F)$ is similar in shape to the pdf $q(x_j)$.The sensitivity of the system performance to the individual components' performances can, thus, be studied by examining the change of the sample distributions at different conditional levels. The histograms of the conditional samples of the components' performances at different conditional levels for a single SS run are shown in Fig. 7.5. It can be seen that the system performance is not very sensitive to the performances of components 1 and 2 in parallel logic, which constitute node 1 of the system (Fig. 5.6), as indicated by the negligible deviation of their empirical conditional distributions (histograms) from the unconditional ones (solid lines). On the contrary, there is a significant leftward shift in the conditional distribution of the performance of component 3, which constitutes node 2 of the system. This result is quite reasonable: in fact, since the unconditional distributions of the components' performances are almost identical (Table 7.2), the importance of each single component in determining the failure of the whole system is almost entirely due to the topology of the system itself. Considering that the performance of the two-nodes series system in Fig. 5.6 is that of the node with the lowest performance and that the two redundant components constituting node 1 sum their individual performances, it is likely that the 'bottleneck' of the system (i.e., the node with the lowest performance) is represented by node 2, i.e., component 3.

7.2 Subset Simulation Applied to a Series–Parallel Discrete-State System

Let us apply SS for performing the reliability analysis of the series–parallel system of Fig. 5.6, where, however, in this case for each component $j = 1, 2, 3$ there are z_j possible discrete states, each one corresponding to a different hypothetical level of performance, $v_{j,l}$, $l = 0, 1, \ldots, z_j - 1$. Each component can randomly occupy the discrete states, according to properly defined discrete probabilities $q_{j,l}$, $j = 1, 2, 3$, $l = 0, 1, \ldots, z_j - 1$.

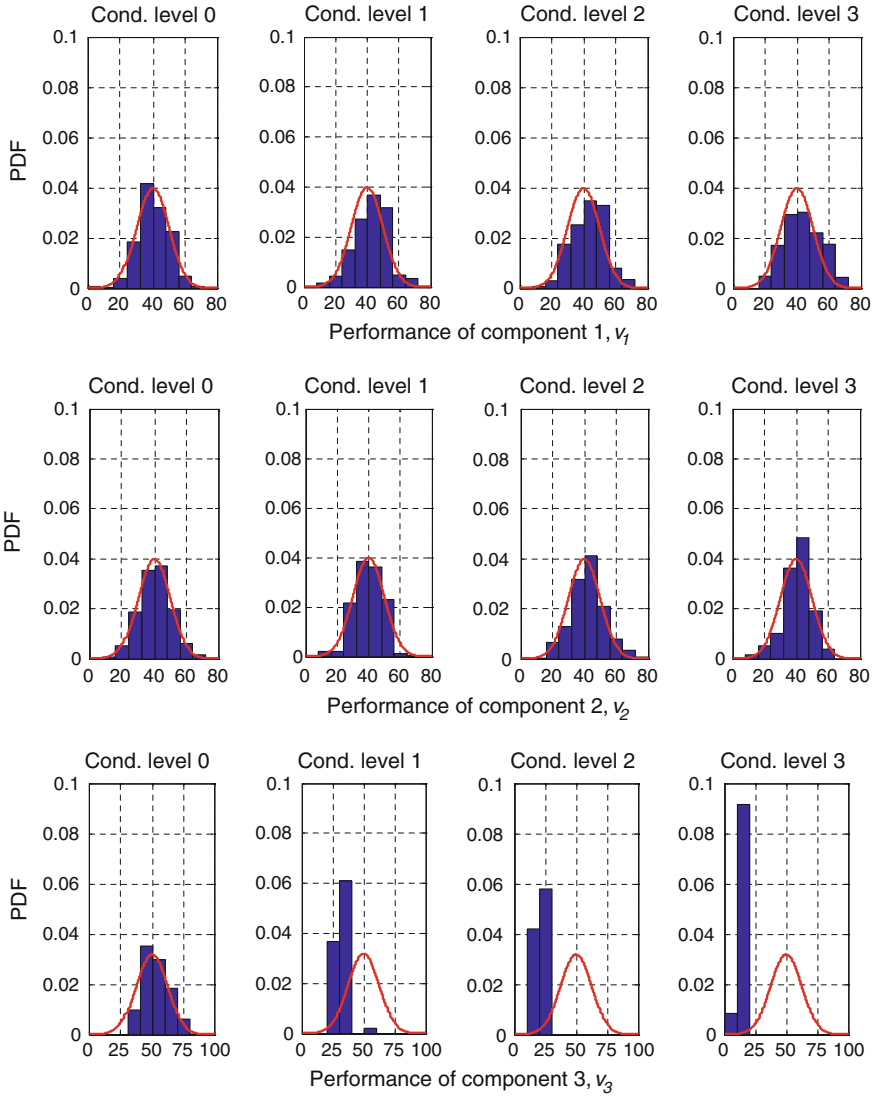

Fig. 7.5 Empirical conditional distributions of the components' performances at different conditional levels (*histograms*) compared to their unconditional distributions (*solid lines*)

For each component $j = 1, 2, 3$, there are $z_j = 11$ possible states each one corresponding to a different hypothetical level of performance $v_{j,l}$, $l = 0, 1, \ldots, 10$; thus, the number of available system states is $\prod_{j=1}^{3} z_j = 11^3 = 1331$. The probabilities $q_{j,l}$ associated to the performances $v_{j,l}$, $j = 1, 2, 3$, $l = 0, 1, \ldots, 10$, are reported in Table 7.4. Obviously, $\sum_{l=1}^{z_j} q_{j,l} = 1, \quad j = 1, 2, 3$.

Table 7.4 Performance distributions of the components of the discrete multistate system of Fig. 5.6

Component index, j	1		2		3	
State index, l	$v_{j,l}$	$q_{j,l}$	$v_{j,l}$	$q_{j,l}$	$v_{j,l}$	$q_{j,l}$
0	0	3.7507×10^{-2}	0	3.4573×10^{-2}	0	6.77×10^{-5}
1	8	7.5013×10^{-2}	8	6.9146×10^{-2}	10	1.354×10^{-4}
2	16	2.522×10^{-2}	16	8.7933×10^{-3}	20	7.314×10^{-4}
3	24	4×10^{-2}	24	1.3×10^{-2}	30	1.4628×10^{-3}
4	32	5.044×10^{-2}	32	1.7586×10^{-2}	40	2.7538×10^{-3}
5	40	3.4573×10^{-2}	40	4.6976×10^{-2}	50	5.5077×10^{-3}
6	48	6.9147×10^{-2}	48	9.3953×10^{-2}	60	2.4953×10^{-2}
7	56	6.9947×10^{-2}	56	8.9943×10^{-2}	70	4.9907×10^{-2}
8	64	1.3989×10^{-1}	64	1.7988×10^{-1}	80	8×10^{-2}
9	72	1.6608×10^{-1}	72	1.5304×10^{-1}	90	3.0482×10^{-1}
10	80	2.9217×10^{-1}	80	2.9309×10^{-1}	100	5.2965×10^{-1}

Table 7.5 Parameters of the probability distributions of the components' performances

	Performance distributions' parameters	
Component index, j	Mean, $\bar{v}_j$	Standard deviation, σ_{v_j}
1	56.48	25.17
2	58.97	23.11
3	92.24	11.15

For clarity sake, the synthetic parameters of the performance distributions of Table 7.4 (i.e., the mean $\bar{v}_j$ and the standard deviation σ_{v_j}, $j = 1, 2, 3$) are summarized in Table 7.5.

Figure 7.6 shows the analytical cdf of the system performance O, obtained by calculating the exact probabilities of all the 1331 available system states; it is worth noting that the probability of the system having performance O equal to 0, i.e., being in the configuration in which each of the three components is in the state $l = 0$, is 1.364×10^{-3}.

As in the previous application, the conditional failure regions are chosen such that a conditional failure probability of $p_0 = 0.1$ is attained at all conditional levels. The simulations are carried out for $m = 3$ conditional levels, thus covering the estimation of failure probabilities as small as 10^{-3}. At each conditional level, $N = 300$ samples are generated. The total number of samples is thus $N_T = 300 + 270 + 270 = 840$, because $p_0 N = 30$ conditional samples from one conditional level are used to start the next conditional level and generate the missing $(1 - p_0)N = 270$ samples at that level.

The failure probability estimates corresponding to the intermediate thresholds, i.e., 10^{-1}, 10^{-2} and 10^{-3}, are computed using a total number of samples equal to $N_T = 300$, 570 and 840, respectively. It is worth noting that the number of samples employed for estimating the probabilities of failure of the system is much (about

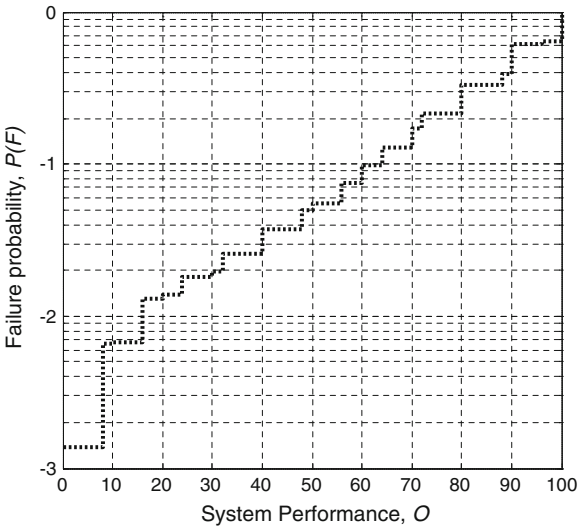

Fig. 7.6 Analytical cdf of the performance O of the series–parallel, discrete multistate system

two times) lower than the total number of available system states, i.e., 1331; thus, the computational time required for estimating the failure probabilities by SS is substantially lower than that necessary for analytically computing them (i.e., for calculating the exact probabilities of all the 1331 system states).

For each component's performance $v_{j,l}$, $j = 1, 2, 3$, $l = 0, 1, \ldots, z_j - 1$, the one-dimensional discrete 'proposal pdf' $p^*_{j,l'}(\xi_{j,l'}|v_{j,l})$ adopted to generate by MCMC simulation the random 'pre-candidate value' $\xi_{j,l'}$ based on the current sample component $v_{j,l}$ is chosen as a symmetric uniform distribution

$$p^*_{j,l'}(\xi_{j,l'}|v_{j,l}) = \begin{cases} 1/(2\Omega_j + 1) & |o' - o| \le \Omega_j \\ 0 & \text{otherwise} \end{cases} \qquad (7.4)$$

$$j = 1,\ 2,\ 3, \quad o' = o - \Omega_j, o - \Omega_j + 1, \ldots, o + \Omega_j - 1, o + \Omega_j$$

where Ω_j is the maximum allowable number of discrete steps that the next sample can depart from the current one. The choice $\Omega_1 = 2$, $\Omega_2 = 2$ and $\Omega_3 = 1$ empirically turned out to offer the best trade-off between estimation accuracy and relatively low correlation among successive conditional failure samples.

Figure 7.7 shows the failure probability estimates for different threshold levels o, obtained in a single simulation run. The results produced by SS with a total of 840 samples (i.e., three simulation levels, each with $N = 300$ samples) and 1110 samples (i.e., four simulation levels, each with $N = 300$ samples) are shown in solid lines. Note that, a single SS run yields failure probability estimates for all threshold levels o up to the smallest one considered (i.e., 10^{-3}). For comparison, the analytical failure probabilities (dashed lines) and the results using standard MCS with 840 and 1110 samples (dot-dashed lines) are shown in the same Fig. 7.7.

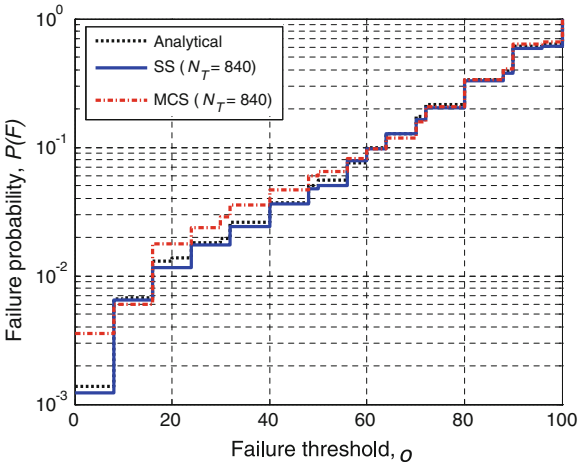

Fig. 7.7 Analytical failure probabilities (*dashed lines*) and their corresponding estimates obtained by SS (*solid lines*) and standard MCS (*dot-dashed lines*) in a single simulation run for different values of the failure threshold o

In order to properly represent the randomness of the SS and MCS procedures and provide a statistically meaningful comparison between the performances of SS and standard MCS in the estimation of a given failure probability $P(F)$ of interest, $S = 200$ independent runs of each method have been carried out. In each simulation $s = 1, 2, \ldots, S$ the relative absolute error $\Delta_s[P(F)]$ between the exact (i.e., analytically computed) value of the failure probability $P(F)$ and the corresponding estimate $\tilde{P}_{F,s}$ (obtained by SS or standard MCS) is computed as follows

$$\Delta_s[P(F)] = \frac{\left|P(F) - \tilde{P}_{F,s}\right|}{P(F)}, \quad S = 1, 2, \ldots S \tag{7.5}$$

The performances of SS and standard MCS in the estimation of $P(F)$ are then compared in terms of the mean relative absolute error $\overline{\Delta}[P(F)]$ over $S = 200$ runs

$$\overline{\Delta}[P(F)] = \frac{1}{S} \cdot \sum_{s=1}^{S} \Delta_s[P(F)] \tag{7.6}$$

The quantity above gives an idea of the relative absolute error made *on average* by the simulation method in the estimation of a given failure probability $P(F)$ of interest *in a single run*.

Table 7.6 reports the values of the mean relative absolute errors $\overline{\Delta}[P(F)]$ made by both SS and standard MCS with 840 samples in the estimation of the failure probability $P(F) = 1.364 \times 10^{-3}$: this value has been chosen as target because it corresponds to the probability of the system having performance O equal to 0, i.e., being in the configuration where all its components are in state 0 which is the most critical for the system and also the less likely one. Only for illustration purposes, the results obtained in four batches of $S = 200$ simulations each are reported.

Table 7.6 Mean relative absolute errors made by both SS and standard MCS with 840 samples in the estimation of the failure probability $P(F) = 1.364 \times 10^{-3}$; these values have been computed for four batches of $S = 200$ simulations each

	Mean relative absolute errors, $\overline{\Delta}[P(F)]$	
	SS $P(F) = 1.364 \times 10^{-3}$	Standard MCS $P(F) = 1.364 \times 10^{-3}$
Batch 1	0.4327	0.7265
Batch 2	0.4611	0.7530
Batch 3	0.4821	0.6656
Batch 4	0.3856	0.6394

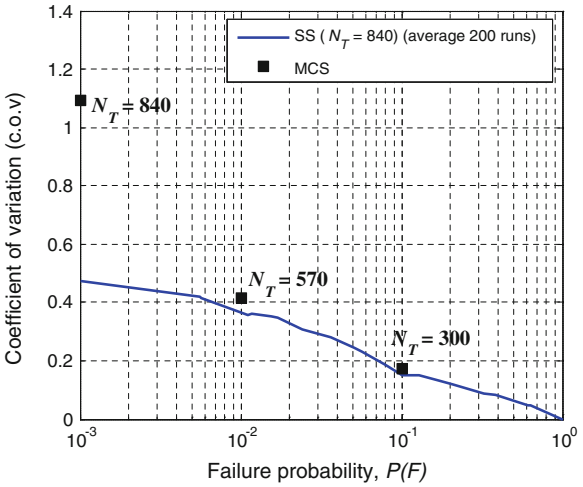

Fig. 7.8 c.o.v. versus different failure probability levels $P(F)$. *Solid lines* sample average over 200 SS runs; *squares* standard MCS (iid samples)

It can be seen from Table 7.6 that in all cases the mean relative absolute errors made by SS are significantly (two to three times) lower than those provided by standard MCS using the same number of samples.

The computational efficiency of SS is reported in Fig. 7.8 (solid line) in terms of the sample c.o.v. of the failure probability estimates obtained by SS in $S = 200$ independent runs. The exact c.o.v. of the MC estimator using the same number of samples ($N_T = 300$, 570, 840, and 1110) at probability levels $P(F) = 10^{-1}$, 10^{-2}, 10^{-3}, respectively, are also shown as squares in Fig. 7.8. As before, the c.o.v. of the standard MCS is seen to grow exponentially with decreasing failure probability whereas the c.o.v. of the SS estimate approximately grows in a logarithmic manner: again, this empirically proves that SS can lead to a substantial improvement in efficiency over standard MCS when estimating small failure probabilities.

To assess quantitatively the statistical properties of the failure probability estimates produced by SS, the sample mean of the failure probability estimates obtained in $S = 200$ independent runs have been computed. For a given failure

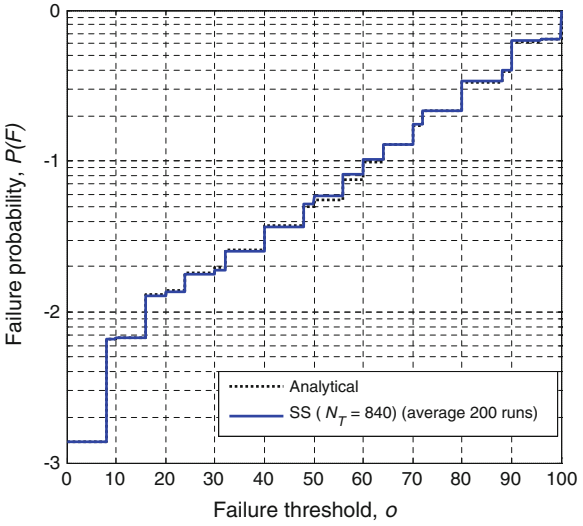

Fig. 7.9 Analytical failure probabilities (*dashed lines*) and sample averages of the failure probability estimates over 200 SS runs (*solid lines*) for different values of the failure threshold o

probability level $P(F)$ of interest, the sample mean $\overline{P}_F$ of the corresponding estimates $\tilde{P}_{F,s}$, $s = 1, 2, \ldots, S$, is

$$\overline{P}_F = \frac{1}{S} \cdot \sum_{s=1}^{S} \tilde{P}_{F,s} \tag{7.7}$$

Figure 7.9 shows the sample means of the failure probability estimates obtained by SS; a comparison with the exact (i.e., analytically computed) failure probabilities is also given (dashed lines).

The sample means of the failure probability estimates almost coincide with the analytical results, except at small failure probabilities, near 10^{-3}, where the estimates seem to be quite biased. As before, a quantitative indicator of the bias associated to the estimate of a given failure probability $P(F)$ can be computed as the relative absolute deviation $\Delta[P(F)]$ between the exact value of the failure probability, i.e., $P(F)$, and the sample average $\overline{P}_F$ of the corresponding estimates

$$\Delta[P(F)] = \frac{\left|\overline{P}_F - P(F)\right|}{P(F)} \tag{7.8}$$

Table 7.7 reports the values of the sample means $\overline{P}_F$ and the corresponding biases $\Delta[P(F)]$ produced by SS in the estimation of $P(F) = 1.364 \times 10^{-3}$. Only for illustration purposes, the results obtained in four batches of $S = 200$ simulations each are reported.

Finally, the sample c.o.v. of the failure probability estimates is plotted versus different failure probability levels $P(F)$ (solid line) in Fig. 7.10, together with the lower (dashed lines) and upper (dot-dashed lines) bounds which would be obtained if the conditional probability estimates at different simulation levels were

Table 7.7 Sample means $\overline{P}_F$ of the failure probability estimates over 200 SS runs and the corresponding biases $\Delta[P(F)]$ produced by SS in the estimation of $P(F) = 1.364 \times 10^{-3}$; these values have been computed for four batches of $S = 200$ simulations each

	Subset simulation	
	$P(F) = 1.364 \times 10^{-3}$	
	Sample mean, $\overline{P}_F$	Bias, $\bar{\Delta}[P(F)]$
Batch 1	1.136×10^{-3}	0.1672
Batch 2	1.145×10^{-3}	0.1606
Batch 3	1.065×10^{-3}	0.2192
Batch 4	1.126×10^{-3}	0.1745

uncorrelated or fully correlated, respectively. It can be seen that the trend of the c.o.v. estimated from the 200 runs follows more closely the upper bound, signaling that the conditional failure probability estimates are almost completely correlated. The high correlation between conditional probability estimates may be explained as follows: differently from continuous-state systems whose stochastic evolution is modeled in terms of an infinite set of continuous states, discrete multistate systems can only occupy a finite number of states; as a consequence, the generation of repeated (thus, correlated) conditional failure samples during MCMC simulation may be significant. Hence, a word of caution is in order with respect to the fact that the estimates produced by SS when applied to discrete multistate systems may be quite biased if the number of discrete states is low.

In conclusion, SS has been shown to be particularly suitable for characterizing the performance of both continuous- and discrete-state systems in their entire range of operation: actually, a single SS run yields failure probability estimates for different threshold levels up to the largest one considered, thus avoiding multiple runs which are instead required by standard MCS.

7.3 Line Sampling Applied to the Reliability Analysis of a Nuclear Passive Safety System

The case study considered regards a safety system for natural convection cooling in a gas-cooled fast reactor (GFR), operating in the conditions of a post-LOCA [9, 10]. The reactor is a 600 MW GFR cooled by helium flowing through separate channels in a silicon carbide matrix core. In case of a LOCA, long-term removal of the decay heat is ensured by natural circulation in a given number N_{loops} of identical and parallel heat removal loops. However, in order to achieve a sufficient heat removal rate by natural circulation, it is necessary to maintain an elevated pressure even after the LOCA. This is accomplished by a guard containment, which surrounds the reactor vessel and power conversion unit and holds the pressure at a level that is reached after the depressurization of the system.

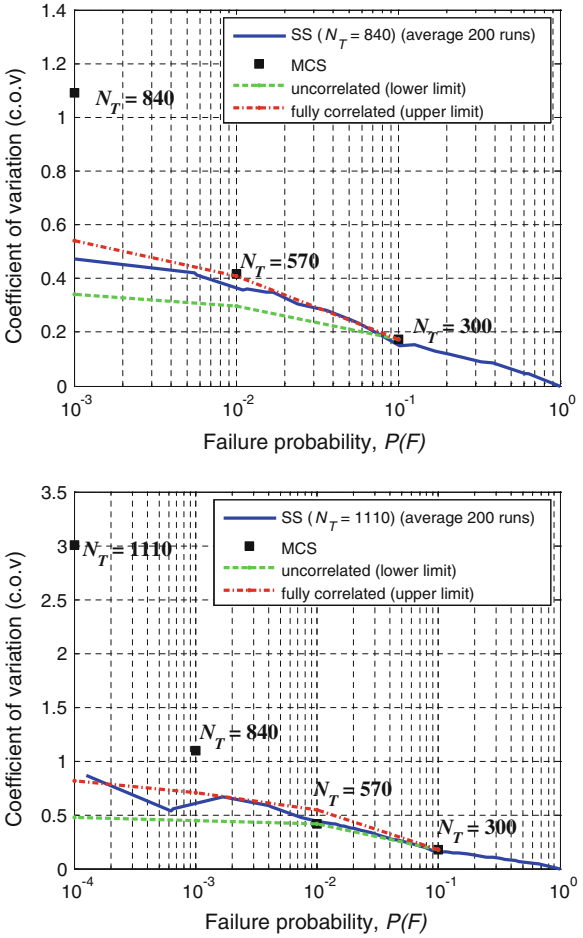

Fig. 7.10 c.o.v. versus different failure probability levels $P(F)$ for Cases 1 (*top*) and 2 (*down*). *Solid line* sample average over 200 SS runs; *dashed lines* sample average of the lower bound over 200 SS runs; *dot-dashed lines* sample average of the upper bound over 200 SS runs; *squares* standard MCS (iid samples)

The GFR decay heat removal configuration considered is shown schematically in Fig. 7.11, with only one loop for clarity of the picture: the flow path of the cooling helium gas is indicated by the black arrows. For numerical modeling purposes, the loop has been divided into $N_{\text{sections}} = 18$ sections; for further technical details about the geometrical and structural properties of these sections, the interested reader may refer to [10–13].

The subject of the present analysis is the quasi-steady-state natural circulation cooling that takes place after the LOCA transient has occurred, assuming successful inception of natural circulation. The average core decay power to be removed is assumed to be 18.7 MW, equivalent to about 3 % of full reactor power (600 MW). To guarantee natural circulation cooling at this power level, a pressure of 1650 kPa is required in nominal conditions. Finally, the secondary side of the heat exchanger (i.e., item 12 in Fig. 7.11) is assumed to have a nominal wall temperature of 90 °C [10].

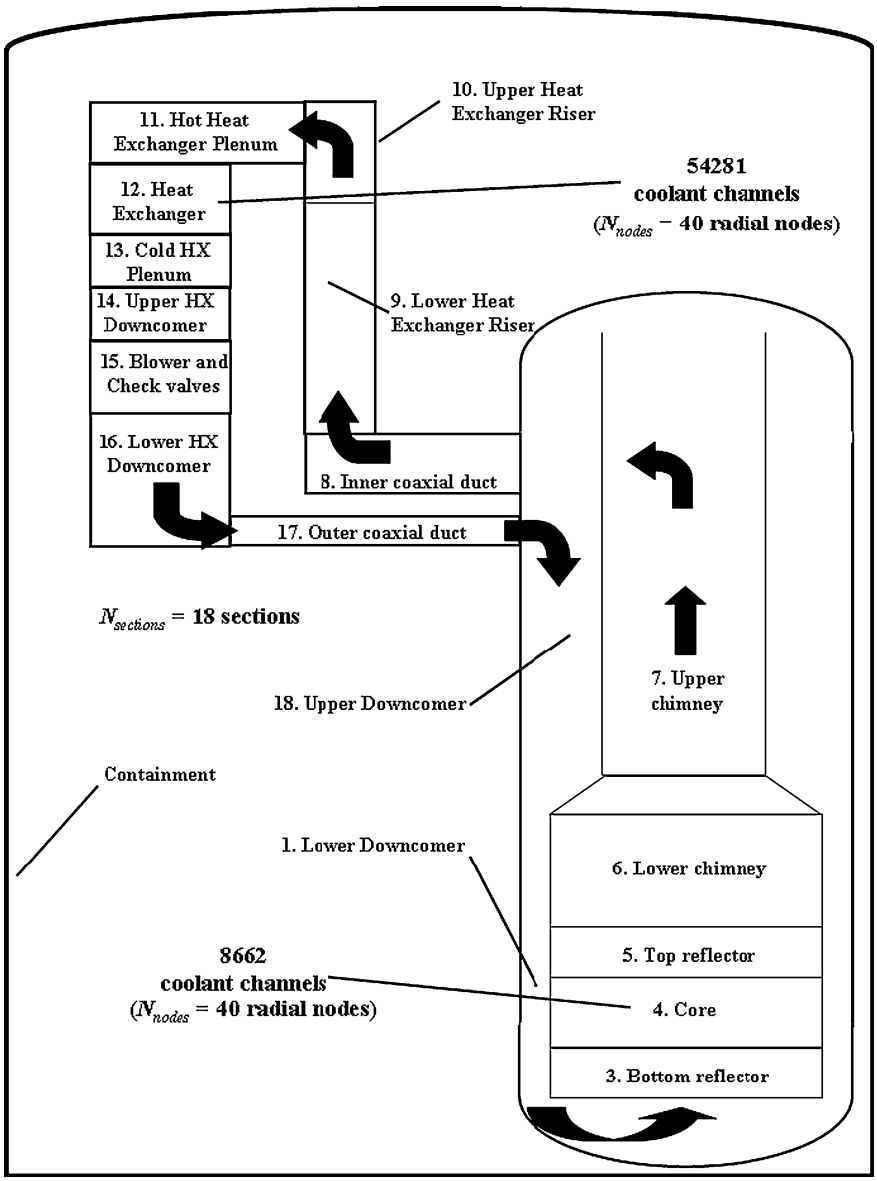

Fig. 7.11 Schematic representation of one loop of the 600 MW GFR passive decay heat removal system [10]; HE=Heat Exchanger

To simulate the steady-state behavior of the system, a one-dimensional Thermal–Hydraulic (T–H) *Matlab*® code developed at the Massachusetts Institute of Technology (MIT) has been implemented [11–13]. The code treats as identical all the N_{loops} multiple loops, each one divided in $N_{\text{sections}} = 18$ sections.

Furthermore, the sections corresponding to the heater (i.e., the reactor core, item 4 in Fig. 7.11) and the cooler (i.e., the heat exchanger, item 12 in Fig. 7.11) are divided in a proper number N_{nodes} of axial nodes to compute the temperature and flow gradients with sufficient detail (40 nodes are chosen for the present analysis). Both the average and hot channels are modeled in the core, so that the increase in temperature in the hot channel due to the radial peaking factor can be calculated.

To obtain a steady-state solution, the code balances the pressure losses around the loops so that friction and form losses are compensated by the buoyancy term, while at the same time maintaining the heat balance in the heater and cooler.

The two following equations govern the heat transfer process in each node $l = 1, 2, \ldots, N_{\text{nodes}}$ of both heater and cooler

$$\dot{Q}_l = \dot{m} c_{p,l} \left(T_{\text{out},l} - T_{\text{in},l} \right) \quad l = 1, 2, \ldots, N_{\text{nodes}}$$

$$\dot{m} c_{p,l} \left(T_{\text{out},l} - T_{\text{in},l} \right) = S_l h_l \left(T_{\text{wall},l} - T_{\text{bulk},l} \right) \quad l = 1, 2, \ldots, N_{\text{nodes}} \tag{7.9}$$

where $\dot{Q}_l$ is the heat flux (kW), $\dot{m}_l$ is the mass flow rate (kg/s), $c_{p,l}$ is the specific heat at constant pressure (kJ/kgK), $T_{\text{out},l}$, $T_{\text{in},l}$, $T_{\text{wall},l}$ and $T_{\text{bulk},l}$ are the temperatures in degrees Kelvin (K) measured at the outlet, the inlet, the wall channel and coolant bulk, respectively, S_l is the heat-exchanging surface (m^2) and h_l is the heat transfer coefficient (kW/m^2K) in the l-th node, $l = 1, 2, \ldots, N_{\text{nodes}}$.

The first equation above states the equality of the enthalpy increase between the flow at the inlet and the flow at the outlet in any node, whereas the second equation regulates the heat exchange between the channel wall and the bulk of the coolant. Notice that the heat transfer coefficients h_l, $l = 1, 2, \ldots, N_{\text{nodes}}$ are functions of the fluid characteristics and geometry and are calculated through proper correlations covering forced-, mixed-, and free-convection regimes in both turbulent and laminar flows; further, different Nusselt number correlations are used in the different regimes to obtain values for the heat transfer coefficients.

The mass flow rate $\dot{m}$ is determined by a balance between buoyancy and pressure losses along the closed loop according to the following equation

$$\sum_{s=1}^{N_{\text{sections}}} \left[\rho_s g H_s + f_s \frac{L_s}{D_s} \frac{\dot{m}^2}{2\rho_s A_s^2} + K_s \frac{\dot{m}^2}{2\rho_s A_s^2} \right] = 0 \tag{7.10}$$

where ρ_s is the coolant density (kg/m^3), H_s is the height of the section (m), f_s is the friction factor, L_s is the length of the section (m), D_s is the hydraulic diameter of the section (m), $\dot{m}$ is the mass flow rate (kg/s), A_s is the flow area of the section (m^2), and K_s is the form loss coefficient of the s-th section of the loop, $s = 1, 2, \ldots, N_{\text{sections}}$ (Fig. 7.11). Such equation states that the sum of buoyancy (first term), friction losses (second term), and form losses (third term) should be equal to zero along the closed loop. Notice that the friction factors f_s, $s = 1, 2, \ldots, N_{\text{sections}}$, are also functions of the fluid characteristics and geometry and are calculated using appropriate correlations.

The deterministic T–H model described in the previous paragraphs provides a mathematical description of the system behaviour. The actual behavior of the natural circulation passive system in reality deviates from its mathematical representation, due to a number of uncertain factors which affect its operation: the outcome of such uncertain behavior must be accounted for in the evaluation of the system reliability [10].

Uncertainties in the passive system operation are mainly due to lack of knowledge about the natural circulation phenomena involved and their conditions of occurrence. These uncertainties translate into uncertainties in the *models* and *parameters* used to represent the system and its processes.

In this example, parameter uncertainties are associated to the reactor power level, to the pressure established in the loops after the LOCA and to the wall temperature of the cooler (i.e., the heat exchanger, item 12 in Fig. 7.11). Model uncertainties are associated to the correlations used to calculate Nusselt numbers and friction factors in forced, mixed, and free convection. Correspondingly, nine uncertain model inputs $\{x_j : j = 1, 2, \ldots, 9\}$ are considered, as summarized in Table 7.8 [10]. The parameters are assumed to be distributed according to normal distributions of given mean μ and standard deviation σ. The practical and conceptual reasons underpinning the choices of the values in Table 1 are described in [10].

The passive decay heat removal system of Fig. 7.11 is considered failed whenever the temperature of the coolant helium leaving the core (item 4 in Fig. 7.11) exceeds either 1200 °C in the hot channel or 850 °C in the average channel: these values are chosen to limit the fuel temperature for avoiding excessive release of fission gasses and high thermal stresses in the cooler (item 12 in Fig. 7.11) and in the stainless steel cross-ducts connecting the reactor vessel and the cooler (items from 6 to 11 in Fig. 7.11).

Letting $\underline{x}$ be the vector of uncertain system inputs (Table 7.8) and $T^{\text{hot}}_{\text{out,core}}(\underline{x})$ and $T^{\text{avg}}_{\text{out,core}}(\underline{x})$ be the coolant outlet temperatures in the hot and average channels, respectively, the failure region F can be written as follows

$$F = \left\{\underline{x} : T^{\text{hot}}_{\text{out,core}}(\underline{x}) > 1200\right\} \cup \left\{\underline{x} : T^{\text{avg}}_{\text{out,core}}(\underline{x}) > 850\right\} \tag{7.11}$$

In order to apply LS, the failure region F has been parameterized with a single parameter so that a single-valued performance function (PF) $g_{\underline{X}}(\cdot)$ arises (Sect. 6.8). This is accomplished as follows. For the failure region F, the system performance indicator $Y(\underline{x})$ can be defined as

$$Y(\underline{x}) = \max\left\{\frac{T^{\text{hot}}_{\text{out,core}}(\underline{x})}{1200}, \frac{T^{\text{avg}}_{\text{out,core}}(\underline{x})}{850}\right\} \tag{7.12}$$

Table 7.8 Parameter and model uncertainties together with the values of the parameters of the related subjective probability distributions for the 600 MW GFR passive decay heat removal system of Fig. 7.11 [10]

	Name	Mean, μ	Standard deviation, σ (% of μ)
Parameter uncertainty	Power (MW), x_1	12	1
	Pressure (kPa), x_2	1650	7.5
	Cooler wall temperature (°C), x_3	90	5
Model uncertainty	Nusselt number in forced convection, x_4	1	5
	Nusselt number in mixed convection, x_5	1	15
	Nusselt number in free convection, x_6	1	7.5
	Friction factor in forced convection, x_7	1	1
	Friction factor in mixed convection, x_8	1	10
	Friction factor in free convection, x_9	1	1.5

Then, it can be easily verified that

$$F = \{\underline{x} : Y(\underline{x}) > 1\} \tag{7.13}$$

Thus, the failure threshold α_Y is equal to 1 and the system PF is written as

$$g_{\underline{X}}(\underline{x}) = Y(\underline{x}) - \alpha_Y = Y(\underline{x}) - 1 \tag{7.14}$$

In the following, the results of the application of LS for the reliability analysis of the 600 MW GFR passive decay heat removal system in Fig. 7.11 are illustrated. First, the probabilities of failure of the system are estimated; then, the sensitivity of the passive system performance with respect to the uncertain input parameters is studied by examination of the important unit vectors $\underline{\alpha}$. For illustration purposes, three different system configurations (with $N_{\text{loops}} = 3$, 4 and 5) are analyzed.

Furthermore, LS is compared to the common method of LHS. For this purpose, LS has been run with a total of $N_T = 10000$ samples in all the cases, whereas LHS has been run with $N_T = 10000$, 100000 and 1000000 for the configurations with $N_{\text{loops}} = 3$, 4, and 5, respectively. Notice that the larger number N_T of samples employed by LHS in the analyses of the configurations with $N_{\text{loops}} = 4$ (where $P(F) = 10^{-5}$) and 5 (where $P(F) = 10^{-6}$) is due to the necessity of producing a number of failure samples sufficient to estimate the related small failure probabilities and their standard deviations with acceptable robustness.

In order to compare the results, the efficiency of the simulation methods under analysis is evaluated in terms of two indices which are independent of the total number N_T of samples drawn: the unitary c.o.v., δu, and the so-called figure of merit (FOM).

The unitary c.o.v. δu is defined as

$$\delta u = \delta \cdot \sqrt{N_T} = \frac{\sigma}{\hat{P}(F)} \cdot \sqrt{N_T} \tag{7.15}$$

where δ is the c.o.v., $\widehat{P}(F)$ is the sample estimate of $P(F)$ and σ is the sample standard deviation of $\widehat{P}(F)$. Since in all MC-type estimators the standard deviation σ (and, thus, the c.o.v. δ) decays with a rate $O(1/\sqrt{N_T})$, then $\delta u = \delta \cdot \sqrt{N_T}$ is independent of N_T. Notice that the lower is the value of δu, the lower is the variability of the corresponding failure probability estimator and thus the higher is the efficiency of the simulation method adopted.

However, in addition to the precision of the failure probability estimator, also the computational time associated to the simulation method has to be taken into account. Thus, the FOM is introduced and defined as

$$\text{FOM} = \frac{1}{\sigma^2 \cdot t_{\text{comp}}} \tag{7.16}$$

where t_{comp} is the computational time required by the simulation method. Since $\sigma^2 \propto N_T$ and approximately $t_{\text{comp}} \propto N_T$, also the FOM is independent of N_T. Notice that in this case the higher is the value of the index, the higher is the efficiency of the method.

Table 7.9 reports the values of the failure probability estimate $\widehat{P}(F)$, the unitary c.o.v. δu and the FOM obtained by LS with $N_T = 10000$ samples and LHS with $N_T = 10000$, 100000 and 1000000 samples in the reliability analysis of the T–H passive system of Fig. 7.11 with $N_{\text{loops}} = 3$, 4 and 5, respectively; the actual number N_{sys} of system performance analyses is also reported together with the computational time t_{comp} (in seconds) required by each simulation method on a Pentium 4 CPU 3.00 GHz. Notice that for LS the actual number N_{sys} of system performance analyses is given by $N_{\text{sys}} = N_s + 2 \times N_T$: in particular, $N_s = 2000$ analyses are performed to generate the Markov chain used to compute the important unit vector $\underline{\alpha}$ as the normalized "center of mass" of the failure domain F (Sect. 3.4); instead, $2 \cdot N_T$ analyses are carried out to compute the N_T conditional one-dimensional failure probability estimates $\left\{\widehat{P}^k(F) : k = 1, 2, \ldots, N_T\right\}$ by linear interpolation.

It can be seen that LS leads to a substantial improvement in efficiency over LHS in all the cases considered, i.e., for failure probabilities $P(F)$ ranging from 10^{-3} ($N_{\text{loops}} = 3$ in Table 7.9) to 10^{-6} ($N_{\text{loops}} = 5$ in Table 7.9). The most significant improvement is registered in the estimation of very small failure probabilities. Indeed, for $P(F) \sim 10^{-6}$ (i.e., $N_{\text{loops}} = 5$ in Table 7.9) the estimate produced by LS is much more robust than the one produced by LHS: actually, the unitary c.o.v. δu (thus, the variability) of the LS estimator is about 770 times lower than that of the LHS estimator (conversely, the FOM is about 105 times larger). Notice that even though the determination of the sampling important direction $\underline{\alpha}$ and the

Table 7.9 Values of the failure probability estimate, unitary coefficient of variation (c.o.v.) δu and FOM obtained by LS with $N_T = 10000$ samples and LHS with $N_T = 10000$, 100000, and 1000000 samples, in the reliability analysis of the passive system of Fig. 7.11 with $N_{\text{loops}} = 3$, 4 and 5, respectively

	$\widehat{P}(F)$	δu	FOM	N_T	N_{sys}	t_{comp} (s)
$N_{\text{loops}} = 3$						
LHS	1.400×10^{-3}	19.05	1.41×10^{3}	10000	10000	32515
LS	1.407×10^{-3}	0.4757	1.00×10^{6}	10000	22000	64328
$N_{\text{loops}} = 4$						
LHS	2.000×10^{-5}	210.82	5.63×10^{4}	100000	100000	321650
LS	1.510×10^{-5}	0.4785	9.87×10^{8}	10000	22000	63482
$N_{\text{loops}} = 5$						
LHS	2.000×10^{-6}	699.80	1.58×10^{5}	1000000	1000000	3223508
LS	3.426×10^{-6}	0.9105	1.60×10^{10}	10000	22000	64281

The actual number N_{sys} of system performance analyses is also reported together with the computational time t_{comp} (in seconds) required by each simulation method on a Pentium 4 CPU 3.00 GHz

calculation of the conditional one-dimensional failure probability estimates $\left\{\widehat{P}^k(F) : k = 1, 2, \ldots, N_T\right\}$ require much more than N_T system analyses to be performed, this is significantly overweighed by the accelerated convergence rate that can be attained.

Finally, it is worth noting that the use of preferential lines (instead of random points) to probe the failure domain F of interest makes the effectiveness of the LS method almost independent of the target failure probability $P(F)$ to be estimated: actually, in this case the value of the unit c.o.v. δu keeps almost constant although the target failure probability $P(F)$ changes by three orders of magnitude (in particular, $\delta u = 0.4757$, 0.4785 and 0.9105 for $P(F) \sim 1.4 \times 10^{-3}$, 1.5×10^{-5} and 3.4×10^{-6}, respectively).

As explained in Sect. 6.8, the important unit vector $\underline{\alpha} = \left\{\alpha_1, \alpha_2, \ldots, \alpha_j, \ldots, \alpha_n\right\}$ points in the "direction of greatest impact" on the PF $g_\theta(\underline{\theta})$ in the standard normal space. In other words, given a specified finite variation $\Delta\underline{\theta}$ in the parameter vector $\underline{\theta}$, the PF $g_\theta(\underline{\theta})$ will change most if this variation is taken in the direction of $\underline{\alpha}$. Equivalently, the vector $\underline{\alpha}$ tells what combinations of parameter variations contribute most to failure and thus gives an idea of the relative importance of the random parameters $\left\{\theta_j : j = 1, 2, \ldots, n\right\}$ in determining the failure of the system under analysis.

Thus, the *sensitivity* of the passive system performance to the individual uncertain input parameters of Table 7.8 can be studied by comparing the magnitude of each component of $\underline{\alpha}$. Table 7.10 reports the values of the components of the LS important unit vectors $\underline{\alpha}$ computed as the normalized "centers of mass" of the failure domain F of the 600 MW passive decay heat removal system of Fig. 7.11 with $N_{\text{loops}} = 3$, 4, and 5.

Table 7.10 LS important unit vector $\underline{\alpha}$ computed as the normalized "center of mass" of the failure domain F of the 600 MW passive decay heat removal system of Fig. 7.11 with $N_{loops} = 3$, 4 and 5

N_{loops}	LS important unit vector, $\underline{\alpha}$								
	α_1 (x_1)	α_2 (x_2)	α_3 (x_3)	α_4 (x_4)	α_5 (x_5)	α_6 (x_6)	α_7 (x_7)	α_8 (x_8)	α_9 (x_9)
3	+0.052	**−0.924**	+0.054	+0.029	**−0.097**	−0.043	+0.019	**+0.351**	+0.060
4	+0.077	**−0.975**	+0.020	+0.003	**−0.133**	+0.001	+0.002	**+0.153**	−0.034
5	+0.071	**−0.987**	+0.064	+0.0110	**−0.0924**	−0.0110	+0.0065	**+0.0796**	−0.0423

The indication of the physical parameters corresponding to one of the vector components are enclosed in parentheses (Table 7.8). The parameters which most contribute to the failure of the passive system are highlighted in bold

It can be seen that the performance of the passive system is strongly sensitive to the pressure level established in the guard containment after the LOCA, as indicated by the large (absolute) values of component α_2 in all the cases considered (in particular $\alpha_2 = -0.9243$, -0.9753, and -0.9868 for $N_{loops} = 3$, 4 and 5, respectively). A (slight) sensitivity of the passive system performance is also observed with respect to the correlation errors in both the Nusselt number (in particular, $\alpha_5 = -0.0976$, -0.1330 and -0.0924 for $N_{loops} = 3$, 4 and 5, respectively) and the friction factor (in particular, $\alpha_8 = +0.3518$, $+0.1534$ and $+0.0796$ for $N_{loops} = 3$, 4 and 5, respectively) in mixed convection. The magnitude of the other vector components is instead negligible with respect to these ones.

Also, the signs of the vector components provide useful pieces of information about sensitivity: in particular, they indicate the direction toward which the corresponding parameters have to move in order to cause the failure of the passive system: for instance, since α_2 and α_5 are *negative* (Table 7.10), failure of the passive system will be caused by a *decrease* in the pressure (x_2) and in the Nusselt numbers in mixed convection (x_5); on the contrary, since α_8 is *positive* (Table 7.10), failure of the passive system will be registered in correspondence of high values of the friction factor in mixed convection (x_8).

These results are physically reasonable. In fact, the pressure of the system strongly affects the density of the coolant helium gas, and thus the extent of the buoyancy force on which the effective functioning of the natural circulation system is based. In particular, a decrease in the system pressure leads to a decrease in the buoyancy force which may not succeed in balancing the pressure losses around the natural circulation loop. Nusselt numbers instead are directly (i.e., linearly) related to the heat transfer coefficients in both the core and the heat exchanger, and thus their variations directly impact the global heat removal capacity of the passive system. In particular, a decrease in the heat transfer coefficient in the heat exchanger (where the wall temperature is imposed) leads to a reduction in the heat flux and consequently to an increase in the coolant. Further, a decrease in the heat transfer coefficient in the core (where the heat flux is imposed as constant) causes an increase in the coolant wall temperature. Thus, both processes lead to a rapid attainment of the coolant temperature limits. Finally, the friction factors

directly determine the extent of the pressure losses which oppose the coolant flow in natural circulation. In particular, an increase in the friction factors determines an increase in the pressure losses along the closed loop and consequently a reduction in the coolant flow rate. The smaller the flow rate in the decay heat removal loop, the higher the coolant temperature rise will be, leading to an earlier attainment of the coolant temperature limits.

References

1. Zio, E., & Podofillini, L. (2003). Importance measures of multi state components in multi-state systems. *International Journal of Reliability, Quality and Safety Engineering, 10*(3), 289–310.
2. Zio, E., & Pedroni, N. (2008) Reliability analysis of a discrete multi state system by means of subset simulation, Proceedings of European Safety and Reliability Conference, ESREL, 22–25 Sept 2008. Valencia, Spain, pp. 709–716
3. Levitin, G., & Lisnianski, A. (1999). Importance and sensitivity analysis of a multi state system using the universal generating function method. *Reliability Engineering and System Safety, 65*, 271–282.
4. Au, S. K., & Beck, J. L. (2001). Estimation of a small failure probabilities in high dimension by subset simulation. *Probabilistic Engineering Mechanics, 16*(4), 263–277.
5. Au, S. K., & Beck, J. L. (2003). Subset simulation and its application to seismic risk based on dynamics analysis. *Journal of Engineering Mechanics, 129*(8), 1–17.
6. Koutsourelakis, P. S., Pradlwarter, H. J., & Schuller, G. I. (2004). Reliability of structures in high dimensions, Part I: Algorithms and application. *Probabilistic Engineering Mechanics, 19*, 409–417.
7. Pradwarter, H. J., Pellisetti, M. F., Schenk, C. A., Schueller, G. I., Kreis, A., Fransen, S., et al. (2005). *Computer Methods in Applied Mechanics and Engineering, 194*, 1597–1617.
8. Au, S. K. (2005). Reliability-based design sensitivity by efficient simulation. *Computers & Structures, 83*, 1048–1061.
9. Zio, E., & Pedroni, N. (2010). An optimized line sampling method for the estimation of the failure probability of a nuclear passive system. *Reliability Engineering and Safety System, 95*(12), 1300–1313.
10. Pagani, L., Apostolakis, G. E., & Hejzlar, P. (2005). The impact of uncertains on the performance of passive system. *Nuclear Technology, 149*, 129–140.
11. Eaoen, J., Hejzlar, P., & Driscoll, M. J. (2002). *Analysis of a natural convection loop for post LOCA GCFR decay-heat removal*. MIT: Department of nuclear engineering.
12. Okano, Y., Hejzar, P., & Driscoll, M. J. (2002). *Thermal-hydraulics and shutdown coolings of supercritical CO_2 GT-GCFRs*. MIT: Department of Nuclear Engineering.
13. Williams. W., Hejzlar, P., Driscoll, M.J., Lee, W.J., Saha, P. (2003) *Analysis of a convection loop fora a GFR post LOCA decay heat removal from a block-type core*. MIT: Department of Nuclear Engineering.

Appendix A
Probability

Definitions

A process whose outcome is a priori unknown to the analyst is called an *experiment* ε. The possible outcomes are all a priori known and classified but which one will occur is unknown at the time the experiment is performed. The set of all possible outcomes of ε is called *sample space* Ω. The sample space can be discrete finite (e.g., for an experiment of a coin or dice toss), countably infinite (e.g., the number of persons crossing the street in a given period of time: in principle, it could be infinite and yet be counted) or continuous (e.g., the value of the dollar currency in the year 3012).

An *event* E is a group of possible outcomes of the experiment ε, i.e., a subset of Ω. In particular, each possible outcome represents an (*elementary) event* itself, being a subset of Ω. Further, the *null set* $\varnothing$ and the sample space Ω can also be considered events. To each event E is possible to associate its complementary event $\overline{E}$, constituted by all possible outcomes in Ω which do not belong to E. Event E occurs when the outcome of the experiment ε is one of the elements of E.

Logic of Certainty

In the *logic of certainty* (Boolean logic), an event can either occur or not occur. Thus, it is represented by a statement, or proposition which can only be either *true* or *false*, and at a certain point in time, after the experiment is performed, the analyst will know its actual state.

Correspondingly, to event E we can associate an indicator variable X_E which takes the value of 1 when the event occurs in the experiment and 0 when it does not. As a counter example, the statement "It may rain tomorrow" does not represent an event because it does not imply a "true" or "false" answer.

E. Zio, *The Monte Carlo Simulation Method for System Reliability and Risk Analysis*, Springer Series in Reliability Engineering,
DOI: 10.1007/978-1-4471-4588-2, © Springer-Verlag London 2013

We define the following operations involving Boolean events:

Negation: Given event E, represented by the indicator variable X_E, its negation $\overline{E}$ is described by

$$\overline{X}_E = 1 - X_E \tag{A.1}$$

Union: The event $A \cup B$, union of the two events A and B, is true, e.g., $X_{A\cup B} = 1$, if any one of A or B is true. Hence,

$$X_{A\cup B} = 1 - (1 - X_A)(1 - X_B) = 1 - \prod_{j=A,B} (1 - X_j) = \coprod_{j=A,B} X_j = X_A + X_B - X_A X_B \tag{A.2}$$

Often in practice this event is indicated as $A + B$ and referred to as the *OR* event, *A OR B*.

Intersection: The event $A \cap B$, intersection of the events A and B, is true, e.g., $X_{A\cap B} = 1$, if both A and B are simultaneously true. Hence,

$$X_{A\cap B} = X_A X_B \tag{A.3}$$

Often in practice this event is indicated as AB and referred to as the joint event *A AND B*.

Mutually exclusive events: Two events A and B are said to be mutually exclusive if their intersection is the null set, i.e.,

$$X_{A\cap B} = 0 \tag{A.4}$$

Logic of Uncertainty

Axiomatic Definition of Probability

At the current state of knowledge, it is possible that the state of an event be *uncertain*, although at some point in the future uncertainty will be removed and replaced by either the true or the false state. Inevitably, if one needs to make decisions based on the current state of knowledge, he or she has to deal with such uncertainty. In particular, one needs to be able to compare different uncertain events and say whether one is more likely to occur than another. Hence, we accept the following *axiom* as a primitive concept which does not need to be proven:

Uncertain events can be compared.

It represents a concept very similar to that of the value of objects and goods which need to be compared for the purpose of exchanging them. In this latter case at one point in history, the monetary scale was introduced as an absolute scale against which to compare different goods with respect to their values. Similarly, it is necessary to introduce a measure for comparing uncertain events.

Let us consider an experiment ε and let Ω be its sample space. To each event E we assign a real number $p(E)$, which we call *probability of E* and which satisfies the following three Kolmogorov axioms:

1. For each event E, $0 \leq p(E) \leq 1$;
2. For event Ω, it is $p(\Omega) = 1$; for event $\varnothing$, it is $P(\varnothing) = 0$;
3. Let $E_1, E_2, \ldots E_n$ be a finite set of mutually exclusive events. Then,

$$p\left(\bigcup_{i=1}^{n} E_i\right) = \sum_{i=1}^{n} p(E_i) \tag{A.5}$$

The latter axiom is called the *addition law* and is assumed to maintain its validity also in the case of countably infinite sample spaces.

This axiomatic view constitutes the Bayesian, or subjectivist, interpretation of probability according to which everything is made relative to an assessor which declares 'a priori' its 'belief' regarding the likelihood of uncertain events in order to be able to compare them. Thus, in this view, the probability of an event E represents a *degree of belief,* or *degree of confidence*, of the assessor with regards to the occurrence of that event. Because the probability assignment is subjectively based on the assessor's internal state, in most practical situations there is no 'true' or 'correct' probability for a given event and the probability value can change as the assessor gains additional information (experimental evidence). Obviously, it is completely 'objective' in the sense that it is independent of the personality of the assessor who must assign probabilities in a coherent manner, which requires obeying the axioms and laws of probability, in particular to Bayes theorem for updating the probability assignment on the basis of newly collected evidence (see Sect. A.4). By so doing, two assessors sharing the same total background of knowledge and experimental evidence on a given event must assign the same probability for its occurrence.

Empirical Frequentist Definition

Let E be an event associated to experiment ε. Suppose that we repeat the experiment n times and let k be the number of times that event E occurs. The ratio k/n represents the relative frequency of occurrence of E. As the number of repetitions n approaches infinity we empirically observe that the ratio k/n settles around an asymptotic value, p, and we say that p is the probability of E.

From a rigorous point-of-view, this empirical procedure does not follow the usual definition of mathematical limit and it can be synthesized as follows,

$$\lim_{n \to \infty} \left| \frac{k}{n} - p \right| < \xi \tag{A.6}$$

with $\xi \geq 0$. Obviously, this definition may be somewhat unsatisfactory as probability is defined in terms of likelihood of a large number of repeated experiments.

Classical Definition

This definition is very similar to the previous empirical one. The only fundamental difference is that it is not necessary to resort to the procedure of taking a limit. Let us consider an experiment with N possible elementary, mutually exclusive and equally probable outcomes $A_1, A_2, \ldots, A_N$. We are interested in the event E which occurs if anyone of M elementary outcomes occurs, $A_1, A_2, \ldots, A_M$, i.e., $E = A_1 \cup A_2 \cup \ldots \cup A_M$.

Since the events are mutually exclusive and equally probable

$$p(E) = \frac{\text{number of outcomes of interest}}{\text{total number of possible outcomes}} \tag{A.7}$$

This result is very important because it allows computing the probability with the methods of combinatorial calculus; its applicability is however limited to the case in which the event of interest can be decomposed in a finite number of mutually exclusive and equally probable outcomes. Furthermore, the classical definition of probability entails the possibility of performing repeated trials; it requires that the number of outcomes be finite and that they be equally probable, i.e., it defines probability resorting to a concept of frequency.

Once a probability measure is defined in one of the above illustrated ways, the mathematical theory of probability is founded on the three fundamental axioms of Kolmogorov introduced earlier, independently of the definition. All the theorems of probability follow from these three axioms.

Probability Laws

As previously mentioned, to the generic random event E is associated an indicator variable X_E which takes the value of 1 when the event occurs in the experiment and 0 when it does not. Correspondingly, a real number $p(E)$ is assigned to measure the *probability of E* and which satisfies the three Kolmogorov axioms. Given the binary nature of the indicator variable, X_E can only take values of 0 or 1 so that

$$p(E) = p(X_E = 1) \cdot 1 + p(X_E = 0) \cdot 0 = E[X_E] \tag{A.8}$$

Union of Non-mutually Exclusive Events

Consider n events E_n not mutually exclusive. Their union E_U is associated with an indicator variable X_U which is the extension of the formula (Eq. A.2) for the union of the two events A and B. For example, for the intersection of the three events A, B, and C we have

$$X_\cup = 1 - \prod_{j=A,B,C} \left(1 - X_j\right) = 1 - (1 - X_A)(1 - X_B)(1 - X_C)$$
$$= X_A + X_B + X_C - X_A X_B - X_A X_C - X_B X_C + X_A X_B X_C \tag{A.9}$$

Following Eq. (A.8), the probability of the event E_U can then be computed applying to Eq. (A.9) the (linear) expectation operator. More generally, for the union of n non-mutually exclusive events

$$P(E_U) = E[X_\cup] = \sum_{j=1}^{n} E\left[X_j\right] - E\left[\sum_{i=1}^{n-1}\sum_{j=i+1}^{n} X_i X_j\right] + \cdots + (-1)^{n-1}\prod_{j=1}^{n} E\left[X_j\right]$$
$$= P(E_j) - \sum_{i=1}^{n-1}\sum_{j=i+1}^{n} P(E_i \cap E_j) + \cdots + (-1)^{n-1}\prod_{j=1}^{n} P(E_j) \tag{A.10}$$

From an engineering practice point-of-view, it is often necessary to introduce reasonably bounded approximations of Eq. (A.10). Keeping only the first sum, one obtains an upper bound (often referred to as the *rare-event* approximation)

$$P(E_U) \leq \sum_{j=1}^{n} P(E_j) \tag{A.11}$$

whereas keeping the first two sums gives a lower bound

$$P(E_U) \geq \sum_{j=1}^{n} P(E_j) - \sum_{i=1}^{n-1}\sum_{j=i+1}^{n} P(E_i \cap E_j) \tag{A.12}$$

More refined upper and lower bounds can then be obtained by alternately keeping an odd or even number of sum terms in Eq. (A.10).

Conditional Probability

In many practical situations, it is important to compute the probability of an event A given that another event B has occurred. This probability is called the *conditional probability of A given B* and it is given by the ratio of the probability of the joint event $A \cap B$ over the probability of the conditioning event B, viz.,

$$P(A|B) = \frac{P(A \cap B)}{P(B)} \tag{A.13}$$

Intuitively, $P(A|B)$ gives the probability of the event A not on the entire possible sample space Ω but on the sample space relative to the occurrences of B. This is the reason for the normalization by $P(B)$ of the probability of the joint event $P(A \cap B)$ in Eq. (A.9).

Based on the conditional probability, it is possible to introduce the concept of statistical independence: event A is said to be statistically independent from event B if $P(A|B) = P(A)$. In other words, knowing that B has occurred does not change the probability of A. From Eq. (A.13), it follows that if A and B are statistically independent $P(A \cap B) = P(A)P(B)$. Note that the concept of statistical independence should not be confused with that of mutual exclusivity introduced earlier $(X_A X_B = 0)$, which is actually a logical dependence: knowing that A has occurred $(X_A = 1)$ guarantees that B cannot occur $(X_B = 0)$.

Theorem of Total Probability

Let us consider a partition of the sample space Ω into n mutually exclusive and exhaustive events E_j, $j = 1, 2, \ldots, n$. In terms of Boolean events, this is written as

$$E_i \cap E_j = 0 \quad \forall i \neq j \quad \bigcup_{j=1}^{n} E_j = \Omega \tag{A.14}$$

whereas in terms of the indicator variables

$$X_i X_j = 0 \quad \forall i \neq j \quad \sum_{j=1}^{n} X_j = 1 \tag{A.15}$$

Given any event A in Ω, its probability can be computed in terms of the partitioning events $E_j, j = 1, 2, \ldots, n$ and the conditional probabilities of A on these events, viz.,

$$P(A) = P(A|E_1)P(E_1) + P(A|E_2)P(E_2) + \cdots + P(A|E_n)P(E_n) \tag{A.16}$$

Bayes Theorem

Assume now that you have experimental evidence that event A has occurred: what is the probability that event E_i has also occurred? This may be considered as a 'reverse' probability with respect to the probability question underlying the previous theorem of total probability. To the joint event $A \cap E_i$ we can apply the conditional probability (Eq. A.13) from both the points of view of A and of E_i

$$P(A \cap E_i) = P(A|E_i)P(E_i) = P(E_i|A)P(A) \tag{A.17}$$

From this, Bayes theorem is readily derived

$$P(E_i|A) = \frac{P(A|E_i)P(E_i)}{P(A)} = \frac{P(A|E_i)P(E_i)}{\sum_{j=1}^{n} P(A|E_j)P(E_j)} \tag{A.18}$$

Equation (A.18) updates the *prior* probability value $P(E_i)$ of event E_i to the *posterior* probability value $P(E_i|A)$ in reflection of the acquired experimental evidence on the occurrence of event A whose unknown probability $P(A)$ is computed by applying the theorem of total probability (Eq. A.16).

Appendix B
HAZID

Definitions

Hazard Identification (HAZID) is the procedure to assess all hazards that could directly and indirectly affect the safe operation of the system. The procedure is broken down and categorized into the two streams that can affect the system both directly and indirectly, i.e., the Internal Hazards and External Hazards studies, respectively.

Main Concepts

A HAZID study is carried out by a team of competent engineers from a mixture of disciplines, led by an analyst who is experienced in the HAZID technique. Each area of the installation is considered against a checklist of hazards. Where it is agreed that a hazard exists in a particular area, the risk presented by the hazard is considered, and all possible means of either eliminating the hazard or controlling the risk and/or the necessity for further study are noted on a HAZID worksheet. Actions are assigned to either discipline groups or individuals to ensure the mitigating control, or further study is completed.

Essentials

1. HAZID Objectives

- Identify hazards to facilities due to design and evaluate potential consequences should the hazards be realized;

E. Zio, *The Monte Carlo Simulation Method for System Reliability and Risk Analysis*, Springer Series in Reliability Engineering,
DOI: 10.1007/978-1-4471-4588-2, © Springer-Verlag London 2013

- Establish safeguards to manage hazards; identify areas where further understanding of safeguard effectiveness is needed;
- Make recommendations to reduce the likelihood of hazard occurrence or mitigate the potential consequences.

2. The HAZID method, accepted as one of the best techniques for identifying potential hazards and operability problems, involves the following:

- Assembly of a team of experienced project personnel;
- Presentations detailing the scope of the HAZID;
- Identify hazards, causes, consequences, and safeguards;
- Make recommendations to address hazards, as appropriate;
- Risk ranking of hazardous events.

3. Key Benefits to Client

- Existing design knowledge is efficiently captured relative to client's projects;
- Numerous procedural, equipment design, testing, and process control recommendations allow expedited development of standardized equipment.

4. Logic diagram

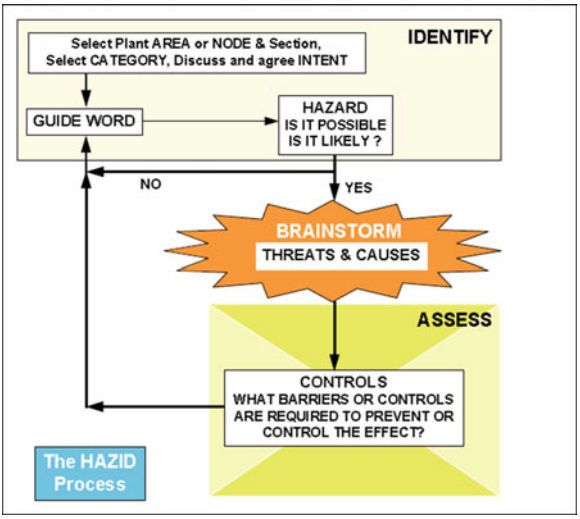

5. Process steps:

1. Define the purpose, objectives, and scope of the study;
2. Select the team;
3. Prepare for the study;
4. Carry out the team review;
5. Record the results.

Appendix C
Fault Tree Analysis

Definitions

For complex multicomponent systems, for example such as those employed in the nuclear, chemical, process, and aerospace industries, it is important to analyze the possible mechanisms of failure and to perform probabilistic analyses for the expected frequency of such failures. Often, each such system is unique in the sense that there are no other identical systems (same components interconnected in the same way and operating under the same conditions) for which failure data have been collected; therefore, a statistical failure analysis is not possible. Furthermore, it is not only the probabilistic aspects of failure of the system which are of interest but also the initiating causes and the combinations of events which can lead to a particular failure.

The engineering way to tackle a problem of this nature, where many events interact to produce other events, is to relate these events using simple logical relationships such as those introduced in Sect. A.2. (intersection, union, etc.) and to methodically build a logical structure which represents the system.

In this respect, Fault Tree Analysis (FTA) is a systematic, deductive technique which allows to develop the causal relations leading to a given undesired event. It is deductive in the sense that it starts from a defined system failure event and unfolds backward its causes down to the primary (basic) independent faults. The method focuses on a single system failure mode and can provide qualitative information on how a particular event can occur and what consequences it leads to, while at the same time allowing the identification of those components which play a major role in determining the defined system failure. Moreover, it can be solved in quantitative terms to provide the probability of events of interest starting from knowledge of the probability of occurrence of the basic events which cause them.

In the following, we shall give only the basic principles of the technique. The interested reader is invited to look at the specialized literature for further details,

E. Zio, *The Monte Carlo Simulation Method for System Reliability and Risk Analysis*, Springer Series in Reliability Engineering,
DOI: 10.1007/978-1-4471-4588-2, © Springer-Verlag London 2013

e.g., [1] and references therein from which the material herein contained has been synthetized.

Fault Tree Construction and Analysis

A fault tree is a graphical representation of causal relations obtained when a system failure mode is traced backward to search for its possible causes. To complete the construction of a fault tree for a complex system, it is necessary to first understand how the system functions. A system flow diagram (e.g., a reliability block diagram) can be used for this purpose, to depict the pathways by which flows (e.g., of mass, signals, energy, information, etc.) are transmitted among the components of the system.

The first step in fault tree construction is the selection of the system failure event of interest. This is called the top event and every following event will be considered in relation to its effect upon it.

The next step is to identify contributing events that may directly cause the top event to occur. At least four possibilities exist [2]:

- No input to the device;
- Primary failure of the device (under operation in the design envelope, random, due to aging or fatigue);
- Human error in actuating or installing the device;
- Secondary failure of the device (due to present or past stresses caused by neighboring components or the environments: e.g., common cause failures, excessive flows, external causes such as earthquakes).

If these events are considered to be indeed contributing to the system fault, then they are connected to the top event logically via an OR event (see Eq. A.2) and graphically through the OR gate (Fig. C.1):

Once the first level of events directly contributing to the top has been established, each event must be examined to decide whether it is to be further decomposed in more elementary events contributing to its occurrence. At this stage, the questions to be answered are:

- Is this event a primary failure?
- Is it to be broken down further in more primary failure causes?

In the first case, the corresponding branch of the tree is terminated and this primary event is symbolically represented by a circle. This also implies that the event is independent of the other terminating events (circles) which will be eventually identified and that a numerical value for the probability of its occurrence is available if a quantitative analysis of the tree is to be performed.

On the contrary, if a first level contributing event is not identified as a primary failure, it must be examined to identify the subevents which contribute to its occurrence and their logical relationships (Fig. C.2).

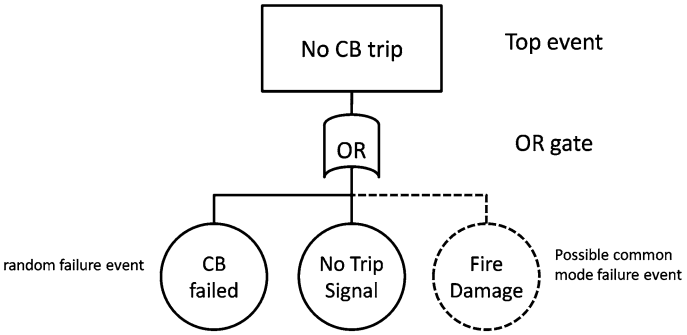

Fig. C.1 Top and first levels of a fault tree for a circuit breaker (*CB*) failing to trip an electrical circuit [3]

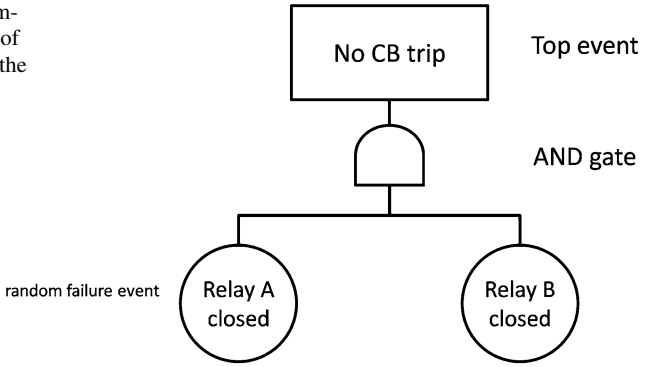

Fig. C.2 AND event example for the circuit breaker of the electrical system with the top event of Fig. C.1 [3]

The procedure of analyzing every event is continued until all branches have been terminated in independent primary failures for which probability data are available. Sometimes, certain events which would require further breakdown can be temporarily classified as primary at the current state of the tree structure and assigned a probability by rule of thumb (typically a conservative value). These underdeveloped events are graphically represented by a diamond symbol rather than by a circle.

For the analysis, a fault tree can be described by a set of Boolean algebraic equations, one for each gate of the tree. For each gate, the input events are the independent variables and the output event is the dependent variable. Utilizing the rules of Boolean algebra, it is then possible to solve these equations so that the top event is expressed in terms of sets of primary events only.

Finally, the quantification of the fault tree consists of transforming its logical structure into an equivalent probability form and numerically calculating the probability of occurrence of the top event from the probabilities of occurrence of the basic events. The probability of the basic event is the failure probability of the component or subsystem during the mission time of interest. The corresponding mathematical details can be found in [1].

Appendix D
Event Tree Analysis

Definitions

Event Tree Analysis (ETA) is an inductive logic method for identifying the various accident sequences which can generate from a single initiating event. The approach is based on the discretization of the real accident evolution in few macroscopic events. The accident sequences which derive are then quantified in terms of their probability of occurrence.

The events delineating the accident sequences are usually characterized in terms of: (1) the intervention (or not) of protection systems which are supposed to take action for the mitigation of the accident (system event tree); (2) the fulfillment (or not) of safety functions (functional event tree); (3) the occurrence or not of physical phenomena (phenomenological event tree).

Typically, the functional event trees are an intermediate step to the construction of system event trees: following the accident-initiating event, the safety functions which need to be fulfilled are identified; these will later be substituted by the corresponding safety and protection systems.

The system event trees are used to identify the accident sequences developing within the plant and involving the protection and safety systems.

The phenomenological event trees describe the accident phenomenological evolution outside the plant (fire, contaminant dispersion, etc.).

In the following, we shall give only the basic principles of the technique. The interested reader is invited to look at the specialized literature for further details, e.g., [1] and references therein from which most of the material herein contained has been synthetized.

E. Zio, *The Monte Carlo Simulation Method for System Reliability and Risk Analysis*, Springer Series in Reliability Engineering,
DOI: 10.1007/978-1-4471-4588-2, © Springer-Verlag London 2013

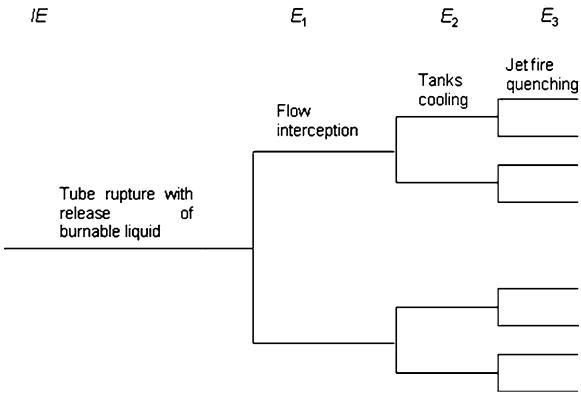

Fig. D.1 Example of functional event tree [1]

Event Tree Construction and Analysis

An event tree begins with a defined accident-initiating event which could be a component or an external failure. It follows that there is one event tree for each different accident-initiating event considered. This aspect obviously poses a limitation on the number of initiating events which can be analyzed in details. For this reason, the analyst groups similar initiating events and only one representative initiating event for each class is investigated in details. Initiating events which are grouped in the same class are usually such to require the intervention of the same safety functions and to lead to similar accident evolutions and consequences.

Once an initiating event is defined, all the safety functions that are required to mitigate the accident must be defined and organized according to their time and logic of intervention. For example (Fig. D.1), if the Initiating Event (IE) is the rupture of a tube with release of inflammable liquid and the sparking of jet-fire, the first function required would be that of interception of the released flow rate, followed by the cooling of adjacent tanks, and finally the quenching of the jet. These functions are structured in the form of headings in the functional event tree. For each function, the set of possible success and failure states must be defined and enumerated. Each state gives rise to a branching of the tree (Fig. D.1). For example, in the typical binary success/failure logic it is customary to associate to the top branch the success of the function and to the bottom branch its failure.

Figure D.2 shows a graphical example of a system event tree: the initiating event is depicted by the initial horizontal line and the system states are then connected in a stepwise, branching fashion; system success and failure states have been denoted by S and F, respectively. The accident sequences that result from the tree structure are shown in the last column. Each branch yields one particular accident sequence; for example, IS_1F_2 denotes the accident sequence in which the IE occurs, system 1 is called upon and succeeds (S_1), and system 2 is called upon but fails to perform its defined function (F_2). For larger event trees, this stepwise

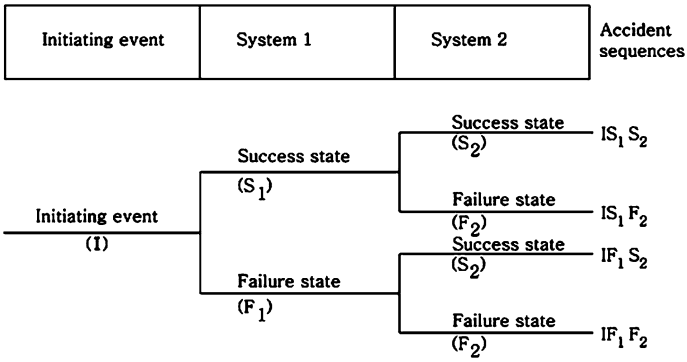

Fig. D.2 Illustration of system event tree branching [3]

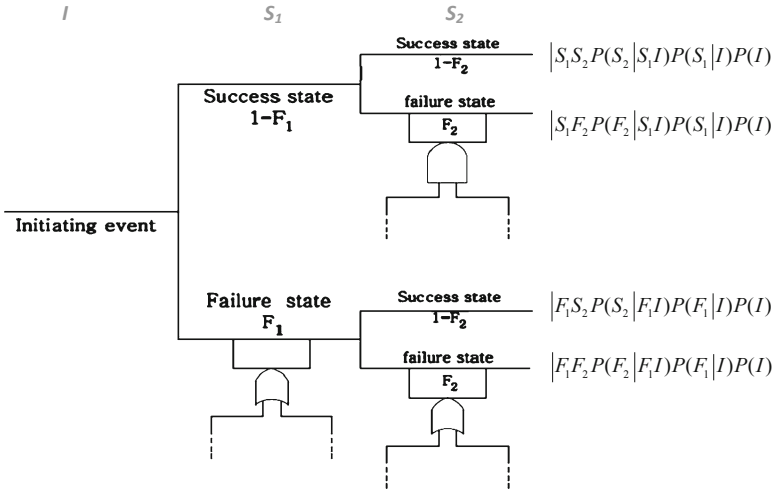

Fig. D.3 Schematics of the event tree and associated fault trees for accident sequences evaluation

branching would simply be continued. Note that the system states on a given branch of the event tree are conditional on the previous system states having occurred. With reference to the previous example, the success and failure of system 1 must be defined under the condition that the initiating event has occurred; likewise, in the upper branch of the tree corresponding to system 1 success, the success and failure of system 2 must be defined under the conditions that the initiating event has occurred and system 1 has succeeded.

Event Tree Evaluation

Once the final event tree has been constructed, the final task is to compute the probabilities of system failure. Each event (branch) in the tree can be interpreted as the top event of a fault tree which allows the evaluation of the probability of occurrence of such event. The value thus computed represents the conditional probability of the occurrence of the event, given that the events which precede on that sequence have occurred. Multiplication of the conditional probabilities for each branch in a sequence gives the probability of that sequence (Fig. D.3).

References

1. Zio, E. (2007). *An introduction to the basics of reliability and risk analysis*. Singapore: World Scientific Publishing Company.
2. Henley, E. J., & Kumamoto, H. (1992). *Probabilistic risk assessment*. New York: IEEE Press.
3. Reliability Manual for Liquid Metal Fast Reactor (LMFBR) Safety Programs, General Electric Company International, Rep. SRD 74-113, 1974.
4. Wash-1400 (NUREG75/014). (1975). *Reactor safety study. An assessment of accidents risk in U.S. Commercial Nuclear Power Plants*.